**The Role of the Histone Tails and their Post-Translational Modifications in Nucleosome Stability and Chromatin Folding**

by

Susan Catherine Moore
B.A., University of British Columbia, 1985
B.Sc., University of Victoria, 1995

A Dissertation Submitted in Partial Fulfillment of the Requirements of the Degree of

DOCTOR OF PHILOSOPHY

in the Department of Microbiology and Biochemistry

We accept this dissertation as conforming to the required standard

Dr. J. Ausió, Supervisor (Department of Microbiology & Biochemistry)

Dr. T. Pearson, Departmental Member (Department of Microbiology & Biochemistry)

Dr. R. Olafson, Departmental Member (Department of Microbiology & Biochemistry)

Dr. W. Kay, Departmental Member (Department of Microbiology & Biochemistry)

Dr. N. Livingston, Outside Member (Department of Biology)

Dr. J. Davie, External Examiner (Manitoba Institute of Cell Biology)

Supervisor: Dr. Juan Ausió

# I. Abstract

The purpose of this thesis was to characterize the impact of the histone tails and their posttranslational modifications on nucleosome stability and chromatin folding dynamics. This was done with a variety of techniques, particularly sedimentation velocity analysis and circular dichroism as well as a range of other procedures including various restriction enzyme digests, DNase I footprinting, and solubility assays. Until recently the methods used to purify histones and their modifications have been somewhat inadequate, particularly with regards to the separation of individually modified histones. Therefore a method which allows the production of native-like histones and their use in reconstituted nucleosomes and chromatin fibers was developed using RP-HPLC fractionation. This has proven particularly useful for the successful purification of modified histones. The importance of the histone tails in chromatin fiber folding was demonstrated using nucleosome trypsinization and *in vitro* investigations using reconstituted polynucleosome arrays and sedimentation velocity analysis. Both the H2A-H2B and H3-H4 tails participate in folding events however the H3-H4 tails have the greatest influence. The structural effects of two specific histone modifications were also examined: acetylation, which occurs on the N-terminal tails of all the core histones; and ubiquitination which occurs primarily on the C-terminal tails of histones H2A and H2B. Examination of different nucleosomes (native, acetylated and trypsinized) using circular dichroism demonstrated that the histone tails have α-helical content which is independent of DNA interactions and increases with acetylation. Closer examination of the histone H4 N-terminal tails with different levels of acetylation showed that this α-helical content

increase as the level of acetylation increases. Examination of histone H2A ubiquitination in nucleosome and polynucleosomal arrays demonstrated that despite the size of this modification, there were no significant structural changes in chromatin fiber folding or nucleosome structure. The results indicate that contrary to expectations uH2A did not prevent chromatin fiber folding and in fact it increased the aggregation of fibers and possibly even increased the stability of the nucleosome. Together the results illustrate the importance of investigating the structural effects of histones modifications and indicate that such modifications may produce very subtle effects rather than the huge structural disturbances often predicted.

Examiners:

Dr. J. Ausió, Supervisor (Department of Microbiology & Biochemistry)

Dr. T. Pearson, Departmental Member (Department of Microbiology & Biochemistry)

Dr. R. Olafson, Departmental Member (Department of Microbiology & Biochemistry)

Dr. W. Kay, Departmental Member (Department of Microbiology & Biochemistry)

Dr. N. Livingston, Outside Member (Department of Biology)

Dr. J. Davie, External Examiner (Manitoba Institute of Cell Biology)

# II. Table of Contents

# III. List of Tables

# IV. List of Figures

# V. Acknowledgements

First and foremost I'd like to acknowledge my family for without you I would not be here figuratively and literally speaking! To my special friends Jennifer, Janet, Lucy, Chris and Andrée - thank you for being there whenever I needed you.

I would also like to acknowledge everyone in the Biochemistry Department for all their help and encouragement over the last few years. Special mention to those unsung heroes: in the office (Claire, Melinda, Deb & John); technical services (Albert, Scott and Steve – technical wizards one and all); and biochemistry stores (the names may change over the years but particular thanks to Sarwan). In one way or another you have all generously shared of your time and knowledge.

To all the members (old and new) of the Ausió lab particularly LeAnn and Miriam, thank you. Additional thanks to John for his computer expertise, I know a few minutes of instruction from you has saved me hours of frustration.

Last, but by no means least, my special thanks and admiration to my supervisor Juan Ausió - thank you for having me in your lab, I am grateful for the experience.

# VI. Dedication

I dedicate this to my family, my parents Elizabeth (Betty) and William (Bill), my grandmother Lily, my sister Joan (& her husband Douglas) and my exceptional niece Elspeth. You are everything wonderful and joyous in my life and there are no words which adequately express my love for you all. To my parents, your love and support have shown no limits for which I am eternally grateful, I couldn't have done this without you.

# VII. Abbreviations

| | |
|---|---|
| $A_{(230, 260 \text{ etc.})}$ | absorbance at 230 nm, or 260 nm, etc. |
| ACN | acetonitrile |
| APS | ammonium persulphate |
| ATP | adenosine triphosphate |
| AU | acetic acid - urea |
| BCIP | 5-bromo-4-chloro-3-indolylphosphate p-toluidine salt |
| bp | base pair |
| BPB | bromophenol blue |
| BSA | bovine serum albumin |
| C-terminal | carboxy terminal |
| $CaCl_2$ | calcium chloride |
| CD | circular dichroism |
| CEL | chicken erythroleukemic |
| $CO_2$ | carbon dioxide |
| Da | Dalton |
| DITC | p-phenylene diisothiocyanate |
| DMEM | Dulbecco's Modified Eagle Media |
| DMSO | dimethyl sulfoxide |
| DNA | deoxyribonucleic acid |
| DTT | dithiothreitol |
| EDTA | ethylenediamine tetraacetic acid |
| EGTA | ethylenebis(oxyethylenenitrilo)-tetraacetic acid. |
| FBS | fetal bovine calf serum |
| GdnHCl | guanidine hydrochloride (aka: guanidine chloride, guanidinium hydrochloride or guanidinium chloride) |
| HAC | acetic acid (concentrated) |
| HAT | histone acetyl transferase |
| HCl | hydrochloric acid |
| HDAC | histone deacetylase |

| | |
|---|---|
| HEPES | [N-[2-hydroxyethyl]piperazine-N'-[2-ethanesulfonic acid] |
| HOS | high order structure |
| HPLC | high performance liquid chromatography |
| HRP | horse radish peroxidase |
| HTP | hydroxyapatite |
| IOS | intermediate order structure |
| IPTG | isopropylthio-β-D-galactoside |
| KCl | potassium chloride |
| KLH | keyhole limpet hemocyanin |
| LB | Luria Bertani medium |
| LOS | low order structure |
| MES | 2-[N-morpholino]ethanesulfonic acid |
| mg | milligram |
| $MgCl_2$ | magnesium chloride |
| ml | milliliter |
| MNase | micrococcal nuclease |
| MWCO | molecular weight cut-off |
| N-terminal | amino-terminal |
| NaCl | sodium chloride |
| NaOH | sodium hydroxide |
| NBCS | newborn calf serum |
| NBT | nitro blue tetrazolium |
| NET | NaCl-EDTA-Tris buffer |
| NDSB | non-denaturing sample buffer |
| PAGE | polyacrylamide gel electrophoresis |
| PBS | phosphate buffered saline |
| Pipes | 1,4-piperazinediethanesulfonic acid |
| PMSF | phenylmethylsulfonyl fluoride |
| PSN | penicillin/streptomycin/neomycin |
| PVDF | polyvinylidene difluoride membrane |
| rpm | revolutions per minute |

| | |
|---|---|
| RP-HPLC | reverse-phase high performance liquid chromatography |
| rRNA | ribosomal RNA |
| s | Svedberg unit ($10^{-13}$s) |
| SDS | sodium dodecyl sulfate |
| S-MEM | minimum essential medium for suspension cells |
| TAE | Tris-acetate-EDTA buffer |
| TBE | Tris-borate EDTA buffer |
| TCA | tricholoracetic acid |
| TE | Tris-EDTA buffer |
| TEMED | *N,N,N',N'* tetramethyl ethylene diamine |
| TFA | trifluoroacetic acid |
| TFE | trifluoroethanol |
| TLCK | N-α-tosyl-L-lysine chloromethylketone |
| Tris | Tris(hydoxymethyl)aminomethane |
| X-gal | 5-bromo-4-chloro-3-indoyl-β-D-galactoside |

# 1.0 INTRODUCTION

## 1.1 Historical Overview of Chromatin Research

Chromatin is most often described as a nucleoprotein complex consisting of DNA and both histone and non-histone proteins. While the molecular structure of these components has been elucidated only relatively recently, the existence of this complex was first discovered over 100 years ago. In 1868 Friedrich Miescher first began to 'purify' a substance from the pus (white blood cells) of hospital patients. It was considered a unique substance with a high phosphorous content which he called "nuclein" (1871). Miescher's 'nuclein' was essentially the first crude preparation of chromatin from cell nuclei. Miescher's subsequent work with salmon sperm (1874) demonstrated that the material in sperm nuclei consisted of both acidic and basic substances. The acidic material proved to be the 'nuclein' which he had previously identified, however the basic material was a new substance which he identified as "protamin". At the end of the decade, it was another scientist, Walter Flemming (1880), who first used the term "chromatin". Using light microscopy and staining techniques he described chromatin as the material within the nuclei which was easily stainable and towards the end of the century the two terms 'nuclein' and 'chromatin' were considered equivalent. A decade after Miescher's work with salmon sperm, Albrecht Kossel provided the next important advance in chromatin research. In 1884 he isolated nuclei from the erythrocytes of geese and also extracted basic proteins. However, Kossel's basic proteins were not equivalent to Miescher's 'protamin' and so he referred to them as "histon". Consequently by the end of the 19$^{th}$ century the major components within the nucleus had already been identified and were known to consist of a complex of both basic proteins - which we now know to be the histones in somatic cell nuclei or the protamines in sperm nuclei - and also the acidic, phosphorous rich component we now know to be DNA. However except for their composition, very little was known about the substances themselves or their functions.

Future work to determine the structural and functional characteristics of chromatin proceeded intermittently over the next several decades. While work progressed on the structure of the nucleic acid (DNA), there was also considerable emphasis on the functional importance of the different components. Consequently during this time there was significant debate as to which of the nuclear components acted as the genetic material. Indeed for many years it was argued that it was the proteins (i.e. histones) which were the genetic component. However during the 1940's and 1950's interest shifted from the protein-gene model to the nucleic acid theory. This idea was given further credence by bacterial transformation experiments which identified DNA as the 'transforming agent' or the genetic material (Avery *et al.*, 1944). In addition, as the purification procedures improved it became obvious that there were far fewer histones than originally thought. As with most endeavours, scientific research is highly dependent upon technological innovation. Consequently further histone research was largely dependent on the development of new purification techniques. The development of gel electrophoresis and new fractionation and chromatographic techniques in the 1950's and 1960's resulted in the accurate identification and purification of the 5 different histones which we now refer to as the core histones (H2A, H2B, H3 and H4) and the linker histones (H1). It also became obvious that the multiple proteins seen in previous experiments were degradation products. Subsequent analysis of the histone proteins has shown that in addition to their small numbers, they are also highly conserved proteins. Indeed their small numbers and conserved nature was one of the strongest arguments against the protein-gene theory and consequently interest in histone research waned. Just as DNA had once been designated as an uninteresting support element for the protein-genes, the situation was now completely reversed and the histone proteins were relegated to a mere structural role with little if any regulatory effects on DNA.

Over the last 15-20 years however there has been a gradual recognition that while the histone proteins are important structural components, they are neither static, inert, uninvolved nor unimportant. Indeed the post-translational modifications which can occur on all histones and their variants, are becoming increasingly important in understanding

the dynamic structural changes which can occur within chromatin. As a result, their effect on modulating and regulating DNA structure impacts on many different cellular processes including DNA replication and repair, transcriptional activation and silencing, and cell cycle progression. Continued structural studies therefore will have an important influence on understanding the functional impact of chromatin structural changes.

## 1.2 Chromatin Structure

The genetic material within a eukaryotic cell is organized to allow its compaction into the nucleus. The DNA, while linear, is not contiguous but is divided into chromosomes of varying sizes. The number, size and shape of the chromosomes is referred to as the karyotype and is highly variable and species specific (Cook, 2001). Each chromosome has two telomeres, one at each end, and a centromere which attaches the chromosomes to the spindle during mitosis. Within the chromosomes, the DNA of eukaryotic cells is organized into a DNA-protein complex called chromatin. The packaging of chromatin into the nucleus compacts the DNA approximately 10,000 fold so that nearly 2 meters of DNA fits into a eukaryotic nucleus which measures approximately 5-10 μm in diameter (Twyman, 1998). This packaging involves extensive folding. However, chromatin is not a static entity but is a dynamic complex which is capable of changing conformation and structure.

The folding and unfolding of DNA is not a haphazard event but is highly organized and controlled. Chromatin has been found to have several orders of structure. Initial studies with light microscopy could visualize only the large scale changes in conformation seen during the cell cycle. The chromosomes in non-dividing cells are not visible even using DNA staining techniques, however during mitosis or meiosis the chromosomes undergo major structural changes. During interphase they are less condensed and more dispersed particularly during the S-Phase when DNA replication occurs. However during metaphase, when they are transcriptionally inactive, they become highly condensed and are visible. Indeed initial information about eukaryotic chromosomal structure was a result of work done with light microscopy and observations of condensed metaphasic

chromosomes from dividing cells. The term 'packaging ratio' is used to express the length of DNA divided by the length into which it is packaged and can be used to describe the amount and differences in DNA packaging which can occur within the cell. For instance at interphase the packaging ratio is $10^3$ whereas during metaphase the packaging ratio increases to $10^5$ (Twyman, 1998).

During the cell cycle therefore there are obvious changes in chromatin structure. Thus while the entire genome must be compacted into the chromosomes within the nucleus, chromatin must still be capable of altering its structure not only during cell cycle progression but must also be accessible for other cellular processes such as DNA replication and repair, and transcriptional activation and silencing. This accessibility must also have specificity because despite the size of the genome, only a small fraction of the genes will be expressed at any given time.

Chromatin is usually designated into two broad categories: euchromatin and heterochromatin. Heterochromatin is generally termed transcriptionally inactive because of its highly condensed structure (even during interphase) and is typified by histone hypoacetylation, DNA hypermethylation, nuclease resistance and asynchronous replication in the S-phase of the cell cycle (Lewin, 1997). Heterochromatin is designated as either constitutive or facultative heterochromatin. Constitutive heterochromatin represents DNA which is permanently silenced and condensed in all cells at all times. This type of chromatin tends to consist of repetitive DNA with few coding sequences. Generally it has a structural role as is most often located at the centromere and telomeres of each chromosome.

Facultative heterochromatin is specifically and selectively inactivated either during certain developmental phases within specific cell types or in response to certain conditions. An example is the X-chromosome inactivation in female mammalian somatic cells. In these cells one of the two homologous X-chromosomes is randomly inactivated (Heard *et al.*, 1997; Lewin, 1997). The inactivated X-chromosome forms the Barr Body which can be stained during interphase and is located at the nucleus periphery.

Euchromatin typically remains 'open' or loosely packaged during interphase. These regions are defined as 'active' chromatin because it is accessible to the transcriptional machinery and is therefore capable of being expressed. However while euchromatin structure is necessary, it is not sufficient for gene expression. Active chromatin or euchromatin is typified by acetylation of histones, nuclease sensitivity, reduced DNA methylation, and normal or synchronous replication timing in the S-phase (Lewin, 1997).

Chromatin organization occurs on a number of different levels. The first level of organization and the lowest level of condensation is the formation of the nucleosome which involves wrapping DNA approximately 1.75 times around a histone core octamer and will be discussed in more detail in Section 1.3. Winding the DNA into nucleosomes compacts the DNA five fold and this conformation, termed a 'low order structure' or LOS, is often referred to as the 10nm fiber (Twyman, 1998). The 10 nm fiber is produced when cell nuclei are lysed in low salt and in electron microscopy experiments it produces a "beads-on-a-string" appearance.

A second level of organization occurs at higher ionic concentrations and in the presence of $Mg^{2+}$ (divalent cations) where the chain of nucleosomes forms a more condensed fiber which is 30-40 nm in diameter (Daban, 2000; Twyman, 1998). This fiber, termed the 30 nm fiber, is an 'intermediate order structure' (IOS) and requires the presence of histone H1. The 30 nm fiber compacts the DNA with a packaging ratio of 40 and is the conformation commonly seen in euchromatin and during interphase (Twyman, 1998). A number of models have been proposed to describe the structure of these fibers and their main differences focuses on the organization and behavior of the linker DNA. Direct visualization of these fibers and the arrangement of individual nucleosomes and linker DNA in these folded states is extremely difficult although recent advances have allowed the visualization of single fibers (Cui & Bustamante, 2000). It appears that the 30 nm fiber is condensed fiber, highly compact with an irregular and uneven arrangement of nucleosomes that is organized three dimensionally (Zlatanova *et al.*, 1999; Daban, 2000; Cui & Bustamante, 2000).

'Higher order structures' (HOS), also require the presence of histone H1, and are even less well characterized than the 30 nm fiber. It appears that the 30 nm fiber is further condensed using loops, folds and anchored coils which help produce organized domains and structures within the genome (Paul & Ferl, 1999; Davie, 1995). The most universally accepted model is that the chromatin loops, which are 30-100 kb long during metaphase, are attached to a flexible nuclear matrix via DNA sequences referred to as the matrix or scaffold attachment regions or MARs/SARs (Paul & Ferl, 1999; Davie, 1995). These HOS are not just formed for packaging purposes however but may have a role in managing the functional organization of the chromatin (Cockell & Gasser, 1999).

## 1.3 Nucleosome Structure

The nucleosome is the most fundamental and basic unit of chromatin and is a highly conserved structure found in all eukaryotes. It is a repeating protein-DNA complex which consists of DNA wrapped around a histone protein complex. Chromatin organized into nucleosomes forms the 'beads on a string' construct visualized with electron microscopy. The length of DNA organized actually varies between 150-250 bp depending on both the organism being studied and the cell type from which the sample was derived.

The term "nucleosome" was first used to describe the approximately 200 bp of DNA wrapped around a histone octamer in 1974 (Kornberg). Digestion of chromatin by micrococcal nuclease (Mnase) results first in the removal of the 'linker' DNA connecting adjacent histone octamers while the 'core' DNA is protected by the histone proteins. If histone H1 is present, 168 bp of DNA is protected and the resulting structure is called the chromatosome (Simpson, 1978). Further digestion results in the release of histone H1 and the removal of an additional 20 bp of DNA. The resulting structure produced is the nucleosome core particle which consists of 146 bp of DNA wrapped around the core

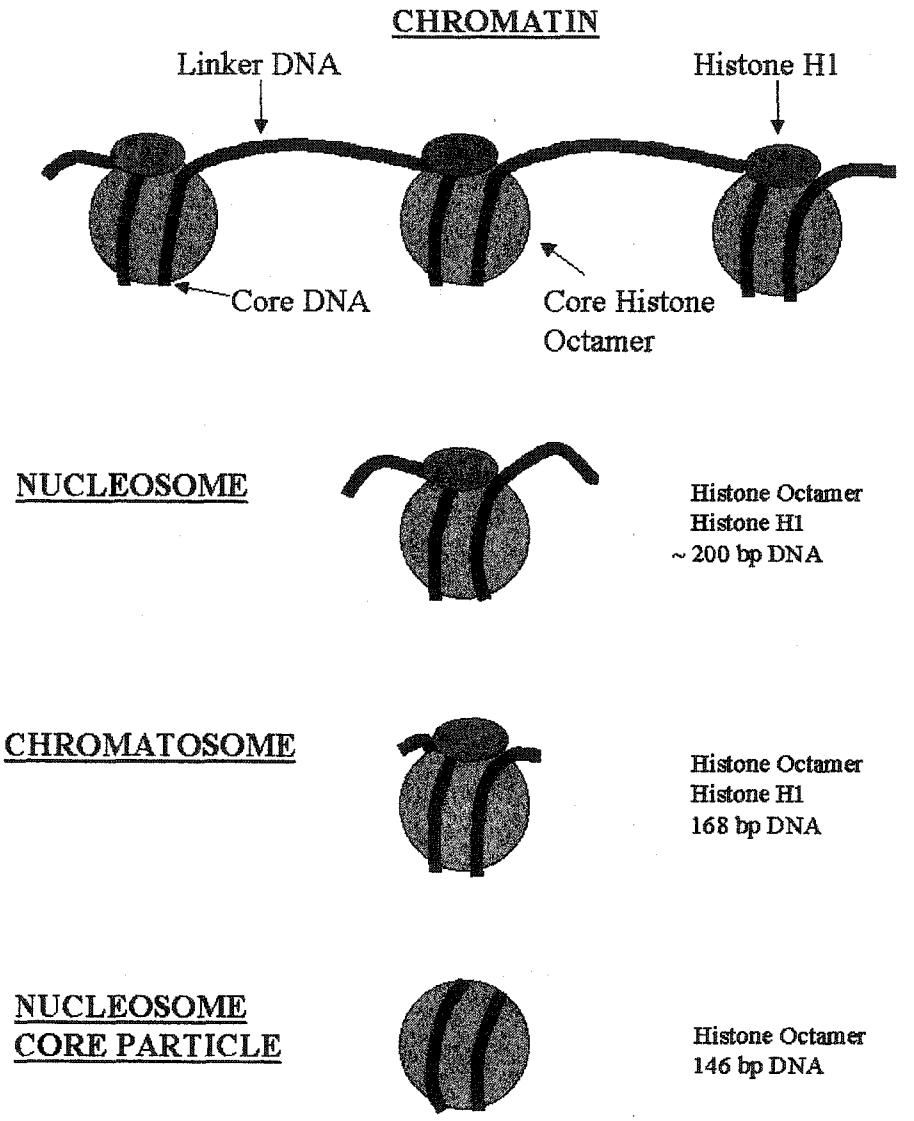


**Figure 1:** **Chromatin Digestion by Micrococcal Nuclease.** The large circle repesents the core histone octamer; the small oval is Histone H1 and the thick dark line is DNA

histone octamer. (Figure 1 shows a schematic representation of Mnase digestion of chromatin).

X-ray crystallography analysis has been used to define the histone-DNA and histone-histone interactions within the nucleosome. A low resolution structure (7 Å) first showed that the DNA wraps around the histone octamer approximately 1.75 times in a left handed superhelical turn (Richmond *et al.*, 1984). Recent studies of the histone octamer at 3.1 Å (Arents *et al.*, 1991) and the nucleosome at 2.8 Å and 3.1 Å (Luger *et al.*, 1997; White *et al.*, 2001; Luger & Richmond, 1998a; 1998b) have shown more clearly the structure of the nucleosome core particle. Such studies have shown that the DNA is not uniformly bent around the octamer and that the octamer contacts the DNA approximately every 10 bp where the DNA minor groove faces inward. The histone-DNA contacts are via electrostatic, hydrogen bonds, and non-polar bonds. The localization of the histone tails is difficult to establish because of their dynamic nature and their structural heterogeneity. While only about a third of the tail's structure has been visualized they are nevertheless capable of protruding or extending from the nucleosome either through or over the DNA gyres. For instance, the N-terminal tails of histone H3 and H2B both pass between the minor-groove channels. In addition it also appears that some of the tails are involved in nucleosome-nucleosome interactions, particularly histones H3 and H4. The accessibility of the histone tails also means that they are capable of being modified even while they are within the nucleosome core particle structure. Indeed it has become increasingly recognized that a key factor in chromatin dynamics is the effect of the histone tail post-translational modifications and several studies have shown that the histone tails are important for chromatin folding (Garcia-Ramirez *et al.*, 1992, Moore & Ausio, 1997).

### *1.3.1 Nucleosome Arrangement*

While histone complexes can show regular spacing in electron microscopy studies, nucleosome placement varies dramatically throughout the chromosome.

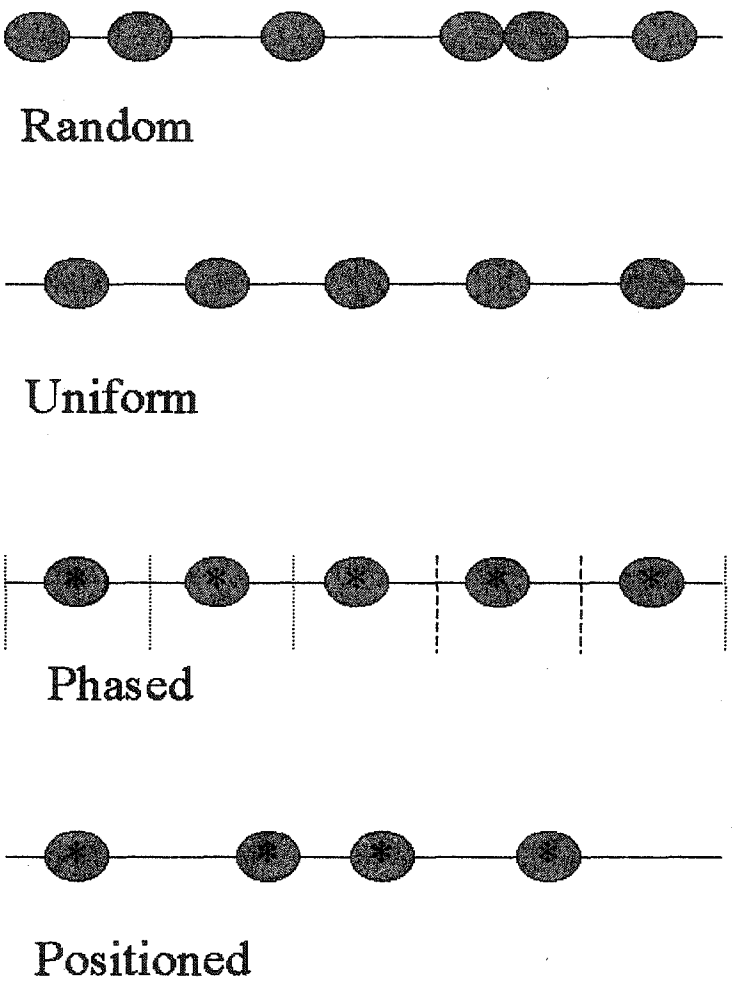


**Figure 2: Nucleosome Arrangements on Chromatin.** The ovals represent nucleosome core particles; the straight lines represent DNA; the vertical dashed lines indicate a repeated DNA sequence; and the asterix (*) indicates that the nucleosome is positioned on a specific DNA sequence. (Adapted from van Holde, 1989).

The terminology used to describe nucleosome arrangements can often be confusing however, the following series of definitions (van Holde, 1989) have been proposed (see Figure 2):

1. Random Nucleosome placement is entirely random and is not dependent on either the position of other nucleosomes or the DNA sequence.

2. Uniform Spacing: Nucleosome arrangement is not dependent on DNA sequence but adjacent nucleosomes are separated by uniform lengths of linker DNA.

3. Phased: Refers to the regular placement of nucleosomes on a repeating sequence of DNA, for example the 208-12 polynucleosome DNA template (see Section 2.11.1)

4. Positioned: Nucleosome placement is directly or indirectly determined by DNA sequence.

Nucleosome placement therefore is affected by a variety of factors. Naturally the DNA sequence itself will influence some positioning as will the presence of other DNA binding proteins which could prevent nucleosome formation. Nucleosomes may often have preferential sites within or near promoters and other regulatory elements (Thoma, 1992; Simpson, 1991). Indeed the nucleosome is becoming a "focal point of transcriptional control" (Kornberg & Lorch, 1999). Nucleosomes are considered to be general repressors as they prevent transcriptional initiation both *in vitro* (Lorch *et al.*, 1987) and *in vivo* (Han & Grunstein, 1988) by packaging promoters thereby making them inaccessible to the transcriptional machinery.

Another aspect of nucleosome positioning is the importance of chromatin remodeling complexes. These multiprotein, ATP-dependent complexes have the ability to change the arrangement of nucleosomes. There appear to be two basic types of complexes some of

# CHROMATIN REMODELING COMPLEXES

| **SWI/SNF GROUP** | Organism | ATPase | Number of Subunits |
|---|---|---|---|
| SWI/SNF (Switch/Sucrose Non-Fermenting) | *S. cerevisiae* | Swi2/Snf2 | 11 |
| RSC (Remodels the Structure of Chromatin) | *S. cerevisiae* | Sth1/Nsp1 | 15 |
| NURD (aka NuRD, NRD) | *H. sapiens* | CHD4 | 18 |
| Brahma | *D. melanogaster* | Brm | ~7-9 |
| **ISWI GROUP** | | | |
| NURF (Nucleosome Remodeling Factor) | *D. melanogaster* | ISWI | 4 |
| CHRAC (Chromatin Accessibility Complex) | *D. melanogaster* | ISWI | 5 |
| ISWI1 (Imitation Switch) | *S. cerevisiae* | ISWI1 | 4 |
| ISWI2 (Imitation Switch) | *S. cerevisiae* | ISWI2 | 2 |

**Table I: Chromatin Remodeling Complexes.** A partial list of known remodeling complexes compiled from a variety of sources including Lorch & Kornberg, 1999; Vignali *et al.*, 2000.

which are listed in Table I. First, the SWI/SNF (switch/sucrose non-fermenting) group of chromatin remodeling complexes appear to work by destabilizing the nucleosome and disrupting DNA-histone contacts therefore allowing the DNA to become more accessible (Kornberg & Lorch, 1999). Indeed one member of this group called RSC (remodels the structure of chromatin), is found in yeast (*Saccharomyces cerevisiae*) and can catalyze the transfer of the complete histone octamer (Lorch, *et al.*, 1999). The other group of complexes are the ISWI (or imitation switch) remodeling complexes which contain a distantly related ATPase called ISWI. These complexes are smaller and appear to redistribute nucleosomes creating nucleosome free regions by sliding octamers to adjacent positions (Hamiche *et al.*, 1999; Langst *et al.*, 1999). The exact mechanisms by which chromatin remodeling complexes operate have yet to be completely elucidated *in vitro* as well as *in vivo,* but it appears that the histone tails may prove to be important components of this process (Georgel *et al.*, 1997).

## 1.4 Histone Proteins

Histone proteins can be divided into two categories: the core histones (H2A, H2B, H3 and H4) which form the core histone octamer; and linker histones (H1) which are required for the formation of higher order chromatin folding. (Table II provides some basic information about the core histones.) These highly basic proteins contain relatively large amounts of positively charged lysine and arginine residues. The positive charges on the histones interact with the negatively charged phosphate backbone of DNA. Analysis of the sequences from many different organisms has shown that the histones are conserved proteins and some also have several variants. The linker histone H1 is the largest histone, shows the most diversity between organisms, is the least conserved with significant microheterogeneity in amino acid sequences (Ausio *et al.*, 2001; van Holde, 1989). In comparison histone H4 is the smallest histone (102 aa – calf thymus), and is the most conserved with 95% identity conserved across species (van Holde, 1989).

| Histone | No. of Residues (a.a.) | Mass (Da) | Acetylation Sites | Ubiquitination Sites |
|---|---|---|---|---|
| H4 | 102 | 11,236 | K5, K8, K12, K16 | None |
| H3 | 135 | 15,273 | K9, K14, K18, K23 | Unknown |
| H2A | 129 | 13,960 | K5 | K119 |
| H2B | 125 | 13,744 | K5, K10, K13, K28 | K120 |

**Table II:** **Characteristics of Calf Thymus Core Histones.**
(Compiled from van Holde, 1989.)

The general histone structure can be divided into two domains, the central core with its histone fold motif (described in more detail below) and the histone tails (See Figure 3). The tails account for approximately 25% of the total mass of the histones. All the core histones have N-terminal tails (see Figure 4) which range in size with H3>H2B>H4> H2A. Except for histone H3, the core histones also have a C-terminal tail (see Figure 5) particularly histones H2A and H2B while histone H4 which has a very small tail (Kornberg & Lorch, 1999).

The histone octamer has a tripartite structure with an $(H3\text{-}H4)_2$ tetramer located at the center of the core particle and also two flanking H2A-H2B dimers at the ends of the octamer (Arents *et al.*, 1991). Each of the histones also share a common structural motif called the histone fold (Arents *et al.*, 1995). The histone fold motif appears to be a widely conserved structure and has also been found in a variety of different proteins including Archaebacteria and transcription factors (Arents & Moudrianakis, 1995; Pereira & Reeve, 1998; Gangloff *et al.*, 2000).

The histone fold is an extended helix-loop and strand-helix domain which contains 3 α-helices. Helix I is approximately 11 residues long and is followed by a short loop and β-strand; Helix 2 is the longest helix which is approximately 27 residues and is followed by another short loop and β-strand; and lastly Helix 3 which is also approximately 11 residues. The histone fold is represented schematically in Figure 3 while Figure 6 highlights the actual residues involved.

The H3-H4 and H2A-H2B heterodimers are formed via their histone folds and they associate head to tail to form a compact handshake-like structure. Each of the H2A-H2B and H3-H4 heterodimers have three DNA binding sites therefore within the nucleosome the histone folds interact with 12 of the 14 possible minor groove sites and 121 bp of DNA (Luger & Richmond, 1998a). Gaps between the DNA gyres allow the N-terminal tails of histones H2B and H3 to pass through the DNA while the N-terminal tails of H2A and H4 and the C-terminal tail of H2A, extend outside the particle and across the face of the nucleosome. Thus the accessibility of some of the histone tails means they are

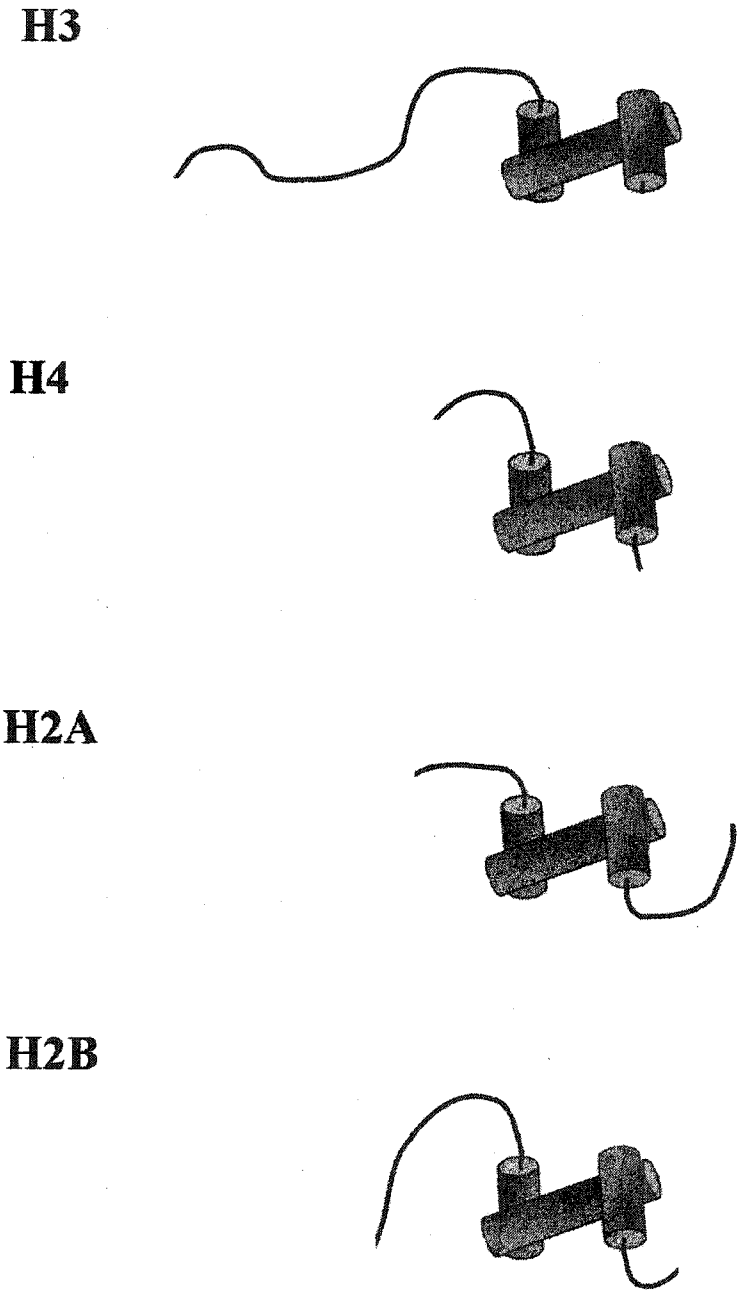


**Figure 3: Schematic Representation of the Core Histones and the Histone Fold Motif.** The four core histones are shown with the histone fold motif (in blue) and the approximate relative sizes of the different N- and C-terminal tails.

## H2A

```
1       5                   15
SGRGKQGGKARAKAK
      *
```

## H2B

```
1       5          12  15       20                              37
PEPAKSAPAPKKGSKKAVTKTQKKGDKKRKKSRKES
      *          *   *        *
```

## H3

```
1            9      14    18      23                              41
ARTKQTARKSTGGKAPRKQLATKAARKSAPATGGVKKPHRY
             *      *     *       *
```

## H4

```
1       5     8       12      16      20
SGRGKGGKGLGKGGAKRHRK
        *     *       *       *
```

**Figure 4: Core Histone N-Terminal Tail Sequences.** All sequences shown are for calf thymus histones (van Holde, 1989). The asterix (*) shows the acetylation sites.

**H2A**

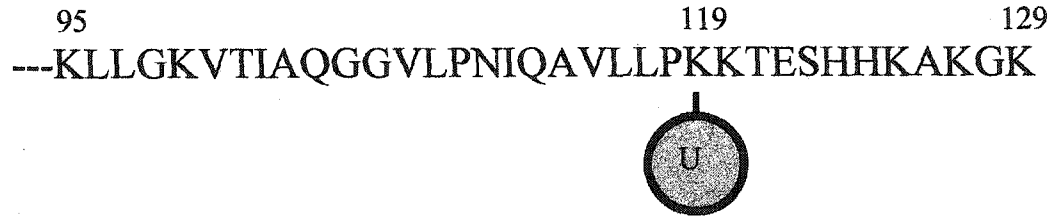


**H2B**

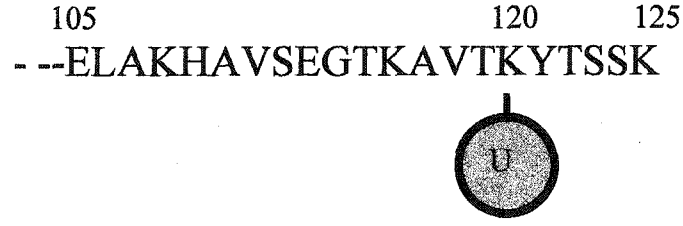


**H4**


**Figure 5: Core Histone C-Terminal Tail Sequences.** All sequences shown are for calf thymus histones (van Holde, 1989). The large circle (U) shows the ubiquitination sites.

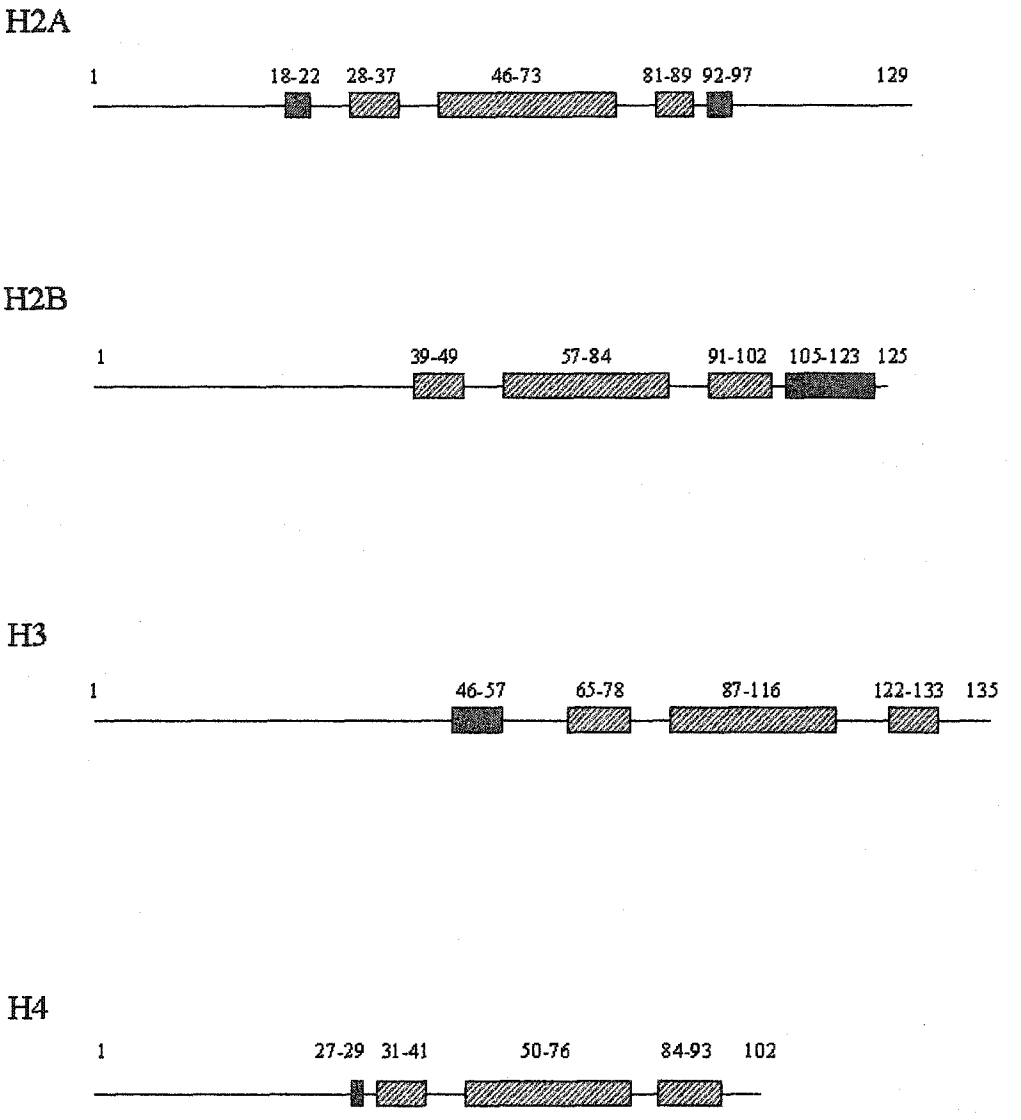


**Figure 6: Core Histone Sequences Forming the Histone Fold Motif.**
A schematic representation of the four core histones showing the histone fold helices (stripped boxes) and other helices (dark boxes) identified from crystal structure data. (Compiled from van Holde, 1989; Luger *et al.*, 1997)

capable of being modified within the nucleosome structure. Since the histone tails are important for fiber folding, interfiber interactions within higher order structures and may also act as recognition sites for recruiting remodeling complexes, it is important to understand the structural and functional impact of their post-translational modifications.

## 1.5 Histone Post-Translational Modifications

While histones are conserved proteins, they are also capable of being post-translationally modified. These modifications include acetylation, ADP-ribosylation, methylation, phosphorylation, and ubiquitination (van Holde, 1989; Ausio *et al.*, 2001; Davie & Spencer, 2001). Most of these variations occur within the N-terminal tails except for ubiquitination which occurs within the C-terminal tail. These modifications are thought to affect chromatin structure by altering histone-histone and histone-DNA interactions as well as interactions with other transacting protein factors. Indeed it has been proposed that modifications like acetylation may constitute a signal or language which is decoded and used by other proteins and/or complexes involved in chromatin remodeling and cellular processes like transcription (Strahl & Allis, 2000). The two modifications examined in this thesis were histone acetylation and ubiquitination which will be discussed below.

### *1.5.1 Acetylation*

Acetylation is the most studied of all the histone post-translational modifications. There are two types of acetylation reactions. The first is an irreversible acetylation reaction that occurs during the synthesis of some histones. In this type of reaction the N-terminal residues of histones H1, H2A, and H4 can be blocked by acetylation of the α-amino group of the N-terminal serine residues. The exact purpose, or role of this type of modification is not yet known. (Van Holde, 1989)

The second type of reaction is far more prevalent. It involves the addition of an acetyl group to the ε-amino group of specific lysine residues within the N-terminal tails of the core histone proteins and (Allfrey *et al.*, 1964). This type of acetylation is a highly

dynamic modification which is reversible and enzyme catalyzed. The reaction is controlled by two groups of enzymes: the histone acetyltransferases or HATs; and the histone deacetylases or HDACs and is shown schematically in Figure 7. While only lysine residues are acetylated, there are four acetylation sites on each of histones H4, H3 and H2B and one on histone H2A (see Figure 4 and Table II for acetylation sites). Consequently there are 26 potential acetylation sites which can be modified within the core octamer which introduces a tremendous amount of variability and creates a huge number of possible configurations.

The possible structural and functional implications of acetylation was recognized almost immediately, particularly with respect to its possible importance in eukaryotic gene transcription (Allfrey *et al.*, 1964). It has been speculated that the loss of positive charge, resulting from the acetylation of a lysine residue, would weaken the histone-DNA interactions. This in turn could produce a looser and more 'open' chromatin conformation which would assist transcription. Indeed acetylation has been correlated with transcriptional activity and a lack of acetylation is seen in inactive chromatin or heterochromatin. Interest in acetylation as a modulator of eukaryotic gene expression has soared in recent years because of the discovery that the HATs and HDACs are components of transcription complexes (Brownell *et al.*, 1996; Brownell & Allis, 1996; Spencer & Davie, 1999; Taunton *et al.*, 1996; Ng & Bird, 2000; Brown *et al.*, 2000). HAT activity has also been shown to be required for activation of genes *in vivo* (Kuo *et al.*, 1998; Krum *et al.*, 1998). Each HAT also appears to produce specific and distinct acetylation patterns which correspond to those seen *in vivo* (Schiltz *et al.*, 1999). This coupled with the apparent presence of multiple HATs in transcription complexes seem to confirm the suggestion that each HAT could have different substrate specificities and functions.

There is already evidence that specific histone acetylation sites have distinct functional/structural roles. For instance, in *Drosophila* the X-chromosome in male cells doubles its transcriptional activity as a form of dosage compensation. The acetylation of lysine 16 on histone H4 is a hallmark of this dosage compensation. The acetylase

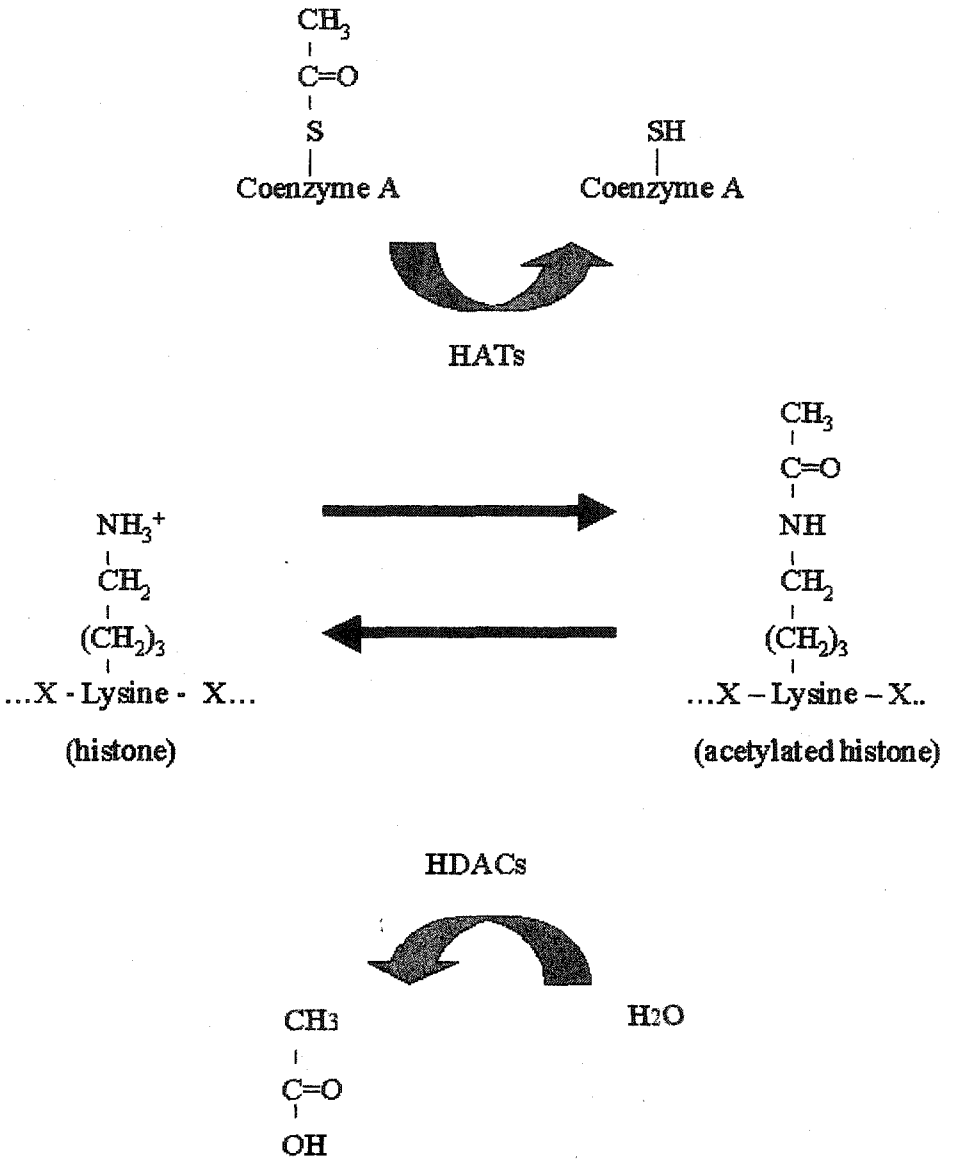


**Figure 7: Histone Acetylation/Deacetylation Reaction.**

responsible for the acetylation of lysine 16, called MOF (males absent on the first), is expressed in both sexes but only associates with the male X-chromosome and is a component of the dosage compensation complex (DCC) in *Drosophila* (Hilfiker *et al.*, 1997; Sterner & Berger, 2000; Turner *et al.*, 1992).

Examination of the structure/function relations of histone H4 lysine residues in yeast (*S. cerevisiae*) indicate that the effects are more complex. Genetic analysis of the four lysine residues (K5, K8, K12, & K16) subject to reversible acetylation in histone H4 have shown that together these lysines are essential as mutation of all four residues to arginine or aspartate was lethal, however no single residue was found to be essential (Megee *et al.*, 1990). If the lysines are mutated to glutamine, the strains were viable but exhibited several different phenotypes which involved mating defects, changes in the length of different stages of the cell cycle, and temperature sensitive growth. This indicates that the lysine residues and their acetylation may have roles in gene expression, replication and nuclear division (Megee, 1990).

In contrast the HDACs which deacetylate histones, are involved in the repression of transcription and in the production and maintenance of inactive DNA conformations. HDACs are components of repressor complexes and are associated with repressors and corepressors (Grunstein, 1997; Kornberg & Lorch, 1999; Ng & Bird, 2000). For example, the deacetylase HDAC1 associates with retinoblastoma protein (Rb) a known tumour suppressor. E2F transcription factors are required for that activation of specific genes which are required for S-phase entry. Rb antagonizes E2F transcription factors and silences these genes by binding to the E2F activation domain. Once bound it can interact with HDAC1 which in turn deacetylates the histones near the promoter helping to repress transcription and preventing gene activation. In many cancers Rb is mutated and is unable to bind E2F or HDAC1 therefore allowing transcription to occur (Brehm *et al.*, 1998; Managhi-Jaulin *et al.*, 1998). Histone acetylation levels therefore can modulate gene expression and have been linked to cancer (Archer & Hodin, 1999), indeed HDAC inhibitors are now being used as a cancer treatments (Conley *et al.*, 1998; Reik *et al.*, 2002).

Another form of negative regulation which involves HDACs is chromatin "silencing" or the formation of heterochromatin. In yeast, heterochromatin is formed at the HML and HMR silencing elements and the telomeres by interactions between the histone, Rap1 and the SIR (silent information regulator) proteins. After the initial binding of Rap1 to DNA, the SIR proteins assemble and these include Sir2, a histone deacetylase, and Sir3 and Sir4 which interact with the hypoacetylated N-terminal tails of histones H3 and H4 (Lewin, 1997; Hennig, 1999; Hecht *et al.*, 1994). The assembly of these proteins can exist over extended regions of DNA thereby preventing transcription.

To better understand how acetylation/deacetylation produces its functional effects, we need to understand the structural implications of this modification. While there are no known inhibitors or activators of acetylases which work *in vivo*, there are inhibitors of the deacetylases. The addition of sodium butyrate to cell cultures has been shown to inhibit the histone deacetylases and thereby lead to a rapid accumulation of hyperacetylated core histones (Boffa *et al.*, 1978). While this has allowed the production of large quantities of highly acetylated histones on demand, the exact structural role of acetylation has remained difficult to ascertain.

At the nucleosome level, the flanking DNA ends do indeed bind less tightly to the histones (Garcia-Ramirez *et al.*, 1995) and adopt a more stretched conformation which results in the acetylated nucleosome particles appearing more asymmetrical (Ausio *et al.*, 1986). While the loss of positive charge resulting from acetylation does allow some weakening of the histone tail interactions as ionic strength is increased (Mutskov 1998), under physiological conditions however, the histone tails remain bound to the nucleosome regardless of the acetylation level (Mustkov *et al.*, 1998; Garcia-Ramirez *et al.*, 1995). Likewise the evidence to support the idea that acetylation could facilitate transcription factor binding to nucleosomally organized DNA has been somewhat controversial (Lee *et al.*, 1993; Howe & Ausio, 1998). For instance, it has recently been shown that binding of the developmental transcription factor HNF3, which preferentially binds to nucleosomal DNA, is not affected by histone acetylation (Cirillo & Zaret, 1999).

The addition of butyrate and the resulting histone hyperacetylation in chromatin does not lead to a general activation of genes (Rubenstein *et al.*, 1979). It is also known that hyperacetylation of the 30nm fiber will not produce a 10 nm fiber (McGhee *et al.*, 1983; Wang *et al.*, 2001) Fibers without H1 do show an extended conformation (Garcia-Ramirez *et al.*, 1995) which has been shown to enhance transcription (Tse *et al.*, 1998). Also acetylation has been shown to maintain the unfolded nucleosome structure for transcription (Walia *et al.* 1998). However when H1 is present, histone acetylation does not appear to produce any significant structural effects on chromatin folding (McGhee *et al.*, 1983). However histone acetylation enhances the solubility of the chromatin fiber (Perry & Chalkley, 1982; Wang *et al.*, 2001).

Another idea recently proposed is that acetylation may act as a histone code (Strahl & Allis, 2000). In this regard, the tails of histone H3 and H4 have been shown to adopt a helical conformation in the nucleosomal DNA (Banares *et al.*, 1997), and their acetylation has been shown to increase their overall α-helical content (Prevelige and Fasman, 1987; Wang *et al.*, 2000). This could be important for protein-protein interactions between these tails and other proteins such as the chromatin remodeling complexes or trans-acting factors. Indeed, it has been recently observed that the histone H4 N-terminal tail plays a critical role in remodeling by ISWI (Clapier *et al.*, 2001). Certainly the specificity of the HATs and multiple acetylation sites could support this theory and may explain the localized and short range effects of acetylation. However there are few transacting factors that have been shown to require acetylation in order to interact with chromatin (Sewack *et al.*, 2001). It has also been demonstrated that acetylation occurs over long stretches of DNA (several kilobases) and this implies a more 'global effect' and argues against a coding hypothesis being the only structural role for acetylation (Vogelaur *et al.*, 2000; Litt *et al.*, 2001). The decrease in internucleosome and chromatin interfiber associations (resulting in an increase in solubility) may play an important role in facilitating the global structural processes involved in transcription initiation and elongation (Garcia-Ramirez *et al.*, 1995; Wang *et al.*, 2001).


**Figure 8:** **Ubiquitin Protein Structure.**

### 1.5.2 Ubiquitination

Ubiquitin is a 8.5 kDa, 76 amino acid protein that is highly conserved and is 'ubiquitously' distributed throughout eukaryotes. It is a globular protein in which residues 1-72 are tightly folded (Vijay-Kumar *et al.*, 1987). Its structure is shown in Figure 8. Ubiquitin attaches to histones via an isopeptide bond between the C-terminal glycine of ubiquitin and the ε-amino group of specific lysine residues. Ubiquitination is a reversible reaction catalyzed by a series of different enzymes (Hershko & Ciechanover, 1998; Pickart, 2001). Conjugation of ubiquitin first requires a single enzyme called the ubiquitin activating enzyme (Uba) or E1 which forms a ubiquitin-E1 thiol ester and then transfers ubiquitin to a member of the ubiquitin conjugating enzymes (Ubc's) or E2 enzymes. Although histone ubiquitination can occur with only the actions of E1 and E2 enzymes (Robzyk *et al.*, 2000), the majority of proteins which are ubiquitinated require an additional enzyme, a ubiquitin ligase or E3 enzyme. These E3 enzymes are highly specific and have multiple families. In contrast the removal of ubiquitin is catalyzed by isopeptidases or ubiquitin proteases (Ubp's) like Ubp3 in yeast (Moazed & Johnson, 1996.

While several E2s are capable of catalyzing the addition of ubiquitin to histones *in vitro* (Pickart & Vella, 1988; Haas *et al.*, 1988), only a few have been identified *in vivo*; for instance Rad6 which ubiquitinates uH2B in yeast (Robzyk *et al.*, 2000), and $TAF_{II}250$ which, in addition to being a coactivator and acetyltransferase, is also a H1 ubiquitin conjugating enzyme in *Drosophila* (Pham & Sauer, 2000).

While most ubiquitination occurs in the cytosol and is associated with proteolytic breakdown and degradation of proteins, histone ubiquitination is not associated with degradation. *In vivo* there appear to be four histones which are capable of being ubiquitinated: H3, H1, H2A and H2B; as well as some histone variants like H2A.Z, and H2A.X (Nickel *et al.*, 1987; Nickel *et al.*, 1989; Bonner, 1988; Chen *et al.*, 1998; Pham & Sauer, 2000). The ubiquitin ligation sites in both H1 and H3 have yet to be identified

and H3 has no apparent ligation points except in its N-terminal or central globular domains (Chen *et al.*, 1998).

By far the most prevalent ubiquitinated histones, and the most studied, are uH2A and uH2B. Indeed H2A, or A-24 as it was then referred to, was the first ubiquitinated protein to ever be identified. Both histones are reversibly ubiquitinated at highly conserved lysines within their C-terminal tails, specifically lysine 119 in H2A (Goldknopf & Busch, 1977) and lysine 120 in H2B (Thorne *et al.*, 1987) (see Figure 5). In higher eukaryotes approximately 5-15% of H2A and 1-2% of H2B are ubiquitinated. Histone ubiquitination does not appear to lead to increased turnover or degradation, indeed histones are conserved over long periods and ubiquitinated histone formation is not linked to DNA replication (Wu *et al.*, 1981). The ubiquitin moiety has a more rapid turnover than the H2A protein itself (Seale *et al.*, 1981) and it is in equilibrium with free ubiquitin within the nucleus (Wu *et al.*, 1981; Carlson & Rechsteiner, 1987).

The fact that mono-ubiquitination does not appear to result in increased histone degradation indicates that this modification must serve some other purpose. Comparison of the relative sizes of the ubiquitin and histone H2A (see Figure 9) indicate that ubiquitination introduces an extremely bulky adduct. Indeed ubiquitin is about 60% of the size of histone H2A. The C-terminal tail of H2A has been shown to extend beyond the core particle in a region close to the site where linker histones and the nucleosome interact (Usachenko *et al.*, 1994). It seems reasonable to assume therefore that such a large modification may have some sort of structural impact on H1 binding, nucleosome structure or chromatin folding.

There are a variety of studies which seem to support the premise that ubiquitination may either prevent chromatin folding or help maintain a more open chromatin conformation. For instance, highly condensed metaphasic chromatin does not appear to contain ubiquitinated histones (Matsui *et al.*, 1979; Mueller *et al.*, 1985). Also, ubiquitinated

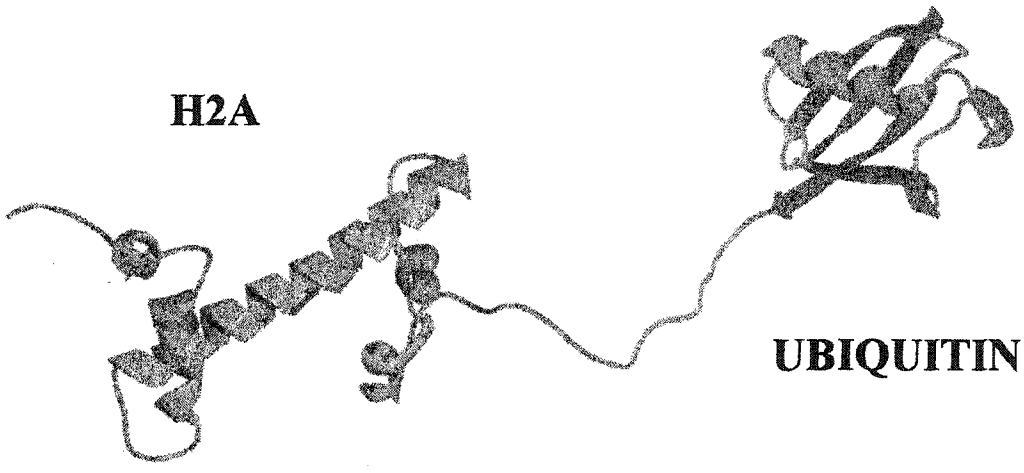


**Figure 9: Proposed Ubiquitinated H2A Structure.** This is a composite of the H2A and ubiquitin crystal structures joined at the appropriate residues.

histones are present at higher levels in chromatin which is depleted of the linker histones (Davie & Nickel, 1987). In yeast (*S. cerevisiae*) the deubiquitinating enzyme UBP3 interacts with Sir4, a protein involved in the *MAT* (mating type) silencing and heterochromatin formation (Moazed & Johnson, 1996).

Based on the crystal structure of the yeast nucleosome, ubiquitination of H2B has also been proposed to alter the internucleosomal contacts mediated by the H2B C-terminal tail (White *et al.*, 2001). The association of ubiquitinated histones, particularly H2B, with transcriptionally active DNA may also support the idea that ubiquitination helps maintain an open chromatin conformation indeed in some cell types the level of uH2B but not uH2A appears to be coupled to transcription (Davie & Murphy, 1990; 1994). Studies with *Tetrahymena* (Nickel *et al.*, 1989; Davie *et al.*, 1990) indicate that uH2B is preferentially located in the transcriptionally active DNA of the macronucleus.

Nevertheless, these observations are by no means universal. For instance uH2A does not appear to be directly coupled with transcription (Ericsson *et al.*, 1986) and other studies do not show correlations between ubiquitinated histones and transcriptional activation (Huang *et al.*, 1986). In addition, there is also physiological evidence which points to a possible role for ubiquitination in chromatin condensation. For instance, uH2A, which is found in the transcriptionally active macronucleus in *Tetrahymena*, is also present in the transcriptionally repressed chromatin of the micronucleus, though at much lower levels (Davie *et al.*, 1990; Nickel *et al.*, 1989). In addition uH2A has also been found in the sex body in mouse spermatids, another inactive heterochromatic structure (Baarends *et al.*, 1999). Studies looking at the distribution of ubiquitinated histones during spermatogenesis in vertebrates, a process in which chromatin undergoes a variety of conformational changes (Oliva & Dixon, 1991), indicate that in some organisms ubiquitinated histones may participate in the chromatin remodeling that occurs during the histone to protamine transition (Agell *et al.*, 1983; Baarends *et al.*, 1999). Since there is no transcription occurring at this time, such a role must be independent of transcription.

It seems probable from the physiological evidence that ubiquitinated histones may have multiple and possibly independent roles. In order to better understand these events it is important to accurately determine the structural impact of ubiquitinated histones on both nucleosome and chromatin dynamics.

Current crystal structures of nucleosome core particles have not included ubiquitinated and acetylated histones. The results from these structures (Luger *et al.*, 1997; White *et al.*, 2001) coupled with trypsin digestion experiments (Bohm *et al.*, 1980; 1982) show that the relative accessibility of the H2A and H2B C-terminal tails is distinctly different. Lysine 119 on H2A is easily accessible whereas lysine 120 on H2B is not. Figure 10 shows the proposed structure of a nucleosome containing two uH2A molecules as well as the indicating the position where ubiquitination of H2B would occur. The difference in accessibility could create differences in nucleosome structure resulting from ubiquitination but as yet no studies have confirmed this possibility.

There have been few studies examining nucleosome structure with or without uH2A or uH2B. Martinson *et al.* (1979) identified uH2A as an integral component of nucleosomes which apparently did not interfere with nucleosome formation. Early work by Kleinschmidt & Martinson (1981) showed that nucleosome particles could be reconstituted with two uH2A molecules without any apparent influence on particle structure or DNase I digestion. Davies and Lindsey (1994) confirmed these results and also showed that core particles with uH2B also appear to behave in a similar way. A preliminary paper on nucleosome arrays (Jason *et al.*, 2001) indicates that uH2A substantially decreases the solubility of the polynucleosome fibers without major effects on magnesium-dependent folding of the fiber.

It has also been proposed that ubiquitination may work synergistically with other histone modifications (Jason *et al.*, 2002) perhaps acetylation, as there is an overlap between histone acetylation and the presence of uH2A during spermatogenesis (Baarends *et al.*, 1999). It is also possible that ubiquitination of uH2A could interfere with histone H1

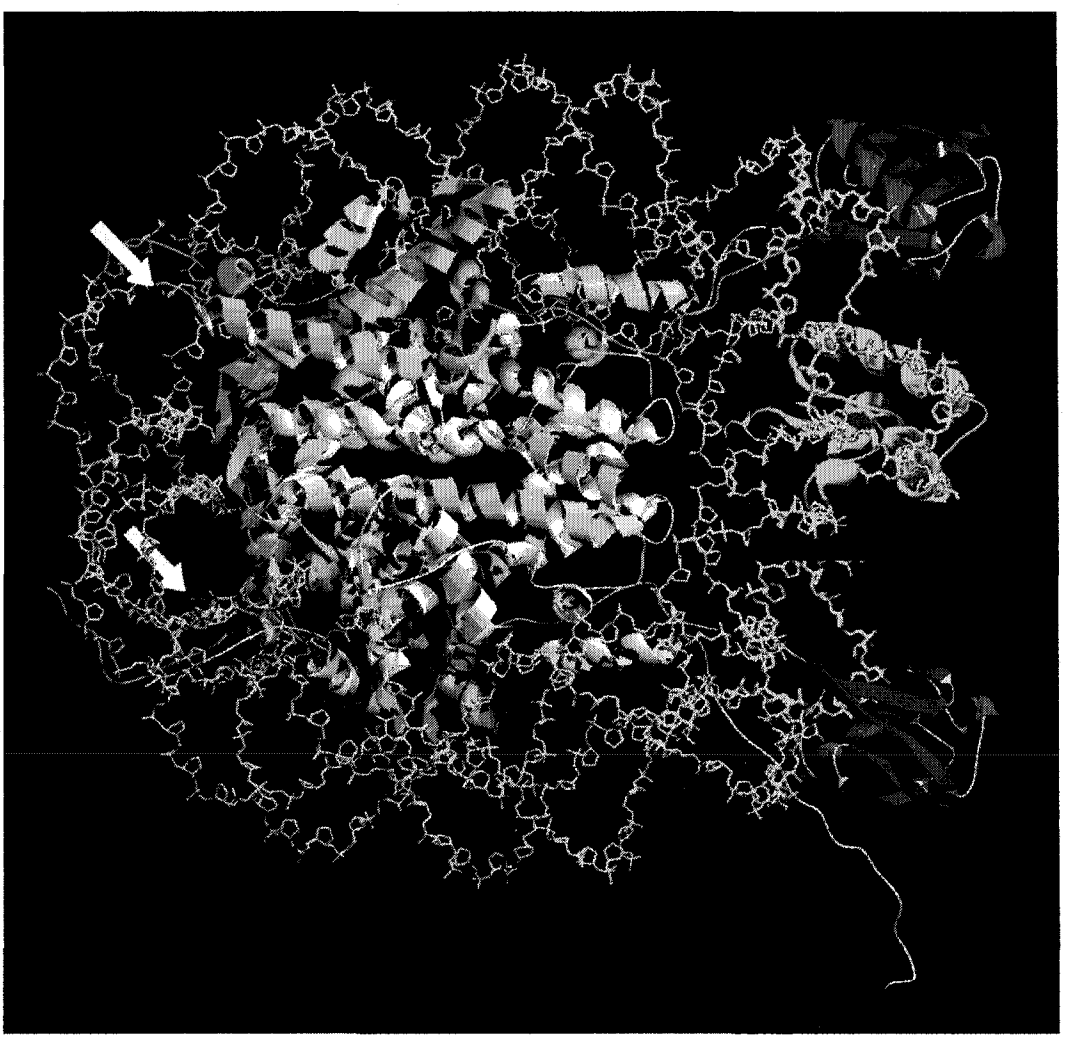

**Figure 10: Proposed Nucleosome Structure with Ubiquitinated H2A.**
H2A shown as gold colour; other core histones in grey; ubiquitin in red; DNA gyres in blue; histone H5 in green. The arrows point to the ubiquitin attachment sites for histone H2B. Nucleosome structure derived from Luger *et al.*, 1997.

binding and consequently affect higher order structures of chromatin. However this has yet to be determined and the exact role and molecular mechanisms involved in the modulation of chromatin structure and function induced from this posttranslational modification remains to be determined. Another proposal (Jason *et al.*, 2002) suggests that ubiquitination may act as a code which ultimately results in the structural modification of chromatin. Recent experiments in yeast seem to support this idea as histone H2B ubiquitinatin has been shown to be a requirement for methylation of specific lysines in histone H3 which in turn mediate gene silencing (Sun & Allis, 2002; Briggs *et al.*, 2002).

## 1.6 Objectives

There were multiple objectives which were undertaken during this thesis and they are listed as follows:

1. To create a method of producing native-like histone proteins from reverse-phase HPLC fractionated histones and determine if they could be used to reconstitute native-like nucleosomes.

2. To determine the importance of the histone tails in chromatin folding.

3. To examine the effects of histone acetylation and determine its impact on histone tail structure.

4. To examine the effects of histone ubiquitination on nucleosome and chromatin structure in both monovalent and divalent salt solutions.

# 2.0 MATERIALS AND METHODS

## 2.1 Sources of Histone Proteins

Histones were obtained from the cell nuclei from a variety of different sources and tissues. These included chicken erythrocytes, HeLa and CEL (chicken erythroleukemic) cell cultures, and solid tissues including calf thymus, and alligator (*Alligator mississipienis*) and lamprey (*Lampetra tridentatus*) testes. Each were obtained, maintained, processed and stored in slightly different ways as detailed below

### *2.1.1 HeLa Cells*

A HeLa cell S3 strain derived from a human cervical epithelioid carcinoma (American type Culture Collection - Rockville, Maryland) was used to produce both control and acetylated chromatin and histone proteins. All HeLa cells were grown in S-MEM media, a Joklik modified minimum essential medium, which was supplemented with sodium bicarbonate (2 g/L) and adjusted to pH 7.4 with 1 N sodium hydroxide. The media was filtered using a 0.45 μm bottle top filter and mixed with 1/10 volume of heat inactivated (56°C for 30 minutes) Newborn Bovine Calf Serum (NBCS) (Gibco-BRL - Burlington, Ont.) and 1/100 volume of PSN antibiotic (Gibco-BRL - Burlington, Ont.) before use, producing an end concentration of 0.05 mg/ml Penicillin, 0.05 mg/ml Streptomycin and 0.1 mg/ml of Neomycin. All media were stored at 4°C and prewarmed to 37°C prior to use. The NBCS and PSN were stored at -20°C and prewarmed to 37°C prior to their addition to S-MEM. If the S-MEM medium was not used within 14 days it was supplemented with 29.2 mg of L-glutamine per 100 mls of medium using a 100 x glutamine stock solution.

To start HeLa cell cultures, stock cultures frozen in liquid nitrogen were quickly thawed and the cells resuspended in 30 ml of prepared S-MEM medium and incubated at 37°C in

a 5% Carbon Dioxide ($CO_2$) air atmosphere for a minimum of 5 hours or overnight. The cell mixture was then transferred to a sterile 50 ml tube and spun at 125 x g for 10 minutes in a Beckman® Model TJ-6 Centrifuge (Beckman Instruments Inc. – Fullerton, CA). The cell pellet was then resuspended in 30 mls of fresh medium and transferred to a fresh culture flask. Cell growth was monitored using light microscopy to ensure cells were replicating normally and that the culture remained uncontaminated. New medium was added as required. Once the cells were confluent or near confluence the cultures were split into additional flasks. To split cultures the media was removed and usually discarded although it could also be centrifuged at 150 x g for 10 minutes to recover any cells in suspension. The cells adhering to the flask were rinsed gently with 5 mls of phosphate buffered saline solution (PBS) which was removed and discarded. Approximately 1 ml of 0.05% Trypsin – 0.53 mM EDTA solution (Gibco-BRL Products - Burlington, Ont.) was added to just cover the cells and were then incubated at 37°C for 2 to 5 minutes to allow the cells to loosen. Exposure time to the trypsin was minimized to prevent cell damage. The flasks were rapped sharply 2 to 3 times to detach the cells and 10 to 15 ml of fresh medium was added to help recover as many cells as possible. The cell culture was centrifuged at 150 x g for 5 to 10 minutes to pellet the cells. The supernatant was discarded and the pellets were resuspended in approximately 10 to 15 ml of fresh medium. After cell counts were done the cells were diluted and split into new culture flasks so that they were in approximately a 1:10 ratio.

Cell counts were performed to determine the viability of the cells, the total number of cells in solution, and the amount of dilution required. Cell counts were done using a mixture of 450 µl cell culture with 50 µl Trypan Blue (Gibco-BRL Products - Burlington, Ont.), which produces a dilution factor of 1.1 and an end concentration of 0.4% trypan blue. Trypan blue stains non-viable cells whereas healthy, viable cells remain clear. A drop of this mixture was placed on a hemocytometer under a coverslip and the average cell counts for several squares were taken. The number of cells per ml of medium equals the average cell count per square x $10^4$ x the dilution factor [i.e. cells/ml = avg. cell count/square x $10^4$ x 1.1]. To determine the total cells in solution the number of cells/ml is multiplied by the original culture volume [i.e. total # cells = (cells/ml) x volume]. The

percentage of cell viability equals the total viable cells divided by the total number of cell and multiplied by 100 [i.e. % viable cells = (viable cell/ total cells) x 100].

To maintain the stocks in storage, new stocks were produced by resuspending cells in 90% NBCS, 10% DMSO (Gibco-BRL Products - Burlington, Ont.) to obtain a concentration of 1 - 5 x $10^7$ cells/ml. Stocks were aliquoted into labelled cryogenic vials, placed overnight in a Nitrogen vapour phase and then stored in liquid Nitrogen.

Once sufficient cells were produced, the cells were resuspended in 200 ml of fresh medium and placed in a 1 liter culture flask so that the final concentration was approximately 1 x $10^5$ cells/ml. Once the cells were in suspension they no longer needed to be maintained in a 5% $CO_2$ air atmosphere and were incubated at 37°C in a Lab-Line Orbit Incubator Shaker Model 3595 (Labline Instruments Inc. - Melrose Park, IL) with gentle swirling. Cells were monitored and cell counts done every 24 to 48 hours and additional media was added as required up to a 1 liter volume. Once the cell concentration reached approximately 1-2 x $10^6$ cells/ml they were harvested and stored until required. To produce highly acetylated cells the cultures were incubated with 10 mM sodium butyrate (pH 7.2) for 20-22 hours prior to harvesting.

To harvest the cells the culture was centrifuged at 3800 x g in a Beckman® Model J2-21 centrifuge for approximately 10 minutes. The pelleted cells from the equivalent of 2 liters of cell culture were resuspended in 160 ml of 40% glycerol in S-MEM medium with or without 5 mM sodium butyrate. The solution was mixed gently via inversion until homogenous and then frozen and stored at -80°C until needed.

### *2.1.2 Chicken Erythroleukemic (CEL) Cells*

CEL cells (chicken erythroleukemic cells transformed by Marek's virus) were generously provided by Dr. Vaughn Jackson (Medical College of Wisconsin - Milwaukee, WI). Subcultures were started by thawing the frozen cells in a 37°C water bath. The cells were then pelleted by centrifugation at low speed, 150 x g, in a Beckman® Model TJ-6 Centrifuge (Beckman Instruments Inc. – Fullerton, CA). The cells were resuspended in

25 ml of 10% Fetal Bovine Calf Serum (FBS) in Dulbecco's Minimal Eagles Medium (DMEM) (Gibco-BRL Products - Burlington, Ont.) and then incubated overnight in a 5% $CO_2$ incubator. DMEM is supplemented with HEPES (4.7 g/litre), glutamine (0.29 g /litre), sodium bicarbonate (3.7 g/litre) and 1/100 volume of PSN antibiotics. After approximately one week the cells recovered and could be split into additional flasks.

The growth and condition of the cells was monitored using light microscropy. Cultures were grown and split until there was approximately 200 ml with a cell density of $10^6$ cells/ml. The cultures were then split two-fold with RPMI 1640 medium (Gibco-BRL Products - Burlington, Ont.) containing 5% bovine calf serum and 5% NBCS and supplemented with sodium bicarbonate (2.5 g/litre) and transferred to a 500 ml erlenmeyer tissue culture flask. Once in suspension the cells no longer need to be maintained in a 5% $CO_2$ atmosphere and were grown in a dry shaking incubator (Lab-Line Orbit Incubator Shaker Model No. 3595) at 37°C with gentle swirling. The cells were maintained in 5% FBS, and 5% NBCS in a 1:1 mixture of DMEM/RPMI 1640 media. Media was added as required and the cells were harvested once a cell density of 1-2 x $10^6$ cells/ml was obtained. If highly acetylated histones were required the cultures were incubated with 5 mM sodium butyrate for 20-22 hours prior to harvesting and the cells were kept in buffers containing 5 mM sodium butyrate during all subsequent procedures. To harvest the cells, the culture was centrifuged at 3800 x g in a Beckman® J2-21 centrifuge (Beckman Instruments Inc. - Fullerton, CA) for 10 minutes at 4°C. The cells were resuspended in a mixture of 40% glycerol in DMEM (+/- 5 mM sodium butyrate as required) at a concentration of 2 x $10^7$ cells/ml and stored at -80°C. Additional stock cultures were made by resuspending non-treated cells in a mixture of 10% DMSO and 10% FBS in DMEM at a concentration of 1-2 x $10^7$ cells/ml and storing at –80°C until required.

### *2.1.3 Chicken Erythrocytes*

Chicken blood was obtained from a commercial slaughter house (Lilydale, Victoria, B.C., Canada) and collected into 10% of its volume in Buffer I (0.15 M NaCl, 15 mM sodium citrate, 10 mM sodium phosphate (pH 7.2), 150 units of heparin/ml of total volume) and

stored on ice. The blood was processed immediately upon return to the lab and all solutions were kept on ice. The blood was filtered through several layers of cheesecloth presoaked in the Buffer I (without heparin) to remove any clotted or unwanted material and then centrifuged at 2000 x g at 4°C for 10 minutes in a Beckman® Model J2-21 centrifuge (Beckman Instruments Inc. – Fullerton, CA). The loose pellet of red blood cells (erythrocytes) was then resuspended in the same volume of Buffer I without heparin. At this point the cells were usually prepared for long-term storage by mixing the cell suspension with an equal volume of 80% glycerol and mixing gently by inversion until homogenous. The suspension was then aliquoted into sterile 50 ml tubes and stored at -80°C. Alternatively, all or part of the erythrocytes were processed using salt extraction of the cell nuclei.

### 2.1.4 Calf Thymus

Histones from calf thymus were a gift from Dr. George Lindsey's lab (University of Cape Town - Cape Town, South Africa) and were prepared in the following way. Calf thymus glands were provided by a local slaughter house and frozen at -80°C. After thawing the blood vessels, fat, and connective tissue were removed and the approximate volume was determined. The thymus was homogenized with a Waring Blender in 5 volumes of 0.14 M NaCl, 0.01 M tri-sodium citrate, 5 mM sodium bisulphite for two minutes. The homogenate was filtered through cheesecloth and centrifuged at 4°C for 10 minutes at 5000 x g. Using a Kinematica Polytron homogenizer, the pellet was rehomogenized in 5 volumes of buffer and centrifuged again. This was repeated four times. The pellet was then homogenized in 10 volumes of 0.4 N HCl to obtain the total acid-extracted histones. The mixture was centrifuged at 4°C for 15 minutes at 10,000 x g and the supernatant was dialyzed against several changes of deionized water and then lyophilized and stored at -20°C. The lyophilized histones were then shipped to Victoria and were stored at -80°C until needed.

### 2.1.5 Alligator and Lamprey Testes

Alligator testes (*Alligator mississipiensis*) were generously provided by Dr. Ruth M. Elsey from the Department of Wildlife and Fisheries at the Rockefeller Wildlife Refuge in Louisiana. Lamprey testes (*Lampetra tridentatus*) were provided by Dr. Harold Kasinsky from the Zoology Department of the University of British Columbia. Both samples were acid extracted in 0.4 N HCl.

The gonadal tissue was stored at either -70°C or at 4°C in 90% ethanol. The samples were homogenized using a Polytron homogenizer in 0.15 M NaCl, 10 mM Tris-HCl (pH 7.5), 0.5% Triton X-100 in the presence of 1/100 (v/v) Complete® Protease Inhibitor (Roche Applied Sciences - Laval, Que.) [Complete® Protease Inhibitor stock solution is made by dissolving 1 pill into 1 ml of sterile, distilled water.] The suspension was then centrifuged at 1500 x g using a Beckman® Model J2-21 centrifuge (Beckman Instruments Inc. – Fullerton, CA) at 4°C. The pellet obtained was resuspended in the same buffer without Triton (0.15 M NaCl, 10 mM Tris-HCl (pH 7.5)) and centrifuged again. The pellet was then resuspended in 0.4 N HCl and homogenized using 10 strokes in a Dounce homogenizer. The mixture was then centrifuged and the recovered supernatant was mixed with 6 volumes of acetone and stored overnight at -20°C to precipitate the histones. The mixture was centrifuged at 12,000 x g for 10 minutes in a Beckman® Model J2-21 centrifuge at 4°C. The pellet was then resuspended in acetone at 20°C and pelleted again using centrifugation. This was repeated twice and the final pellet was dried in a dessicator under vacuum and stored at -80°C until required.

# 2.2 Chromatin Preparation

## 2.2.1 Spectrophotometric Determination of Chromatin Concentration

Absorption measurements were determined on a Cary® 1 UV-Visible Spectrophotometer (Varian Inc. – Mississauga, Ont.) using 1 ml samples and quartz cuvettes. The absorption coefficient for DNA at 260nm ($A_{260}$) is 20 $cm^2mg^{-1}$ therefore an $A_{260}$ of 20 is equivalent to 1 mg/ml of double stranded oligonucleotides. Measurement of chromatin (DNA) concentration within unlysed cell nuclei required special procedures. Measurements were done using a 1/200 dilution of the cell nuclei in a mixture of water and SDS. Specifically 50 µl of the cell suspension was thoroughly mixed with 9.5 ml of distilled water after which 0.5 ml of a 10% SDS solution was added and the solution was mixed via inversion. DNA concentration was then determined using this mixture and adjusting for the dilution factor.

## 2.2.2 HeLa Cells- Salt Extraction of Cell Nuclei

Previously frozen cell cultures (usually the equivalent of 2 litres of harvested cells/container) were thawed and centrifuged at 3800 x g for 15 minutes at 4°C using a Beckman® Model J2-21 centrifuge (Beckman Instruments Inc. – Fullerton, CA) and a JA-14 rotor. The pellet was resuspended in 30 mls of Buffer A (0.25 M sucrose, 60 mM KCl, 15 mM NaCl, 10 mM MES (pH 6.5), 5 mM $MgCl_2$, 1 mM $CaCl_2$, 0.5% (w/v) Triton X-100, 0.1 mM PMSF) so there was approximately 5 ml/g of pellet. The mixture was split into two 30 ml tubes polycarbonate tubes and centrifuged at 3000 x g for 10 minutes at 4°C in a JA-20 rotor. This step was repeated 1-2 times using 15 ml of Buffer A per pellet. The pellets were then resuspended in a total of 15 to 20 ml of Buffer B (50 mM NaCl, 10 mM Pipes (pH 6.8), 5 mM $MgCl_2$, 1 mM $CaCl_2$, 0.1 mM PMSF) and centrifuged at 3000 x g for 10 minutes at 4°C. The pelleted cell nuclei were resuspended in approximately 10-15 ml total volume of Buffer B and the chromatin concentration was measured as outlined in Section 2.2.1. Once the concentration of this mixture was determined, the volume of the nuclear suspension was adjusted with Buffer B until the

DNA concentration was 20 mg/ml ($A_{260}$ = 40). The mixture was then prewarmed to 37°C in a Model 3545 Lab-Line Orbit Shaking water bath (Labline Instruments Inc. – Melrose Park, IL) and then digested with 50 units/ml of MNase (Worthington Biochemical Corp. - Freehold, NJ) for 5 minutes at 37°C. If shorter chromatin fragments were required, for instance nucleosome core particles, then the digestion was done using 60 units/ml MNase for 7 minutes. The digestion was stopped by bringing the mixture to 10 mM EDTA and storing on ice. The solution was centrifuged at 10,000 x g for 10 minutes at 4°C. The supernatant or SI fraction consists mainly of small chromatin fragments and mononucleosomes which have leaked out of the cell nucleus and contain hyperacetylated histones. The $A_{260}$ of the SI fraction was measured and 1/100 (v/v) of Complete® Protease Inhibitor (Roche Applied Science - Laval, Que.) was added prior to storage on ice at 4°C.

The pellet was then resuspended in 0.25 mM EDTA, 0.1 mM PMSF and stirred for 1 hour at 4°C in order to lyse the nuclear membranes. The mixture was centrifuged at 10,000 x g for 20 minutes at 4°C and the supernatant or SII fraction was collected and its concentration determined using $A_{260}$ measurements. A 1/100 (v/v) of Complete® Protease Inhibitor (Roche Applied Sciences - Laval, Que.) was added and the fraction was stored on ice at 4°C. The SII fraction is the fraction which contains the most chromatin and it is usually used to produce both nucleosome core particles and histones.

Additional histones can be extracted from the pellet by either acid extraction or via continued salt extraction with 0.6 M NaCl, 20 mM Tris-HCl (pH 7.5), 0.1 mM PMSF and then 2 M NaCl, 20 mM Tris-HCl, (pH 7.5). After each resuspension, the mixture is centrifuged at 10,000 x g for 15 minutes at 4°C, the supernatant is recovered, its $A_{260}$ measured, and the supernatant was brought to 1/100 (v/v) with Complete® Protease Inhibitor (Roche Applied Sciences - Laval, Que.) and stored on ice.

### 2.2.3 CEL Cells - Salt Extraction of Cell Nuclei

The procedure for the salt extraction of CEL cell nuclei follows the HeLa cell procedure (Section 2.2.2) until after the collection of the SI fraction. After collecting the SI fraction, the remaining pellets were resuspended in total of 15 ml of Buffer C (100 mM NaCl, 10 mM Pipes (pH 6.8), 5 mM $MgCl_2$, 1 mM $CaCl_2$ ). Chromatin extraction was done by pipetting up and down with a glass pipette and incubating on ice for 30 minutes with occasional mixing using a Vortex Genie 2 (VWR Canlab - Mississauga, Ont.). The mixture was then centrifuged at 4°C in a Beckman Model J2-21 Centrifuge (Beckman Instruments Inc. – Fullerton, CA) at 10,000 x g for 10 minutes. The supernatant (SII fraction) was recovered, its $A_{260}$ was measured, and then brought to 1/100 (v/v) with Complete® Protease Inhibitor (Roche Applied Science - Laval, Que.). The remaining pellet was resuspended in Buffer D (350 mM NaCl, 10 mM Tris-HCl (pH 7.5), 5 mM $MgCl_2$, 2 mM EGTA) plus 1/100(v/v) Complete® Protease Inhibitor (Roche Applied Science - Laval, Que.) by pipetting up and down and incubated on ice for 30 minutes. The mixture was centrifuged at 4°C for 10 minutes at 10,000 x g which produced a supernatant which is poorly acetylated. Additional histones can be recovered using either acid extraction (Section 2.5.3) or continued salt extraction as per the HeLa cell procedures (Section 2.2.2).

### 2.2.4 Chicken Erythrocytes - Salt Extraction of Cell Nuclei:

Fresh or previously frozen chicken erythrocytes in Buffer I without heparin (0.15 M NaCl, 15 mM sodium citrate, 10 mM sodium phosphate (pH 7.2), 0.1 mM PMSF) and 40% glycerol were centrifuged in a Beckman® J2-21 Centrifuge (Beckman Instruments Inc. – Fullerton, CA) at 4°C and 2000 x g for 15 minutes (usually 100 mls of frozen nuclei was split into 4 polycarbonate tubes). The supernatant was removed and the loose pellet was resuspended in Buffer I without heparin (0.15 M NaCl, 15 mM sodium citrate, 10 mM sodium phosphate (pH 7.2) 0.1 mM PMSF). The mixture was centrifuged at 2000 x g for 10 minutes, and the buffer decanted off. Each pellet (still fairly loose) was gently resuspended in approximately 25 mls of Buffer II with Triton (0.1 M KCl, 50 mM Tris-HCl (pH7.5), 1 mM $MgCl_2$, 0.5% (w/v) Triton X-100, 0.1 mM PMSF). After

incubating on ice for 10 minutes the mixture was centrifuged at 3500 x g for 5-10 minutes at 4°C. These steps were repeated 2-4 times until the pellet was a straw/white colour with no residual pink colour which would result if unlysed erythrocytes were still present. Each pellet was then resuspended in 25 ml of Buffer II without Triton (0.1 M KCl, 50 mM Tris-HCl (pH 7.5), 1 mM $MgCl_2$ and 0.1 mM PMSF) and centrifuged at 3500 x g for 5 minutes at 4°C. This step was repeated 1 or 2 times to remove the Triton X-100. Each pellet was then gently resuspended in approximately 3ml of Buffer III (0.1 M KCl, 50 mM Tris-HCl (pH 7.5), 1 mM $CaCl_2$, 0.1 mM PMSF). The total volume was measured, and the $A_{260}$ was determined using a 1/200 dilution (as per section 2.2.1). The volume of the sample was then adjusted with Buffer III until the concentration was 6 mg/ml ($A_{260}$ = 120).

The nuclear suspension was then digested with 9 units/ml of Mnase (Worthington Biochemical Corp. - Freehold, NJ) for 5 minutes at 37°C. If shorter chromatin fragments were required, digestion was done using 15 units/ml for 7 minutes at 37°C. To stop the reaction the solution was brought to 10 mM EDTA and kept on ice. The digest was centrifuged at 12,000 x g for 5 minutes at 4°C. The supernatant (SI fraction) was recovered and the $A_{260}$ was measured to determine the chromatin concentration and 1/100 (v/v) of Complete® Protease Inhibitor (Roche Applied Science - Laval, Que.) was added. The pellet was resuspended in 0.25 mM EDTA (pH 7.5) using half the previous volume and stirred at 4°C for 1 hour to lyse the nuclei. The mixture was then centrifuged at 8000 x g for 15-20 minutes at 4°C. The supernatant (SII fraction) was recovered, the $A_{260}$ was measured to determine the chromatin concentration and 1/100 (v/v) of Complete® Protease Inhibitor (Roche Applied Science - Laval, Que) was added. Additional histones could be recovered as described in Section 2.2.2.

### *2.2.4 Preparation of H1 Depleted Chromatin*

Chromatin prepared from the the salt extraction of cell nuclei is used for this procedure. The chromatin mixture was brought to 0.35 M NaCl by the addition of the appropriate volume of 4 M NaCl which was added dropwise with stirring. The H1 proteins were removed by the addition of CM Sephadex C-25 resin (Amersham Pharmacia Biotech –

Baie d'Urfé, Que.) using 12 mg resin/mg of DNA for chicken chromatin or 24 mg resin/mg of DNA for HeLa chromatin. Since the resin swells to 6 times its original volume when wet, the resin was preequilibrated with the appropriate buffer containing 0.35 M NaCl before the chromatin sample was added. The chromatin/resin mixture was gently tumbled for 2 hours at 4°C in a 50 ml sterile tube and then centrifuged at 4°C in a Beckman J2-21 Centrifuge (Beckman Instruments Inc. – Fullerton, CA) for 10 minutes at 3,000 x g to pellet the resin. This centrifugation was repeated if necessary to ensure no resin was retained in the supernatant. The supernatant containing H1 depleted chromatin was then collected and the loss of histone H1 was confirmed using SDS-PAGE (Section 2.13.2). The chromatin was then dialyzed versus 25 mM NaCl, 10 mM Tris-HCl (pH 7.5), 0.1 mM PMSF using Specta/Por® 3 (3500 MWCO) dialysis tubing (VWR Canlab – Mississauga, Ont.). After dialysis the solution is collected, its concentration was determined using $A_{260}$ measurements and then stored on ice. If no further digestions were required a 1/100 (v/v) of Complete® Protease Inhibitor (Roche Applied Science – Laval, Que.) was added to the solution.

## 2.3 Nucleosome Core Particle Preparation

Nucleosome core particles (mononucleosomes) were prepared from H1 depleted chromatin from the SI or SII fractions of salt extracted cell nuclei and Figure 11 shows a simplified schematic of this process. The H1-depleted chromatin fraction was usually dialyzed overnight versus 25 mM NaCl, 10 mM Tris-HCl (pH 7.5) and 1 mM $CaCl_2$ at 4°C using Spectra/Por® 3 (3500 MWCO) dialysis tubing (VWR Canlab – Mississauga, Ont.). However they could also be brought to 1 mM $CaCl_2$ without further dialysis if the chromatin was already in the appropriate buffer. The chromatin mixture was prewarmed to 37°C and digested with 30 units of MNase (Worthington Biochemical Corp. – Freehold, NJ) per mg of chromatin for 12 minutes at 37°C with gentle swirling Model 3545 Lab-Line Orbit shaking waterbath (Lab-Line Instruments Inc. – Melrose Park, IL). The solution was brought to 10 mM EDTA and put on ice to stop the reaction.

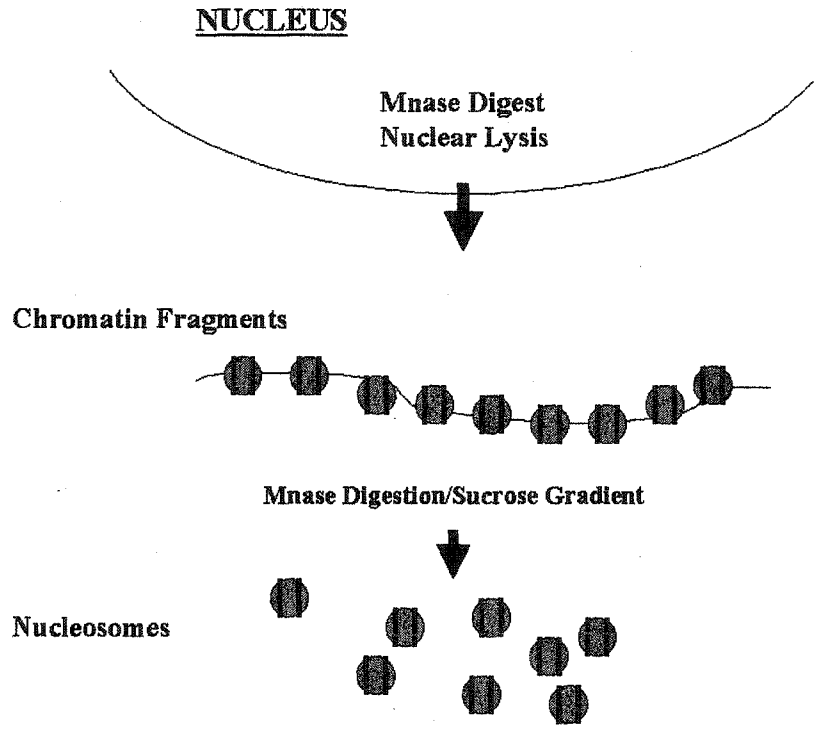


**Figure 11: Schematic of Nucleosome Core Particle Production.**

The mononucleosomes were then separated from oligonucleosomes and other chromatin fragments using a sucrose gradient. If necessary the chromatin solution was first concentrated with a Centriprep 50 (Millipore Amicon – Bedford, MA) to reduce the volume loaded onto the gradient. A 5% to 20% (w/v) linear sucrose gradient in 25 mM NaCl, 10 mM Tris-HCl (pH 7.5), 1 mM EDTA was prepared in Nalgene thin-wall ultratube SW-28 tubes (Nalge Nunc International – Lynwood, WA) using a BRL Gradient Former (Gibco BRL – Burlington, Ont.). These tubes hold a total volume of 38 mls of which a maximum of 3 mls would consist of the sample loaded onto the top of the preformed gradient. Smaller quantities could also be fractionated using Nalgene thin-wall ultratube SW-41 tubes (Nalge Nunc International – Lynwood, WA) which hold a total of 11 mls of which 1 ml would be sample. All solutions, containers and samples were kept on ice at all times. Once the gradient was formed the samples were carefully loaded on top of the gradient using a pasteur pipette. Opposite tubes were balanced to within 0.005 g using sample buffer only. SW-28 tubes were centrifuged in either a Beckman® L8-70M Ultracentrifuge or a Beckman® L5-65 Ultracentrifuge (Beckman Instruments Inc. – Fullerton, CA) using a SW-28 Ti swing bucket rotor at 82,000 x g for 24 hours at 4°C or at 100,000 x g for 20 hours at 4°C. SW-41 tubes were centrifuged in a SW-41 Ti swing bucket rotor at 125,000 x g for 17 hours at 4°C. Centrifugation was stopped without braking.

The resulting sucrose gradients were carefully placed on ice and 1 ml fractions were collected from the bottom of the gradient using an autoclaved glass capillary tube and a BioRad Model 2110 fraction collector (Bio-Rad Laboratories – Hercules, CA) with a Pharmacia Peristaltic pump (Amersham Pharmacia Biotech – Baie d'Urfé, Que.) set at 1 ml/min. The presence of nucleosomes in the fractions was determined using $A_{260}$ measurements of a 1/200 dilution (in water) of the different fractions. The results were confirmed using 4% Native (non-denaturing) polyacrylamide gel electrophoresis (PAGE) (see Section 2.13.5) to determine which peaks were mono-, di-, tri- and oligo-nucleosomes. Fractions containing nucleosome core particles were combined and the sucrose was removed by dialysis versus 10 mM Tris-HCl (pH 7.5), 1 mM EDTA

(or 25 mM NaCl, 10 mM Tris-HCl (pH 7.5), 0.5 mM EDTA) at 4°C overnight using Spectra/Por® 3 (3500 MWCO) dialysis membrane (VWR Canlab – Mississauga, Ont.). The mononucleosomes were then collected, their concentration determined using $A_{260}$ measurements and 1/100 (v/v) Complete® Protease Inhibitor (RocheApplied Science – Laval, Que.) was added prior to storage on ice at 4°C.

## 2.4 Oligonucleosome/Chromatosome Preparation

Oligonucleosomes such as di-, tri-, and tetra-nucleosome particles and also chromatosomes (a core histone particle with 168 bp DNA) were produced both with or without H1 following similar procedures as for the production of nucleosome core particles. The size of the particles required determined the duration of the MNase digestion so that the larger the particle the less MNase and shorter digestion times were required. Digestion times were determined using pilot digestions and the results confirmed with 4% Native PAGE (Section 2.13.5).

After the main digestion, the different sized particles were separated on a sucrose gradient using 5% and 30% sucrose in 25 mM NaCl, 10 mM Tris-HCl (pH 7.5), 1 mM EDTA and processed as per Section 2.3. The $A_{260}$ of a 1/200 dilution (in water) of the collected fractions was determined and those containing the appropriate sized particles were confirmed using 4% Native PAGE. The relevant fractions were combined, and the sucrose removed using dialysis versus 100 mM NaCl, 20 mM Tris-HCl (pH7.5), 0.5 mM EDTA.

# 2.5 Core Histone Octamer Preparation

## 2.5.1 Spectrophotometric Determination of Histone Protein Concentration

To determine the concentration of histone proteins the absorption of histone solutions was measured at 230 nm. Absorption measurements ($A_{230}$) were done using either a Cary® 1 UV-Visible Spectrophotometer (Varian Inc. – Mississauga, Ont.) using 1 ml samples and quartz cuvettes; or a Beckman® Du-65 Spectrophotometer (Beckman Instruments Inc. – Fullerton, CA) using 100 µl samples and quartz cuvettes. At 230 nm the histone extinction coefficient is 4.3 $cm^2mg^{-1}$ (Stein, 1979).

## 2.5.2 Hydroxyapatite Column Chromatography

Hydroxyapatite (HTP) column chromatography can be used to obtain core histones from chromatin samples containing or depleted of histone H1 and from nucleosome core particles derived from the salt extraction of cell nuclei. The procedure varies slightly depending on the sample used. A fresh 1.5 cm x 15cm hydroxyapatite column (Bio-Gel® HTP, DNA grade; Bio-Rad Laboratories – Hercules, CA) was prepared and equilibrated with 0.1 M potassium phosphate (pH 6.8) at a flow rate of 8 to 10 ml/hour. Nucleosome core particles or H1-depleted chromatin (usually 8 to 20 mg) were loaded onto the column at a flow rate of 5 to 8 ml/hour. In this type of chromatography, the sample volume is not critical and relatively large volumes can be loaded. The column is then run with two bed volumes of 0.1 M potassium phosphate (pH 6.8) buffer. The total core histones from samples without H1 can be eluted from the column with a buffer of 2 M NaCl in 0.1 M potassium phosphate (pH 6.8) buffer. For chromatin samples containing H1, the sample was loaded as above and the column was run with 0.35 M NaCl in 0.1 M potassium phosphate (pH 6.8) buffer for several hours to elute the H1 histone. Removal of H1 can be confirmed by $A_{230}$ measurements and SDS-PAGE of the eluted fractions. After H1 is removed, the total core histones can be obtained by elution with 2 M NaCl in 0.1 M potassium phosphate (pH 6.8) buffer. Generally fractions of

1 to 2 ml were collected and the presence of histones was determined by $A_{230}$ measurements and confirmed with SDS-PAGE. Combined fractions were dialyzed at 4°C versus several changes of distilled water using Spectra/Por® 3 (3500 MWCO) dialysis tubing (VWR Canlab – Mississauga, Ont.). The histones were collected, their concentration determined using $A_{230}$ measurements, and then lyophilized using a VirTis Sentry Condenser Vacuum Lyophilizer (Canberra Packard Canada – Mississauga, Ont.), and stored at -20°C or -80°C until needed.

### 2.5.3 Acid Extraction

Acid extraction can be used to remove histones from many different types of samples and tissues. This method extracts total histones, not just core histones, and therefore depending on the sample being used, histone H1 will also be extracted.

For soluble chromatin samples (e.g. SI, SII fractions) the solution was brought to 0.4 N HCl by the addition of an equal volume of 0.8 N HCl and stirred for 1 hour at 4°C. The mixture was centrifuged at 4°C in either a Beckman J2-21 Centrifuge (Beckman Instruments Inc. – Fullerton, CA) or a Eppendorf 5415C Microcentrifuge at 12,000 x g for 10 minutes. The supernatant containing the histones was retained and the histones were precipitated using 6 volumes of acetone and kept at -20°C for a minimum of 1 hour. The tubes were then centrifuged at 12,000 x g for 15 minutes at 4°C. The acetone was removed via aspiration and the histones were dried in a Jouan RC 10-10 Centrifugal Evaporator (Canberra Packard Canada – Mississauga, Ont.). The dried histones were then stored at -20°C until required.

Histones could also be acid extracted from the pellets produced during the salt extraction of cell nuclei. The pellet was mixed with one volume of 0.4 N HCl. The histones were extracted using 10-15 strokes in a Dounce homogenizer. The mixture was centrifuged at 12,000 x g for 10 minutes at 4°C. The supernatant containing the histones was retained and the histones were precipitated by adding 1 ml of cold acetone (4°C) for every 250 ul of supernatant. The mixture was stored at -20°C for a minimum of 1 hour and then

centrifuged at 12,000 x g for 10 minutes at 4°C to precipitate the histones which were then dried and stored at -20°C.

The procedures used to acid extract solid samples depends greatly on the sample tissue being used. The acid extraction procedure for calf thymus tissue is detailed in Section 2.1.4. The procedures for acid extraction of testes samples from alligator (*Alligator mississipienis*) and lamprey (*Lampetra tridentatus*) were previously described in Section 2.1.5.

## 2.6 Fractionation and Separation of Histones

The complete separation of individual core histones can be done using a variety of methods which depends on how the histones were first prepared. For instance, acid extracted histones must be processed differently than salt extracted samples because they may contain histone H1 and they have already been purified from DNA so hydroxyapatite chromatography can not be used. Generally the two methods used to separate the histones were liquid column chromatography and high performance liquid chromatography (HPLC).

### *2.6.1 Liquid Column Chromatography*

For samples derived from the salt extraction of cell nuclei such as chromatin (with or without H1) or nucleosome core particles (control, acetylated, trypsinized or ubiquitinated) the first step in fractionating histones was hydroxyapatite (HTP) column chromatography.

The sample was loaded a freshly prepared 1.5 cm x 15 cm HTP column (Bio-Gel HTP, DNA grade; Bio-Rad Laboratories – Hercules, CA) equilibrated with 0.1 M potassium phosphate (pH 6.8) at 5 to 8 ml/hour. If H1 was present, it was selectively eluted first by running the column (usually overnight) with 0.35 M NaCl in 0.1 M potassium phosphate (pH 6.8) buffer. Once eluted the H1 histones were recovered via dialysis versus several

changes of distilled water at 4°C using Spectra/por® 3 (3500 MWCO) dialysis tubing (VWR Canlab – Mississauga, Ont.) and then lyophilized and stored at -20°C until required.

The core histones were then separated into H2A-H2B and H3-H4 histones by elution with a salt gradient in the 0.1 M potassium phosphate (pH 6.8) buffer. The gradient can be 0 to 2 M NaCl or 0.4 to 2 M NaCl depending on whether the starting chromatin sample contained histone H1 or not. After the sample was loaded, several bed volumes of the first buffer is allowed to run through the column to remove any unbound sample. For a 1.5 cm x 15 cm column run at 5 to 8 ml/hour and loaded with approximately 10 to 15 mgs of sample, a gradient was formed with 80 mls of each buffer using a Series 1200 Gradient Former (Gibco BRL – Burlington, Ont.). One ml samples were collected and $A_{230}$ measurements were used to determine which fractions contained histones. Figure 12 shows a typical elution profile. The first peak eluted at around 0.8 M NaCl and contained histones H2A and H2B while the second peak eluted at around 1.2 M NaCl and contained histones H3 and H4. The linearity of the salt gradient was confirmed by measurement of the refractive index of the fractions using a Carl Zeiss Jena Refractometer. SDS-PAGE confirmed the presence and type of the histones present, however high concentrations of salt can interfere in electrolysis, therefore the histones were precipitated prior to SDS-PAGE using trichloroacetic acid (TCA) precipitation as outlined in Sections 2.13.1 and 2.13.2. The relevant fractions were then combined and dialyzed versus several changes of distilled water using Spectra/Por® 3 (3500 MWCO) dialysis tubing (VWR Canlab – Mississauga, Ont.) at 4°C. The concentration of the different histone peaks was determined using $A_{230}$ measurements and the histones were lyophilized and stored at -20°C until required.

To separate H2A from H2B or H3 from H4, the lyophilized histones were redissolved in 2 to 3 ml of 8 M urea (Ultrapure® Urea from ICN Biomedicals – Costa Mesa, CA), 4% β-mercaptoethanol and incubated at room temperature for 30-60 minutes. A 1.5 cm x 114 cm P60 (Bio-Rad Laboratories – Hercules, CA) (100-200 mesh) gel filtration column was prepared and equilibrated at 8 to 10 ml/hour with a 20 mM HCl, 50 mM NaCl buffer.

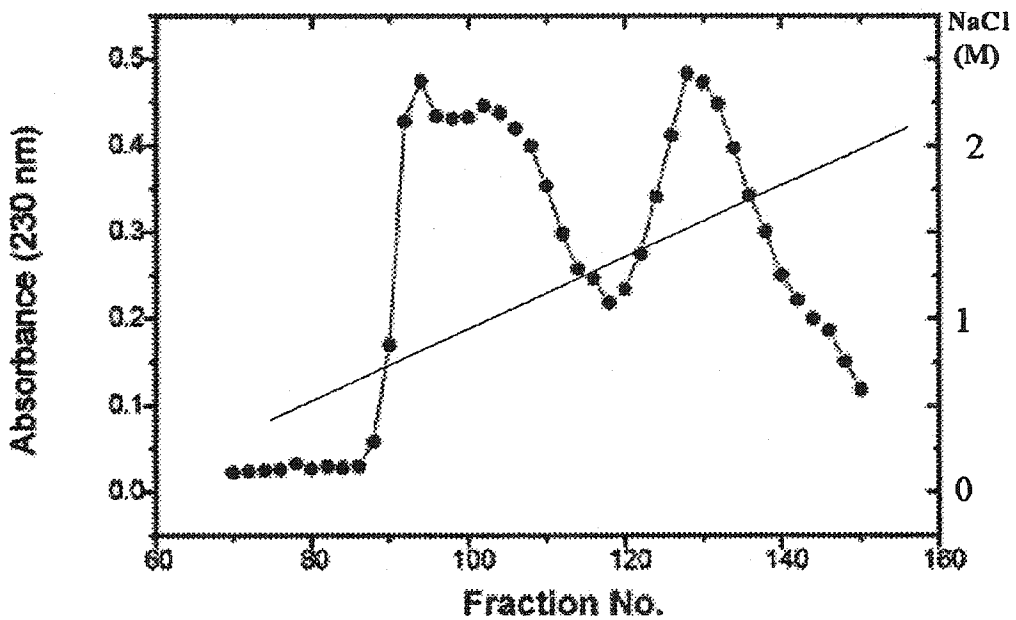


**Figure 12: Histone Elution Profile from a HTP Column.** A 1.5 x 15 cm HTP column was loaded with 15 mg of the SII fraction from the salt extracted, hyperacetylated HeLa cell chromatin. Histones were eluted with a 0 to 2 M NaCl gradient in potassium phosphate buffer (pH 6.8) with the gradient shown as the line overlaying the profile. Two ml fractions were collected and $A_{230}$ measurements were taken to determine histone presence. The first peak contains H2A/H2B; the second H3/H4 as confirmed by SDS-PAGE.

The sample was loaded onto the column and 1-2 ml fractions were collected at 5 ml/hour using the same buffer. The $A_{230}$ of the fractions was measured to determine the presence of histones and aliquots were run on SDS-PAGE to determine the type and purity of the histones present. Purified fractions were combined, dialyzed against several changes of distilled water, collected, the concentration determined using $A_{230}$ measurements, quick frozen in liquid nitrogren, lyophilized and stored at -20°C until needed.

### 2.6.2 Acid Extracted Histones

Since acid extracted histones can not be separated into H2A/H2B and H3/H4 peaks using HTP column chromatography, fractionation requires a slightly different procedure. The acid extracted histones (with or without H1) were first separated using gel filtration on a 2.5 cm x 95 cm P60 column (Bio-Rad Laboratories – Hercules, CA). The column had been previously equilibrated at 15 ml/hour with 20 mM HCl, 50 mM NaCl buffer. The lyophilized histones (70-90 mg) were resuspended in 3 ml of 8 M urea, 4% β-mercaptoethanol for 30-60 minutes and then loaded onto the gel. The column was then run at 12 ml/hour with the 20 mM HCl, 50 mM NaCl buffer while 3 ml fractions were collected. Histone presence was determined using $A_{230}$ measurements and SDS-PAGE. This system usually separated the histones into an H1 peak (if present) which tended to overlap slightly with a H2B/H3 peak which merged into a H2B/H3 peak and lastly and H4 peak. H4 and H1 were the only histones which were purified at this point and any purified fractions were dialyzed versus water, aliquoted, lyophilized and stored at -20°C. The H2B/H3 or H2A/H3 mixtures were run separately on a 1.5 cm x 114 cm Sephadex G100 (Amersham Pharmacia Biotech - Baie d'Urfé, Que.) size exclusion column previously equilibrated at 8 to 10 ml/hour with 20 mM HCl, 50 mM Tris-HCl (pH7.5). The lyophilized samples were resuspended in a maximum 2 ml of 8 M urea, 4% β-mercaptoethanol and incubated at room temperature for 30-60 minutes and loaded onto the column. The histones were eluted at 5 ml/hour using the 20 mM HCl, 50 mM NaCl buffer and 1 ml fractions were collected. One peak was usually produced with a trailing tail end, with histone H3 being eluted at the beginning and H2A at the end of the peak as confirmed by SDS-PAGE. Purified histones were usually obtained after a second

separation on this column and were dialyzed versus distilled water, quantified, aliquoted, lyophilized and stored until required.

### *2.6.3 Purification of Histones using HPLC*

Salt or acid-extracted histones from different sources were dissolved in 1 ml of HPLC grade 25% (v/v) acetonitrile (ACN), 1% (v/v) trifluoroacetic acid (TFA). For preparative purposes usually 5 to 10 mg of histones were injected onto a 25 cm x 1 cm C4 or C18 Vydac (Hesparia, CA) column (300 Å pore size, 5 μm particle size) and eluted at 3 ml/min using an ACN gradient and monitoring at 230 nm. Generally, the acetonitrile gradient parameters were as follows: 25% ACN for 5 minutes; 25-37% over 15 minutes; 37-49% over 110 minutes; 49-80% over 10 minutes; 80-80% for 5 minutes and 80-0% over 10 minutes. Smaller sample sizes (500 μg to 1 mg) and columns (25 cm x 0.45 cm C18 Vydac (Hesperia, CA) column - 300 Å pore size, 5 μm particle size) were used for analytical purposes and were eluted using the same gradient conditions at 1 ml/minute. Aliquots from the different peaks were dried using a Jouan RC 10.10 Centrifugal Evaporator (Canberra Packard Canada – Mississauga, Ont.) and then resuspended for SDS-PAGE to confirm histone identity and purity. Once the identity of the different histones was confirmed, the HPLC samples were lyophilized and stored at -80°C until required.

#### 2.6.3.1 Renaturation of RP-HPLC separated histones

Lyophilized RP-HPLC purified histone fractions were resuspended at 2 mg/ml in 6 M guanidium hydrochloride, 20 mM β-mercaptoethanol, 50 mM Tris-HCl (pH 7.5) and incubated for 30 minutes at room temperature. The sample was then dialyzed against distilled water (2 liters/ml of sample) for 1 hour at 4°C using Spectra/por® 3 (3500 MWCO) dialysis tubing (VWR Canlab – Mississauga, Ont.). The histones were then renatured by dialysis overnight at 4°C versus 2 litres of 2M NaCl, 50 mM Tris-HCl (pH 7.5), 1 mM EDTA, 1 mM DTT. At this point the histones could be used for reconstitution experiments or stored at -20°C or -80°C after dialysis against water and lyophilization.

## 2.7 Trypsinized Histones

Treatment of nucleosomes with trypsin will remove both the C- and N-terminal domains of the core histones. To prevent overdigestion, an immobilized trypsin rather than soluble a trypsin enzyme was used. Two types of immobilized typsin were used, the first was trypsin bound to DITC glass beads (Sigma Aldrich – Oakville, Ont.). An enzyme to substrate ratio (E:S) of 50:1 was used (i.e. 50 mg of immobilized trypsin: 1 mg DNA). The trypsin beads were equilibrated for 1 hour at room temperature in 20 µl of 25 mM NaCl, 10 mM Tris-HCl (pH 7.5) buffer per mg of trypsin. The supernatant was removed after centrifugation at 800 x g in a Eppendorf Model 5415C Microcentrifuge for 30 seconds. The core nucleosomes were digested at room temperature with mild rotary shaking. The length of digestion was determined by pilot time course digestion monitored by SDS-PAGE. Generally the nucleosomes were incubated for 90 minutes with rotation at room temperature. The reaction was stopped by centrifuging the mixture at 800 x g for 30 seconds at 4°C to pellet the trypsin beads. The supernatant was retained and digestion confirmed using SDS-PAGE.

Alternatively, L-1-tosylamido-2-phenylethyl chloromethyl ketone-treated trypsin immobilized on beaded agarose (Pierce – Rockford, IL) was also used. The beads come in a suspension of 200 units/ml. The trypsin suspension was equilibrated by washing with 3 volumes of 25 mM NaCl, 10 mM Tris-HCl (pH 7.5) buffer and centrifuging at 800 x g for 30 seconds and discarding the supernatant. This was repeated a total of 5 times. After the last wash, the nucleosomes in 25 mM NaCl, 10 mM Tris-HCl (pH 7.5) were added to the trypsin pellet at an enzyme to substrate ratio of 50:1. The mixture was tumbled for 50-60 minutes at room temperature. The immobilized trypsin was then removed by centrifugation at 800 x g for 30 seconds and the recovered supernatant containing the trypsinized nucleosomes was brought to 1:100 (v/v) with Complete® Protease Inhibitor (Roche Applied Science – Laval, Que.) and stored on ice. Trypsinized histones were purified from the trypsinized nucleosomes by HTP column chromatography as detailed previously (2.6.1).

# 2.8 Acetylated Histones

## 2.8.1 Cell Cultures

Acetylated histones were usually produced using either CEL or HeLa cell lines. Prior to harvesting, the cell cultures were grown to an approximate density of 1 to 2 x $10^6$ cells/ml and then incubated in the presence of 10 mM sodium butyrate for 20-22 hours before harvesting. Chromatin and nucleosome core particles were produced using salt extraction of cell nuclei (see Sections 2.2.2 or 2.2.3) and histones were purified using hydroxyapatite chromatography (see Section 2.6.1). The key modification was that all buffers used in the salt extraction, sucrose gradients and the hydroxyapatite column chromatography also contained 10 mM sodium butyrate.

## 2.8.2 Acetylated Histone H4 Tails

Acetylated nucleosomes produced from the salt extracted cell nuclei of CEL cultured cells were loaded onto a HTP column and the H2A-H2B and H3-H4 histones were eluted using a 0.4 to 2.0 M NaCl gradient in 0.1 M potassium phosphate (pH 6.8). The H3-H4 peak was collected, combined, dialyzed against water, lyophilized and stored at -20°C. The H4 histones were then purified from H3 using reverse-phase HPLC. The histones were resuspended in water and 1% TFA and loaded onto a 1.0 cm x 25 cm Vydac C4 (5 μm) column (Vydac – Hesperia, CA) column and the histones were eluted with a 0 - 60% acetonitrile gradient in 175 minutes in 0.1% TFA at a flow rate of 2 ml/min. The peak containing acetylated H4 (as verified by SDS-PAGE) was collected and lyophilized.

Purified acetylated H4 was used to obtain the mono-,di-, tri-, and tetra-acetylated histone tails, while the non- and mono-acetylated tails were generally obtained from purified control H4 histones. The H4 histones were digested with Asp-N, an endoproteinase (Roche Applied Science – Laval, Que.), in either 100 mM ammonium bicarbonate (pH 8.0) or in 50 mM Tris-HCl (pH 6.0) at room temperature using an enzyme to substrate ratio of 1:1500 (w/w). Asp-N cleaves histone H4 on the N-terminal side of

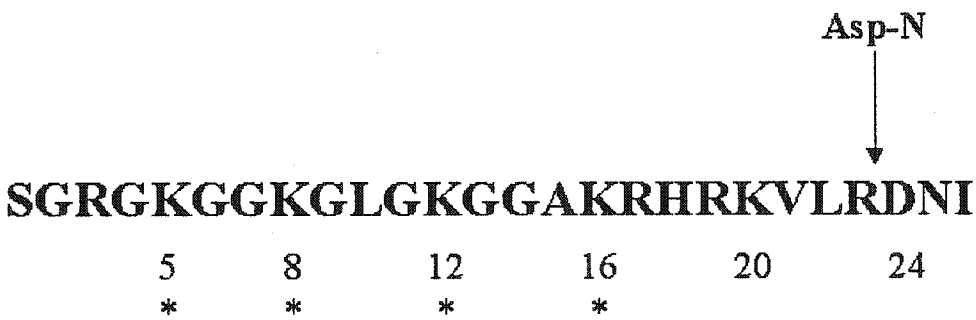


**Figure 13:** **Asp-N Cut Site on Histone H4 N-Terminal Tail.**
Histone acetylation sites indicated by asterix (*).

aspartic acid (D) with differing specificity depending on pH. Figure 13 shows the Asp-N cut site on the histone H4 N-terminal tail. The digested sample was then loaded on a RP-HPLC 0.46 x 25 cm Vydac C18 column (5 μm) (Vydac - Hesperia, CA) and eluted with a linear acetonitrile gradient in 0.1% TFA at a flow rate of 1 ml/min. The gradient was as follows: 0.1% TFA for 10 minutes; 0-10% ACN over 10 minutes; 10–25% over 60 minutes; 25-80% over 10 minutes; 80% for 5 minutes; 80-0% over 5 minutes. Fractions containing the differently acetylated H4 tails were identified and confirmed using SDS-PAGE. The purified tails were then lyophilized and stored until required.

## 2.9 Ubiquitinated Histones

Attempts were made to purify ubiquitinated histones from both HeLa cell nuclear extracts and chicken erythrocytes using both column chromatography and RP-HPLC. However the quantities obtained were too small for experimental purposes and large scale purification using these techniques would have been prohibitively expensive. Consequently ubiquitinated histones were purified using liquid column chromatography of large quantities of acid extracted histones obtained from calf thymus tissue.

Approximately 280 to 315 mg of lyophilized calf thymus histones were resuspended in 5 ml of 8 M urea (Ultrapure® Urea; ICN Biomedicals – Costa Mesa, CA), 4% β-mercaptoethanol, and incubated at room temperature for 60 minutes. Histones were then separated using a 4.1 cm x 120 cm Bio-Gel® P60 column (100-200 mesh) (Bio-Rad Laboratories –Hercules, CA) run with 20 mM HCl, 50 mM NaCl buffer at 40 ml/hour at room temperature and collecting 1 fraction every 9 minutes. Fractions enriched in uH2A (or uH2B) were determined using SDS-PAGE and western blotting. The relevant fractions were combined, dialyzed versus water and lyophilized.

Lyophilized samples from three such Bio-Gel® P60 columns were combined and dissolved in 10 ml of 6 M urea, 50 mM sodium acetate (pH 5.4) and incubated for 60 minutes at room temperature. The sample was then run on a 1.5 cm x 16.5 cm Whatman CM-52 cellulose (Fisher Scientific – Napean, Ont.) ion exchange column

equilibrated with 50 mM NaCl, 50 mM sodium acetate (pH 5.4), 6 M urea at room temperature. The histones were eluted with a linear gradient of increasing salt concentration which was created with a Series 1220 Gradient Former (Gibco BRL – Burlington, Ont.) using 160 mls each of 110 mM NaCl or 175 mM NaCl in 6 M urea, 50 mM sodium acetate (pH 5.4). The buffers were brought to pH 5.4 with HCl. The column was run at 15 ml/hour, and 4 fractions/hour were collected at room temperature. Fractions containing uH2A (or uH2B) were verified using SDS-PAGE and western blotting, and were combined, dialyzed versus water and lyophilized.

Lyophilized samples from the CM-52 column were then resuspended in 5 ml of deionized 8 M urea, 2 mM Tris-HCl (pH 7.5), 10% (v/v) β-mercaptoethanol. The deionized sample buffer was made by mixing 10 ml of buffer with 0.25 g of analytical grade mixed bead resin AG®501-X8(D) (20-50 mesh) (Bio-Rad Laboratories – Hercules, CA) and incubating with vigourous shaking at room temperature for 1 hour. Half the buffer (5 mls) was mixed with the sample which was then incubated at room temperature for 1 hour, and then 3 hours at 4°C. The mixture was brought to pH 2.2 with 1.2 N HCl and was centrifuged at 12,000 x g in a Beckman Model J2-21 centrifuge (Beckman Instruments Inc. – Fullerton, CA) at 4°C for 10 minutes to pellet the resin. The supernatant was recovered and loaded onto a 2.5 cm x 120 cm Bio-Gel® P60 column (Bio-Rad Laboratories –Hercules, CA) which was run at room temperature at 5 ml/hour using a fully deionized 7 M urea, 2 mM Tris-HCl (pH 2.2) buffer and collecting 4 fractions/hour. This column had to be run continuously to prevent the column from plugging therefore several samples were usually run sequentially to maximize efficiency. The elution of pure uH2A (or uH2B) was determined using SDS-PAGE and western blotting (Section 2.14.3). Purified samples were dialyzed versus water and lyophilized until needed. Samples still containing a mixture were usually recombined and rerun on the column.

## 2.10 DNA Preparation – General Procedures

The general procedures for plasmid transformation into competent cells, plasmid amplification and growth, DNA precipitation, and determination of DNA concentration are outlined below followed by the specific procedures for the preparation of specific sized DNA fragments.

### *2.10.1 Spectrophotometric Determination of DNA Concentration*

Absorption measurements were determined on a Cary® 1 UV-Visible Spectrophotometer (Varian Inc. – Mississauga, Ont.) using 1 ml samples and quartz cuvettes. Smaller samples were measured on a Beckman® DU-65 Spectrometer using 100 µl samples and quartz cuvettes. An absorption coefficient for DNA at 260nm ($A_{260}$) is 20 $cm^2mg^{-1}$ therefore an $A_{260}$ of 20 is equivalent to 1 mg/ml of double stranded polynucleotides.

### *2.10.2 Preparation of Competent Cells*

Using strict sterile technique, an overnight culture of *E. coli* strain JM109 cells in 5 ml of LB broth (10 g bacto™tryptone, 5 g bacto™-yeast extract, 10 g NaCl in 1 litre of water and autoclaved) [bacto™ = trademark or Becton Dickinson & Company – Sparks, MD] was grown at 37°C without ampicillin. Next day, 500 µl of the culture was added to 50 ml of LB broth and grown with shaking at 37°C for approximately 2 hours until the $A_{260}$ was between 0.4 and 0.6. The culture was then centrifuged at 4°C in a Beckman Model J2-21 Centrifuge (Beckman Instruments Inc. – Fullerton, CA) at 1500 x g for 10 minutes after which the supernatant was removed. The pelleted cells were resuspended in a total of 25 ml of cold 50 mM $CaCl_2$ and incubated on ice for 20 minutes. The mixture was spun at 3000 x g, 4°C for 10 minutes and the supernatant was removed. The pellet was resuspended in a total volume of 3-5 ml total in 50 mM $CaCl_2$, 15% (w/v) glycerol and incubated on ice for 3 hours after gentle mixing by inversion. The cells were then stored in 200 µl aliquots at -70°C until required.

### 2.10.3 Transformation of Competent Cells

Plasmid DNA was mixed with a 200 µl aliquot of quickly thawed competent cells in a 1.5 ml microfuge tube. Since the cells are very fragile, a wide bore pipet tip was used to allow gentle mixing. The mixture was incubated on ice for 30 minutes then heated at 42°C for 90 seconds and immediately put on ice for 1 minute. Next 500 µl of LB broth was added and the mixture was incubated at 37°C for 45 minutes. A 100 µl aliquot was plated onto an LB plate (2.5 bacto™-tryptone, 1.25 g bacto™-yeast extract, 2.5 g NaCl, 2.5 g Agar in 250 mls water, autoclaved; bacto™ = trademark of Becton Dickinson & Company – Sparks, MD) containing appropriate antibiotics and any other reagents required for screening purposes (for instance: if using a bluescript plasmid then both X-Gal and IPTG (Gibco BRL – Burlington, Ont.) are added to allow for blue/white screening). The remaining mixture was spun at 1300 x g for 3 minutes in an Eppendorf Model 5415C Microcentrifuge. Most of the supernatant was discarded and the pellet was resuspended in any residual supernatant and streaked onto LB plates with appropriate antibiotics. The plates were grown overnight at 37°C, and positive colonies were individually selected and grown overnight in 5 mls of LB broth with 0.05 µg/µl penicillin. Mini-plasmid preps were done to ensure that the plasmid with the correct insert was present and bacterial stocks were made by mixing 500 ml of culture with 200 µl of 80% glycerol and stored at -80°C.

### 2.10.4 Small-Scale Plasmid Preparation (Miniplasmid Preps)

Bacterial stocks transformed with plasmid were streaked onto LB plates with 0.05 µg/ul penicillin and grown overnight at 37°C. A single bacterial colony was selected and grown in 5 ml of LB medium with 0.05 mg/ml penicillin in a Lab-Line Orbit Shaking Water Bath Model 3545 (Labline Instruments Inc. – Melrose Park, IL) overnight at 37°C. The bacterial mixture was transferred into a 1.5 ml microfuge tube and centrifuged at 12,000 x g for 30 seconds at 4°C in an Eppendorf Model 5415C Microcentrifuge. The supernatant was removed and each pellet was resuspended in 100 µl of ice-cold 50 mM glucose, 25 mM Tris-HCl (pH 8.0), 10 mM EDTA (pH 8.0) and mixed vigorously. Next

200 µl of freshly prepared 0.2 N NaOH, 1% SDS was added to each tube and mixed via inversion and incubated on ice for 10 minutes. Next 150 µl of ice cold 3 M sodium acetate (pH 4.8) was added, mixed via inversion and incubated on ice for 3-5 minutes. The mixture was centrifuged at 12,000 x g for 5 minutes at 4°C. The supernatant was transferred to a fresh tube and 5 µl of RNase A (DNase free) (Roche Applied Science – Laval, Que.) was added and incubated for 30 minutes at 37°C. The DNA was precipitated with 2 volumes of cold 95% ethanol, mixed and stored at –20 °C (or -80°C) for a minimum of 15 minutes. The precipitated DNA was pelleted by centrifuging 12,000 x g for 5 minutes at 4°C. The supernatant was removed and the pellet washed with cold 70% ethanol. The ethanol was removed and the pellet dried in a Jouan RC 10-10 Centrifugal Evaporator (Canberra Packard Canada – Mississauga, Ont.) for 10 minutes. The pellet was redissolved in 20 µl of water and then analyzed, for instance, with restriction enzyme digestion to ensure that the proper sized insert was present.

### 2.10.5 Large Scale Plasmid Preparation

Once it was determined using mini-plasmid preps that the stock cultures were not contaminated and that they contained the proper plasmid and insert, a large scale plasmid prep was done to amplify and purify sufficient quantities of the DNA fragments necessary for future reconstitution experiments.

As with the mini-prep protocol, stocks were streaked onto LB plates and some of the resulting colonies were then innoculated into 5ml cultures and grown overnight. Each 5 ml culture was then innoculated into 500 ml of LB broth with 0.05 mg/ml Penicillin in a Fernbach flask and grown overnight at 37°C in a Lab-Line Orbit Incubator Shaker No. 3595 (Lab-Line Instrument Inc. - Melrose Park, IL). During harvesting and processing, the cells were kept on ice unless stated otherwise. Cells were centrifuged at 3800 x g in a Beckman® Model J2-21 Centrifuge (Beckman Instruments Inc. – Fullerton, CA) for 15 minutes at 4°C. Each pellet was resuspended in 10 ml of ice cold lysis buffer (25 mM Tris-HCl (pH7.5), 10 mM EDTA, 15% (w/v) sucrose, 3 mg/ml lysozyme) and incubated on ice 20 minutes. The solution was transfered to six 30 ml polycarbonate tubes and 13.3 ml of freshly prepared 0.2 M NaOH, 1% SDS was added to each tube and mixed

quickly and vigorously by inversion. The solution was incubated on ice for approximately 10 minutes until solutions were clear. After lysis, 8.3 ml of 3 M sodium acetate (pH 4.8) was added to each tube, mixed gently by inversion and incubated on ice 20 minutes. The tubes were centrifuged at 12,000 x g for 20 minutes at 4°C. To remove any solid material, the mixture was strained through several layers cheesecloth presoaked in 0.3 M sodium acetate (pH 4.8) and the volume was recorded. The solution was warmed to 37°C, and 200 µg of RNase A (DNase free) (Roche Applied Science – Laval, Que.) was added. The solution was incubated at 37°C for 1 hour and then cooled to room temperature. Next, 0.6 volumes of isopropanol was added, mixed via inversion, and incubated at room temperature for 10 minutes. The solution was centrifuged at 12,000 x g for 15 minutes at 4°C. The supernatant was removed and the pellet dried in a vacuum dessicator for approximately 10 minutes. Each pellet was then redissolved in 10 ml of water. Proteins were removed using phenol:choloroform extraction and the DNA was ethanol precipitated at -80°C.

### 2.10.6 Phenol:Chloroform Extraction of Proteins

Unwanted proteins, enzymes for instance, can be removed from DNA/protein mixtures using phenol extraction. An equal volume of 25:24:1 (v/v/v) of phenol: chloroform: isoamyl alcohol was added to an aqueous DNA solution and vigorously mixed until emulsified. The solution is then centrifuged at 1600 x g in a Beckman® J2-21 Centrifuge (Beckman Instruments Inc. – Fullerton, CA) for 5 minutes at 4°C. The top aqueous layer was recovered while the precipitated proteins at the interface and the lower phenol layer were discarded. This step was repeated if considered necessary. Next the residual phenol and any remaining proteins were removed by adding an equal volume of 24:1 (v/v) chloroform: isoamyl alcohol, mixing vigourously, and centrifuging as above. The top aqueous layer containing the protein free DNA was recovered. The DNA solution was then ethanol precipitated and stored at -20°C.

### 2.10.7 Ethanol Precipitation of DNA

Ethanol precipitation is used to concentrate DNA solutions and remove salts in the buffers. First the volume was accurately measured and a 1/10 volume of 3 M sodium acetate (pH 4.8) was added and mixed by inversion. Next 2.5 volumes of ice cold 95% ethanol was added and the mixed solution was stored at -80°C or -20°C for a minimum of 30 minutes or for long term storage. To recover the DNA, the mixture was centrifuged at 12,000 x g in a Beckman Model J2-21 centrifuge (Beckman Instruments Inc. – Fullerton, CA) for 20 minutes at 4°C. The ethanol was removed and the pellet was washed with cold 70% ethanol. After the removal of the 70% ethanol, the DNA pellet was dried in a vacuum dessicator for approximately 10 minutes and then resuspended in water or TE buffer (10 mM Tris-HCl (pH 7.5), 0.5 mM EDTA). The DNA concentration was determined using $A_{260}$ measurements.

## 2.11 Production of DNA Fragments

A variety of different sized DNA fragments, which were either of random or defined sequence, were used throughout the procedures. DNA fragments with defined sequences were inserted within a plasmid which was maintained in a bacterial stock. Non-defined or random sequences DNA fragments were obtained from chicken erythrocyte chromatin. The different DNA fragments were used in reconstitution experiments.

### 2.11.1 208-12 DNA

The p5S-208-12 plasmid containing the 208-12 DNA template (a tandemly repeated array of twelve copies of a 208 bp fragment of the 5S rRNA gene from the sea urchin *Lytechinus variegatus*) was originally provided by Dr. Robert T. Simpson Pennsylvania State University – State College, PN) and is maintained in an *E. coli* HB101 strain bacterial stock (Simpson *et.al.* 1985). The plasmid was amplified and purified using a large scale plasmid prep and ethanol precipitated. Plasmid DNA was separated from *E. coli* genomic DNA by column chromatography. The precipitated DNA was recovered

and resuspended in 2-5 ml of TE buffer (10 mM Tris-HCl (pH 7.5), 0.5 mM EDTA) and loaded on a previously equilibrated 2.5 cm x 60 cm Sephacryl S-1000 (40-105μm wet bead diameter) (Amersham Pharmacia Biotech – Baie d'Urfé, Que.) column using TE buffer at a 1 ml/minute flowrate. Two ml fractions were collected and $A_{260}$ measurements confirmed which fractions contained DNA. Plasmid DNA was eluted first in a small peak and its position was verified using 1% agarose gel electrophoresis. Fractions containing plasmid DNA were combined and concentrated using Centriprep 30 or 50 concentrators (Millipore-Amicon; Bedford, MA) until approximately 3 ml in volume. The DNA concentration was determined using $A_{260}$ measurements. The 208-12 insert was excised from the plasmid using restriction enzyme digestion with *Hha*I (New England Biolabs Ltd. – Mississauga, Ont.). Pilot digests were used to determine digestion times. Generally 1.8 mg of plasmid DNA in 6 mls total volume was digested with 560 units of *Hha*I /ml and digested overnight at 37°C. Digestion was verified using 1% agarose gel electrophoresis. After digestion, the solution was phenol extracted and the DNA ethanol precipitated. To separate the insert from the remainder of the plasmid DNA, the precipitated mixture was resuspended in approximately 3-4 ml of TE buffer and loaded onto the same 2.5 cm x 60 cm Sephacryl S-1000 column (Amersham Pharmacia Biotech – Baie d'Urfé, Que.) and run with TE buffer at a 1 ml/min flowrate. Once again 2 ml fractions were collected and $A_{260}$ measurements and 1% agarose gels were used to determine the presence of the insert and its purity. Fractions containing the purified insert were combined and concentrated using a Centriprep 30 (Millipore-Amicon – Bedford, CA) until approximately 1 to 2 ml in volume. The DNA concentration was determined and the DNA was ethanol precipitated and stored at -20°C until needed.

### 2.11.2 196 bp DNA

Purified 208-12 DNA insert was digested with *Eco*R I (New England Biolabs Ltd. – Mississauga, Ont.) to produce identical 196 bp fragments. Figure 14 outlines the production of the 196 bp fragments.The digestion was generally done overnight at 37°C using 600 units *Eco*R I per mg of DNA. The mixture was then phenol extracted to remove the enzyme and the DNA ethanol precipitated and stored at -20°C until required.

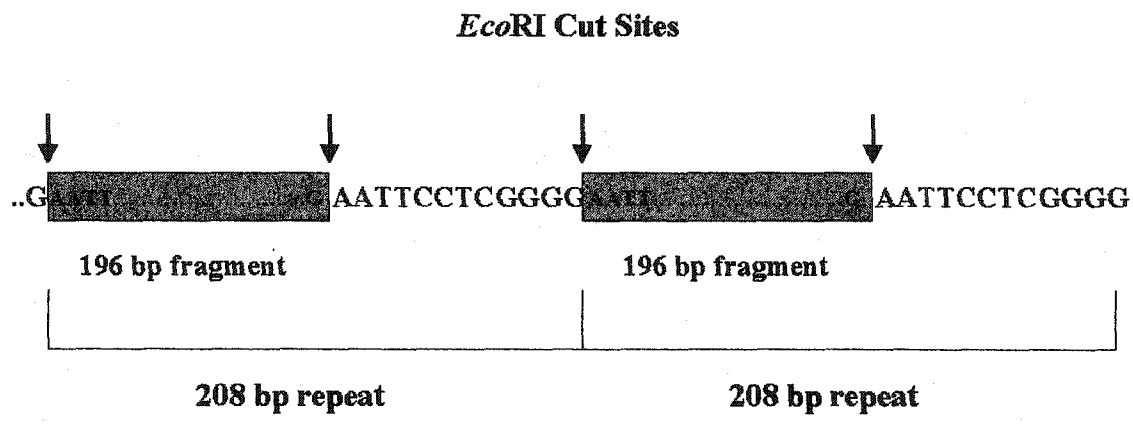


**Figure 14: *Eco*RI Cut Sites on the 208-12 DNA Template.** Cut sites are indicated by arrows, dark boxes show the resulting 196 bp fragment.

### 2.11.3 146 bp DNA

Random sequence 146 bp DNA fragments were derived from chicken erythrocyte core nucleosomes purified by salt extraction of cell nuclei and sucrose gradients as detailed previously in Sections 2.2.3 and 2.3. Core nucleosomes were loaded onto a new hydroxyapatite column and the histones and DNA were eluted as detailed above in Section 2.11.3. The recovered DNA was ethanol precipitated at stored at -20°C until required.

## 2.12 Reconstitution of Histone-DNA Complexes

### 2.12.1 Preparation of Histone Octamers

Lyophilized cores histones (control and/or modified) were resuspended in water and combined in stoichiometric amounts as confirmed by SDS-PAGE. Their concentration was determined using $A_{230}$ measurements and the histone mix was lyophilized. To ensure that only histone octamers were used in future reconstitution experiments the histone were run on a Sephacryl S300 (Amersham Pharmacia Biotech – Baie d'Urfé, Que.) size exclusion column. The previously mixed and lyophilized histones (usually 0.7 to 1.2 mg) were resuspended in 200 µl of 10 mM Tris-HCl (pH 8.0) and 4% β-mercaptoethanol for 30 minutes at room temperature. The mix was then brought to 8 M urea by adding 800 µl of a 10 M urea buffer (Ultrapure® Urea from ICN Biomedicals - Costa Mesa, CA) and incubated at room temperature for a further 30 minutes. The mixture was dialyzed in Spectra/Por® 3 dialysis tubing (3500 MWCO) (VWR Canlab – Mississauga, Ont.) versus 2 M NaCl, 10 mM Tris-HCl (pH7.5) overnight at 4°C. The histones were collected and loaded onto a 0.9 cm x 80 cm Sephacryl S-300-HR (25-75 µm wet bead diameter (Amersham Pharmacia Biotech – Baie d'Urfé, Que.) size-exclusion column run at 4°C and 4 ml/hour with 2 M NaCl, 10 mM Tris-HCl (pH 7.5). One ml fractions were collected and $A_{230}$ measurements and SDS-PAGE were used to determine which fractions contained histone octamers. Fractions containing complete

octamers were combined, their concentration determined using $A_{230}$ measurements, and stored on ice for future reconstitution experiments.

### 2.12.2 DNA Preparation

Ethanol precipitated DNA fragments were recovered as per Section 2.10.7. The DNA pellet was resuspended in water at approximately 2 mg/ml and the concentration was confirmed using $A_{260}$ measurements. The DNA was then brought to 2 M NaCl, 10 mM Tris-HCl (pH 7.5).

### 2.12.3 Preparation of Histone-DNA Complexes

The concentrations of the histone octamers and DNA fragments, both in 2 M NaCl, 10 mM Tris-HCl (pH 7.5), were accurately determined using $A_{230}$ and $A_{260}$ measurements respectively. An absorption coefficient of $A_{260}$ = 20 $cm^2mg^{-1}$ was used for DNA and $A_{230}$ = 4.3 $cm^2mg^{-1}$ for the core histone octamers (Stein, 1979). Since equimolar quantities of octamers and DNA were mixed together, the (w/w) ratios actually used were highly dependent on the calculations of molecular weight for the histones (i.e. control, acetylated, ubiquitinated or trypsinized) and the DNA fragments used (146 bp or 208-12). Since the amino acid sequences for the core histone proteins are very well defined, calculating their molecular weight is relatively simple and were calculated from the amino acid sequences of the individual histones and trypsinized histone (Bohm & Crane-Robinson, 1984; Ausio *et al.*, 1989). The molecular mass of a control histone octamer is 108,768 Da (10.8 x $10^4$ g/mol). The molecular mass of octamers containing uH2A must be adjusted to include the molecular mass of the additional ubiquitin protein (8,565 Da) therefore an octamer containing two uH2A histones will have a molecular mass of 125,768 Da (12.5 x $10^4$g/mol). Trypsinized histones lack both carboxyl- and amino-terminal tail domains, therefore a trypsinized octamer has a molecular mass of 8.3. x $10^4$ g/mol. With acetylated histones, since acetyl groups are relatively small, the molecular weight of acetylated histone octamers is usually assumed to be the same as control octamers. For DNA, the average molecular mass is 662 Da/bp so 146 bp DNA has an average molecular mass of 96,798 Da (9.67 x $10^4$ g/mol). Therefore for each

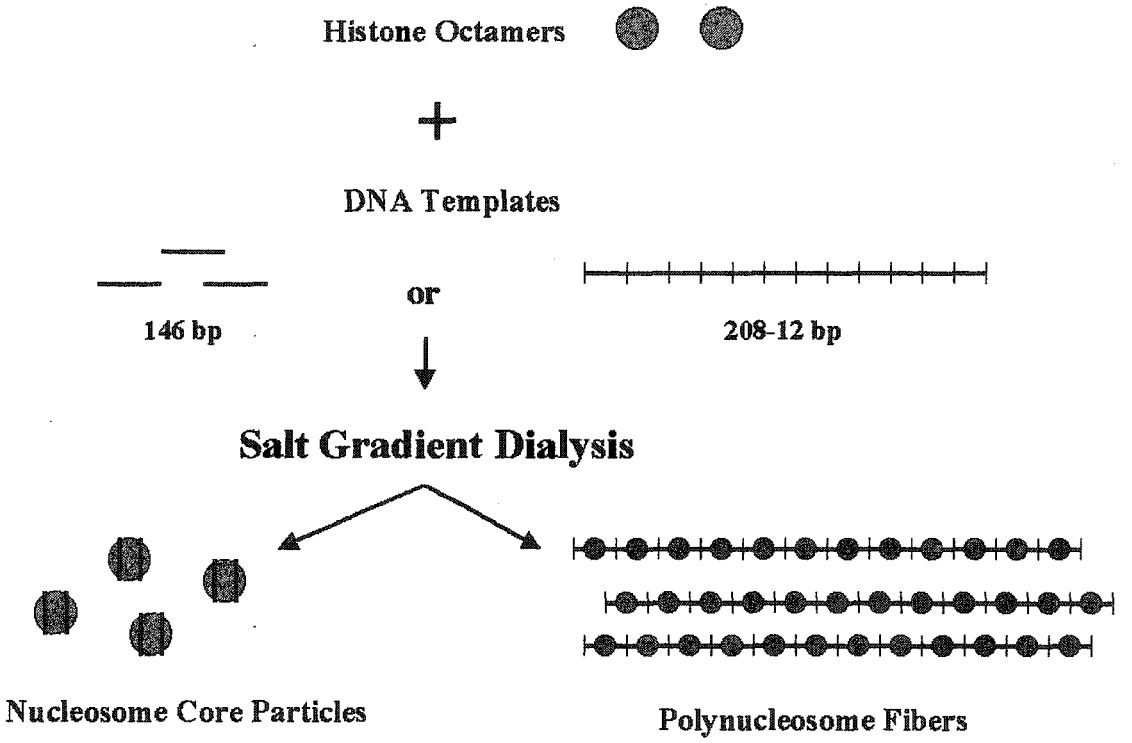


**Figure 15: Schematic of Salt Gradient Dialysis.**

combination of histone octamers and DNA they were combined using equimolar (w/w) quantities of each component.

### 2.12.4 Salt Gradient Dialysis

The combined histone and DNA samples were complexed together using salt gradient dialysis (Tatchell & van Holde, 1977). The two solutions (in 2 M NaCl buffer) were mixed together and dialyzed overnight at 4°C in Spectra/Por® 3 dialysis tubing (3500 MWCO) (VWR Canlab – Mississauga, Ont.) versus 2 M NaCl, 20 mM Tris-HCl (pH 7.5), 0.1 mM EDTA. The next morning the dialysis buffer was changed to 1.5 M NaCl, 20 mM Tris-HCl (pH 7.5), 0.1 mM EDTA and throughout the day the salt concentration was gradually reduced from 1.5 M NaCl to 1.2 M, 1.0 M, 0.6 M, 0.3 M and then 0.15 M in the same buffer every 2 to 2.5 hours. The last dialysis was done overnight at 4°C versus 10 mM Tris-HCl (pH7.5), 0.1 mM EDTA. After dialysis the sample was collected and its volume and concentration determined using $A_{260}$ measurements. The samples were then stored on ice at all times prior to analysis. Figure 15 shows a representation of this process.

## ANALYSIS TECHNIQUES

## 2.13 Gel Electrophoresis

### 2.13.1 Trichloroacetic Acid (TCA) Precipitation of Histones

High concentrations of salt can interfere with electrophoresis, therefore histone samples containing salt must be TCA precipitated to remove the salt buffer. The solution, usually containing 3-5 μg of histones, was brought to 20% TCA using either a 95% or 100% TCA stock solution. The mixture was incubated on ice for 10 minutes and then centrifuged for 10 minutes at 12,000 x g in an Eppendorf Model 5415C Microcentrifuge at 4°C and the supernatant was then removed. If the original buffer was very high in salt, then this step could be repeated using 500 μl of a 20% TCA solution and repeating the incubation and centrifugation. After the supernatant was removed 500 μl of cold 0.25 N

HCl in acetone was added and incubated on ice for 10 minutes. The mixture was then centrifuged at 12,000 x g for 10 minutes at 4°C and the supernatant was removed. The tubes containing the pelleted histones were the dried in a Jouan RC 10-10 Centrifugal Evaporator (Canberra Packard Canada – Mississauga, Ont.). Once dry, the histones were resuspended in water and the appropriate sample buffer for gel electrophoresis.

### 2.13.2 SDS-PAGE

SDS-PAGE gels (Laemmli, 1970) were used to examine the histone composition of native and reconstituted histone and nucleoprotein complexes.

A vertical mini-gel system from Idea Scientific (Minneapolis, MN) was used. The 7.3 cm x 10.2 cm x 0.75 cm SDS-PAGE was prepared with a 15% separating gel [5 ml of a 30:0.8% acrylamide:bis-acrylamide stock solution; 2.5 ml of 1.5 M Tris-HCl (pH 8.8), 100 µl of 10% SDS, 2.32 ml of $H_2O$, 57 µl of 10% APS and 4.5 µl of TEMED] and a 6% stacking gel [400 µl of a 30:0.8% acrylamide:bis-acrylamide stock solution, 500 µl of 0.5 M Tris-HCl (pH 6.8), 20 µl 10% SDS, 1.06 ml $H_2O$, 20 µl 10% APS, 2 µl TEMED]. Samples were resuspended in water and mixed with an equal volume of 2 x SDS Sample Buffer [0.04% SDS, 20% glycerol, 10% (v/v) β-mercaptoethanol, 0.0125 M Tris-HCl (pH 6.8) and 0.025% (w/v) bromophenol blue]. Samples generally contained 1 µg of histones and were boiled for 5-10 minutes prior to loading.

Various histone markers with and without histone H1 were made using acid extracted or salt extracted samples which were dialyzed versus water, lyophilized and then resuspended in equal volumes of water and 2 x SDS Sample Buffer to a concentration of 0.25 µg/µl. All markers were boiled for 10 minutes and stored at -20°C until required.

The gels were loaded and run cathode (-) to anode (+) at 200 volts using a 0.05 M Tris-base, 0.38 M glycine, 0.1% SDS running buffer at 4°C for approximately 20-30 minutes or 100 volts at room temperature for approximately 60 minutes until the bromophenol blue tracking dye was at the bottom of the gel. The gels were stained in 10% acetic acid,

25% isopropanol, 0.2% Coomassie Blue G-250 for 40 to 60 minutes and then destained in 10% isopropanol, 10% acetic acid with several changes of destain or left overnight. Pictures of the gels were taken using Kodak® 667 film and the gels were then dried.

### 2.13.3 SDS-PAGE (20% Acrylamide)

Samples requiring a higher resolution of separation were run on an SDS-PAGE with 20% acrylamide. The gels were made as above (Section 2.13.2) except that there was a 20% acrylamide separating gel [using 3.3 ml 60:0.4% acrylamide:bis-acrylamide stock solution, 2.5 ml of 1.5 M Tris-HCl (pH 8.8), 3.99 ml $H_2O$, 100 µl of 10% SDS, 57 µl 10% APS, 4.5 µl of TEMED] and a 6% stacking gel [using 400 µl 60:0.4% acrylamide:bis-acrylamide solution, 1.0 ml 0.5 M Tris-HCL (pH 6.8), 2.52 ml of $H_2O$, 40 µl of 10% SDS, 40 µl 10% APS and 4 µl of TEMED]. These gels were run at room temperature only at 100 volts with the same running buffer, staining, and destaining conditions for SDS-PAGE as outlined in Section 2.13.2.

### 2.13.4 Acetic Acid - Urea (AU) Gels

Acetic Acid-Urea gels (Panyim & Chalkley, 1969; Hurley, 1977) were also used to look at histone proteins, particularly post-translational modifications like acetylation because unlike SDS-PAGE, AU-PAGE can separate both acetylated and non-acetylated histones. The 2.5 M urea, 5% HAC, 15% acrylamide gels [using 4 ml of 30:0.2% acrylamide:bis-acrylamide solution, 2 ml of 10 M urea, 1 ml of 43% HAC, 1ml of $H_2O$, 7 mg of thio-urea and 45 µl of 30% hydrogen peroxide) were 7.3 cm x 10.2 cm x 0.75 cm and were run using a vertical mini-gel system from Idea Scientific (Minneapolis, MN).

Samples were prepared in a variety of ways. Histones which were suspended in water or buffers without salt were generally mixed with an equal volume of the 2 x AU-sample buffer (8 M urea, 10% acetic acid, 0.1% Pyronin Y). Samples in buffers containing high salt concentrations however were TCA precipitated first as per Section 2.13.1. In order to reduce the H3-H3 dimers, samples were treated with a reducing buffer (700 µl of $H_2O$, 3.5 µl of 1 M Tris-HCl (pH 7.5), 3.5 µl of β-mercaptoethanol). An aqueous histone solution was mixed in a 1:1 (v/v) ratio with this reducing buffer and incubated for 1 hour

at room temperature after which an equal volume of 2 x AU-sample buffer was added. To visualize histones contained in nucleoprotein samples (i.e. nucleosomes or oligonucleosomes), the histones had to be removed from the DNA first. To do that the samples were mixed with 2 x AU-sample buffer containing 0.3% protamines in order to displace the histones from the DNA and allow them to be visualized on the gel. Various histone markers (with and without H1) were made using acid extracted or salt extracted samples which were dialyzed versus water and lyophilized. When needed, the histones were resuspended in equal volumes of water and reducing buffer (as described above) to a concentration of 0.5 µg/µl and incubated for 60 minutes at room temperature. Then an equal volume of 2 x AU-sample buffer was added and the end concentration was 0.25 µg/µl. Markers were stored at -20°C until required.

The gels were run anode (+) to cathode (-) at 80-100 volts with a 5% HAC running buffer at room temperature until the pyronin dye was about 0.5 cm from the bottom of the gel. The gels were stained in 10% acetic acid, 25% isopropanol, 0.2% Coomassie Blue G-250 for 40 to 60 minutes and then destained in 10% isopropanol, 10% acetic acid with several changes of destain or left overnight. Pictures of gels were taken using Kodak® 667 film and the gels were then dried.

### 2.13.5 4% Native (Non-Denaturing) PAGE

Native polyacrylamide gels were used to visualize DNA fragments or nucleoprotein complexes like nucleosomes, chromatosomes, etc., without denaturing or displacing the histone proteins (Yager & van Holde, 1984). A vertical mini-gel system from Idea Scientific (Minneapolis, MN) was used. The 4% acrylamide gels [2 ml of 20:1 acrylamide:bis-acrylamide solution, 1.67 ml 6E buffer (6E = 240 mM Tris-HCl (pH 7.2), 6 mM EDTA (pH 8.0), 120 mM sodium acetate), 6.3 ml of $H_2O$, 70 µl 10% APS, 10 µl TEMED) were 7.3 cm x 10.2 cm x 0.75 cm in size.

Samples in which just the DNA fragments were to be visualized were prepared by adding 1/6 volume of 6 x NDSB (0.25% bromophenol blue, 0.25% xylene cyanol FF, 30% glycerol). Nucleoprotein samples in which the histones were not to be displaced from the

DNA were mixed with an equal volume of either 2 x native sample buffer without dye (80 mM Tris-HCl (pH 7.2), 1 mM EDTA, 20 mM sodium acetate, 10% glycerol) or an equal volume of 10% glycerol only. A tracking dye was loaded into an empty well to help track gel running times. The DNA marker used with these gels consisted of pBR22 plasmid DNA digested with 2 units of *Hha*I (New England Biolabs Ltd. – Mississauga, Ont.) per μg of DNA and mixed 6 x NDSB and stored at –20°C until required.

Gels were run cathode (-) to anode (+) at 60 volts in 1E running buffer (40 mM Tris-HCl (pH 7.2); 1 mM EDTA; 20 mM sodium acetate) at room temperature until the bromophenol blue dye front was about 1cm from the bottom of the gel. Gels were stained with 0.1 mg/ml ethidium bromide solution for approximately 15 minutes and then rinsed in water for 10-15 mintues. The DNA was visualized using an ultraviolet transilluminator and photographed with an AlphaImager 2000 Documentation Analysis System (Alpha Innotech Corporation – San Leandro, CA).

### 2.13.6 1% Agarose Gel Electrophoresis

Agarose gels were used for the analysis of DNA fragments. Generally a 1% agarose (Omnipur® Agarose from EM Science – Gibbstown, NJ) gel in 1x TAE buffer (40 mM Tris-acetate, 1mM EDTA) was prepared. The gel was 15 cm x 11 cm x 1 cm in size and was run in a Chameleon Submarine Gel Apparatus (Idea Scientific – Minneapolis, MN). Samples were prepared by adding a 1/6 volume of 6 x NDSB (0.25% bromophenol blue, 0.25% xylene cyanol FF, 30% glycerol). The DNA markers used consisted of Lamba (λ) DNA digested with *BstE* II (New England Biolabs Ltd. – Mississauga, Ont.)

Gels were run cathode (-) to anode (+) at 60 to 80 volts in 1 x TAE buffer for approximately 30 minutes at room temperature. The movement of the bromophenol blue tracking dye was approximately equivalent to a 200 bp DNA fragment. Gels were stained in 0.1 mg/ml ethidium bromide solution for approximately 15 minutes and then rinsed in water for 10-15 minutes. The DNA was visualized using an ultraviolet transilluminator and photographed with a AlphaImager 2000 Documentation and Analysis System (Alpha Innotech Corporation – San Leandro, CA).

## 2.13.7 DNase I Footprinting and DNA Sequencing Gels

DNase I footprinting gels were prepared to examine the effect of post-translationally modified histones and the histone tails on the digestion of nucleosomes by DNase I. Comparison of the DNase I digestion patterns helped determine if digestion had been inhibited or enhanced by the histone modifications. Sequencing gels were done to determine or verify the sequence of specific DNA fragments which were produced. Except for the differences in sample preparation, both gels used the same protocol and procedures in preparing, running and analyzing the gels.

### 2.13.7.1 Gel Preparation

A vertical 10% acrylamide (20:1 acrylamide:bis-acrylamide), 7 M urea, 1 x TBE (89 mM Tris-borate, 2 mM EDTA (pH 8.0)) denaturing gel was prepared which was 39 cm x 31 cm x 0.4 mm in size. The acrylamide/urea/TBE stock solution was mixed with 1/100 of 10% APS and 1/2000 of TEMED. The gel was polymerized at room temperature for a minimum of 2 hours and then pre-run at 60 Watts using a 1 x TBE running buffer for 30 minutes prior to loading using a Model S2 Sequencing Gel Electrophoresis System (Gibco BRL – Burlington, Ont.) and a Fisher Biotech Model FB600 Constant Power supply (Fisher Scientific – Nepean, Ont.). Prior to loading the wells were rinsed to remove any urea. The gels were run cathode (-) to anode (+) at 60 Watts until the tracking dye was 0.5 – 1.0 cm from the bottom of the gel. The gel was then fixed in 2 liters of 10% (v/v) acetic acid, 10% (v/v) methanol for 60 minutes. The gel was then dried on electrophoresis blotting paper grade 238 (Scientific Specialties Group – Hollywood Springs, PA) for one hour at 80°C using the Jouan GF10 gel dryer (Canberra Packard Canada – Mississauga, Ont.). The gel was then autoradiographed with Kodak® BioMax MR (maximum resolution) Autoradiography film (VWR Canlab – Mississauga, Ont.).

### 2.13.7.2 DNase I Digest Sample Preparation

Nucleosomes particles (usually 30 μg) were 5'-end labelled with [$\gamma$-$^{32}$P] ATP (Amersham Pharmacia Biotech – Baie d'Urfé, Que.). The nucleosomes in 50 mM Tris-HCl (pH 7.5),

2 mM $MgCl_2$, 1 mM EDTA were mixed with 1 μM [$\gamma$-$^{32}$P] ATP (10 Ci/mM). Then 0.5 units/μl of T4 Polynucleotide Kinase (New England Biolabs Ltd. – Mississauga, Ont.) was added and the mixture was incubated at 37°C for 30 minutes. After labelling, excess [$\gamma$-$^{32}$P]-ATP was removed by dialysis with a Centricon 30 Microconcentrator (Millipore Amicon - Beverly, MA) using 10 mM or 25 mM NaCl, 10 mM Tris-HCl (pH 7.5) buffer. This was done 5-8 times for 10 minutes at 3500 x g in a Beckman Model J2-21 centrifuge (Beckman Instruments Inc. – Fullerton, CA) in a JA-20 rotor. Radioactivity was analyzed by doing scintillation counts (with 1μl) of both the sample and the filtrate in a Beckman Gamma 8000 Scintillation Counter (Beckman Instruments Inc. – Fullerton, CA) to verify that labelling was successful and unlabelled isotope had been removed.

The labelled nucleosomes were brought to 1 mM $MgCl_2$ and then digested with DNase I (Roche Applied Science – Laval, Que.) on ice. Pilot digestions were done but generally nucleosomes were digested about 80 minutes with 70 DNase I units/ ml at 0°C. Any required dilutions of DNase I were done using DNase I dilution buffer (25 mM Tris-HCl (pH 7.6), 50% glycerol, 100 μg/ml BSA, 1 mM DTT, 50 mM NaCl). Immediately after digestion the samples were heated to 100°C for 1 minute to heat inactivate the enzyme, then cooled and deproteinized with proteinase K (Roche Applied Science – Laval, Que.) for 1 hour at 37°C using an enzyme to substrate ratio of 1:10. The samples were then mixed with an equal volume of 98% (v/v) deionized formamide, 10 mM EDTA (pH 8.0), 0.4% bromophenol blue, 0.4% xylene cyanol FF and stored at -20°C until needed. Prior to loading the samples were incubated at 90-100°C for 10 minutes.

### 2.13.7.3 Sequencing Samples

DNA sequencing was done to ensure that the DNA fragments used were still present in the plasmid constructs with their proper orientation and sequence. The plasmid DNA was amplified and purified using small-scale plasmid preps. Prior to sequencing the DNA was processed with the Wizard® DNA Clean-up System (Promega – Madison, WI) which removes any unwanted enzymes, proteins, kinases, exo- and endo-nucleases, salts, etc., without the use of organic extractions and precipitations. Approximately 50-500 μl of DNA was mixed with 1 ml of resin in a 1.5 ml microcentrifuge tube and inverted

several times. A syringe barrel with an attached minicolumn was attached to a vacuum manifold. The resin/DNA mix was loaded into the syringe barrel. After applying a vacuum, the resin forms a minicolumn in the syringe and the column was then washed with 2 ml of 80% isopropanol and dried for 30 seconds. The column was transferred to a microcentrifuge tube and centrifuged at 10,000 x g for 2 minutes in an Eppendorf Model 5415C microcentrifuge to remove any residual isopropanol. The column was then transferred to a new tube and 50 µl of prewarmed (65° to 70°C) water was applied and allowed to sit for 1-5 minutes. The column was then centrifuged at 10,000 x g for 20 seconds to elute the purified DNA which was then stored at -20°C.

The DNA sample was labelled for sequencing using the Sequenase Version 2.0 DNA Sequencing Kit (Amersham Pharmacia Biotech – Baie d'Urfé, Que.) and [$\alpha$-$^{35}$S]-dATP (Amersham Pharmacia Biotech - Baie d'Urfé, Que.). Once complete, the samples were loaded onto the sequencing gel.

## 2.14 Western Blotting

Western blotting of both SDS-PAGE and AU-PAGE gels was performed to detect ubiquitinated H2A (uH2A) and H2B (uH2B) histone proteins during purification and analysis procedures.

### *2.14.1 Antibody Production*

A rabbit polyclonal antibody to ubiquitin was produced using New Zealand white rabbits. Since ubiquitin is a highly conserved protein and a poor immunogen, it was necessary to attach it to a more immunogenic carrier protein. Consequently, bovine ubiquitin protein (Sigma Aldrich – Oakville, Ont.) was attached to the maleimide activated carrier protein Imject® Keyhole Limpet Hemocyanin (KLH) (Pierce Biotechnology Inc. – Rockford, IL). Since ubiquitin has only one sulfhydryl group, the KLH crosslinker, a sulfhydryl reactive maleimide group, binds to the ubiquitin at one location and thus should increase the specificity of the immune response.

Two mg of lyophilized KLH were used to produce a 10 mg/ml KLH solution in 83 mM sodium phosphate (pH 7.2), 0.9 M NaCl and 0.1 M EDTA. An excess of ubiquitin (4 mgs) was resuspended in 500 µls of the same buffer and the two solutions were mixed and allowed to conjugate for 2 hours at room temperature. The conjugated proteins were loaded onto a pre-packed Pharmacia Sephadex G25 column (Amersham Pharmacia Biotech – Baie d'Urfé, Que.) equilibrated with the running buffer (83 mM sodium phosphate (pH 7.2), 0.9 M NaCl). Fractions of 1 ml were collected dropwise by gravity. The $A_{280}$ of the fractions was measured and those containing the conjugated ubiquitin-KLH were combined. The 5 mls of the 0.4 mg/ml solution of ubiquitin-KLH solution were used for subsequent innoculations. Prior to the first innoculation, 6 to 10 mls of blood was collected into Vacutainers containing coagulants. The "pre-bleed" mixture was allowed to stand for 30 to 60 minutes, the blood clot was then loosened from the side and the tubes were centrifuged at 1300 x g for 10 minutes in a Beckman® Model TJ-6 Centrifuge (Beckman Instruments Inc. – Fullerton, CA). The clear, straw coloured serum was collected, brought to a 0.1% sodium azide ($NaN_3$) concentration and aliquoted and stored at -80°C.

The first injection was a mixture of 100 ugs (in 250 µl) of the ubiquitin-KLH conjugate brought to 1.2 ml with PBS solution mixed with 2.1 ml of Freund's Complete Adjuvant (Pierce Biotechnology Inc. – Rockford, IL), an emulsion of water and mineral oil with heat killed *Mycobacterium*. The mixture was emulsified with a Model W-385 Ultrasonic Disrupter (Heat Systems Ultrasonics Inc.) until it formed a milky, paste-like consistency. Approximately 0.5 ml was injected intramuscularly into the thigh muscle of the hind leg and the remainder was divided into 0.25 ml aliquots (a maximum of 1 ml total) and injected subcutaneously under the loose skin on the shoulders and flanks of the rabbit. Twenty-five days after the first injection the first booster shots were administered to induce a secondary immune response. Booster shots were prepared as above except that Freund's Incomplete adjuvant (Pierce Biotechnology Inc. – Rockford, IL) consisting of a water in mineral oil emulsion was used. Boosters were then given every 7 to 10 days and test bleeds of 6 - 10 ml of blood were collected and processed as previously described one week after administration of the booster shot. The sera collected were then assayed

for anti-ubiquitin and anti-KLH antibodies using using ELISA. Once it was determined that the antibody titre was no longer increasing after booster shots, the rabbit was euthanized and the sera was brought to 0.1% sodium azide, aliquoted and stored at -80°C until required for western blot analysis.

### 2.14.2 ELISA ASSAYS

An indirect ELISA assay was performed to measure anti-ubiquitin and anti-KLH antibody levels in the pre-bleed and various test-bleed serum samples collected after booster injections. Antigen samples of pure ubiquitin protein (Sigma Aldrich – Oakville, Ont.) and the ubiquitin-KLH conjugate were diluted with water to a concentration of 0.01 μg/μl. Using a polystyrene microtitre ELISA plate (96 well), selected wells were coated with antigen; Rows A-D (columns 1-9) each contained 1μg (in 100 μl) of ubiquitin protein in solution; rows E-H (columns 1-9) contained 1μg (in 100 μl) of the ubiquitin-KLH conjugate. Columns 10-12 contained 100 μl of water as a control. The plate was incubated at 37°C overnight. Unbound sites were blocked for 1 hour at 37°C using 200 μl/well of 3% (w/v) powdered milk (Carnation Instant Milk – Safeway) in PBS (pH 7.4). Each well was then quickly rinsed 3 times with PBS-Tween solution (0.5% (w/v) Tween-20 in PBS). Each serum sample being tested was then diluted to 1/100 in 1% (w/v) BSA in PBS-Tween. These solutions were then serially diluted until a 1/1,024,00 dilution was reached and the wells contained 100 μl of the different dilutions. Controls contained only 1% (w/v) BSA in PBS-Tween solution. The plate was incubated with agitation at 37°C for 60 minutes (or at room temperature for 2 hours) and then rinsed 3 times with PBS-Tween. The secondary antibody, an alkaline phosphatase conjugated goat anti-rabbit (IgG) antibody (Perkin Elmer Life Sciences Inc. – Boston, MA), was diluted 1/2000 in 1% (w/v) BSA- PBS-Tween and 100 μl was added to each well and incubated at 37°C for 1 hour. The wells were then washed with PBS-Tween three times quickly and then three times for 5 minutes each. After rinsing, 100 μl of the 1 mg/ml phosphatase substrate (p-nitro-phenyl-phosphate) was added to each well and incubated in the dark for 15-20 minutes until sufficient colour development was achieved. [The phosphatase buffer contained one 5mg phosphatase tablet in 2ml of room temperature diethanolamine buffer (97 ml diethanolamine, 800 ml water, 0.2 g $NaN_3$, 100 mg $MgCl_2.6H_2O$, made up to 1

liter and adjusted to pH 9.8 with HCl and stored at 4°C in the dark until needed.)] The absorbance of the yellow product, p-nitrophenol, was measured at 405 nm using an ELISA reader. The $A_{405}$ values were plotted versus the serum dilution to determine the antibody titre. From the plots of the ELISA results it was determined that there were insignificant amounts of anti-KLH antibodies in the samples and that anti-ubiquitin antibodies were present (See Figure 16). Subsequent western blotting indicated that pure ubiquitin was detectable with even a 1/20,000 dilution and western blots using HRP detection could easily detect uH2A and uH2B in cellular extracts and column chromatography fractions with a 1/6000 dilution.

### 2.14.3 Western Blots of SDS-PAGE gels

Duplicate samples were run on SDS-PAGE . One set was stained (see Section 2.13.2) to visualize the proteins while the gel containing the second set of samples was equilibrated in transfer buffer (25 mM Tris base, 192 mM glycine) for 10-15 minutes. Sequi-Blot™ polyvinylidene difluoride (PVDF) Membrane (Bio-Rad Laboratories – Hercules, CA) was cut to size and moistened first in 100% methanol, immediately transfered to deionized water for 5 minutes, and then put into transfer buffer for 15 to 20 minutes. The western blot apparatus was assembled with the membrane on the anode (+) side and the gel on cathode (-) side. The assembly was immediately put into a BioRad Mini Trans-Blot® Electrophoretic Transfer Cell apparatus (Bio-Rad Laboratories – Hercules, CA) with an ice cooling unit and 500 mls of 4°C transfer buffer. The proteins were transfered for 2 hours at 100 volts at 4°C with stirring. Ubiquitinated proteins were generally detected using horse radish peroxidase (HRP) detection although alkaline phosphatase detection was also possible. HRP detection was preferred because it was far more sensitive and the membrane could be stained after detection.

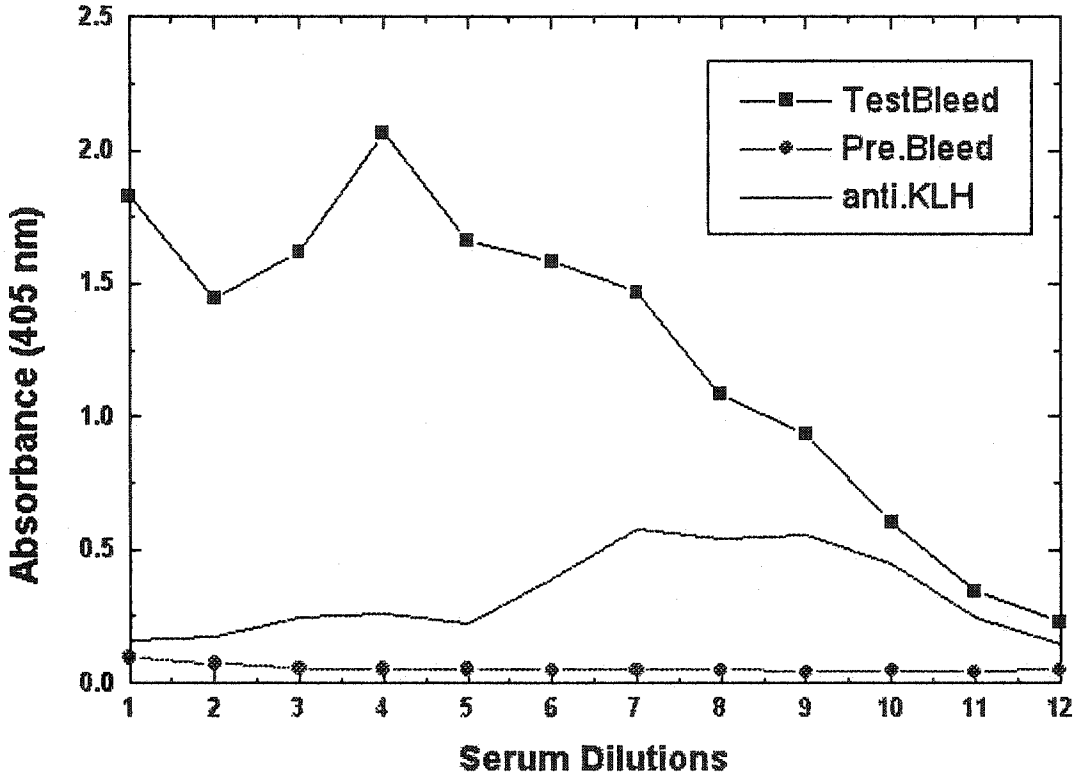


**Figure 16: Plot of Anti-Ubiquitin Antibody ELISA Results.** All absorbances were read at 405 nm. Serial dilutions of serum; 1 = 1/500; 2 = 1/1000; 3 = 1/2000; 4 = 1/4000; 5 = 1/8000; 6 = 1/16000; 7 = 1/32000; 8 = 1/64000; 9 = 1/128000; 10 = 1/256000; 11 = 1/1512000; 12 = 1/1024000. Pre-bleed serum obtained prior to introduction of ubiquitin-KLH antigen and tested for anti-ubiquitin and anti-KLH antibody activity; Test Bleed serum obtained after second booster shot and tested for anti-ubiquitin antibody activity. Test bleed serum also tested for anti-KLH antibody to ensure specificity of anti-ubiquitin antibody.

### 2.14.3.1 Horse Radish Peroxidase (HRP) Detection

After the transfer the membrane was blocked using 3% (w/v) powdered skim milk, 0.1% (w/v) Tween-20 in PBS buffer. The membrane was shaken at room temperature for 60 minutes and then stored overnight at 4°C. The rabbit serum containing the anti-ubiquitin antibody was diluted 1/6000 in 0.1% Tween-20, 1% powdered skim milk, 350 mM NaCl, in PBS buffer. The membrane was incubated with the anti-ubiquitin antibody at room temperature for 60 minutes with shaking. The membrane was then washed in 0.1% (w/v) Tween-20 in PBS buffer for 4 x 15 minutes, 3 x 5 minutes. The secondary antibody, the HRP-conjugated goat anti-rabbit (IgG) antibody (Pierce Biotechnology Inc. – Rockford, IL) was diluted 1/3000 in 0.1% (w/v) Tween-20, 1% (w/v) powdered milk, 350 mM NaCl in PBS solution and incubated at room temperature for 60 minutes with shaking. The membrane was washed 4 x 15 minutes with PBS/Tween, then 4 x 10 minutes with PBS, and rinsed with water immediately prior to HRP detection. Using Rennaissance® Western Blot Chemiluminescence Reagents (Perkin Elmer Life Sciences Inc. – Boston, MA), the blot was incubated for 30 seconds in the dark with 2 ml of each of the developing buffers. The blot was then sandwiched between Saran® wrap and placed in a cassette with Kodak® BioMax MR film (VWR Canlab – Mississauga, Ont.) which was exposed for different times and then developed. After development, the blot was then stained for 2 minutes in 10% (v/v) acetic acid, 25% isopropanol, 0.2% Coomassie Blue G-250 and then destained in 50% (v/v) methanol, 10% (v/v) acetic acid for 10 minutes with multiple changes of destain. This staining confirmed the transfer of proteins and allowed the easy identification of appropriate bands.

### 2.14.3.2 Alkaline Phosphatase Detection

Blocking, washing, and incubation with the α-ubiquitin antibody proceeded as with the HRP detection. However the secondary antibody, an alkaline phosphatase conjugated goat α-rabbit (IgG) antibody (Perkin Elmer Life Sciences Inc. – Boston, MA) was diluted 1/1250 and incubated for 60 minutes. The blot was then washed 3 x 10 minutes in 40 ml of alkaline phosphatase buffer (100 mM Tris-HCl (pH 9.5), 10 mM NaCl,

50 mM $MgCl_2$) at room temperature with shaking. The blot was then incubated in developing buffer (10 ml alkaline phosphate buffer, 33.3 µl BCIP and 44 µl of NBT) with shaking at room temperature until sufficient colour development was seen. The reaction was stopped by rinsing the blot with cold water. Pictures of the blot were then taken with the AlphaImager 2000 Documentation and Analysis Sytem (Alpha Innotech Corporation – San Leandro, CA).

### 2.14.4 *Western Blotting of Acetic Acid-Urea Gels*

The basic protocol for AU gels is the same as the SDS-PAGE except that different buffers were used. The transfer buffer was 0.7% HAC. The rabbit serum containing the first antibody was diluted 1/1000 in NET buffer (150 mM NaCl, 5 mM EDTA, 50 mM Tris-HCl (pH 7.5)). All washes were done using 0.5% (w/v) Tween-20 in NET buffer. The secondary antibody was also diluted in NET buffer. Detection could be done with either the alkaline phosphatase or HRP methods dependent upon which secondary antibody had been used, i.e. alkaline phosphatase or HRP conjugated goat anti-rabbit polyclonal antibody.

## 2.15 *Eco*R I Digestion of Oligonucleosomes

Reconstituted oligonucleosomes were digested with *Eco*R I (New England Biolabs, Ltd. – Mississauga, Ont.) to assess the number of histone octamers bound to the 208-12 template. Digestions were done in low-ionic-strength buffer (15 mM Tris-HCl, (pH 7.5), 15 mM NaCl, 1 mM $MgCl_2$, 5 mM DTT) for 3.5 hours at 37°C. *Eco*R I sites flank the preferred octamer position on the template therefore digestion produces a mixture of mononucleosomes and 196 bp DNA if any nucleosome sites are unoccupied. The digestion was run on a 4% native acrylamide gel and stained with ethidium bromide.

## 2.16 Solubility Assays

The solubility of 208-12 polynucleosome fibers with post-translationally modified or control histones were compared by mixing the fibers with varying concentrations of either divalent ($MgCl_2$ ) or monovalent (NaCl) ions. Equivalent amounts of the polynucleosome fibers in 1 mM Tris-HCl (pH 7.5) were mixed with different quantities of NaCl or $MgCl_2$ in 1 mM Tris-HCl (pH 7.5) buffer to produce mixtures with the same volume but with concentrations of NaCl ranging from 5 mM to 300 mM or $MgCl_2$ ranging from 0 mM to 6 mM. The mixtures were incubated on ice for 60 minutes and then centrifuged at 4°C and 12,000 x g in an Eppendorf Model 5415C Microcentrifuge for 10 minutes. Fibers which oligomerized and precipitated out of solution were pelleted and the quantity of fibers remaining soluble was determined by $A_{260}$ measurements of the supernatant. The percent solubility was determined by comparison to the zero sample (i.e. 1 mM Tris-HCl (pH 7.5) with no $MgCl_2$ or NaCl) which was taken as 100%.

## 2.17 Protamine Displacements Assays

Nucleosome core particles containing control or modified histones were dialyzed overnight versus 50 mM NaCl, 10 mM Tris-HCl (pH 7.5), 1 mM EDTA, 2% sucrose at 4°C using Spectra/Por® 3 dialysis tubing (3500 MWCO). Once recovered, the concentration was determined using $A_{260}$ measurements and adjusted with buffer to 1.5 μg/μl. To determine the quantity of protamines to be used we determined the positive to negative (+/-) charge ratio, i.e. the number of positively (+) charged arginines in the protamines versus the negative (-) charges of the DNA per weight. Nucleosomes have a negative charge every 330 Da while squid protamines have a positive charge every 188.3 Da. Therefore it was assumed that there was a positive (+) charge every 190 Da for the protamines, and consequently the +/- ratio was 330/190 = 1.74.

The protamine proteins were resuspended in 50 mM NaCl, 10 mM Tris-HCl (pH 7.5), 1 mM EDTA, 2% sucrose. Squid protamines were combined with ratios of 0, 1, 2, and 3. Each tube contained the same total volume and 15 μg of nucleosomes and the appropriate quantity of protamines. The tubes with the different mixtures were each mixed for 10 seconds and then stored overnight at 4°C. The next morning they were mixed for 10 seconds every hour for 3 hours. Total incubation time was 19 hours, total mixing time was 40 seconds and the mixture was allowed to incubate for 30 minutes after the last mixing. The tubes were then centrifuged at 12,000 x g for 10 minutes at 4°C. The pellet contained DNA bound to protamines and non-displaced histones, while the supernatant contained displaced histones and unbound protamines. The supernatant was recovered, the $A_{260}$ was determined and the sample was then dried in a Jouan RC 10-10 Centrifugal Evaporator (Canberra Packard Canada). Once dry the samples were resuspended in equal volumes of water and 2 x AU sample buffer and run on an Acetic Acid-Urea gel. The gels were scanned using the AlphaImager 2000 Documentation and Analysis System (Alpha Innotech Corporation – San Leandro, CA).

## 2.18 Circular Dichroism

Circular dichroism was used to identify and measure changes in the molecular conformation of the histone tails, histone octamers and nucleosome structure as a result of histone post-translational modifications. The percentage of alpha(α)-helices, beta(β)-sheets and random coil structures was determined for each sample and this allowed direct comparison between structures containing control and modified histones.

All experiments were performed at 20°C on a Jasco J-720 spectropolarimeter (Jasco Incorporated – Easton, Maryland) using a wavelength range of 310 to 190 nm. Histone samples had an $A_{230}$ of approximately 1.2 while nucleosome or DNA samples had an $A_{260}$ of approximately 0.8. Measurements were taken in quartz cells with either a 1 cm or 0.1 cm path length.

CD data is measured in mdeg (1 mdeg = 0.001 degrees) and is expressed as ellipticity (θ). For macromolecules such as histone proteins and nucleic acids, these data are expressed as the mean residue molar ellipticity [θ] which is measured in deg.cm$^2$.decimole$^{-1}$ and is calculated using the equation:

$$[\theta] = \theta / (10 \,.\, C_r \,.\, l)$$

where θ is the measured ellipticity (mdeg); 10 is a constant (decimole/mole); $l$ is the path length of the cell (cm); and $C_r$ is the mean residue molar concentration (mol/L). The path length ($l$) is determined by the cell used. Therefore for the histone tails and histone proteins a 0.1 cm cell was used and for DNA and nucleosomes a 1 cm cell was applied. For all samples the mean residue molar concentration ($C_r$ in mol/L) was determined by calculating concentration using absorbance values ($A_{230}$ or $A_{260}$) and extinction coefficients and dividing by the mean residue molecular weights ($M_r$ in g/mol). For histone proteins the absorption coefficient at $A_{230}$ = 4.3 cm$^2$mg$^{-1}$; for DNA $A_{260}$ = 20 cm$^2$mg$^{-1}$; for octamer particles $A_{260}$ = 0.23 cm$^2$mg$^{-1}$; for native nucleosome particles $A_{260}$ = 9.5 cm$^2$mg$^{-1}$; and trypsinized nucleosome particles = $A_{260}$ = 10.5 cm$^2$mg$^{-1}$ (Ausio *et al.*, 1984). The mean residue molecular weight ($M_r$) values used for the average amino acid residue for native histones was 110.6 g/mol and for trypsinized histones 110.4 g/ml as determined from amino acid analysis of the two proteins. In the case of the histone H4 tail, $M_r$ values of 103.2, 105, 106.6, 108.4 and 110.2 were used for the non-, mono-, di-, tri-, and tetraacetylated forms, respectively, as calculated from the amino acid sequence. The average $M_r$ (for a nucleotide) used for the DNA was 331.

DNA, nucleosomes particles and histone proteins were generally examined in 25 mM NaCl, 5 mM Tris-HCl (pH 7.5) or 2 M NaCl, 0.1 mM DTT, 10 mM Tris-HCl (7.5). Purified histone H4 N-terminal tails were examined in either 25 mM NaCl, 5 mM Tris-HCl (pH 7.5) or 90% trifluoroethanol (TFE). TFE was used because it has been shown to stabilize pre-existing regions of α-helical conformation in peptides which may not be maintained in a strictly aqueous solution (Lehrman *et al.*, 1990; Segawa *et al.*, 1991). Figure 17 shows the typical shapes of CD spectra for different secondary structures.

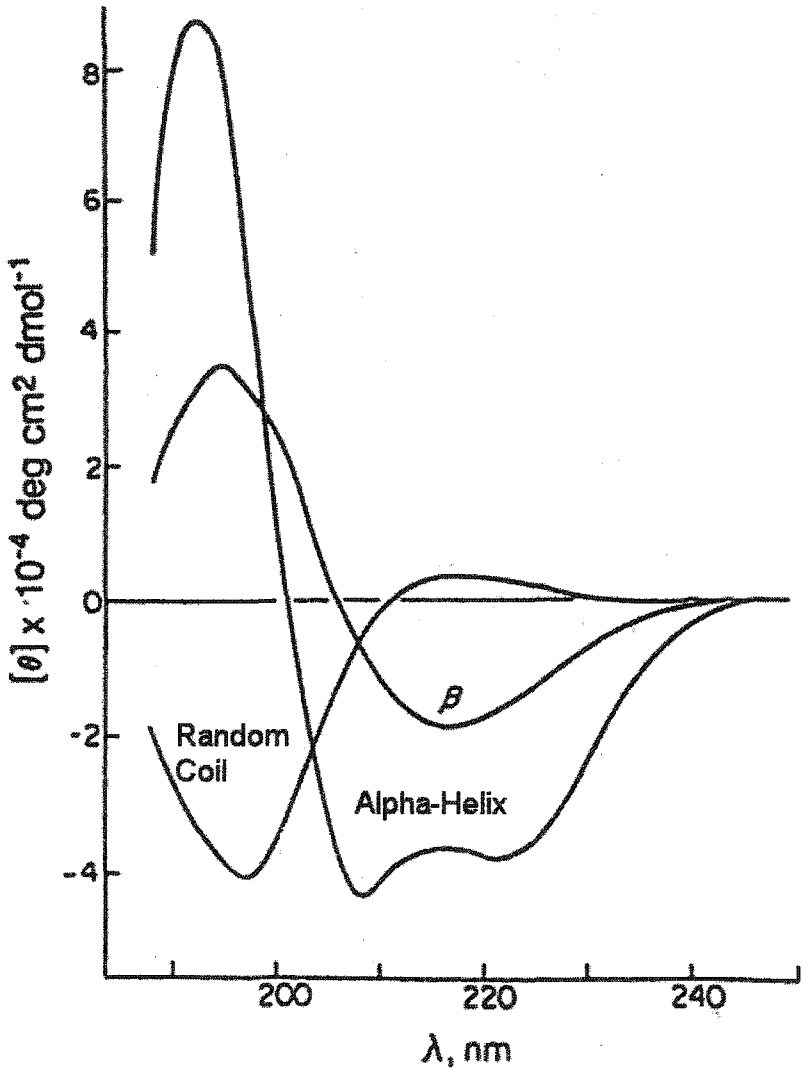


**Figure 17: CD Spectra for Different Secondary Structures.** The random coil spectra shows a single dip at approximately 195 nm; the alpha helix has a double dip typically at 208 nm and 222 nm. All samples are $(lysine)_n$ proteins under different conditions. (Figure adapted from Greenfeld, 1969).

### 2.18.1 Secondary Structure Prediction

Secondary structure prediction was carried out with the help of the DNASTAR Program (DNASTAR Inc. – Madison, WI) using the Protean analysis system tool. Since histone have very little β-sheet structure (Luger *et al.*, 1997; Arents *et al.*, 1991), α-helix content (i.e. percentage) was calculate in two ways using the ellipticity values [θ] at either 220 nm (Verdagauer *et al.*, 1993) or at 222 nm:

Equation 1: $\alpha = 8.9 - 2.4 \times [\theta]_{220} \times 10^{-3}$

or

Equation 2: $\alpha = -3.1\,(1 + [\theta]_{222} \times 10^{-3})$

Equation 2 is based on the assumption that only random coil and helical regions are present.

## 2.19 Analytical Ultracentrifugation

Analytical ultracentrifugation is an effective and important method for characterizing macromolecules like nucleosomes and chromatin fragments (Ausio, 2000). Sedimentation velocity analysis was used to determine sedimentation coefficients and monitor changes in conformation (tertiary and quaternary) and sedimentation equilibrium analysis was used to determine molecular mass and association constants in macromolecular interactions.

This method is useful because sedimentation coefficients can be related to both molecular mass (M) and the translational friction coefficient (f) using the equation:

$$s = M(1 - \acute{\upsilon}\rho)/Nf = M(1 - \acute{\upsilon}\rho)/RTD$$

Where ύ represents the partial specific volume of the macromolecule; ρ, the density of the solvent (g/ml); N, Avogadro's Number; R, the gas constant; T, absolute temperature; and D, the diffusion coefficient. Therefore since the frictional coefficient (f) relies on shape (conformation), the sedimentation values can be used to examine changes in conformation in macromolecules. Partial specific volumes and the estimated molecular masses of the different complexes were determined as described in (Ausio *et al.*, 1989). All sedimentation coefficients (s) are in Svedberg units (S) which are equivalent to $10^{-13}$ seconds.

All analytical ultracentrifugation runs were carried out at 20°C in a Beckman Analytical XL-A Ultracentrifuge (Beckman Spinco Division, Palo Alto, CA) using 12 mm aluminum filled Epon double sector centerpieces. Sedimentation velocity runs used a An-55 (aluminum) rotor whereas sedimentation equilibrium runs used a An-60 (Titanium) rotor. For sedimentation velocity runs nucleosome particles were centrifuged at 40,000 rpm while oligonucleosome particles were centrifuged at 18,000 or 20,000 rpm. Sedimentation Velocity scans were analyzed to determine the sedimentation coefficients using either the Ultrascan-Origin Version 2.93 Sedimentation Data Analysis Software or the XL-A Ultra Scan version 4.1 sedimentation data analysis software (Borries Demeler, Missoula, MT) which employs a published method of boundary analysis (van Holde & Weischet, 1978). Sedimentation equilibrium scans were analyzed using the XLA Data Analysis Software using a nonlinear, least squares, curve fitting algorithm (Johnson, *et al.*, 1998). Figure 18 shows an example of sedimentation velocity data collected before (1) and after (2) van Holde/Weischet analysis.

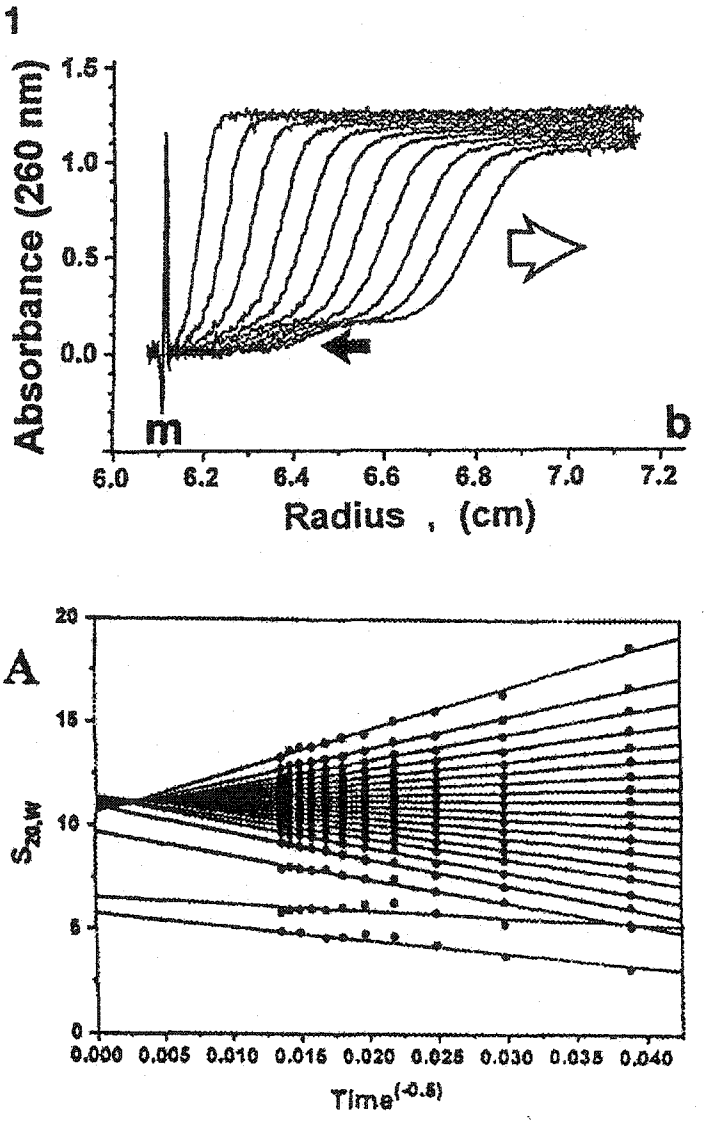


**Figure 18: Examples of Ultracentrifuge Data.** Sedimentation velocity analysis first creates a boundary analysis plot (1) of the data. M, meniscus; dark arrow shows presence of free DNA; large arrow shows boundary movement of the macromolecule. Determining the midpoint of the boundary curves and using van Holde-Weischet analysis of the data produces a van Holde-Weischet plot (A) . This fan-plot is used to obtain the sedimentation coefficient by determining the intersection point on the y-axis. This data was obtained for native chicken erythrocyte nucleosome core particles and all data was recorded at 20°C and 40,000 rpm on a Beckman XL-A analytical ultracentrifuge.

# 3.0 RP-HPLC FRACTIONATED HISTONES AND THE PRODUCTION OF NATIVE-LIKE NUCLEOSOMES PARTICLES AND CHROMATIN COMPLEXES

In order to examine the effects of specific post-translational modifications on both nucleosome and chromatin structure, it is necessary to fully fractionate the core histones. Complete fractionation allows for the subsequent substitution of modified histones for control histones and their comparison in both reconstituted nucleosomes and chromatin complexes. However, production of native-like histones from the various fractionation procedures currently available has been somewhat problematic.

Acid extraction of the histone proteins from cell nuclei was the first method used to purify the basic histone proteins. Modifications combining acid extraction with organic solvents make it possible to purify four different histone fractions (Johns *et al.*, 1964) However, the histones are not fully fractionated and the possibility of protein denaturation and alteration of native conformation, makes their use in subsequent structural studies somewhat suspect.

Salt extraction of cell nuclei and the subsequent use of hydroxyapatite resins and a salt gradients allows the differential disassociation of histones from chromatin into H1, H2A/H2B and H3/H4 fractions (Burton, *et al.*, 1978). The use of salts means that the histones are not denatured however even this method does not accomplish complete separation (See Figure 12). While it is possible to use size exclusion liquid chromatography to successfully fractionate histones, the columns used are very large, require huge quantities of starting material, and literally take several days to complete which increases the probability of possible degradation or contamination problems.

Recently high performance liquid chromatography has become widely used for quick and efficient separation of proteins and peptides. RP-HPLC is capable of purifying individual

histones quickly and efficiently, however there have been concerns about the use of these histones in subsequent structural studies because of possible alterations in native conformation.

The objective of this section was to determine whether RP-HPLC fractionated histones could be successfully used in structural studies. To test this hypothesis histones were extracted from a variety of different sources using different extraction methods. The histones were then purified using RP-HPLC and both native and fractionated histones were reconstituted into either nucleosome core particles or chromatin complexes. These were then compared to native structures using a variety of techniques to see if the reconstituted particles exhibited native-like behavior.

## 3.1 RP-HPLC Fractionation of Core Histones

Reverse-phase HPLC is able to effectively purify even small quantities of proteins, including histones. Depending on the conditions it can now be used to purify some modified and variant histones (Helliger *et al.*, 1988; Gurley *et al.*, 1983; Lindner *et al.*, 1997). Its purification ability is demonstrated in Figure 19 which shows the elution profile of acid-extracted chicken erythrocyte histones. The profile shows that the different histones have been successfully separated in under two hours using 0.1% Trifluoroacetic Acid (TFA) and an increasing concentration gradient of acetonitrile. Figure 20 shows an acetic-acid urea (AU)-PAGE of the different peaks eluted which are numbered 1-6. This gel verifies the complete fractionation of the different core histones with lane 1 being histone H5; lane 2, H1; lane 3, H2B; lane 4, H4; lane 5, H2A, and lane 6, H3 monomers (m) and dimers (d). These histones were also examined using SDS-PAGE in Figure 21. The purified core histones from peaks 3-6 were recombined in stoichiometric amounts and run in lane 3. Lanes 1 and 4 are markers which allow comparison with the total histones (lane 1) or core histones (lane 4) from salt extracted chicken erythrocyte cell nuclei and the total histones from an acid extracted sample

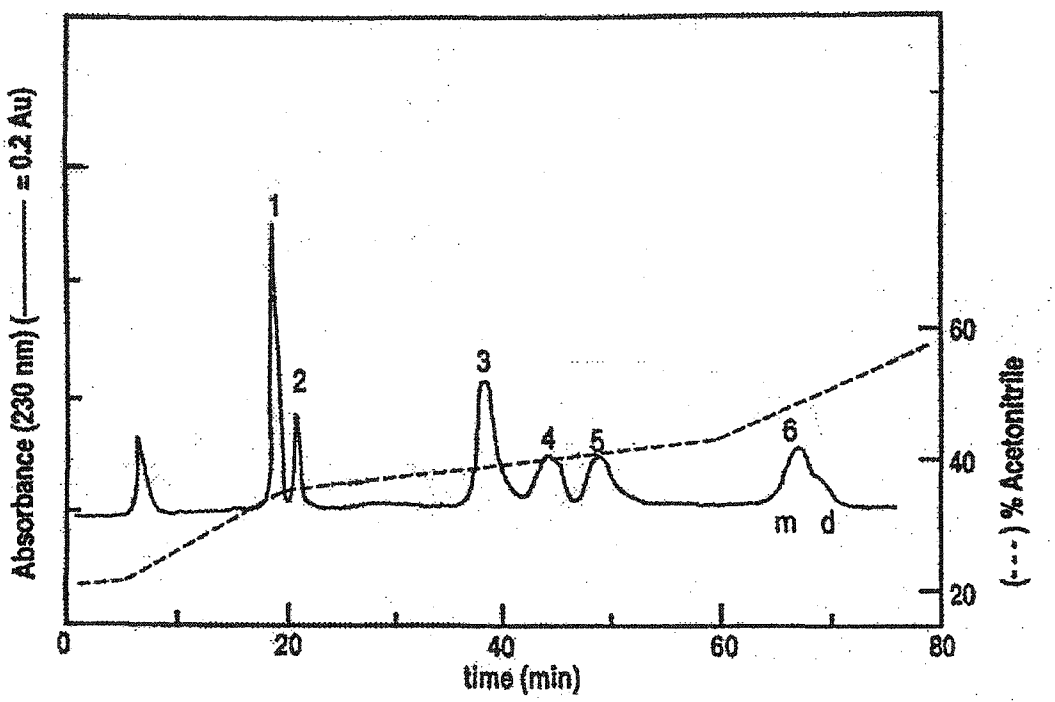


**Figure 19: Histone RP-HPLC Elution Profile.** Approximately 600 μg of acid extracted chicken erythrocyte histones histones were loaded onto a Vydac C18 (0.46cm x 25 cm) column and eluted at 1 ml/min with an acetonitrile gradient (dashed line) in the presence of 0.1% TFA. Absorbances were measured at 230 nm. (Gradient: 25% acetonitrile for 5 minutes; 25-35% over 15 minutes; 37-43% over 40 minutes; and 43-69% over 20 minutes). Aliquots from the six numbered peaks were analyzed by AU-PAGE in Figure 20.

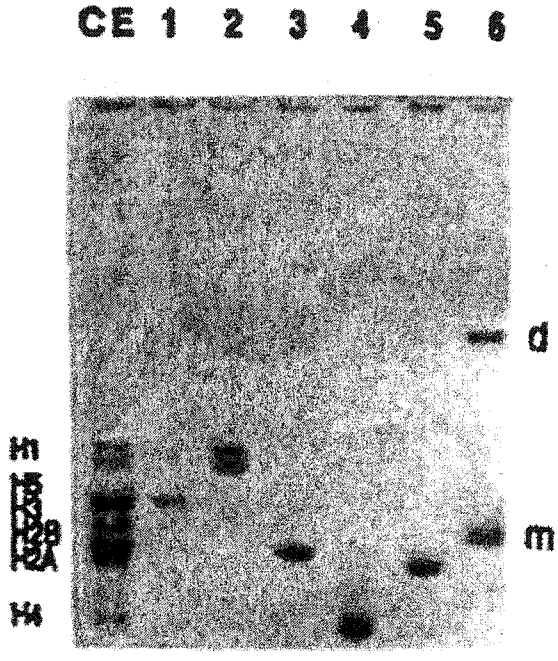


**Figure 20: AU-PAGE of Histone RP-HPLC Elution Profile Fractions.** The numbers (1-6) correspond to the elution peaks from Figure 19. M and d refer to the histone H3 monomers and dimers respectively; CE represents an acid extracted chicken erythrocyte total histone standard. Samples were mixed with 2x AU sample buffer and run on a 2.5 M urea, 5% acetic acid, 15% acrylamide gel at 80 volts in a 5% acetic acid running buffer and stained with Coomassie Blue.

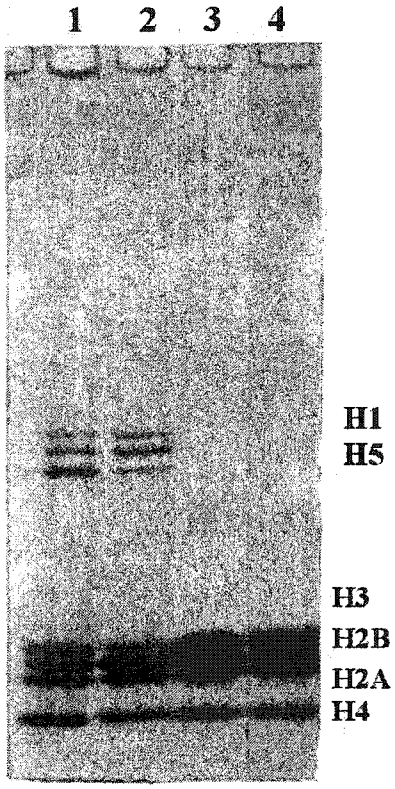


**Figure 21: SDS-PAGE of Histone RP-HPLC Elution Profile Fractions.** Lane (1) salt extracted chicken erythrocyte total histone standard; (2) acid extracted chicken erythrocyte total histone standard; (3) stoichiometric mixture of RP-HPLC fractionated core histones combined from elution peaks 3-6 (see Figure 19); and (4) salt extracted chicken erythrocyte core histone standard. All samples were mixed with 2x SDS sample buffer and boiled for 5 minutes prior to loading on a 6% stacking, 15% separating SDS-PAGE which was run at 100 volts in a 0.05 M Tris-base, 0.38 M glycine, 0.1% SDS running buffer. The gel was stained with Coomassie Blue.

(lane 2). Comparisons of lane 3 and 4 show that the fractionated histones appear comparable to core histones obtained from salt extraction of native chicken erythrocyte nucleosomes.

While the elution profile (Figure 19) and gels (Figures 20, 21) show that fractionation is possible and that the histones appear normal, however there are still concerns as to whether such histones should be used in subsequent structural studies. This is because the buffers used to elute the proteins, namely 0.1% (v/v) TFA and the organic solvent acetonitrile (ACN). Acetonitrile in high concentrations can adversely affect protein structure (Hallin *et al.*, 1985). If ACN alters the native conformation of the histones, this would greatly affect the validity and implications of any structural studies they may be used for.

To analyze the affects of RP-HPLC on histone structure, native and RP-HPLC fractionated histones were compared and examined using analytical ultracentrifugation and sedimentation velocity analysis and circular dichroism. (Figure 22 shows an experimental outline). Nucleosome core particles were produced from salt extracted chicken erythrocyte cell nuclei and the total core histones were obtained using hydroxyapatite column chromatography with 2 M NaCl in 0.1 M potassium phosphate (pH 6.8) buffer. Half the histones were used as a native control and the other half were dialyzed versus water, lyophilized and then separated by RP-HPLC (as per Figure 19). The peaks corresponding to the core histones were mixed in stoichiometric amounts and lyophilized. For the sedimentation velocity analysis the different histone samples were dialyzed against 2 M NaCl, 10 mM Tris-HCl (pH7.5), 1 mM EDTA as under these conditions the histones associate into the histone octamers. Figure 23 shows the sedimentation velocity results for both samples.

The sedimentation velocity analysis of the native core histones (Figure 23, sample 1) indicates that the native sample is very homogenous as shown by the convergence of the fan plot to one point. The sedimentation value was determined by the y-axis intercept point was found to be $3.8 \pm 0.2$S which was as expected and is in agreement with

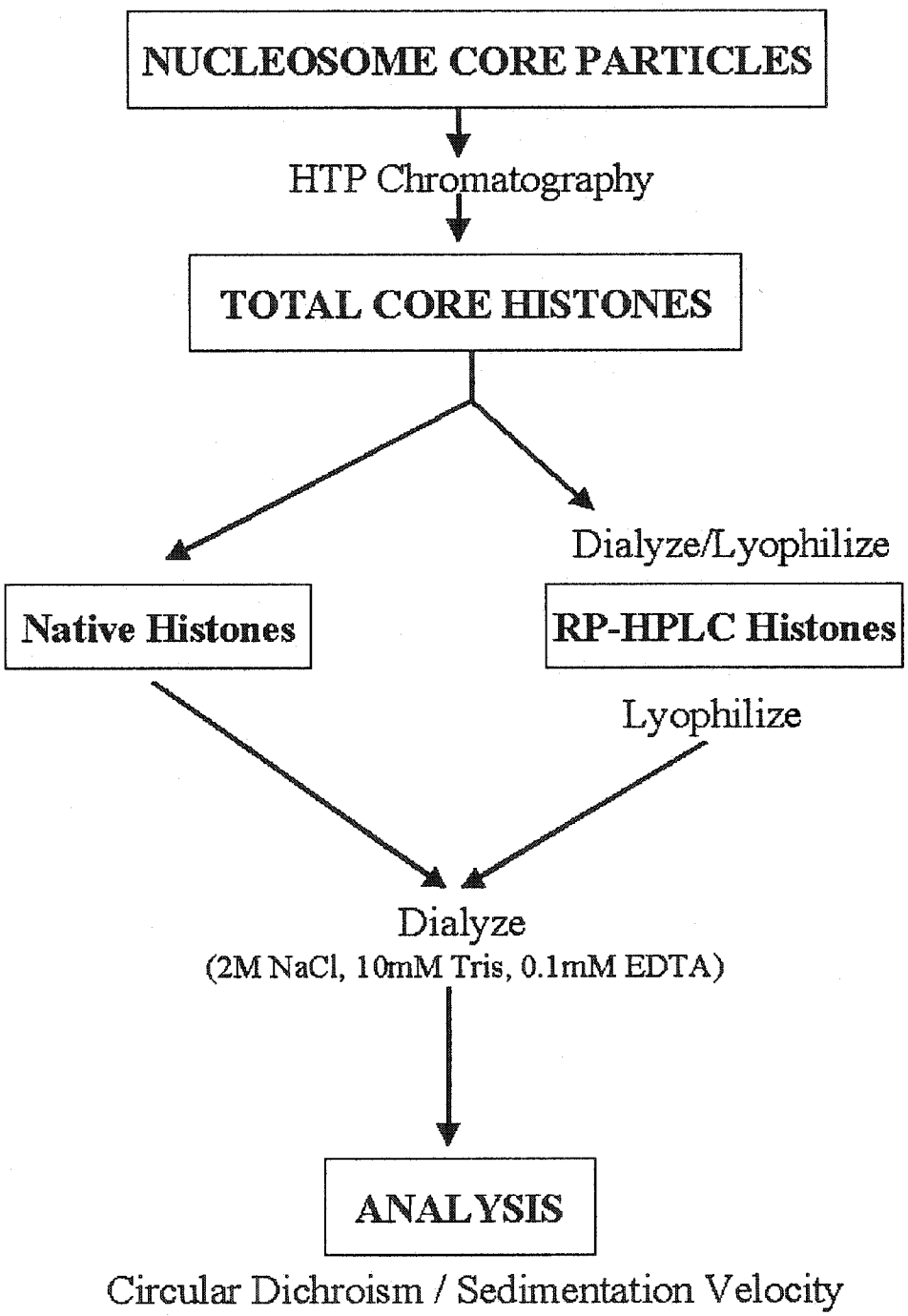


**Figure 22: Experimental Outline to Analyze Native and RP-HPLC Fractionated Histones.**

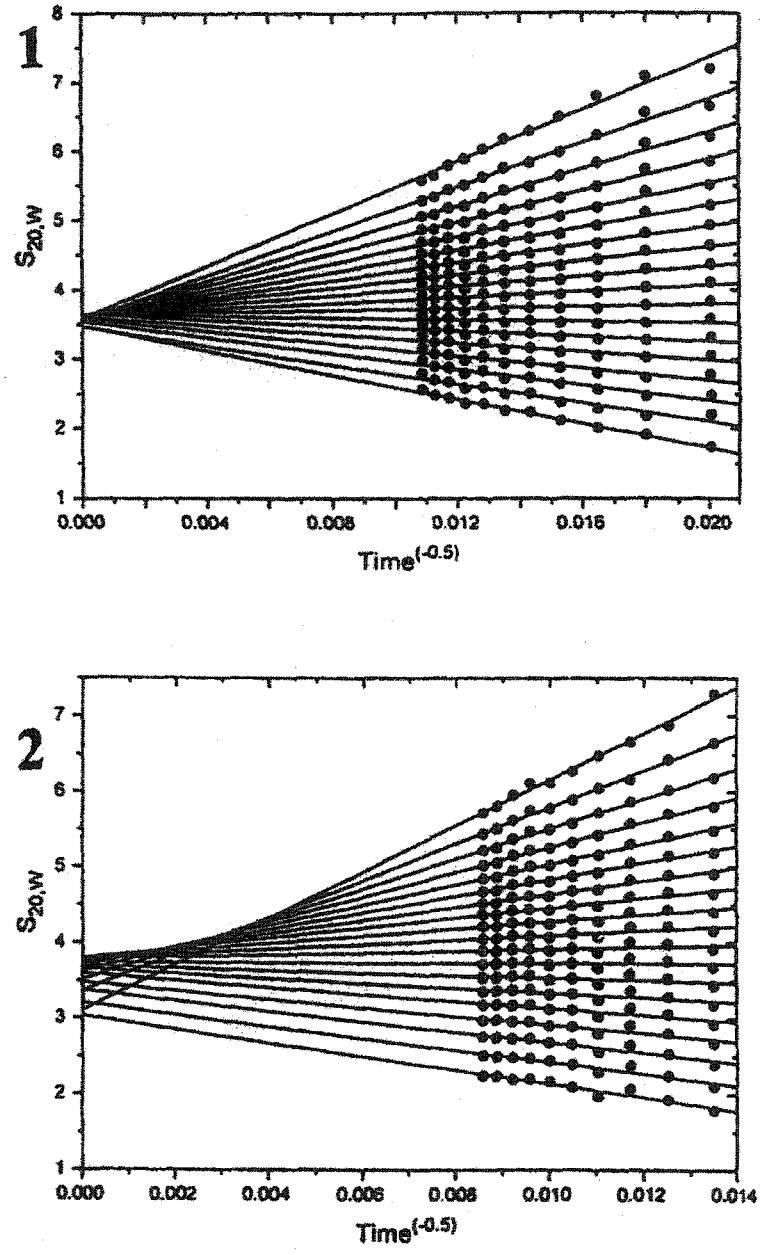


**Figure 23: Sedimentation Velocity Analysis of Native and RP-HPLC Fractionated Histones.** (1) native core histones; (2) RP-HPLC fractionated core histones. Both samples were dialyzed against 2M NaCl, 10 mM Tris-HCl (pH 7.5). Samples were analyzed at 20°C and 44,000 rpm in a Beckman XL-A analytical ultracentrifuge.

previous reports (Chung, *et al.*, 1978). The RP-HPLC fractionated histones (Figure 23, sample 2) however do not sediment as well as the native histones. The more dispersed fan plot shows that there is a significant amount of heterogeneity. Only about 50% of the sample sediments at 3.8S while the rest of the sample has lower $S_{20,w}$ values. This indicates that these histones have an altered configuration, do not appear to associate properly and therefore do not behave in a completely native-like manner.

In order to look at the secondary structure of the histones more closely, the two samples were dialyzed against a low salt buffer (10 mM sodium phosphate pH 7.2) and then analyzed using circular dichroism (CD). Circular dichroism is an effective way to detect changes in protein secondary structure and can be used to determine the percentage of α-helical content in a protein. The CD results for both samples are shown in Figure 24. The native histones (sample 1) produced a spectrum which is typical of proteins containing α-helices, i.e. there are two peak minima at approximately 208 nm and 222 nm, and the results are almost identical to that previously reported by Prevelige & Fasman (1987). The RP-HPLC fractionated histones (Sample 2) while having a similar shaped spectrum is shifted upwards which indicates a significant reduction in the molar ellipticities at 222 nm and 208 nm. At 222 nm this represents decrease of approximately 15% in the overall α-helical content of the histones. This upwards shift of the spectrum is a clear indication that there are changes in the secondary structure and that acetonitrile does appear to denature the histone proteins. As a result of the denaturation the histones are unable to associate correctly which produces the heterogeneity and variation in sedimentation values demonstrated by the sedimentation velocity analysis.

## 3.2 Reconstituted Nucleosome Core Particles with RP-HPLC Fractionated Histones

The use of acetonitrile during HPLC fractionation of the histones clearly has some denaturing effects on the proteins. Therefore if the histones could be renatured after

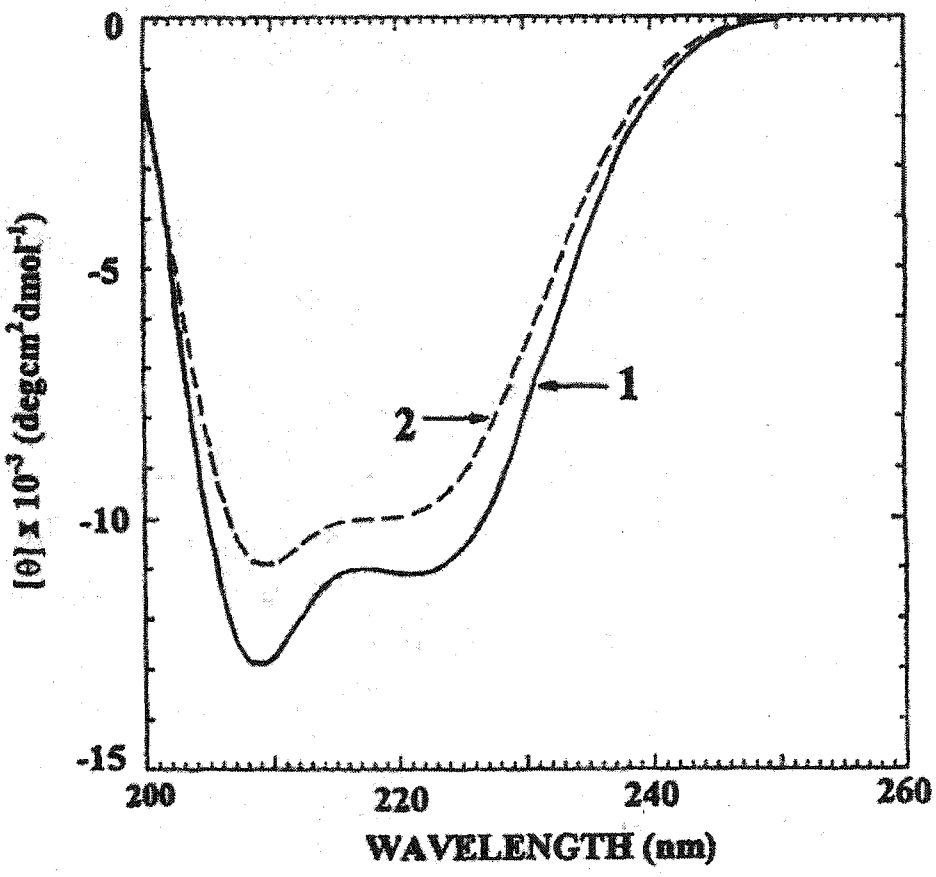


**Figure 24: CD Analysis of Native and RP-HPLC Fractionated Histones.** 1, Native histones; 2, RP-HPLC fractionated histones. For analysis both samples were dialyzed against 10 mM sodium phosphate (pH 7.2) buffer prior to analysis. CD spectra were recorded at 20°C on a Jasco J-720 spectropolarimeter.

separation it may be possible to produce native-like proteins which can be used in subsequent studies. It was decided to test whether treatment with 6 M guanidine hydrochloride (GdnHCl) after RP-HPLC fractionation would be able to renature the histones and produce native-like proteins which would allow them to be used for nucleosome reconstitution experiments and further structural analysis.

A flowchart (Figure 25) outlines the general strategy used for this series of experiments. As before, nucleosome core particles from salt extracted chicken erythrocyte cell nuclei were produced. A fraction of these core particles (Sample A) was kept as a control for native, untreated nucleosomes. Histones were obtained from the remaining nucleosomes using hydroxyapatite chromatography. After the core histones were eluted from the HTP column, the random sequence chicken 146 bp DNA fragments were also eluted from column using 0.5 M potassium phosphate (pH 6.8) buffer and were dialyzed versus the buffer and retained for future reconstitutions. The native histones were then divided into three fractions. The first fraction (Sample B) was kept as a positive control for native histones. The second fraction (Sample C) were separated using RP-HPLC and then processed as before, i.e. lyophilized and then resuspended in a 2 M NaCl buffer. This fraction (C) therefore acted as a negative control as RP-HPLC fractionated histones have already been shown to be denatured. The last fraction (Sample D) was also fractionated using RP-HPLC but processing was modified in an attempt to renature the proteins. After fractionation, the lyophilized histones were resuspended and incubated at 2 mg/ml in 6M GdnHCl, 20 mM β-mercaptoethanol buffer which was later removed by dialysis. All three histone samples (B-D) were dialyzed overnight against 2 M NaCl buffer and reconstituted into nucleosome core particles using 146 bp DNA and salt gradient dialysis. The reconstituted nucleosomes (B-D) were compared to the native nucleosomes (A) using sedimentation velocity analysis, circular dichroism and DNase I footprinting.

Analytical ultracentrifugation and sedimentation velocity analysis of the four samples are shown in Figure 26. The letters A-D correspond to the samples designated in the flowchart in Figure 25. Beside each plot is an SDS-PAGE profile of the corresponding

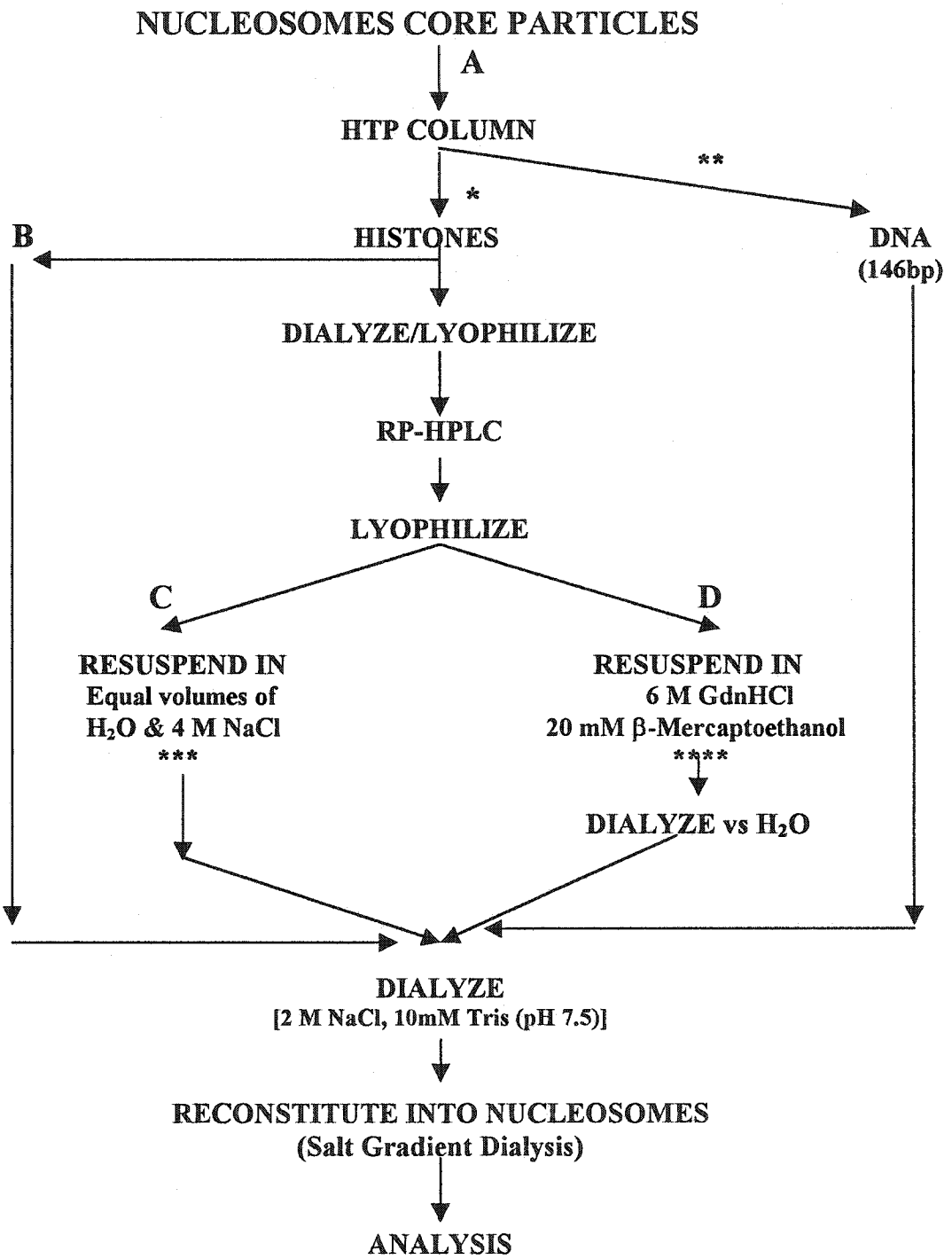


**Figure 25: Experimental Outline to Analyze Nucleosomes Reconstituted with Native and RP-HPLC Fractionated Histones.** Native (A) and reconstituted nucleosome core particles using native (B) and RP-HPLC fractionated histones (C, D) were prepared. (*) Histones eluted in 2 M NaCl, 0.1 M potassium phosphate buffer (pH 6.8). (**) Nucleosomal DNA eluted in 0.5 M potassium phosphate buffer (pH 6.8). (***)Final buffer was 2 M NaCl, 50 mM Tri-HCl (pH 7.5), 1 mM EDTA, 1mM DTT. (****) 6M GdnHCl in 50 mM Tris-HCl (pH 7.6).

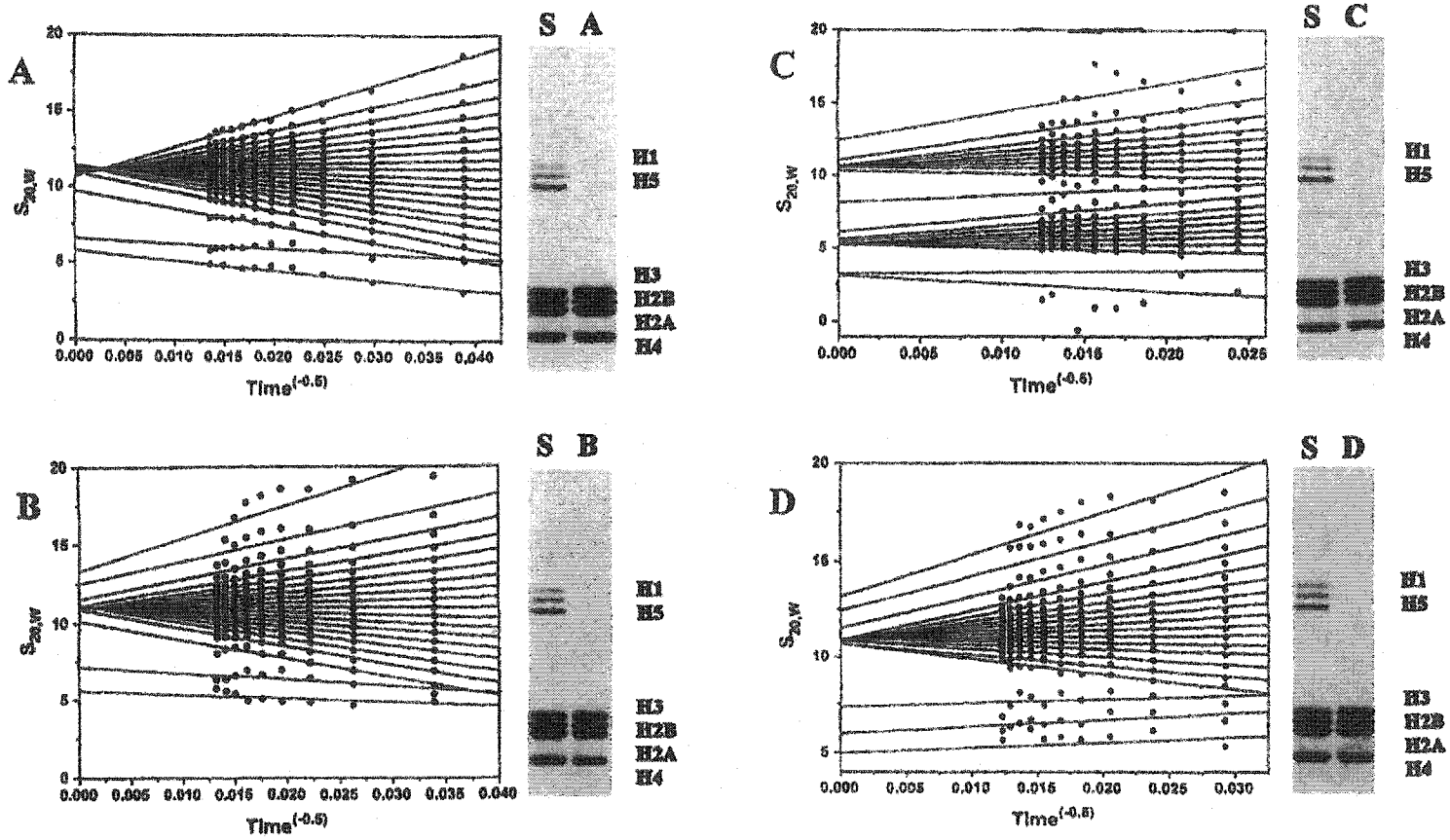


**Figure 26: Sedimentation Velocity Analysis of Nucleosomes Reconstituted with Native and RP-HPLC Fractionated Histones.** (A) native nucleosome core particles (B) reconsituted nucleosomes with HTP purified core histones; (C) reconstituted nucleosomes with RP-HPLC fractionated histones; (D) reconstituted nucleosomes with RP-HPLC purified histones treated with guanidine hydrochloride. Sedimentation velocity runs were performed at 20°C and 40,000 rpm in 0.1 M NaCl, 20 mM Tris-HCl (pH 7.5), 0.5 mM EDTA in a Beckman XL-A Analytical Ultracentrifuge. $S_{20,w}$ (Svedbergs) and analysis done according to van Holde and Weischet (1978). SDS-PAGE of each sample (A-D) are shown to right of corresponding plot where S is a chicken erythrocyte whole histone standard. SDS-PAGE 6% stacking 15% separating gel run at 100 volts in 0.05 M Tris-base, 0.38 M glycine, 0.1% SDS running and stained with Coomassie Blue.

nucleosomal histones compared to a chicken erythrocyte whole histone marker. The SDS-PAGE show that all the core particles produced contained stoichiometric amounts of proteins.

Comparison of the sedimentation velocity analysis results show that the native nucleosomes (A), and reconstituted nucleosomes with either native (B) or GdnHCl treated RP-HPLC fractionated histones (Sample D) all have very similar shaped fan plots. The sedimentation coefficients determined from each of the plots for samples A, B, and D were consistent and were determined to be 11.06, 11.07, and $10.9 \pm 0.2$S respectively. In contrast the reconstituted nucleosomes with untreated RP-HPLC fractionated histones (C) shows distinct differences from the other three samples.

The fan plot for Sample C has two distinct populations. The first group are nucleosomes which sediment at $10.6 \pm 0.2$S. The second group sediments at $5.4 \pm 0.2$S and represents free 146 bp DNA (Ausio *et al.*, 1984). Comparing the plots for the RP-HPLC fractionated histones clearly shows a distinct difference between the RP-HPLC histones which were untreated or treated with GdnHCl. The untreated histones (C) show distinct structural differences from the native nucleosomes (A) whereas the GdnHCl treated histones (D) are virtually indistinguishable from both the native nucleosomes (A) as well as nucleosomes reconstituted with native histones (B). This appears to indicate that treatment with GdnHCl was successful and helps to renature RP-HPLC fractionated histones.

Next the nucleosomes were analyzed using circular dichroism to determine if there were any obvious changes in secondary structure. The circular dichroism results are shown in Figure 27. Once again the native core particles (A) and nucleosomes reconstituted with histone fractions B and D all show very similar profiles. However the spectra for nucleosomes reconstituted with untreated HPLC fractionated histones (C) shows a definite change in structure as indicated by the distinct upward shift of the spectra. This shift is attributed to the presence of a larger quantity of free DNA. These data therefore

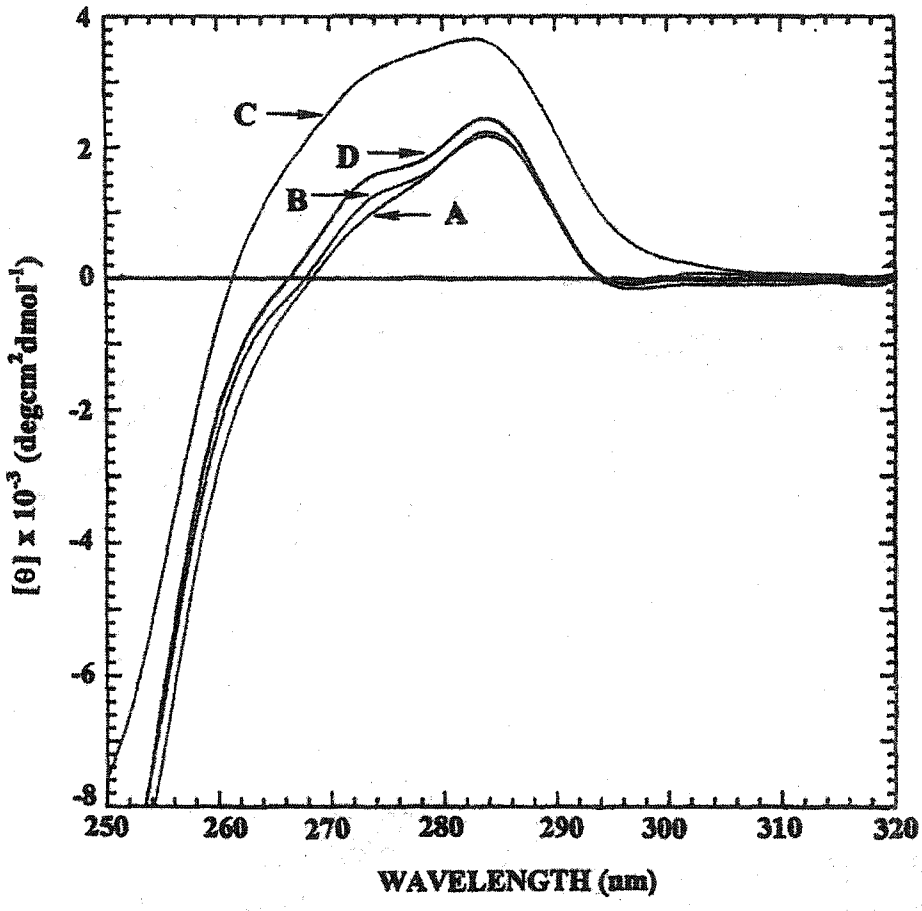


**Figure 27: CD Analysis of Nucleosomes Reconstituted with Native and RP-HPLC Fractionated Histones.** CD spectra for native nucleosome core particles (A); nucleosome core particles reconstituted with native histones (B); RP-HPLC fractionated and untreated histones (C); and RP-HPLC fractionated histones renatured with guanidine hydrochloride (D). All CD spectra were recorded at 20°C on a Jasco J-720 spectropolarimeter in 25 mM NaCl, 5 mM Tris-HCl (pH 7.5) buffer.

support the premise that guanidine hydrochloride treatment of RP-HPLC fractionated histones helps to create native-like histones and therefore nucleosomes.

To further investigate the properties of the different nucleosome samples, possible differences in nuclease accessibility were examined using DNase I footprinting. The different nucleosomes samples (A-D) plus nucleosomes reconstituted with histones previously frozen at -80°C prior to reconstitution (Sample B*) were 5'end-labelled with [$\gamma$-$^{32}$P]-ATP and then digested with DNase I (as per Section 2.13.7). The resulting DNA fragments were run on a 10% (v/v) 20:1 acrylamide:bis-acrylamide, 7M urea gel to visualize the DNase I cleavage sites and Figure 28 shows the DNase I footprint produced with the different nucleosome particles. The preferred DNase I cleavage sites are designated as S1 to S14. This gel indicates that the native nucleosomes (A) and reconstituted nucleosomes with either native histones (B & B*) or HPLC fractionated histones treated with guanidine hydrochloride (D) all show identical profiles. The reconstituted nucleosomes with untreated RP-HPLC fractionated histones (C) however do show some differences in digestion which is most obvious between the S2 and S4 preferred cleavage sites. The increased intensity of bands between the preferred sites and the decrease in intensity at the preferred sites, are obvious indications of a change in cleavage behavior which is probably due to the larger quantity of free DNA present.

The results of the circular dichroism, sedimentation velocity and DNase I footprinting, all indicate that the untreated RP-HPLC fractionated histones are denatured and therefore produce anomalous results. However if these histones are processed with guanidine hydrochloride prior to reconstitution they then produce native-like histones and nucleosomes which appear to be virtually indistinguishable from their native counterparts.

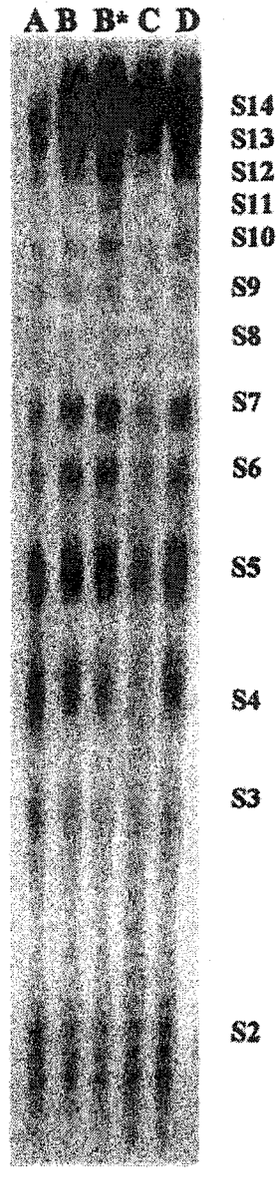


**Figure 28: DNase I Footprint of Nuclueosomes Reconstituted with Native and RP-HPLC Fractionated Histones.** Native nucleosomes (A); nucleosome core particles reconstituted with: native histones (B); untreated RP-HPLC fractionated histones (C); or RP-HPLC fractionated histones renatured with GdnHCl (D). (B* native histones frozen prior to reconstitution). S1-S14 represent preferential DNase I cleavage sites with respect to the labelled 5'-end of the nucleosome core particle. All samples were 5'-end labelled with [$\gamma$-$^{32}$P]ATP and digested with 70 units DNase I/ml at 0°C. All samples were heated at 90°C for 10 minutes prior to loading on a 10% acrylamide (20:1 acrylamide:bis-acrylamide), 7M urea, 1xTBE gel and run at 60 watts for approximately 2 hours using a 1xTBE running buffer. The gel was fixed in 10% acetic acid, 10% methanol for 60 minutes, dried and autoradiographed.

## 3.3 Effects of Extraction Method and Biological Source

Since it is now possible to use RP-HPLC fractionated histones to produce native-like histones and nucleosome particles, it was decided to investigate whether either the method of histone extraction or the biological source of the histones would have any effect on this procedure. To compare biological source, three different samples of histones were used namely: chicken erythrocyte cell nuclei, and alligator and lamprey testes. To compare extraction methods chicken erythrocyte cell nuclei were both acid extracted and salt extracted. All RP-HPLC fractionated histones were treated with GdnHCl, reconstituted into nucleosomes and their structures compared to native nucleosomes and each other using PAGE, sedimentation velocity analysis and DNase I digestion.

### *3.3.1 Biological Source*

Figure 29 shows an SDS-PAGE of the three acid extracted histone samples. Lane 1 is a chicken erythrocyte total histone standard which was compared to the acid extracted chicken (lane 2), alligator (lane 4) and lamprey (lane 6) starting samples. The acid extracted samples, particularly the chicken (lane 2) and alligator (lane 4) show a depletion of H3 and H4 histones which indicate that the acid extraction method can be problematic by producing a non-stoichiometric mix of histones. All three samples (2, 4, 6) were then individually fractionated by RP-HPLC and the purified core histones were mixed in stoichiometric amounts and reconstituted into nucleosomes after guanidine hydrochloride treatment. The same histones after fractionation, GdnHCl treatment and reconstitution are shown; chicken in lane 3, alligator in lane 5 and lamprey in lane 7. When these samples (lanes 3, 5, 7) are compared to their pre-fractionation counterparts (lanes 2, 4, 6) you can see that they now show a stoichiometric mix of strictly core histones which run the same as the total histone standard (lane 1).

Sedimentation velocity results for the three reconstituted nucleosome samples are shown in Figure 30. The fan plots show that all the acid extracted samples produced

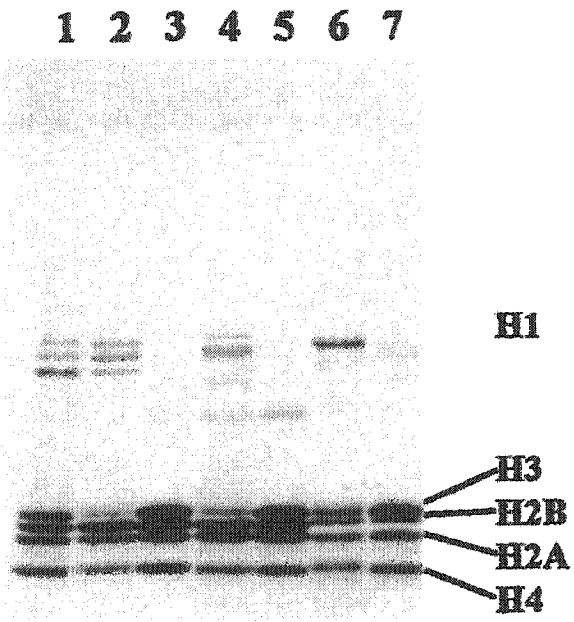


**Figure 29: SDS-PAGE of Acid-Extracted Histones from Different Biological Sources.** The linker and core histones are identifed at the side of the gel. Lane 1, chicken erythrocyte total histone marker; Lanes 2-7 are acid-extracted histones before (lanes 2, 4, 6) and after RP-HPLC fractionation (lanes 3, 5, 7). Biological sources used were chicken erythrocytes (lanes 2, 3), alligator testes (lanes 4, 5) and lamprey testes (lanes 6, 7). All samples were mixed with SDS sample buffer and boiled 5 minutes prior to loading. The 6% stacking gel, 15% separating SDS-PAGE was run at 100 volts in a 0.05 M tris, 0.38 M glycine, 0.1% SDS running buffer and stained with Coomassie Blue.

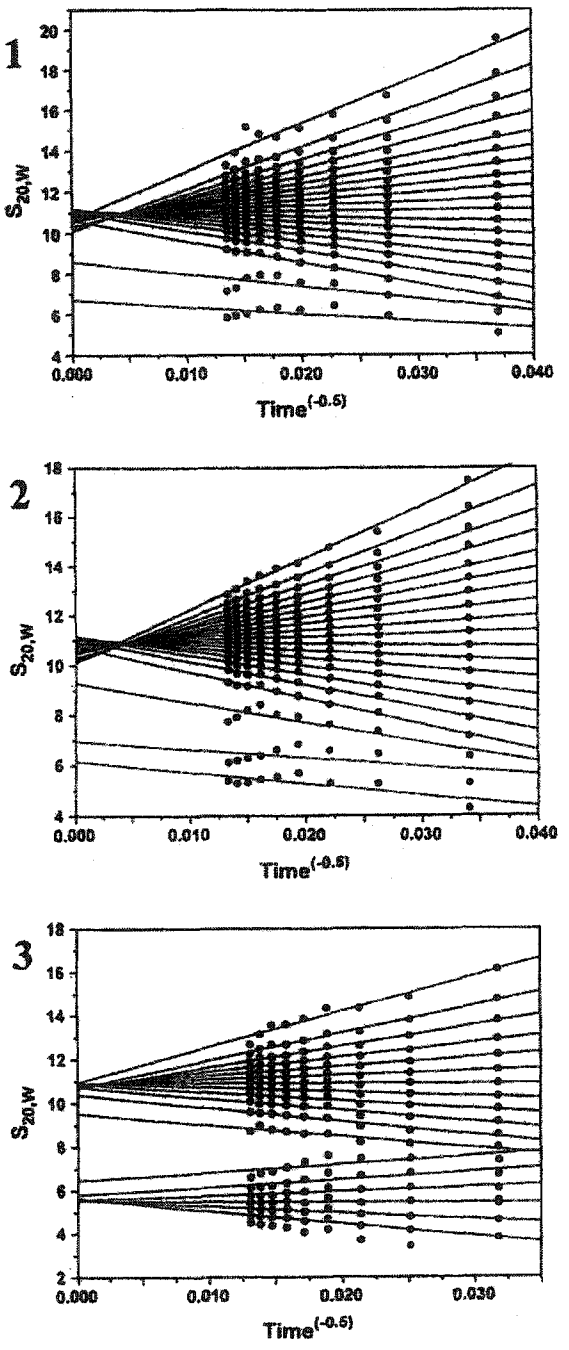


**Figure 30: Sedimentation Velocity Analysis of Nucleosomes with Histones from Different Biological Sources.** All samples; (1) chicken erythrocyte, (2) alligator, (3) lamprey; used acid extracted, RP-HPLC fractionated histones treated with GdnHCl prior to reconstitution of nucleosomes. Sedimentation velocity runs done in a Beckman XL-A analytical ultracentrifuge at 20°C and 40,000 rpm in 0.1 M NaCl, 20 mM Tris-HCl (pH 7.5), 0.5 mM EDTA buffer. Analysis carried out according to van Holde and Weischet (1978).

nucleosome particles with sedimentation values of approximately 10.9 $\pm$ 0.2S which is within expected values and compare well to the native nucleosomes at 11.06 $\pm$ 0.2S seen in Figure 26 (Sample A). However the lamprey sedimentation fan plot (Figure 30, sample 3) does show a discrepancy in that while approximately 60-70% of the reconstituted sample consists of nucleosomes which sediment at 10.8 $\pm$ 0.2S there is about 30% of the sample which sediments at 5.7S and corresponds to naked DNA. This is a significant amount of free DNA when compared to that seen in the other samples and indicates nucleosomal instability. A lack of sample meant that it was not possible to determine whether the decrease in nucleosome stability was an intrinsic property of lamprey histones or a result of handling or reconstitution problems prior to its analysis. Consequently, with the exception of the lamprey sample, the source of histone sample does not appear to affect the ability of guanidine hydrochloride treatment to reverse the structural changes introduced by RP-HPLC fractionation. Both the acid-extracted chicken and alligator samples produced consistent plots and results with the sedimentation velocity analysis.

To further examine the effect of sample source, a DNase I digestion of the three reconstituted nucleosomes was also done. The results are shown in Figure 31 and indicate that all three samples chicken (lane 1), alligator (lane 2) and lamprey (lane 3) produced nucleosomes which appear normal with no obvious differences in DNase I digestion patterns. Even the lamprey nucleosomes show no significant differences which indicates that the nucleosomes produced did behave normally under these conditions.

### 3.3.2 Comparison of Extraction Methods

It has been speculated that acid extraction may change the histone's native conformation. As previously shown in Figure 29, an SDS-PAGE of acid extracted histones from chicken erythrocyte cell nuclei can produce non-stoichiometric mixtures of histones (lane 2) when compared to their salt extracted equivalents (lane 1) indicating that extraction methods can have a significant impact on histones. However stoichiometric mixtures can

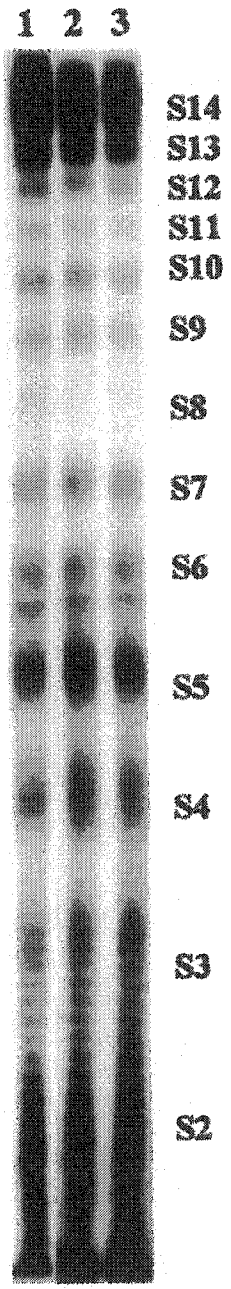


**Figure 31: DNase I Footprint of Nucleosomes with Histones from Different Biological Sources.** All samples: (1) chicken, (2) alligator and (3) lamprey; used acid extracted, RP-HPLC fractionated, guanidium chloride treated histones prior to reconstitution. Nucleosomes were 5'-end labelled with [$\gamma$-$^{32}$P]ATP, digested with 70 units DNase I/ml at 0°C for 80 minutes. All samples (in 10 mM NaCl, 10 mM Tris-HCl (pH 7.5), 1mM EDTA) were run on a 10% acrylamide (20:1 acrylamide:bis-acrylamide), 7M urea, 1xTBE gel at 60 watts for approximately 2 hours in a 1xTBE running buffer. The gel was fixed, dried and autoradiographed. S1-14 are sites of preferential DNase I cleavage with repect to the labelled 5'-end of the nucleosome core particle.

be produced from histones which have been RP-HPLC fractionated and treated with GdnHCl. Therefore acid and salt extracted histones from chicken erythrocytes were compared to assess the effectiveness of the GdnHCL treatment of RP-HPLC fractionated histones.

The sedimentation velocity results for nucleosomes reconstituted with RP-HPLC fractionated, GdnHCL treated acid extracted histones and salt extracted native nucleosome samples are shown in Figures 32, 33 and 34. Figure 32 shows the initial boundary analysis of the two samples which are similar and indicate the presence of some free DNA (see solid arrows). When these data are analyzed using the van Holde-Weischet method (1978), typical fan plots (shown in Figure 33) are produced that allow the determination of the sedimentation coefficients from the Y-axis intersection points. Comparison shows that both samples produce nucleosomes (N) with sedimentation coefficients of $11.06 \pm 2S$ and $10.9 \pm 2S$ for the native salt extracted (1) and acid extracted (2) samples respectively. The presence of some free DNA is also shown (D). The data can also be presented to show the integral distribution of the sedimentation coefficients using the van Holde-Weischet method (Figure 34). The method shows the sedimentation coefficients ($S_{20,w}$) more clearly by the positioning of the data points over the X-axis and indicates the presence of nucleosomes and free DNA (solid arrow). The SDS-PAGE of the nucleosomal histones from both samples compared to a chicken erythrocyte total histone marker are shown as an inset for each figure and indicate that both samples contain stoichiometric amounts of histones. Consequently the sedimentation velocity data indicates that the extraction method has no affect on the production of native-like nucleosome particles using this method.

DNase I digestion of both nucleosome samples are compared in Figure 35. These results also indicate that there are no significant changes in the digestion patterns thereby confirming the sedimentation velocity results. Together these results indicate that the regardless of the extraction method used, native-like nucleosomes can be produced from RP-HPLC fractionated histones which have been treated with guanidine hydrochloride prior to reconstitution.

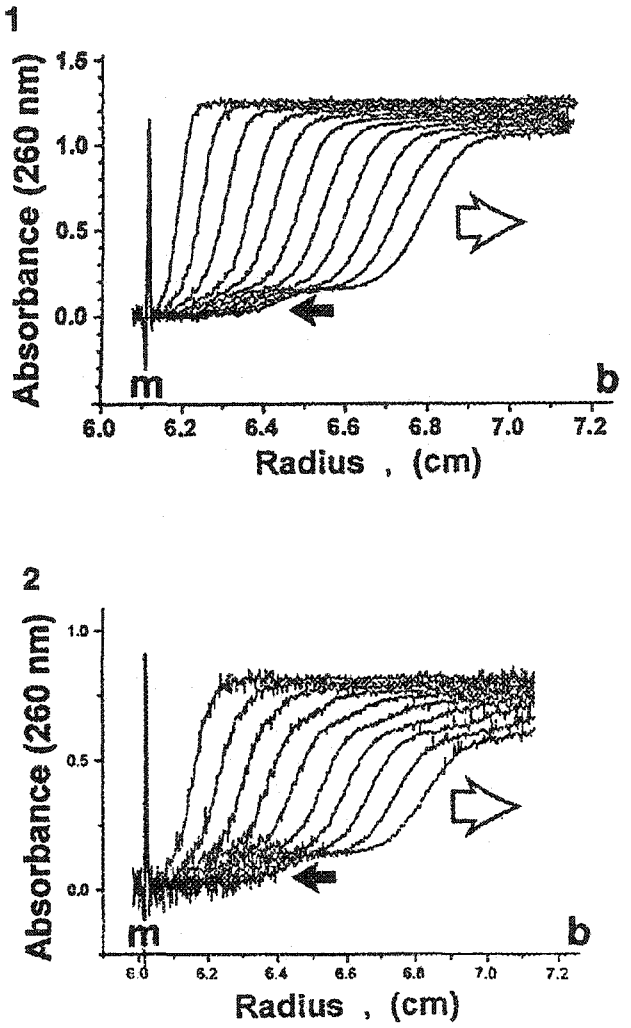


**Figure 32: Sedimentation Velocity Boundary Analysis of Nucleosomes with Histones from Different Extraction Methods**. (1) Native nucleosomes – salt extracted; (2) reconsituted nucleosomes – acid extracted, RP-HPLC purified, GdnHCl treated histones. Both samples produced from chicken erythrocytes. Solid arrow points to the presence of naked (146 bp) DNA; open arrows shows the direction of sedimentation; M, meniscus; b, bottom of cell. The sedimentation velocity analysis was carried out at 40,000 rpm in 0.1 M NaCl, 20 mM Tris-HCl (pH 7.5), 0.5 mM EDTA at 20°C in a Beckman XL-A ultracentrifuge.

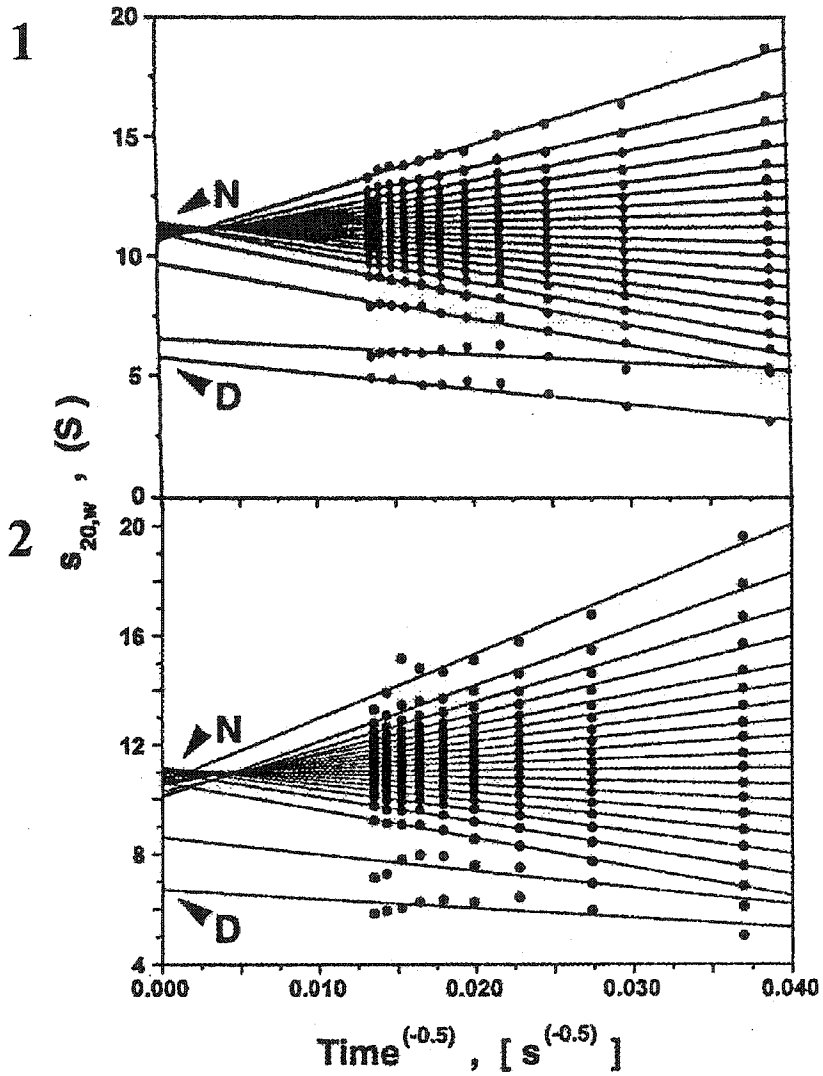


**Figure 33: Sedimentation Velocity van Holde/Weischet Analysis of Nucleosomes with Histones from Different Extraction Methods.** (1) native nucleosomes – salt extracted; (2) reconsituted nucleosomes - acid extracted, RP-HPLC purified, GdnHCl treated histones. Both samples were produced from chicken erythrocytes. Analysis was carried out according to van Holde and Weischet (1978). The lines converge toward a common $S_{20,w}$ value (S in Svedberg units), N for nucleosomes, D for free DNA. Time units are in seconds. Analysis was carried out at 20°C and 40,000 rpm in 0.1 M NaCl, 20 mm Tris-HCl, 0.5 mM EDTA (pH 7.5) in a Beckman XL-A ultracentrifuge.

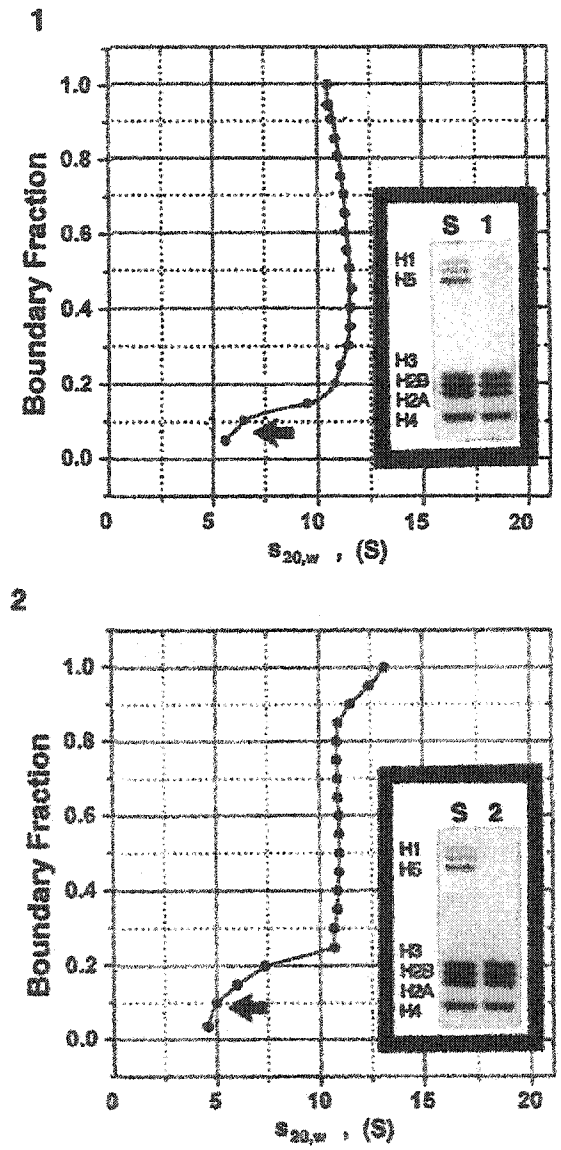


**Figure 34: Sedimentation Velocity Integral Distribution Analysis of Nucleosomes with Histones from Different Extraction Methods.** (1) native nucleosomes – salt extracted; (2) reconstituted nucleosomes - acid extracted, RP-HPLC purified, GdnHCl treated histones. Both samples produced from chicken erythrocytes. The graphs represent the integral distribution of the sedimentation coefficient (in Svedberg units, S) obtained after analysis of the boundaries shown in Figure 32 using van Holde and Weischet method (1978). The ordinate represents the fraction of material sedimenting with an $s_{20,w}$ given on the abscissa. Solid arrows point to presence of naked DNA (146 bp). The sedimentation velocity analysis was carried out at 40,000 rpm in 0.1 M NaCl, 20 mM Tris-HCl (pH 7.5), 0.5 mM EDTA at 20°C in a Beckman XL-A analytical ultracentrifuge. The insets show an SDS-PAGE of the histones from the corresponding nucleosomes where S is chicken erythrocyte histone standard.

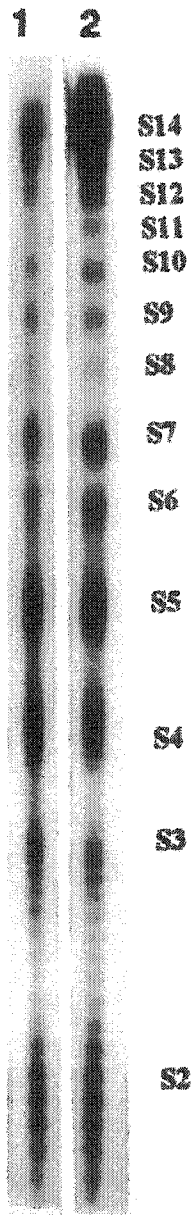


**Figure 35: DNase I Footprint Analysis of Nucleosomes with Histones from Different Extraction Methods.** Both samples are produced from chicken erythrocytes. (1) native nucleosome core particles and (2) reconstituted nucleosome core particles from RP-HPLC purified, GdnHCl treated histones. The S2-S14 indicate preferential DNase I cleavage sites with respect to the 5' end of the nucleosome core particle. All samples were 5'-end labeled with [γ-32P]ATP and digested with 70 units DNase I/ml at 0°C for 80 minutes. All samples (in 10 mM NaCl, 10 mM Tris-HCl (pH 7.5), 1 mM EDTA buffer) were run on a 10% acrylamide (20:1 acrylamide:bis-acrylamide), 7 M urea, 1x TBE gel at 60 watts for approximately 2 hours using a 1xTBE running buffer. The gel was fixed, dried and autoradiographed.

## 3.4 Reconstitution of Chromatin Complexes with RP-HPLC Fractionated Histones.

While the production of native-like proteins and nucleosomes is important, it was also necessary to determine if RP-HPLC fractionated, GdnHCl treated histones could be used to produce native-like chromatin complexes. (Figure 36 shows the experimental outline). To reconstitute chromatin complexes, the histones were once again either acid extracted or salt extracted from chicken erythrocyte cell nuclei, purified using RP-HPLC, renatured using GdnHCl and then reconstituted onto a chromatin DNA template using salt gradient dialysis. The chromatin DNA template was a sequence specific oligonucleosome fiber consisting of 12 tandem repeats of a 208 bp fragment of the 5S rRNA gene from the sea urchin *Lytechinus variegatus* (Simpson *et al.*, 1985). The reconstituted chromatin complexes therefore produce homogenous oligonucleosome fibers which were analyzed using restriction enzyme digestion, PAGE and sedimentation velocity analysis.

To ensure that the reconstitution of the chromatin complexes was complete, the complexes were digested with *Eco*RI. Digestion with this enzyme cuts the fibers between the 208 repeats producing fragments of 196 bp of DNA (see Figure 14). If the reconstitution is not complete, there will be fewer than 12 histone octamers present and the *Eco*RI digestion will produce 196 bp DNA fragments. Figure 37 shows a 4% native-PAGE of the oligonucleosome complexes reconstituted with the RP-HPLC purified and treated histones. A marker (M) shows a *Cfo*I digest of the plasmid pBR322 which produces fragments ranging from 131 to 395 bp and allows estimation of nucleosome and DNA fragment sizes. Lane 1 shows an incomplete digest of naked 208-12 DNA which produces 196 bp DNA (D) and larger DNA fragments. Digestion of the reconstituted complexes (Lane 2) shows the position of the nucleosome monomer (1N), dimer (2N), and trimer (3N) fragments, however there is no band corresponding to 196 bp indicating there is no naked DNA present and that the reconstitution was successful.

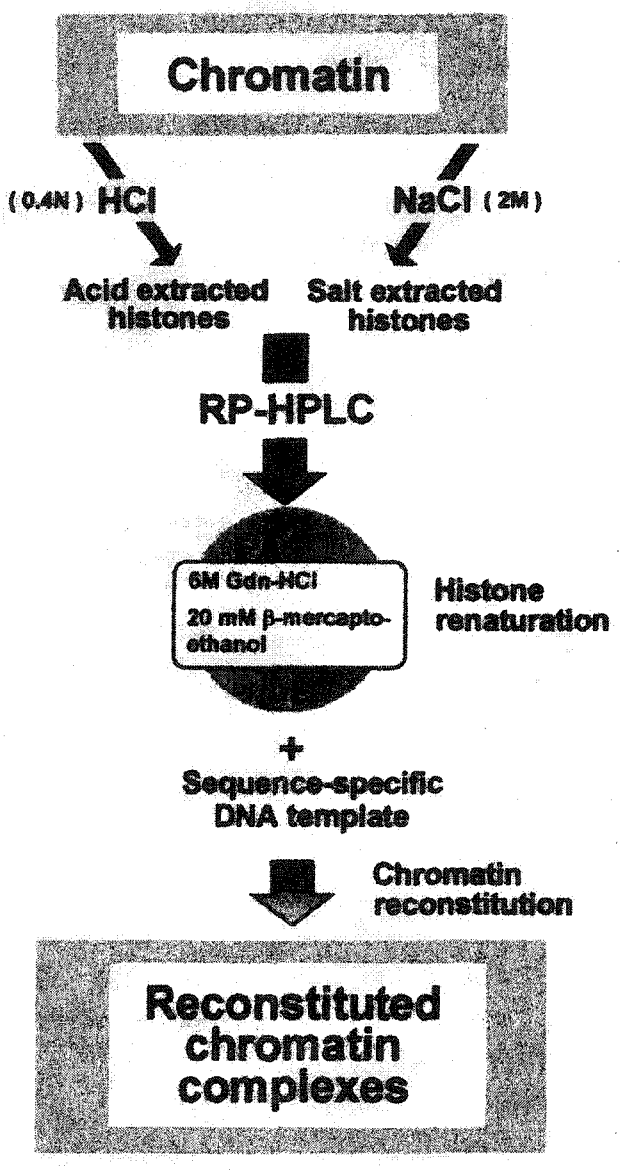


**Figure 36: Experimental Outline to Produce Chromatin Complexes with RP-HPLC Purified Histones.**

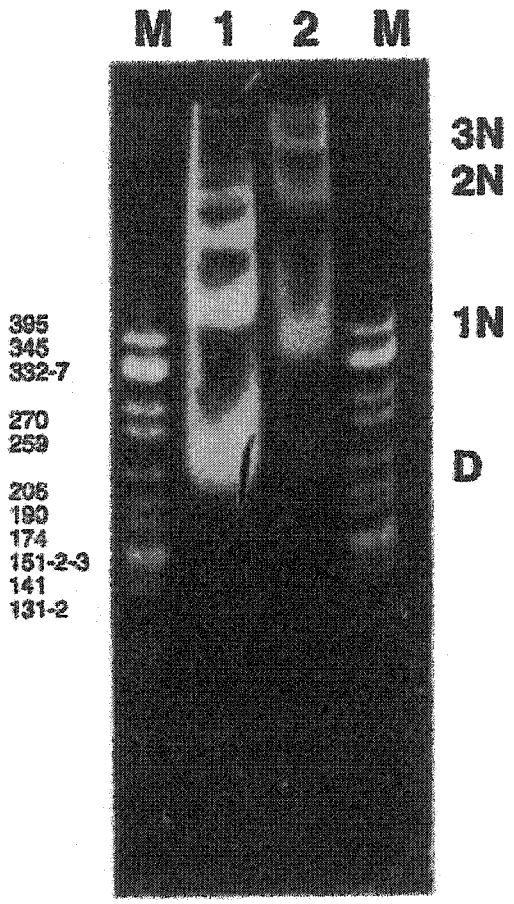


**Figure 37: Native 4% Acrylamide PAGE Analysis of 208-12 Oligonucleosome Complexes Reconstituted with RP-HPLC Purified Histones.** These complexes were reconstituted with RP-HPLC purified, GdnHCl treated histones. Lane 1 is an incomplete *Eco*RI digest of naked 208-12 DNA; Lane 2 - oligonucleosome fibers digested with *Eco*RI for 3.5 hours at 37°C; M - marker, *Cfo*I digest of pBR322 (DNA fragment sizes shown at the side of gel). D is 196 bp DNA; 1N, 2N, and 3N are nucleosome monomers, dimers and trimers. The non-denaturing gel was run at 60 volts in 1xE running buffer and stained with ethidium bromide.

Sedimentation velocity analysis of the reconstituted chromatin complexes was done under a variety of different ionic strengths between 0 mM to 150 mM NaCl and the combined results are shown in Figure 38. Under these conditions without the presence of histone H1, the chromatin complexes will exhibit ionic strength dependent folding. (Hansen *et al.*, 1989, Garcia-Ramirez *et al.*, 1995) This folding event is also represented schematically in Figure 38 where the fiber is relatively unfolded at 0 mM NaCl but folds into a more compact structure as ionic strength is increased to 0.15 M NaCl. This is a reversible reaction so that folded complexes at higher salt concentrations can unfold as the ionic strength of the buffer is decreased. The sedimentation values for complexes reconstituted with native histones have been previously determined (Garcia Ramirez *et al.*, 1992) and are represented by the solid line. The values obtained at different ionic strengths using the reconstituted chromatin complexes containing the RP-HPLC fractionated histones treated with GdnHCl are represented by the solid circles in the same figure. The figure clearly shows that the values obtained for the complexes with the RP-HPLC purified and treated histones are virtually identical to their native counterparts and therefore appear to retain the same inter- and intra-nucleosomal interactions.

## 3.5 Discussion

In order to look at structural changes and events which result from post-translational modifications to histones, it is necessary to have an efficient and effective means of purifying the histones, their variants and their modified forms. The ability to use purified histones and reconstitute them onto nucleosome and chromatin DNA templates allows the opportunity to investigate nucleosome structure and chromatin folding events. Together these investigations allow us to speculate on *in vivo* events and structures.

However these studies require the complete purification of individual histones. While salt extraction and acid extraction are both extremely successful in producing histones from a variety of samples, the use of acid-extracted histones in structural studies is somewhat controversial because of suspected changes in secondary structure (Voordow

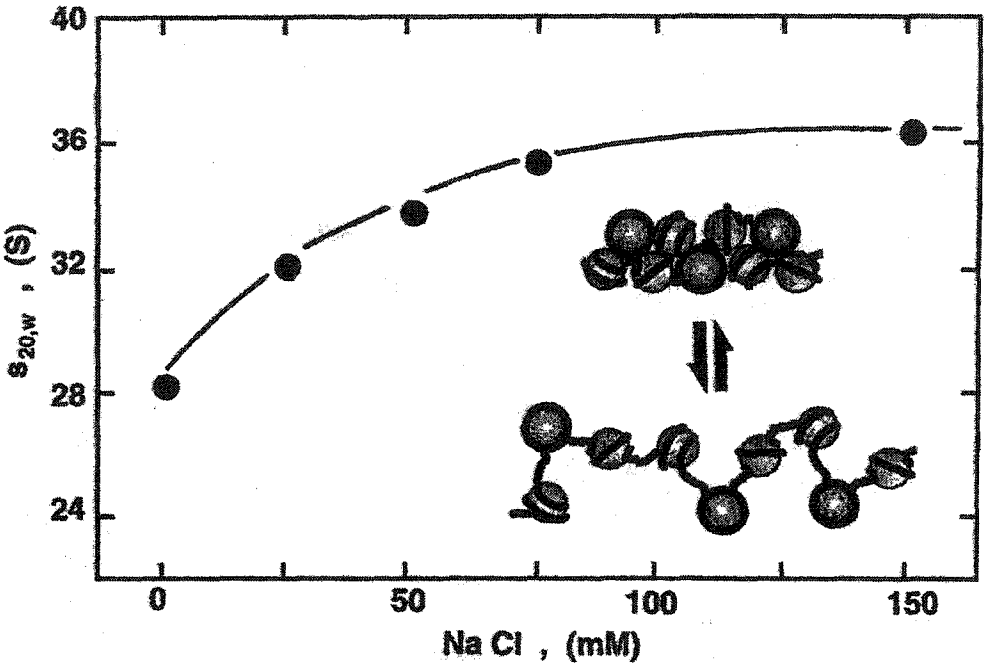


**Figure 38: Sedimentation Velocity Analysis of 208-12 Complexes at Different Ionic (NaCl) Concentrations.** The effect of ionic strength (NaCl concentration) on the average sedimentation coefficient of a reconstituted 208-12 oligonucleosome complex with RP-HPLC purified, guanidine hydrochloride treated histones (solid dots). The fitting line represents the same analysis for a native histone H1-depleted native chromatin fraction consisting of an average of 12 nucleosomes (Garcia-Ramirez, 1992). The increase in $s_{20,w}$ with the salt concentration is due to an increase in the folding of the chromatin complex which is shown schematically in the inset. Analysis was carried out at 20,000 rpm at 20°C in a Beckman XL-A analytical ultracentrifuge.

*et al.*, 1977). Naturally if the conformation of these histones is somehow changed during acid extraction then the results of any biophysical or structural analyses using these histones would also be suspect.

The advent of RP-HPLC has proven very successful in purifying proteins and peptides including modified histones and histone variants which are often present in relatively small quantities and may not be capable of being purified by other methods. However, their use in structural studies has also been controversial because of possible conformational changes due to the buffers used in the separation process which can have a destructive effect on secondary and tertiary protein structure (Hallin & Khan, 1985). Indeed our comparison of native and RP-HPLC fractionated histones show that there are distinct changes in secondary structure and association properties with the RP-HPLC fractionation (Figures 23 and 24). The major damaging effect of RP-HPLC appears to be due to the high concentrations of acetonitrile used during the process as neutralization of the TFA with NaOH before lyophilization of the fractions had no impact (results not shown).

The sedimentation results show conclusively that it is possible to successfully use RP-HPLC fractionated histones for structural analysis if the samples are treated with guanidine hydrochloride after their fractionation. Sedimentation velocity analysis under these conditions show that nucleosome core particles reconstituted with GdnHCl treated RP-HPLC fractionated histones had the same native-like characteristics as native nucleosomes or those reconstituted with salt extracted histones (Figure 26 – Samples D, A and B respectively). The presence of free DNA in virtually all the samples analyzed (including the native nucleosome core particles – sample A) is an intrinsic characteristic of nucleosome core particles in solution. It represents a reversible dissociation equilibrium (See Figure 39) which depends on the ionic strength and temperature of the buffer was well as on the sample concentration (Ausio *et al.*, 1984; Yager *et al.*, 1984; Cotton *et al.*, 1981).

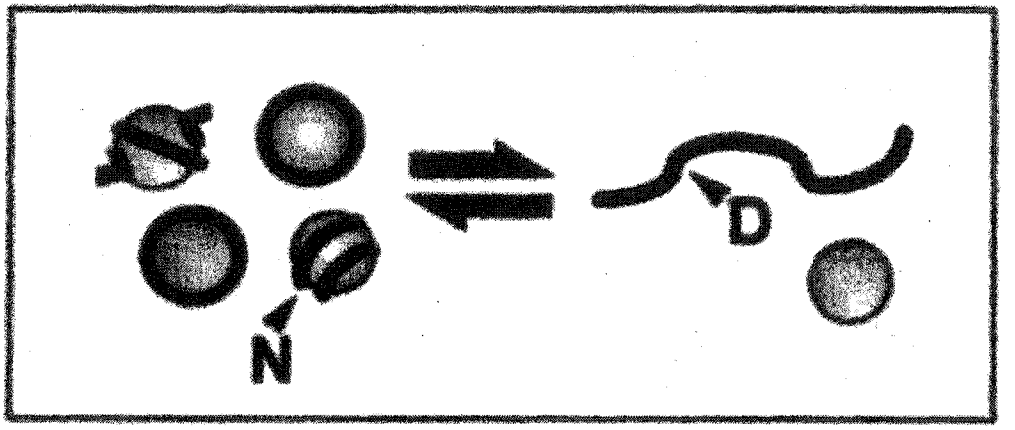


**Figure 39: Schematic Representation of the Reversible Dissociation Equilibrium of Nucleosomes in Solution. N, nucleosome particle; D, DNA.**

The use of GdnHCl appears to produce native-like histones by completely denaturing the histones after their exposure to large concentrations of acetonitrile during fractionation, and this allows their complete renaturation once GdnHCl is removed. In addition, this method has proven successful regardless of the histone extraction method used. With regards to possible effects due to the source of the histones, the results appear to indicate that biological source is not a factor as shown by comparison of chicken and alligator samples. However that is not completely conclusive as Lamprey samples did appear to show changes in nucleosome stability. While this may be an intrinsic property of the histones themselves it could also be a result of undiagnosed problems during the procedure. Unfortunately a lack of sample precluded further investigation into either possibility.

While the production of native-like nucleosomes was important, the production of native like chromatin complexes was also crucial because it allows us to speculate on *in vivo* chromatin dynamics. Analysis of ionic strength-dependent folding of the artificially reconstituted chromatin fibers without H1 exhibited the same folding behavior as their histone H1-depleted native counterparts (Figure 38) indicating that the reconstituted chromatin complexes retained the same inter- and intra-nucleosome interactions.

The development of RP-HPLC is extremely useful for the quick fractionation of very small amounts of starting sample. Histone fractionation using conventional chromatographic techniques requires large amounts of starting material which was often a limiting factor to its usefulness. Recently however RP-HPLC has proven effective in fractionating individual multi-phosphorylated subtypes of histone H1 variants (Lindner *et al.*, 1997) and should be capable in separating other modified histones as well. The ability to purify these post-translationally modified histones, which often represent a very small fraction of the total histones, opens up tremendous possibilities for future analysis of their possible structural and functional relationships of individual and combined modifications. Examining chromatin complexes containing specifically modified histones will be a powerful tool in developing a better understanding of chromatin structure and function.

# 4.0 ROLE OF THE HISTONE TAILS IN CHROMATIN FIBER FOLDING

While the folding of the chromatin fiber has been characterized in the past (van Holde, 1989), the mechanisms of this folding and the importance of the different histones and their domains in this process are still being investigated. Previous work using chromatin fibers without H1 at different ionic concentrations and under physiological conditions have shown that even without histone H1, such fibers are capable of forming an intermediate state of chromatin folding (IOS) (See Figure 38 – inset) and it is the tails of the core histones that are mainly responsible for this state event (Garcia-Ramirez *et al.*, 1992, 1995). In this chapter the contribution of the histone H2A-H2B dimer and H3-H4 tetramer tails to H1 depleted fiber folding is investigated. The purpose was to determine which, if any, make a greater contribution to fiber folding.

The experimental procedure is outlined in Figure 40. Essentially salt extracted chicken erythrocyte native nucleosome core particles were either left untreated (N) or were trypsinized (T) using immobilized trypsin. Trypsinization removes both the histone N- and C-terminal histone tails. Purified native and trypsinized H2A-H2B dimers and H3-H4 tetramers were then recombined into four different octamer complexes:
native: $2(H2A\text{-}H2B)_N + [(H3\text{-}H4)_N]_2$;
hybrids: $2(H2A\text{-}H2B)_N + [(H3\text{-}H4)_T]_2$; or $2(H2A\text{-}H2B)_T + [(H3\text{-}H4)_N]_2$; and
fully trypsinized: $2(H2A\text{-}H2B)_T . [(H3\text{-}H4)_T]_2$.
The different octamer complexes were then reconstituted onto 208-12 chromatin DNA templates using salt gradient dialysis to form homogenous, polynucleosomal complexes. Comparison of these complexes using PAGE, solubility assays and sedimentation velocity analysis should provide information as to which of the histone tails most affect fiber folding and association.

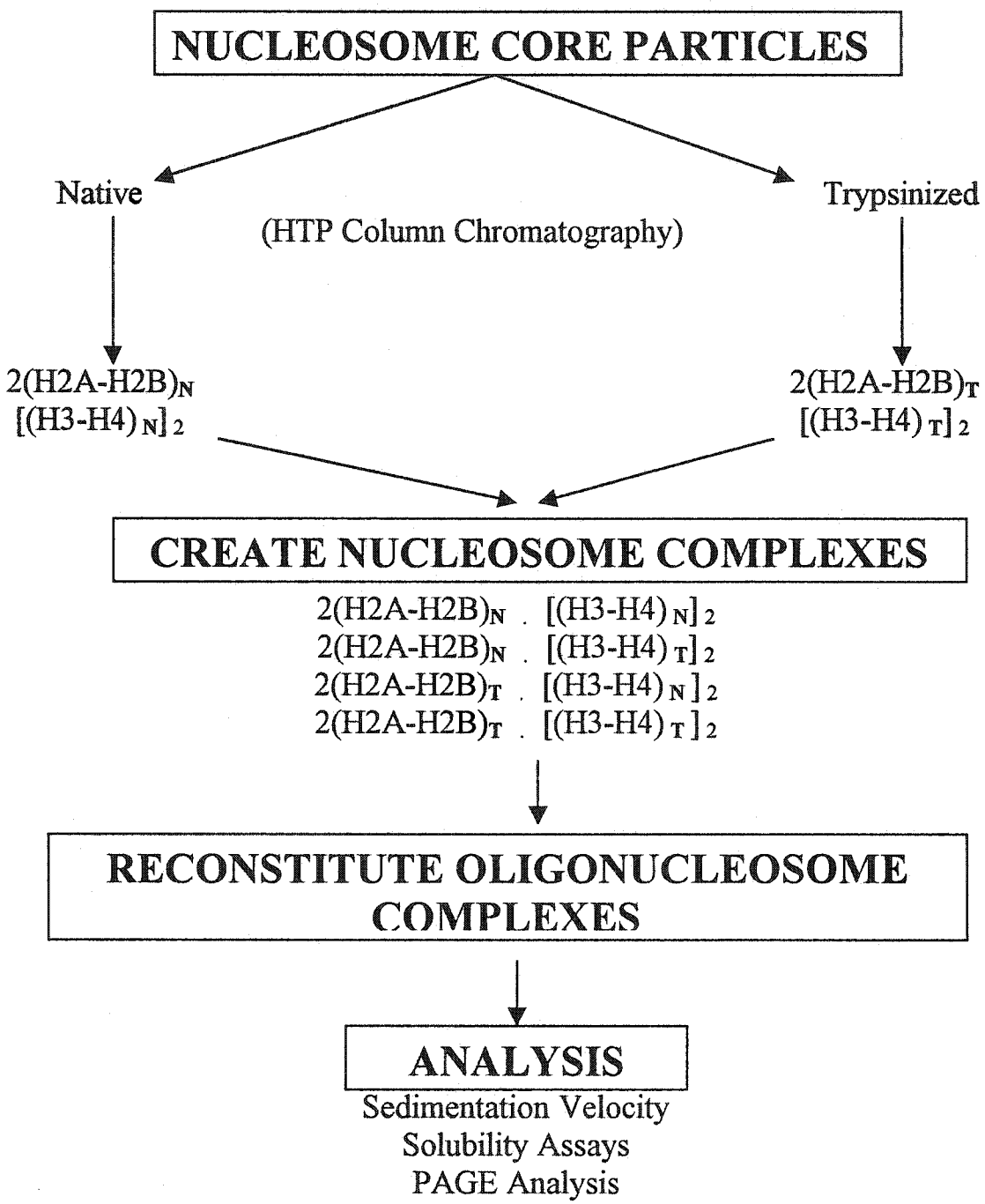


**Figure 40: Experimental Outline to Analyze the Importance of the Histone Tails in Chromatin Folding.**

## 4.1 Creation of Hybrid Octamers

An SDS-PAGE shown in Figure 41 compares the histone composition of the different polynucleosome complexes created to a total histone chicken erythrocyte marker (M). Because trypsinization removes the histones tails, there is a decrease in the molecular weight of the histones. Consequently trypsinized histones have less mass and run farther on an SDS-PAGE. The composition of the different octamers means that each type of octamer will run differently on the gel making them easy to distinguish. Figure 41 shows the successful formation of the different complexes: the fully native (Lane 1); the fully trypsinized (Lane 2) and the hybrids containing either trypsinized H2A-H2B (Lane 3) or trypsinized H3-H4 (Lane 4). The identification of the different histones is listed at the side of the gel.

## 4.2 Sedimentation Velocity Analysis

The folding dynamics of the different polynucleosome fibers generated were analyzed by analytical ultracentrifugation and sedimentation velocity analysis. Each of the fibers reconstituted with the different octamers were analyzed at varying concentrations of monovalent ions (NaCl) to determine their salt dependent sedimentation behaviour. The combined results are shown in Figure 42. The fibers with intact (native) histones are designated by the solid circle (●) and the dashed line. The fully trypsinized octamer is designated by an open circle (○) and a dashed line. As expected the two complexes behave very differently. The fully trypsinized complexes have much lower sedimentation values which is expected because of their lower mass. However a folding event clearly still occurs but the sedimentation values indicate that it is not as great as that seen in the native fibers. Examination of the two hybrid fibers indicated that the complexes containing the trypsinized H2A-H2B and native H3-H4 histones, (represented by ◒ and a solid line), most closely resemble the fully intact complexes. In contrast, the complexes with the native H2A-H2B and trypsinized H3-H4 histones, (represented by ◓ and a solid line) exhibit a salt dependence with is clearly intermediate to that of the fully intact

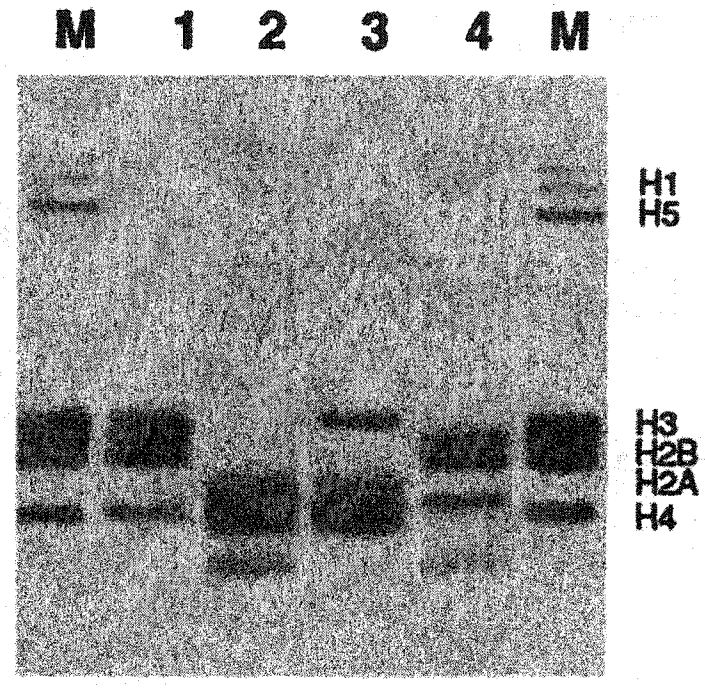


**Figure 41: SDS-PAGE of Native, Trypsinized and Hybrid Histones.**
Lane 1: native - $2(H2A\text{-}H2B)_N.[H3\text{-}H4]_N]_2$ ; Lane 2: fully trypsinized - $2[(H2A\text{-}H2B)_T]$ . $[H2\text{-}H4)_T]_2$ ; Lane 3: hybrid with trypsinized H2A-H2B - $2[(H2A\text{-}H2B)_T]$ . $[(H3\text{-}H4)_N]_2$; Lane 4: hybrid with trypsinized H3-H4 - $2(H2A\text{-}H2B)_N$ .$[(H3\text{-}H4)_T]_2$. M, total chicken erythrocyte histones identified at the side of the gel. All samples mixed with 2x SDS sample buffer and boiled for 5 minutes prior to loading on a 6% stacking, 15% separating SDS-PAGE gel. The gel was run at 100 volts in a 0.05 M Tris, 0.38 M glycine, 0.1% SDS running buffer and stained with Coomassie Blue.

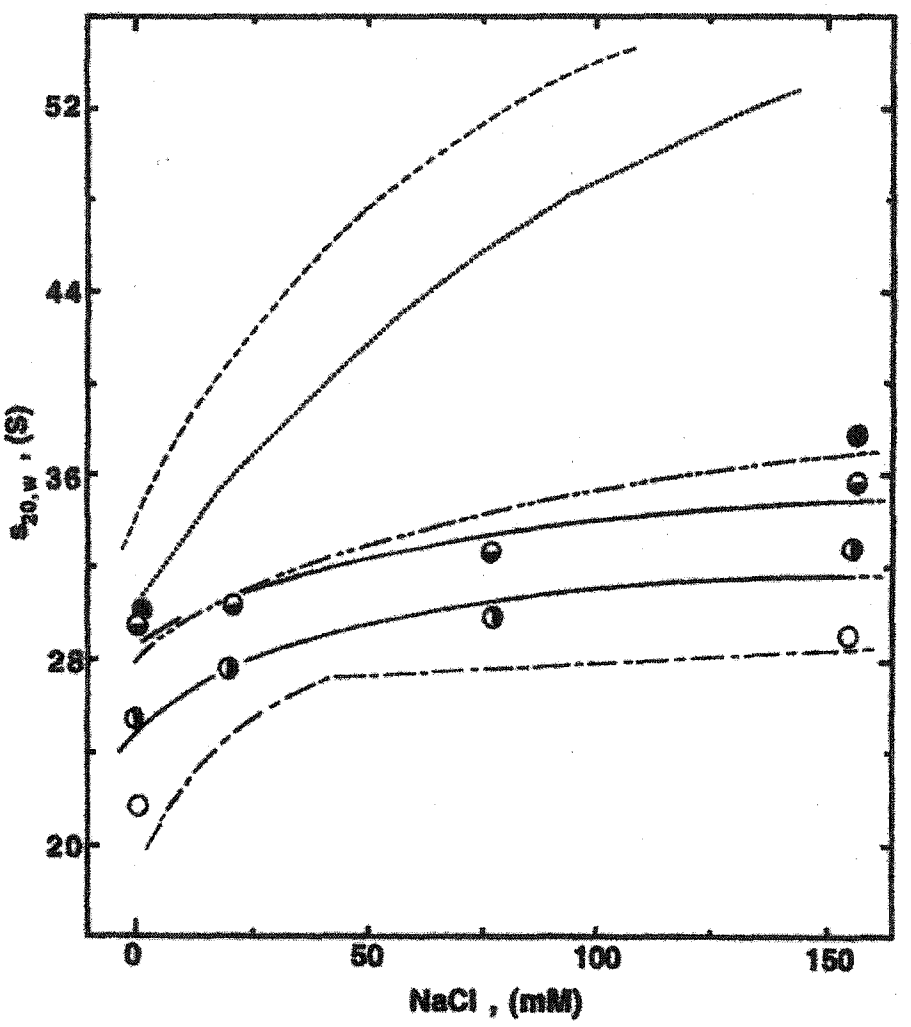


**Figure 42: Salt-dependent Sedimentation Behaviour of 208-12 Polynucleosome Fibers Reconstituted with Native, Trypsinized and Hybrid Histone Octamers.** Polynucleosome fibers with: (●) non-trypsinized histones; (○) fully trypsinized histones; ( ◒ ) hybrids with native H3-H4 histones $\{2(H2A\text{-}H2B)_T .[(H3\text{-}H4)_N]_2\}$; ( ◔ ) hybrids with native H2A-H2B histones $\{2(H2A\text{-}H2B)_N .[(H3\text{-}H4)_T]_2\}$. Also shown is the salt-dependent sedimentation behaviour of native chicken erythrocyte chromatin with a DNA size distribution of approximately 12-13 nucleosomes with histone H1 (.... or - - -) from (Ausio *et al.*, 1984b; Butler & Thomas, 1980 respectivel. All sedimentation runs were carried out at 20,000 rpm at 20°C in a Beckman XL-A analytical ultracentrifuge. Sedimentation values $S_{20,w}$ are in Svedbergs (S).

or fully trypsinized complexes. Together these results show that both the H2A-H2B and H3-H4 tails contribute to the folding of the polynucleosome fibers as indicated by their intermediate positioning. However it is clearly evident that the H3-H4 tails provide the largest contribution to the salt dependent folding and sedimentation behavior of the polynucleosome complexes since the hybrids containing the intact H3-H4 histones exhibit behavior which is closest to that of the fibers with fully intact histones.

## 4.3 Solubility Assays

Reconstituted chromatin fibers are also known to undergo folding in the presence of divalent ions like magnesium. This is due to the divalent cations binding to the DNA reducing the residual charge (Clark & Kimura, 1990). It was decided to further investigate the differential folding behavior of the different complexes by looking at the behavior of their magnesium-mediated folding association and solubility. Each of the complexes were incubated with different concentrations of magnesium chloride buffer. Under these conditions the polynucleosome fibers will undergo a folding event in the presence of increasing concentrations of divalent cations. This is a reversible association behavior and occurs because the divalent cations bind to DNA reducing its residual charge. By incubating the fibers with increasing amounts of magnesium chloride, any polynucleosome complexes which fold and aggregate will be precipitated and the quantity of soluble chromatin fibers can be determined by optical density readings at 260 nm and comparison to the results in zero $Mg^{2+}$ buffer. The results of the solubility assays with the different polynucleosome fibers are shown as a solubility curve in Figure 43. The first curve shown (dashed line) is for native chicken erythrocyte chromatin containing 12-13 nucleosomes with a full complement of linker histones as previously determined by Ausio *et al.* (1986). This curve shows that when H1 is present the oligonucleosome fibers will precipitate very quickly in less than 2 mM $MgCl_2$. The H1 histone tails bind to the linker DNA separating adjacent nucleosome core particles, thereby screening the repulsive negative charges and allowing adjacent nucleosomes to come together during fiber folding. The solubility curves for the different reconstituted complexes are also shown. The complexes with non-trypsinized histones (●) are shown

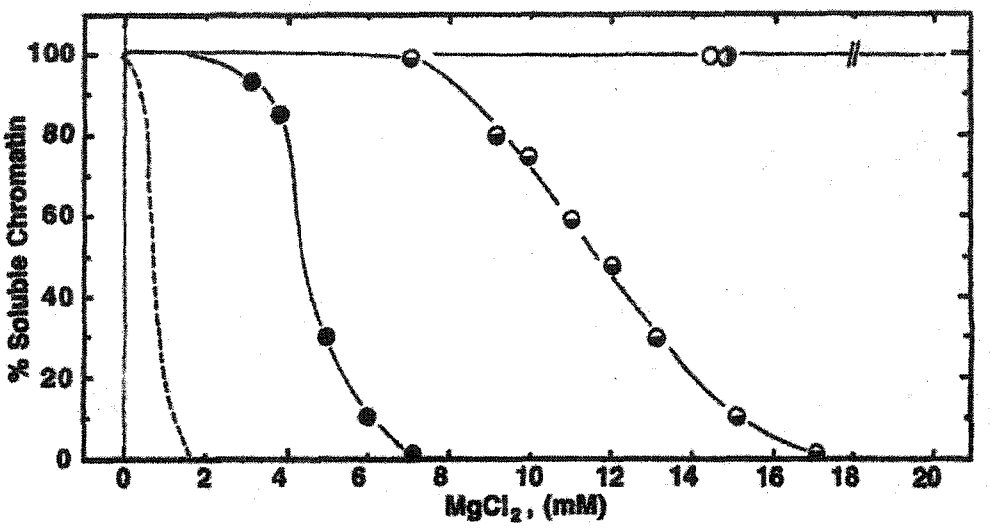


**Figure 43: Solubility Assay of 208-12 Polynucleosome Fibers Reconstituted with Native, Trypsinized and Hybrid Histone Octamers.** Solubility as a function of $MgCl_2$ concentration in 10 mM Tris-HCl (pH 7.5) was determined using $A_{260}$ measurements. Polynucleosome fibers with: (●) non-trypsinized histones; (○) fully trypsinized histones; (◒) hybrids with native H3-H4 histones $\{2(H2A\text{-}H2B)_T .[(H3\text{-}H4)_N]_2\}$; and (◓) hybrids with native H2A-H2B histones $\{2(H2A\text{-}H2B)_N .[(H3\text{-}H4)_T]_2\}$. Also shown is the solubility behaviour of native chicken erythrocyte chromatin (- - -) (Ausio *et al.*, 1986). The % solubility is relative to 0 mM $MgCl_2$ results.

next and have a higher degree of solubility which is as expected due to the lack of linker histones. The complexes with fully trypsinized histones (○) lack both histone H1 and the core histone tails and are therefore expected to remain more soluble than their native and hybrid counterparts. This was confirmed as these complexes remain soluble even when magnesium concentrations greater than 20 mM were used. Examination of the hybrid complexes showed that those containing the trypsinized H2A-H2B and intact H3-H4 ( ◒ ) produced a solubility which was intermediate to that of the wholly trypsinized (○) and the fully intact (●) histone complexes. However the hybrid with the trypsinized H3-H4 and intact H2A-H2B ( ◔ ) shows a solubility behavior identical to the complex containing the wholly trypsinized histones (○). Both these complexes remained soluble even with magnesium concentrations greater than 50 mM. These assays clearly indicate that the H3-H4 tails have a much greater impact than the H2A-H2B tails on folding events in solutions containing divalent cations. It is clear that the participation of the linker histones and the histones tails on these processes follow a defined hierarchy where histone H1>>H3-H4>H2A-H2B. Figure 44 shows this hierarchy in a schematic representation of the polynucleosome complexes and their folding behavior.

## 4.4 Discussion

The major aim of this study was to determine the role played by the tails of the H2A-H2B dimers and H3-H4 tetramer in the process of folding and association of chromatin fibers without histone H1. Polynucleosome complexes reconstituted with individually purified trypsinized or non-trypsinized histones allowed comparison of the relative importance of the different histone tails. Since trypsinization removes both the N- and C-terminal tails of the histone proteins, comparison of polynucleosome chromatin complexes which differ only in the presence or absence of specific histone tails, provides an opportunity to determine the importance of the different histone tails chromatin folding behavior. The folding behavior of the chromatin fibers were examined using salt dependent sedimentation behavior and magnesium mediated association.

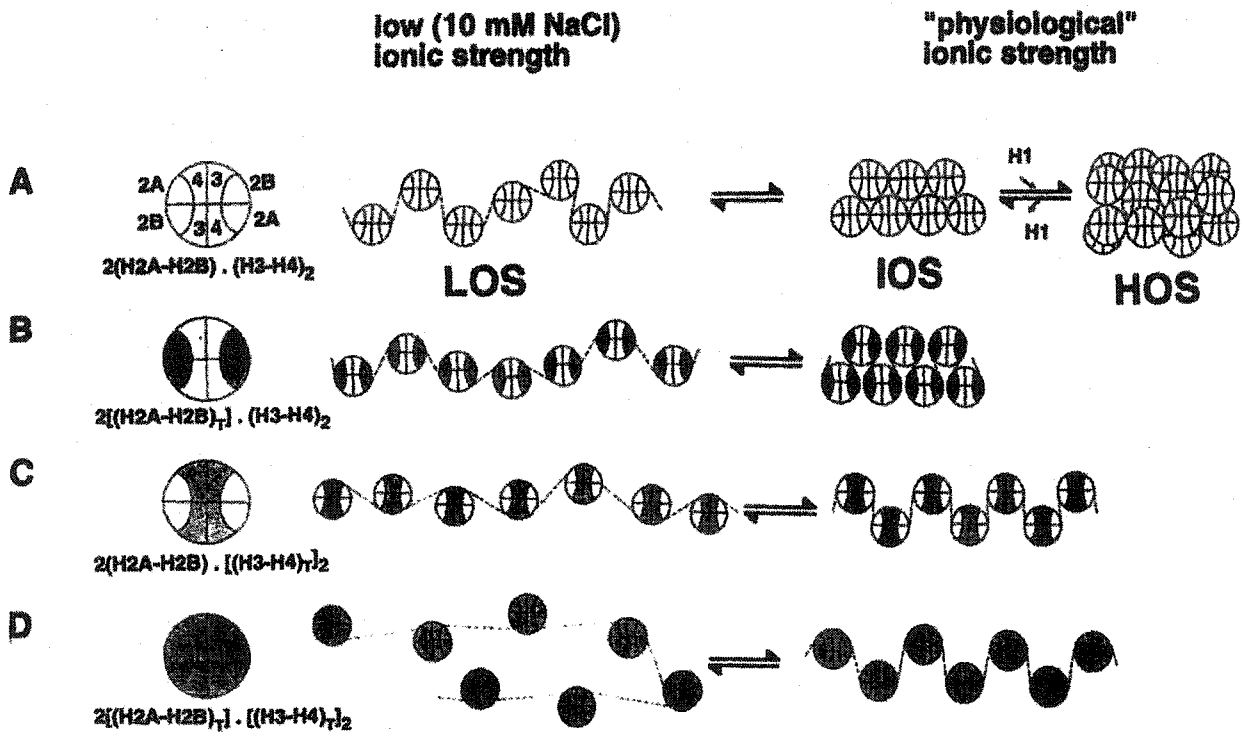


**Figure 44: Schematic Representation of the Folding Behaviour of Different 208-12 Polynucleosome Complexes Reconstituted with Native, Trypsinized or Hybrid Histone Octamers.** (A) native histones $2(H2A\text{-}H2B).(H3\text{-}H4)_2$; fully trypsinized histones $\{2[(H2A\text{-}H2B)_T].[(H3\text{-}H4)_T]_2\}$; hybrids with native H3-H4 histones $\{2[(H2A\text{-}H2B)_T].[(H3\text{-}H4)_N]_2\}$; and hybrids with native H2A-H2B histones $\{2[(H2A\text{-}H2B)_N].[(H3\text{-}H4)_T]_2\}$. LOS: low order structure; IOS: intermediate order structure (determined by Garcia-Ramirez *et al.*, 1992); and HOS: higher order structure. The shaded domains of the histone octamers shown on the left-hand side of the figure correspond to those lacking the histone tails. The folding pattern of native chromatin ($\pm$ H1) is shown in the upper row (A) (HOS).

Analysis of the sedimentation behaviour of the reconstituted complexes (Figure 42) clearly show that as salt concentration increases from 0 to 150 mM (i.e. to physiological concentrations), the hybrid containing the trypsinized H3-H4 and native H2A-H2B octamer has a folding which is intermediate to that of the complexes which are either fully trypsinized (folds the least) or fully intact (folds the most). In contrast the hybrids with the trypsinized H2A-H2B and intact H3-H4 fold to almost a similar extent as the complex with completely intact histones. Our results were also compared to native chromatin complexes with 12-13 nucleosomes and a full complement of histones including histone H1. These results are also shown in Figure 42 (dotted lines - Ausio *et al.*, 1984; Butler & Thomas, 1980). These native fragments have a sedimentation value of 50 $\pm$ 2S which is very close to the 51.5S value predicted for a 208-12 complex folded into a higher order conformation (Hansen *et al.*, 1989).

It has been shown that monovalent cations affect the folding of the fiber by primarily screening the residual charge of DNA, whereas divalent cations bind to DNA thereby reducing its residual charge (Clark & Kimura, 1990). It is possible that the histone 'tails' bind to the nucleosomal DNA in a fashion similar to histone H1 binding linker DNA. This screening of the repulsive negative charge would allow for adjacent nucleosomes to come together during the folding of the fiber and would also allow for the reversible association behaviour of these particles in the presence of magnesium (Scwartz *et al.*, 1996). Examination of the magnesium induced folding (Figure 43) shows unequivocally that the histone H3-H4 tails make a greater contribution to the folding than their H2A-H2B counterparts.

Native chromatin fibers complete with H1 fold to a much greater extent than fibers without H1. From the results in Figures 42 and 43 it is clear that in the folding and association behavior of the reconstituted polynucleosome complexes and native chromatin with H1, the participation of the tails follow a hierarchy with H1>>H3-H4>H2A-H2B. The folding behaviour of the different constructs characterized is represented schematically in Figure 44. The low order structures (LOS) at low ionic strength, i.e. 10 mM NaCl, show that the fully trypsinized polynucleosomes fibers have

the lowest sedimentation values and therefore have the most open structure. They are followed by the H3-H4 trypsinized hybrids, trypsinized H2A-H2B hybrids, and then the fully intact histones. As ionic strength increases, the intermediate order structures are formed with the fully intact and the hybrid containing native H3-H4 having a more folded structure than either the hybrid containing trypsinized H3-H4 or the fully trypsinized fibers. If the fully intact polynucleosomes are mixed with histone H1, then higher order structures (HOS) would form producing higher sedimentation values as shown with the native chromatin samples.

The results indicated that the tails of histone H3 and H4 have a greater effect on folding than those of the H2A-H2B tails. However both play an important role in the inter-(folding) and intra- association in the polynucleosome fiber. The results also support recent trypsinization studies *in situ*, i.e. within the nucleus, which showed that the 'tails' of H3-H4 play a critical role in chromatin folding (Kragewski & Ausio, 1996).

# 5.0 STRUCTURAL EFFECTS OF HISTONE TAIL ACETYLATION

Acetylation is the most studied of the histone post-translational modifications, however its precise role and structural impact on chromatin remains elusive. Given the relevance of both acetylation and the histones tails in the process of chromatin folding it was decided to determine more precisely the structural effect of acetylation on the histone tails. Circular dichroism allows analysis of protein structure and molecular conformational changes by determining secondary structure and the percentage of α-helices, β-sheet and random coil structures present in a molecule. An earlier study indicated that histone acetylation increases the overall α-helical content of these proteins in a way that was not defined (Prevelige & Fasman, 1987). A more recent paper has shown that the tails of the core histones adopt a helical conformation in nucleosomal DNA (Baneres *et al.*, 1997). However it was not shown whether the helical conformation pre-existed in the histone tails or was a result of their interaction with DNA. Given the relevance of both acetylation and the histone tails in the processes of chromatin folding (Garcia-Ramirez *et al.*, 1992, 1995), it was decided to use circular dichroism analysis to characterize the secondary structure of the histones tails and particularly the effects of their acetylation. This was done by comparison of control, trypsinized, and acetylated nucleosomes. In addition the conformation of the N-terminal tails in the presence and absence of interaction with nucleosomal DNA was also examined as well as the individual N-terminal tails of histone H4 with varying levels of acetylation. Figure 45 shows a summary of the experimental procedures used.

## 5.1 PAGE Analysis

Native, acetylated and trypsinized nucleosome core particles were prepared and analyzed using different types of PAGE. Figure 46 shows a 4% native polyacrylamide gel of acetylated (n1), native (n2) and trypsinized (n3) nucleosome core particles and their

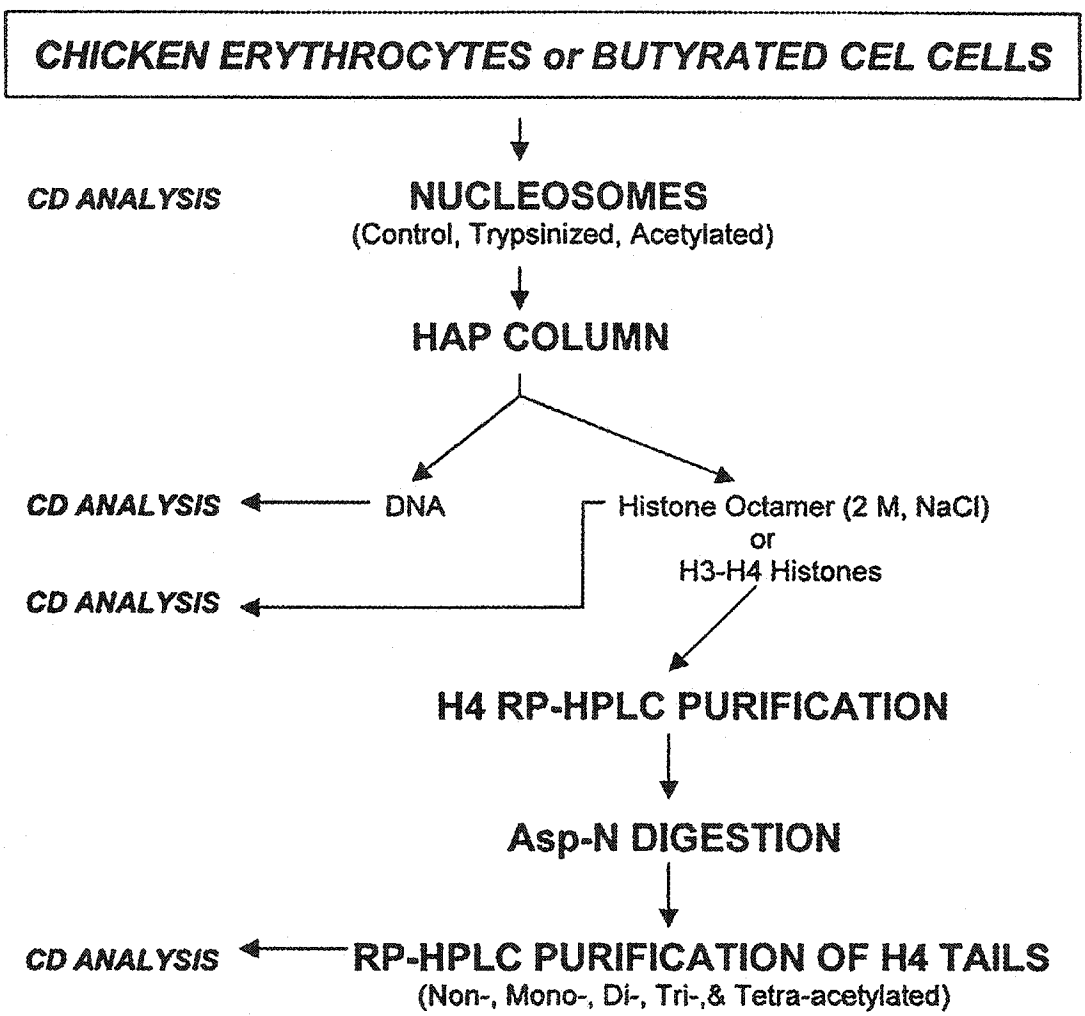


**Figure 45:** **Experimental Outline for Analysis of Histone Acetylation.**

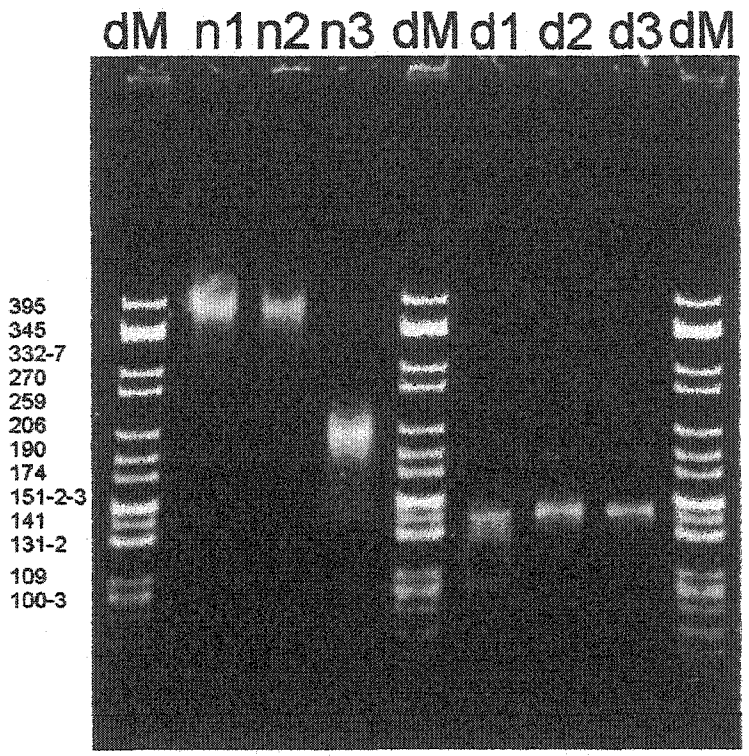


**Figure 46: Native 4% Acrylamide PAGE of Acetylated, Native and Trypsinized Nucleosomes.** Acetylated (*n*1), native (*n*2), and trypsinized (*n*3) nucleosome core particles and their corresponding DNA (*d*1, *d*2, and *d*3 respectively). DNA marker (*d*M ) obtained by digesting pBR 322 with *Hha*I. The non-denaturing gel was run at 60 volts in a 1xE running buffer and stained with ethidium bromide.

respective DNA fragments (d1, d2 and d3) as compared to a DNA marker prepared by digesting pBR322 with *Hha*I. The gel shows that all three types of nucleosomes contain equivalent sized 146 bp DNA (d1-d3) and that the nucleosomes run as expected. Since the native and acetylated nucleosomes are very similar in size they run to the same position on the gel whereas the trypsinized nucleosomes migrate faster due to their lower mass resulting from the loss of the histone tails.

The nucleosomal histones were also analyzed using SDS-PAGE as shown in Figure 47. The histone proteins from the acetylated (h1) , native (h2), and trypsinized (h3) nucleosomes were compared to a chicken erythrocyte total histone marker. This gel again illustrates that because the trypsinized histones have less mass they run faster on the gel. All the samples appear to have equimolar quantities of core histones although the H3-H4 histones in the acetylated (h1) sample appear slightly fuzzy when compared to their native counterparts (h2). This fuzzy appearance in this type of gel is a result of the increased acetylation levels of these histones (Georgieva & Sendra, 1999).

Since the individual acetylated forms of the core histones do not show up well on SDS-PAGE, the same samples: acetylated (h1); native (h2); and trypsinized(h3); were also run on an AU-PAGE which is shown in Figure 48. The samples were compared to the chicken erythrocyte total histone marker (hM) and the histones are identified at the side of the gel. The AU-PAGE clearly shows that the histones in acetylated nucleosome fraction (h1) contain many bands which represent the differently acetylated histones. The numbers 0 through 4 represent the different acetylated histone H4 forms with the numbers indicating the number of acetylated lysines present. These results, together with the other types of PAGE analysis, indicate that the histones and nucleosomes being examined appear normal and clearly show that the histones in the acetylated nucleosomes, particularly histone H4, have a high level of acetylation.

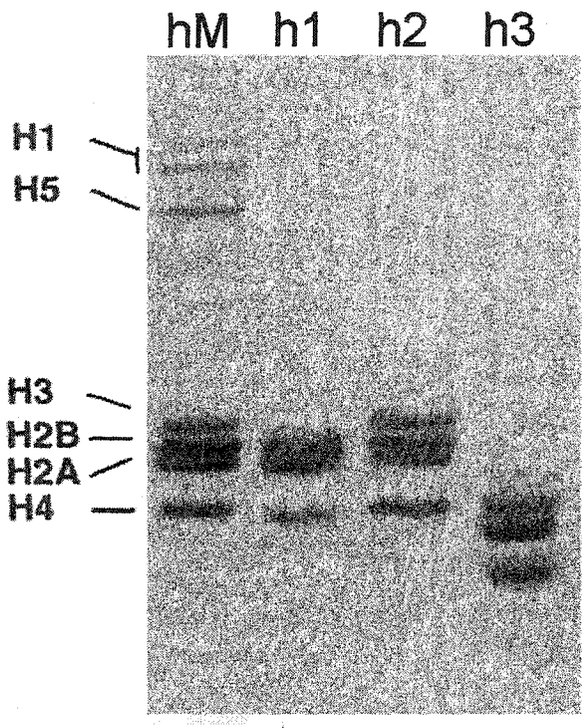


**Figure 47: SDS-PAGE of Acetylated, Native and Trypsinized Nucleosomes.** Acetylated (h1), native (h2), and trypsinized (h3) histones; hM, chicken erythrocyte histone marker with histone identities are located at the side of the gel. All samples mixed with 2x SDS sample buffer and boiled for 5 minutes prior to loading on a 6% stacking, 15% separating SDS-PAGE. The gel was run at 100 volts in a 0.05 M Tris-base, 0.38 M glycine, 0.1% SDS running buffer. Gels were stained with Coomassie Blue.

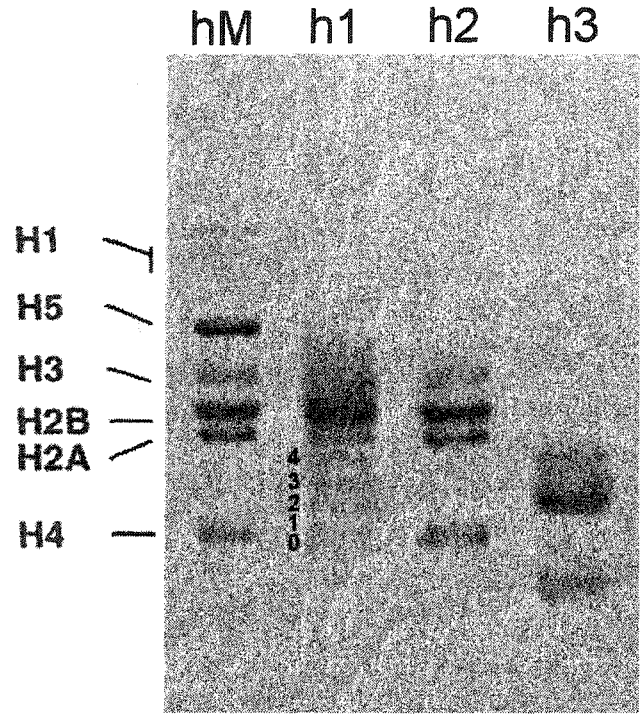


**Figure 48: AU-PAGE of Acetylated, Native and Trypsinized Nucleosomes.** Acetylated (h1), native (h2), and trypsinized (h3) histones; hM, chicken erythrocyte total histone marker with histone identities located at the side of the gel. The numbers in lane h1 represent the number of acetylated histones for histone H4. All samples were mixed with 2 x AU-sample buffer and loaded onto the 2.5 M urea, 5% acetic acid, 15% acrylamide gel. The gel was run at 80 volts in a 5% acetic acid running buffer. Gels were stained with Commassie Blue.

## 5.2 CD Analysis of the Native Nucleosomes

Figure 49 shows the circular dichroism spectra between 200 to 310 nm of both the trypsinized (thick dashed line) and native (thick solid line) nucleosomes and the 146 bp nucleosomal DNA (thin solid line). The thin dashed line is the trypsinized nucleosome spectra which has been normalized for the loss of mass resulting from the loss of the histone tails after trypsin treatment. The near UV region, (i.e. 250-310 nm), is enlarged and shown as an insert in Figure 49. From this spectra is can be seen that the histone octamer has the strongest contribution in the far UV region (190-250 nm) whereas the DNA has the greatest contribution in the near UV region (250-310 nm). The results for the native (N) and trypsinized (T) nucleosomes in the near UV region produce spectra which are identical to those reported in an earlier paper (Ausio *et al.*, 1989). There is an ellipticity increase of approximately 17% at the maxima 282.5 nm for the trypsinized (T) nucleosomes compared to the native nucleosomes (N) (see inset). We can also see that the DNA (D) exerts its major influence in this region of the spectra.

Examination of the far UV region in Figure 49 (190-250 nm) shows that in this area it is the histone octamer which provides the strongest contribution. If the DNA spectra is subtracted from the nucleosomal spectra it is possible to obtain a protein spectrum for just the nucleosomal octamers and this is shown in Figure 50. Figure 50 compares the spectra for the native (thin line) and trypsinized (dashed line) nucleosome core particles to a spectrum obtained for histone octamers only (thick line) in 2M NaCl conditions in which the octamer exists as a stable entity (Arents *et al.*, 1991; Eickbush *et al.*, 1978). These spectra show the typical double minima (at 208 and 222 nm) of a $\alpha$-helical protein and are obviously remarkably similar. It is possible to estimate the amount (i.e. percentage) of $\alpha$-helices present using the ellipticity values $[\theta]$ at either 220 nm or at 222 nm and the following equations:

Equation 1: $\alpha = 8.9 - 2.4 \times [\theta]_{220} \times 10^{-3}$

or

Equation 2: $\alpha = -3.1\,(1 + [\theta]_{222} \times 10^{-3})$

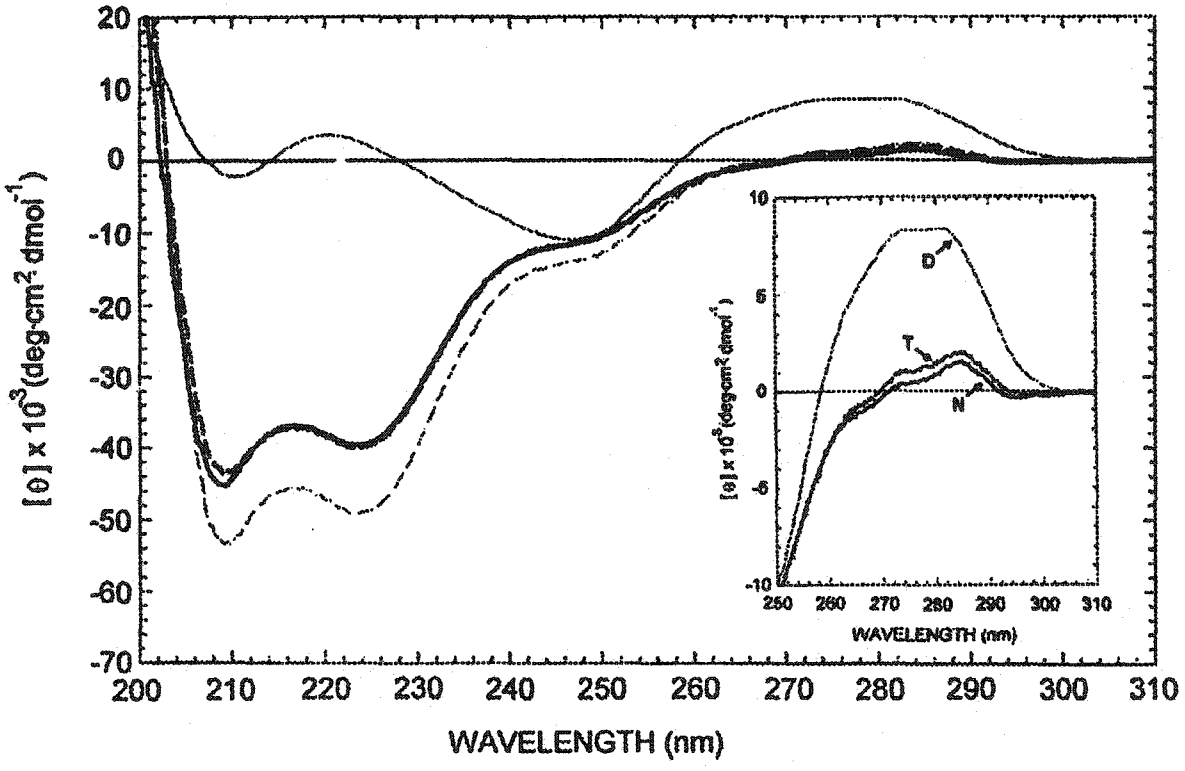


**Figure 49: Circular Dichroism Analysis of Native and Trypsinized Nucleosome Core Partcles.** Native nucleosomes (thick line), trypsinized nucleosomes (thick dashed line), and nucleosomal DNA (thin line) in 25 mM NaCl, 5 mM Tris-HCl (pH 7.5). Trypsinized nucleosomes (thin dashed line) after normalization for the loss of mass due to trypsinization. The inset represents an enlarged view of the near UV region portion of the same spectra. For clarity, the normalized spectrum of the trypsinized nucleosomes is not shown in the inset. D, DNA; N, Native nucleosome core particles; T, trypsinized nucleosome core particles. All data were recorded at 20°C on a Jasco J-720 spectropolarimeter.

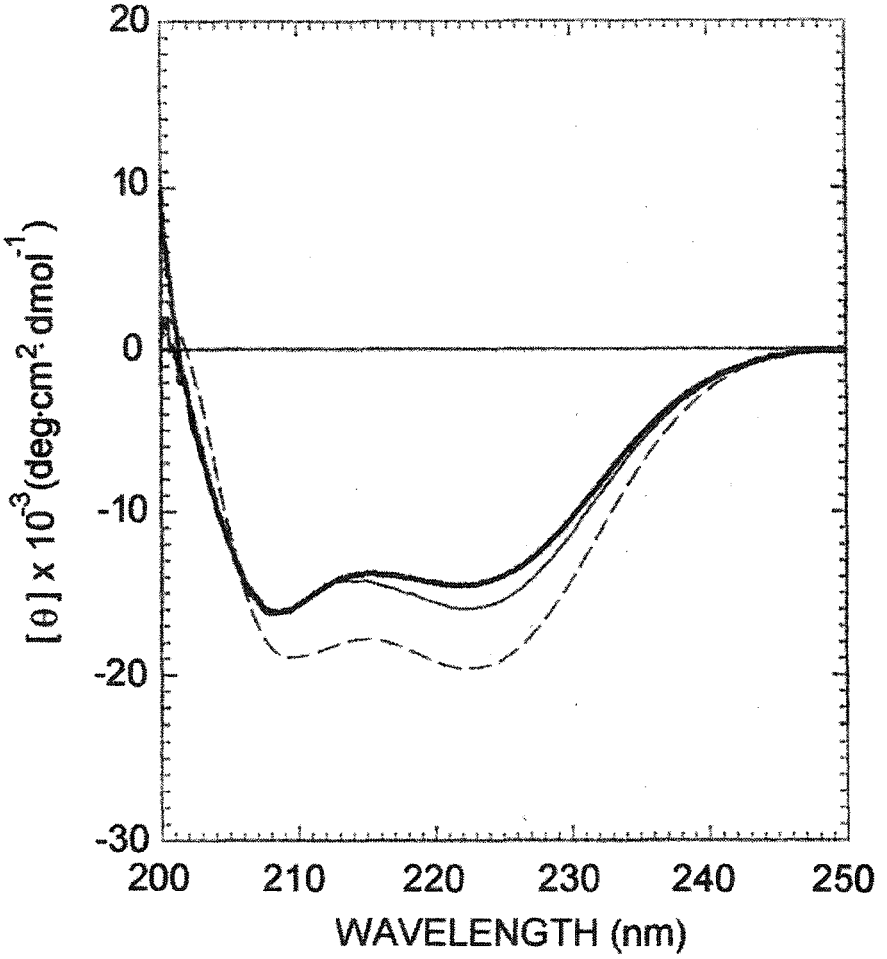


**Figure 50: CD Analysis of Native Histone Octamer and Native and Trypsinized Nucleosome Histones.** All samples were in 2 M NaCl, 0.1 mM DTT, 10 mM Tris-HCl (pH 8.0). Histone octamer (thickline); native (thin line) or trypsinized (thin dashed line) nucleosome core particles. The spectra for the nucleosomal octamers were obtained by subtraction of the nucleosomal DNA spectrum shown in Figure 49. The trypsinized nucleosome spectrum was corrected for the loss of protein mass due to trypsinization. All spectra were recorded at 20°C on a Jasco J720 spectropolarimeter.

For equation 1 the result for the histone octamer only was 46.6% while the native nucleosomal octamer was 43.7%. For equation 2 the histone octamer only was 52.5% whereas the native nucleosomal octamer was 48.7%. Crystallographic structures had determined that the α-helical content of the histone octamer to be 49.4% (Luger *et al.*, 1997). Therefore the results for equation 2 compare very well with the crystallographic value. This indicates that it is possible to use the far UV region of the nucleosomal spectrum to effectively determine the spectrum of the histone octamer and that the results obtained were reliable.

## 5.3 CD Analysis of Trypsinized Nucleosomes

The native (thick line) and trypsinized (thick dashed line) nucleosome core particle spectra is also shown in Figure 49. The initial spectra look remarkably similar, particularly in the far UV region, while the near UV region (Figure 49 inset) does show some difference. However the spectrum for the trypsinized nucleosomes should be normalized to take into account the histone loss of mass resulting from trypsinization. The normalized spectra for the trypsinized nucleosomes are shown in Figures 49 and 50 as the thin dashed line. These spectra show an obvious downward shift in the spectrum and thus a corresponding increase in the negative ellipticity values. Using the ellipticity values at 222 nm the total α-helical content is calculated to be 64.4%, an increase of 11.6% over that calculated for the intact native nucleosome which was 52.8%. This corresponds well to the value of 62% which was previously estimated from the nucleosome crystallographic data (Luger *et al.*, 1997). Considering the relative molecular masses of the two types of nucleosomes (native nucleosomes have 20% more mass than their trypsinized counterparts) it is possible to estimate the α-helical content of the tail domains to be approximately 17%.

It has been hypothesized that the α-helical conformation of the histone tails may be a result of their interactions with nucleosomal DNA (Banares *et al.*, 1997). To determine if this was so, native nucleosomes were analyzed in solutions with ionic strengths ranging from 25 to 600 mM NaCl. Nucleosomes retain their integrity within this range of salt

concentration (Ausio *et al.*, 1984) and as ionic strength increases it has been shown that the histone tails dissociate completely from any interactions with DNA (Walker *et al.*, 1984). Analysis of the far UV spectrum showed no significant changes in the spectrum or molar ellipticities at 222 nm indicating that the α-helical conformation seen in the nucleosomal histones tails does not appear to be a result of their interaction with nucleosomal DNA [results not shown].

## 5.4 CD Analysis of Acetylated Nucleosomes

It is possible that the ionic environment and electrostatic interactions between the histone tails and nucleosomal DNA may have an important impact on the histone tail structure. If charge neutralization of the histone tails results from DNA interaction and is responsible for α-helical conformation (Banares *et al.*, 1997) then acetylation of lysine residues, which decreases the positive charge, should favour this conformation. To examine this possibility hyperacetylated nucleosome core particles were prepared from butyrate treated CEL cell cultures and compared to their native counterparts using CD analysis.

Figure 51 shows the CD spectra produced for the acetylated (dashed line) and native (thick solid line) nucleosomes and the naked nucleosomal DNA (thin solid line). The inset of Figure 51 is an enlargement of the near UV region (250 - 310 nm). The main influence of the DNA is in the near UV region and there is a very slight increase in the ellipticity of the acetylated nucleosomes (A) at 282.5 nm which corresponds to that previously reported (Ausio *et al.*, 1986). For the far UV region, the nucleosomal spectrum of the acetylated nucleosomes (dashed line) has a small downwards shift and a subsequent increase the negative ellipticity. As before the DNA spectrum was subtracted and the far UV regions were replotted and are shown in Figure 52. This spectra shows a small but reproducible increase in the negative ellipticity between the two nucleosome samples of approximately 2-3% . This clearly indicates that the α-helical content of the histone tails increases with acetylation of the lysine amino acids.

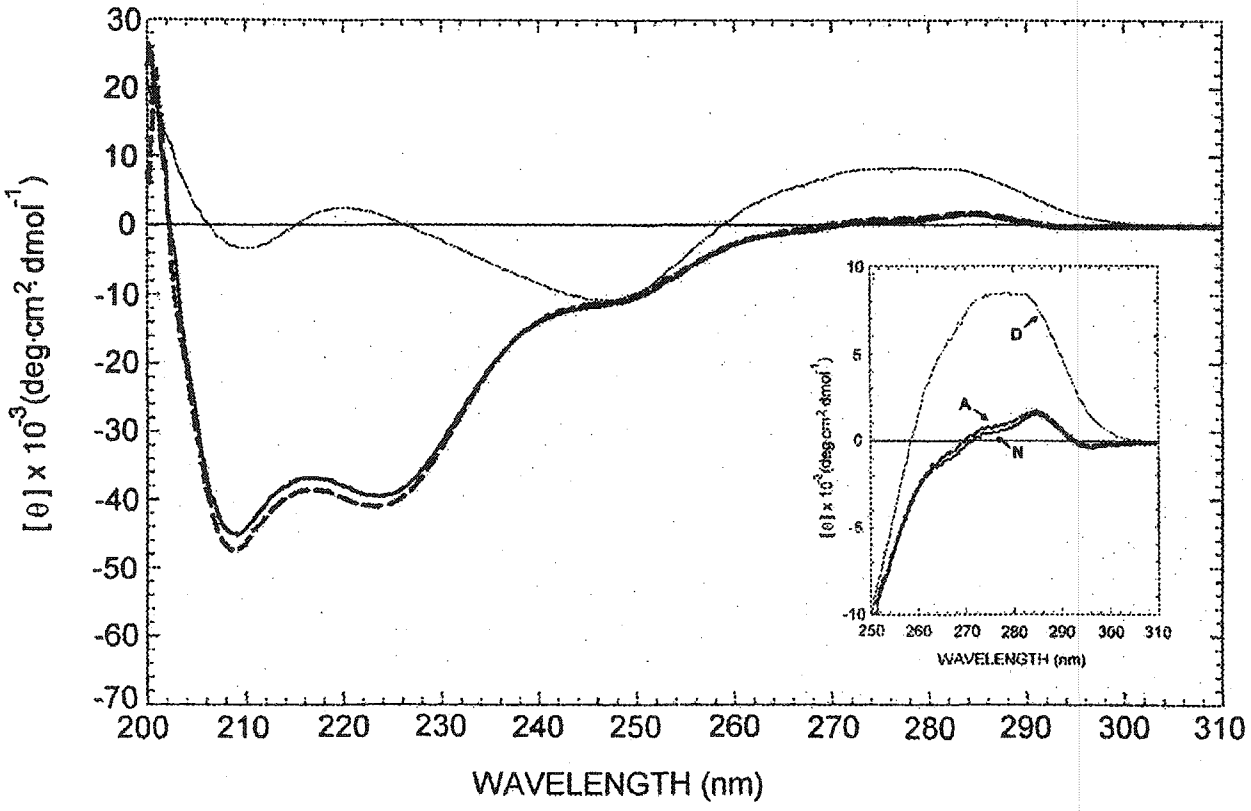


**Figure 51: CD Analysis of Native and Acetylated Nucleosomes.** Native nucleosomes (thick line); acetylated nucleosomes (thick dashed line); and nucleosome DNA (thin line) in 25 mM NaCl, 5 mM Tris-HCl (pH 7.5). The inset represents an enlarged view of the near UV region portion of the same spectra. A, acetylated nucleosome core particles; D, DNA; N, native nucleosome core particles. All data were recorded at 20°C on a Jasco J-720 spectropolarimeter.

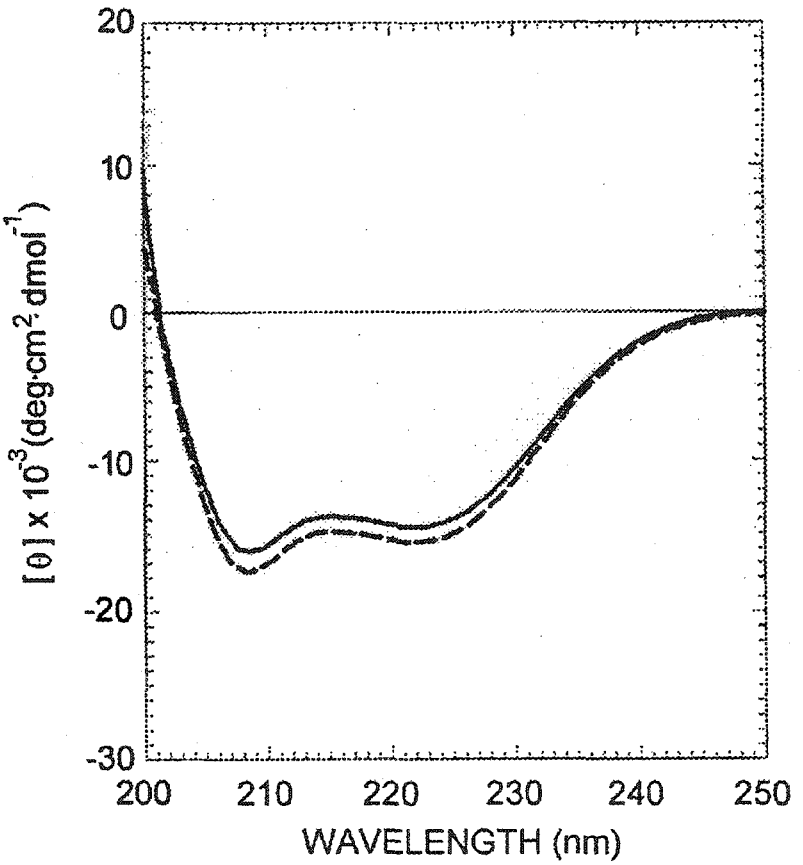


**Figure 52: CD Analysis of Native and Acetylated Nucleosomal Histones.** Native (thick line) and acetylated (thick dashed line) nucleosome core particle histone octamers. The spectra for the nucleosomal octamers were obtained by subtraction of the nucleosomal DNA spectrum shown in Figure 51. All spectra were recorded at 20°C on a Jasco J-720 spectropolarimeter.

## 5.5 CD Analysis of Acetylated N-Terminal Histone H4Tails

CD analysis of the nucleosomes has shown that the histone tails contain α-helices regardless of the presence of nucleosomal DNA and that the α-helical content increases in acetylated nucleosomes. It was decided to use CD to investigate the affect of acetylation on the histone tails directly by examining the histone H4 N-terminal tail with varying levels of acetylation. The experimental procedure is outlined in Figure 45. Histone H4 was purified from both control and hyperacetylated nucleosome samples using HTP column chromatography and RP-HPLC. Purified histone H4 was digested with Asp-N to remove the N-terminal tail (see Figure 13) and RP-HPLC was used to purify N-terminal tails with different levels of acetylation which were then analyzed using circular dichroism and PAGE analysis.

Figure 53 shows an AU-PAGE of the peptides produced by Asp-N digestion of histone H4. Digestions were initially done under two different conditions as recommended. However it was decided to do digestions at pH 8.0 (100 mM ammonium bicarbonate - lane 2) rather than at pH 6.0 (50 mM Tris-HCl - lane 1) because the later conditions produced an internal peptide which co-eluted with the tetra-acetylated N-terminal tail (Figure 53 - solid arrow). Figure 53 shows the different levels of acetylation on the H4 N-terminal tails very clearly and indicates that Asp-N digestion was successful. The RP-HPLC elution profile for the peptides produced from Asp-N digestion of histone H4 are shown in Figure 54. The numbered bars under the peaks within the elution profile indicate the fractions run on an AU-PAGE shown in Figure 55. The AU-PAGE shows that these peaks (Figure 54) also represent the different acetylated histone H4 tails in that the peak numbers (0-4) also correspond to the acetylation levels i.e. non-, mono-, di-, tri-, and tetra-acetylated H4 N-terminal tails (lanes 0-4 respectively in Figure 55). The other lanes on the gel correspond to histone H4 before (fB) and after digestion (fC) with Asp-N. Consequently this gel indicates that the purification procedure was successful.

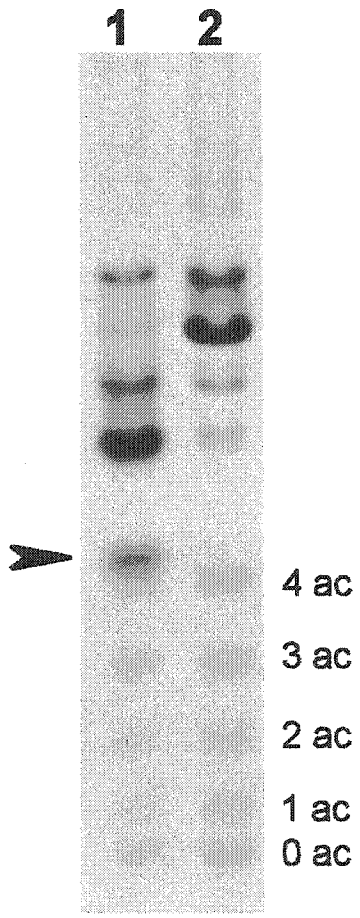


**Figure 53: AU-PAGE Analysis of AspN Digested Histone H4.** RP-HPLC purified H4 from acetylated chromatin obtained from CEL cell nuclei were digested with Asp-N endoproteinase in 50 mM Tris-HCl (pH 6.0) [lane 1] or 100 mM ammonium bicarbonate (pH 8.0) [lane 2]. The arrow points to an internal peptide that elutes in the same position as the RP-HPLC purified tetracetylated N-terminal peptide (amino acids 1-23). The numbers 0 to 4 ac refer to the different acetylation levels of the N-terminal H4 tails. All samples were mixed with 2 x AU sample buffer and loaded onto the 2.5 M urea, 5% acetic acid, 15% acrylamide gel. The gel was run at 80 volts in a 5% acetic acid running buffer. The gel was stained with Coomassie Blue.

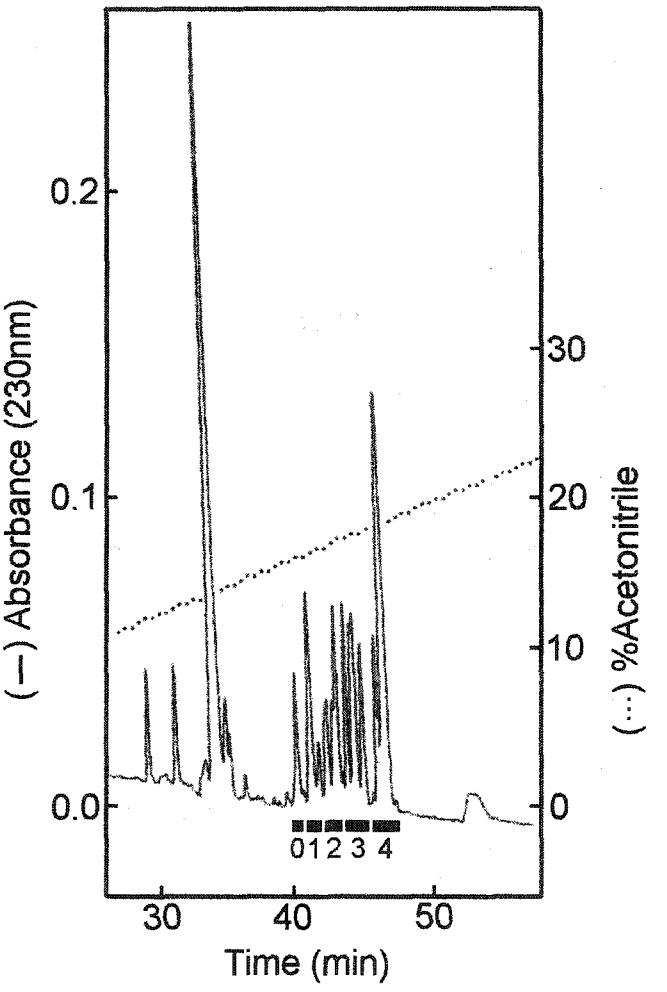


**Figure 54: RP-HPLC Elution Profile of AspN Digested Histone H4.**
Histone H4 was digested with Asp-N at pH 8.0. The % of acetonitrile is shown on the right hand axis, with the gradient shown as the dotted line. The numbered bars represent the fractions collected which contain the H4 tails with different levels of acetylation (0-4). A RP-HPLC 0.46 x 25 cm Vydac C18 column was used and histones were eluted with an acetonitrile gradient in 0.1% TFA at flow rate of 1 ml/minute. Absorbance was measured at 230 nm.

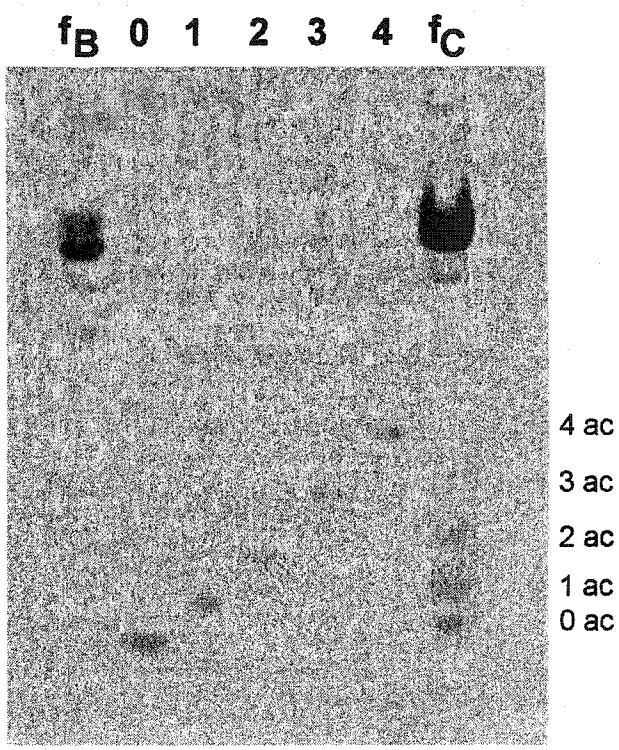


**Figure 55: AU-PAGE Analysis of RP-HPLC Purified Asp-N Digested Histone H4 N-Terminal Tails.** The lanes 0-4 correspond to the fractions collected in Figure 54. The histone H4 N-terminal tails with different levels of acetylation are indicated by the number 0-4 ac labeled on the side of the gel. Undigested acetylated histone H4 (fB); acetylate histone H4 digested with Asp-N at pH 8.0. All samples were mixed with 2 x AU sample buffer and loaded onto the 2.5 M urea, 5% acetic acid, 15% acrylamide gel. The gel was run at 80 volts in a 5% acetic acid running buffer. The gel was stained with Coomassie Blue.

CD analysis of the different purified H4 N-terminal tails, i.e. non-, mono-, di-, tri- and tetra-acetylated forms was initially done in an aqueous solution of 25 mM NaCl, 5mM Tris-HCl (pH 7.5). Figure 56 shows the CD spectra of the non-acetylated (solid line) and tetra-acetylated (dashed line) H4 N-terminal tail peptides. The spectra produced are typical of a random coil conformation and show a single peak at approximately 195 nm (Greenfield, 1969). It is obvious that acetylation does cause an increase in the negative ellipticity as evidenced by the downward shift of the acetylated spectra. The variation of ellipticity at 195 nm for all the differently acetylated H4 tails was plotted in Figure 57 with ellipticity as a function of the number of acetylation groups. This produces an inverse linear relationship with ellipticity decreasing as the number of acetyl groups increases. This probably occurs as a result of some protein compaction and the charge neutralization effects of acetylation.

It was decided to repeat the CD analysis using 90% trifluoroethanol. This solvent stabilizes existing α-helical secondary structure, but does not induce helix formation in sequences which do not already contain them (Lehrman *et al.*, 1990; Segawa *et al.*, 1991). TFE enhances the structure of small protein fragments in solution, therefore peptides which have α-helices will retain their α-helical structure in TFE whereas in an aqueous solution, they would appear as strictly random coil conformations.

Figure 58 shows the CD spectra of both the non- (dashed line) and tetra-acetylated (solid line) H4 tails in 90% TFE. Instead of the spectra produced in Figure 56, the same sample produces a spectra indicative of an α-helical conformation with absorption minima at approximately 208 and 222 nm. The tetra-acetylated sample is shifted downwards and to the right. Using the ellipticity values the percentage of α-helices was calculated. In the non-acetylated tail the value was approximately 17% which increased to 24% in the tetra-acetylated tail. The results from the different forms of acetylated H4 N-terminal tails were plotted in Figure 59 with the % of α-helices versus the number of acetyl groups on the H4 tail. This produces a relationship which increases exponentially with the level of acetylation. The data show that increasing levels of acetylation lead to an increase in α-helical content within the H4 N-terminal tail.

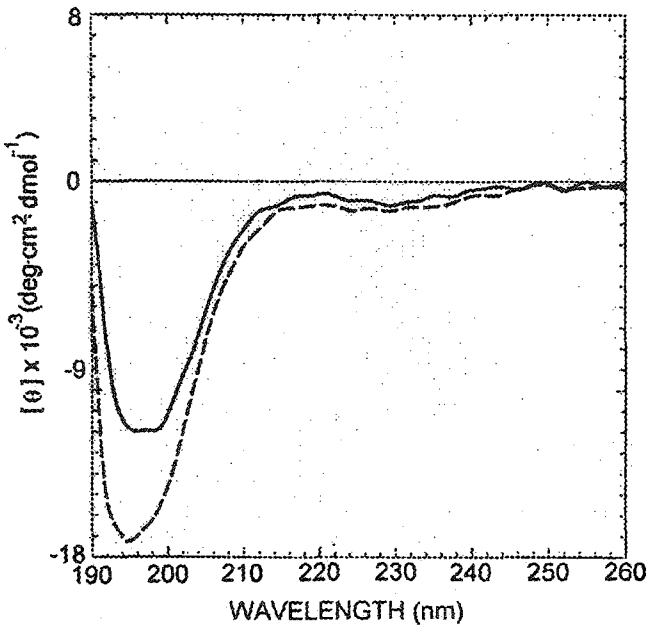


**Figure 56: CD Analysis of Non- (solid line) and Tetra-Acetylated (dashed line) Histone H4 N-terminal peptides.** Histone H4 N-terminal peptide is amino acids 1-23. Both samples were in 25mM NaCl, 5 mM Tris-HCl (pH 7.5) and the spectra were recorded at 20°C on a Jasco J-720 spectropolarimeter.

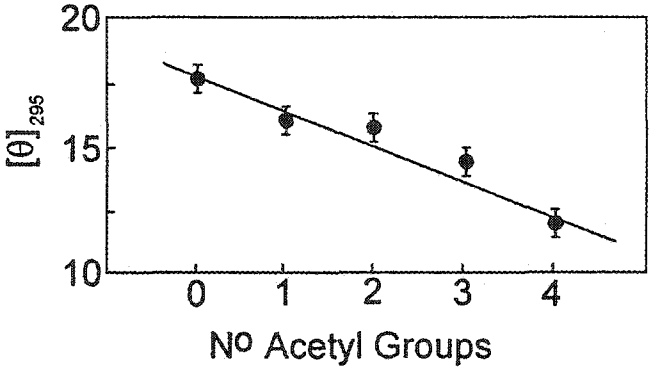


**Figure 57: Plot of Ellipticity at 195 nm versus the Level of Acetylation of the Histone H4 N-Terminal Tails.** Ellipticity values were determined using CD spectra in 25 mM NaCl, 5 mM Tris-HCL (pH 7.5) as per Figure 56

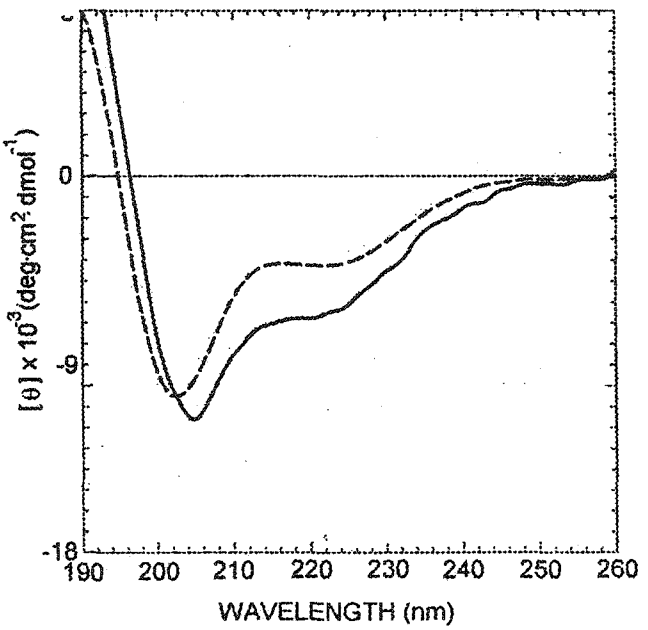


**Figure 58: CD Analysis of Native (dashed line) and Tetra-acetylated (solid line) Histone H4 N-terminal Peptides.** The N-terminal peptide was amino acids 1-23 in 90% TFE. Spectra were recorded at 20°C on a Jasco J-720 Spectropolarimeter.

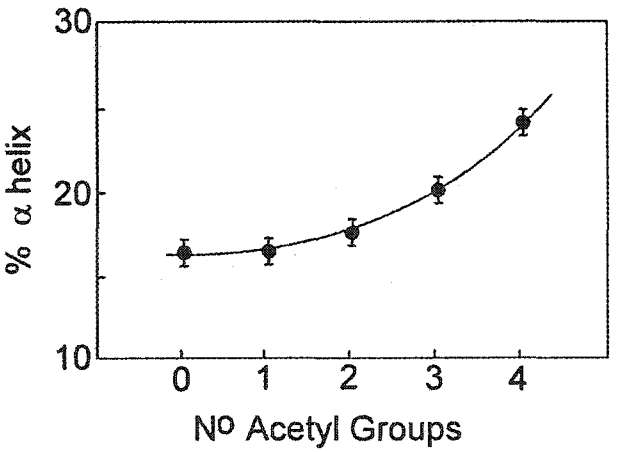


**Figure 59: Plot of % α-Helical Content versus the Number of Acetylated Lysine Residues for Histone H4 N-Terminal Peptides.** The amount of α-helix was determined by calculating the α-helical content from CD spectra (as represented by Figure 58).

## 5.6 Discussion

The importance of the histone tails in chromatin folding, particularly histones H3 and H4, means that it is important to examine and understand the structural impact of the post-translational modification which are known to occur in the N- and C-terminal histone tails. The ability to use RP-HPLC to fractionate some of these modified histones means that such investigations are now becoming possible. The most prevalent histone modification seen is histone acetylation which can occur on all the histone N-terminal tails. Interest in this modification has grown due to the discovery that HATs and HDACs are integral parts of transcriptional and silencing complexes respectively. Understanding the structural impact of this modification therefore has taken on an added significance.

Previous studies to examine the structural effects of acetylation have shown there are few differences at physiological pH. Studies have indicated that there is α-helical content within the histone tails in nucleosomes and that acetylation increases the overall α-helical content in an undefined way (Prevelige & Fasman, 1987; Banares *et al.*, 1997) Our studies have focused on histone conformation with and without acetylation using circular dichroism. CD is an excellent method of examining conformational changes in macromolecules and can be used to determine the quantity of α-helices present. Therefore CD was used to determine if acetylation affects the helical properties of the histone tails both alone and within the nucleosome and whether α-helical content was a direct result of interaction between the histone tails and nucleosomal DNA.

Initial analysis of native nucleosomes and the histone octamer (Figures 49 and 50) illustrated that it was possible to use CD analysis of the nucleosome to obtain reliable data about the histone octamer. Indeed the α-helical content of the octamer as determined from the nucleosomal data was found to be 48.7% (equation 2) which corresponded very well to the value of 49.4% determined from the crystal structure (Luger *et al.*, 1997; Arents *et al.*, 1991). The crystal structures have shown that the structure of the histones is almost exclusively α-helices or random coil. Both of the equations used to calculate percentage of α-helices from our data are based on models

containing α-helices and random coil only. Equation 2 proved to be better probably because it is derived from analysis of many globular proteins containing α-helices of approximately 10-20 residues which corresponds to the size of helices found in the histones, for instance within the histone fold.

Analysis of trypsinized nucleosomes (Figures 49 and 50) indicated that the histone tails contain about 17% α-helices. The results with acetylated nucleosome core particles and acetylated octamers (Figures 51 and 52) show conclusively that histone acetylation increases the α-helical content. Experiments using model peptides have shown that acetylation and the subsequent removal of the positive charges at lysine residues stabilizes helical structure and our results support these observations (Xu *et al.*, 1995). The fact that histone acetylation increases the α-helical content and that this occurs both in solution and when bound to DNA suggests that such an increase is not dependent on the interaction of the affected regions with DNA. If histone-DNA interactions were involved in the α-helical conformation then changes in the spectra should have been apparent when the nucleosomes were examined in buffers with increased NaCl concentrations which result in the salt-dependent dissociation of the histones, however no changes were apparent.

Examination of the purified histone H4 tails in both aqueous and TFE solutions have shown that the TFE stabilizes α-helical conformation. Importantly the percentage of α-helices increases exponentially with increasing levels of acetylation. Different secondary structure prediction methods were used to determine the domains predicted to have α-helical content within the histone H4 N-terminal tail (Figure 60). With all the models used the most consistent area predicted to contain α-helices in the N-terminal histone H4 tail is between residues 15 and 21. This area contains lysine 16, which is the only lysine residue to be acetylated in this region, therefore it is the most likely residue responsible for the increase in α-helical content. Acetylation of lysine 16 has already been shown to be important in a variety of organisms. In addition, as previously mentioned in the

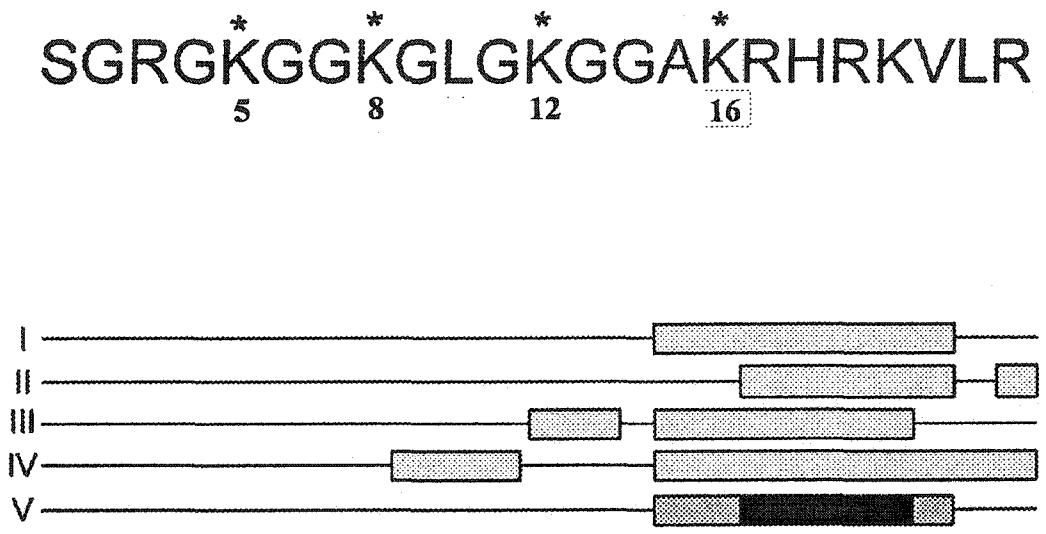


**Figure 60: Amino Acid Sequence of Histone H4 N-terminal Tail and Predicted α-Helical Structure.** The asterix (*) and numbers represent the lysine residues which can be acetylated. The predicted α-helical domains (grey boxes) for this sequence were determined using different prediction methods are listed: I, Chou & Fasman (1978); II, Double Prediction Method (Deleage & Roux, 1987); III, Gilbrat method (Gilbrat *et al.*, 1987); IV, α-amphipathic regions (Eisenberg *et al.*, 1984); V, consensus region for α-helices; the black area indicates the highest region of consensus.

introduction, acetylation of lysine 16 is crucial for dosage compensation and the increased transcriptional activation of the male X-chromosome in *Drosophila*. Indeed the acetyltransferase MOF, which acetylates lysine 16 in histone H4, is a component of the dosage compensation complex. Therefore the importance of lysine 16 acetylation in these processes may be coupled with the increased α-helical content. It is also possible of course that acetylation affects will be greater in other histone tails. For instance both histones H3 and H2B have predicted α-helical regions which are larger than that predicted for histone H4 (residues 15-21). Histone H3 has a predicted α helical region between residues 16-26 while H2B has one between 15-24 (using Fasman *et al,* 1976) and both these areas contain two lysines which can be acetylated: K18 and K23 in histone H3; and K15 and K20 in histone H2B.

The results provide the first experimental evidence that acetylation increased the α-helical content of the histone tails. It appears therefore that the structural effects of acetylation changes do not result in the huge changes in conformation that had previously been proposed or predicted, but rather are far more discrete.

It is possible that acetylation exerts its effects by operating in conjunction with other modifications or by modulating interactions with other proteins. If the 23 amino acids in the N-terminal tail are organized into a helical wheel, which is represented in Figure 61, then the proximity of serine 1 to the four lysine residues (K5, K8, K12, K16) which can be acetylated (indicated by *) can be seen. Serine 1 can be phosphorylated and this phosphorylation would neutralize the two positively charged arginine (R3 & R19) residues if they were part of a helix. Therefore if serine 1 is phosphorylated then together with acetylation of some if not all of the lysines, there may be a much greater impact on structure and a much greater increase in α-helical content than seen with acetylation alone. There is evidence that both modifications can occur simultaneously during spermiogenesis in trout and the resulting replacement of the histones by protamines, it has been shown that histone H4 is acetylated and serine 1 is phosphorylated (Sung & Dixon, 1970).

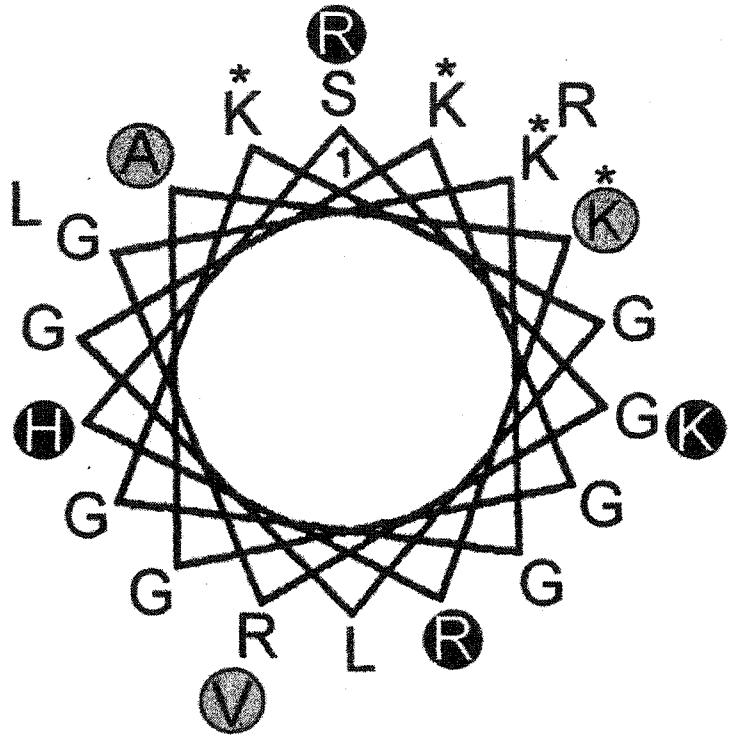


**Figure 61: Helical Wheel Representation of Histone H4 N-terminal Tail.**
The highlighted residues (grey and black) correspond the the consensus region residues shown in Figure 60 method V. Asterix (*) show lysines (K) residues which can be acetylated.

With regards to acetylation, the increase in α-helical content may play a role in affecting or modulating interactions with other complexes like chromatin remodeling complexes. Recently it has been shown that a small amphipathic α-helical region of approximately 10 amino acids is sufficient for transcriptional activation of Stat5 (Wang *et al.*, 2000a). This is a transcription factor involved in signal transduction and activation of transcription. Therefore since acetylation induces α-helical conformation it may be that interactions with histone α-helical regions may have important structural and functional implications.

It appears therefore that structural changes induced by acetylation are far more subtle than previously anticipated. However this does not preclude combinations of modifications working together to produce larger effects, nor does it prevent histone acetylation from having an important structural and functional impact on chromatin dynamics.

# 6.0 STRUCTURAL ANALYSIS OF NUCLEOSOMES AND POLYNUCLEOSOME FIBERS CONTAINING uH2A

The structural impact of histone post-translational modifications and their effect on nucleosome structure and chromatin folding remains a crucial area of investigation in chromatin research. It is known that the histone tails are important components in chromatin folding, therefore it is a reasonable assumption that their many post-translational modifications will also play a key role in chromatin dynamics. This chapter looks at the effects of one of the least studied modifications, specifically ubiquitination of histone H2A. Ubiquitin is a small globular, highly conserved protein which is conjugated *in vivo* to histones H1, H3, H2A and H2B (Goldknopf *et al.*, 1977; Chen *et al.*, 1980; Pham & Sauer, 2000). The most commonly ubiquitinated histones are H2A and H2B. In uH2A, ubiquitin reversibly attaches to one specific lysine in the C-terminal tail, namely lysine 119. Crystal structures have shown that the C-terminal tail of histone H2A extends from the nucleosome and its accessibility means it is available for post-translational modification and possible interactions with other proteins or nucleosomes (Luger *et al.*, 1997; Luger & Richmond, 1998b). The function of histone ubiquitin is as yet unknown but it does not appear to tag histones for degradation (Seale, 1981; Wu *et al.*, 1981). uH2A has been correlated with transcriptionally active chromatin although this has not been a universal observation. Regardless, coupled with the fact that some cell cycle observations indicate that uH2A decreases to non-detectable levels during the metaphase (when chromatin is highly condensed), has led to speculation that histone ubiquitination may affect chromatin folding and prevent more compact structures from forming (Ericsson *et al.*, 1986; Davie & Murphy, 1990). With this premise in mind, the impact of uH2A on both nucleosome structure and chromatin folding was examined (see Figure 62 for outline).

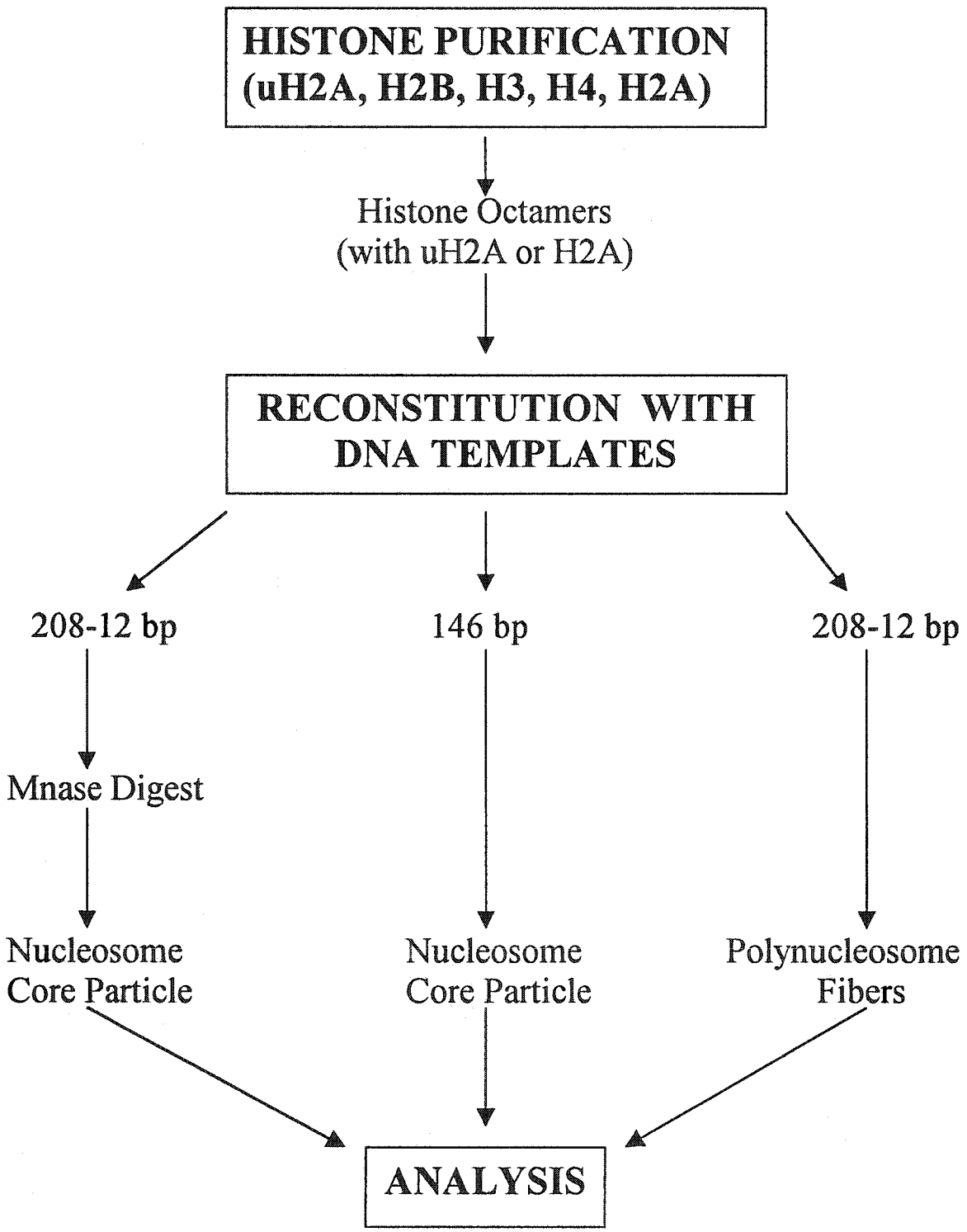


**Figure 62: Experimental Outline to Analyze Nucleosomes and Chromatin Fibers Reconstituted with uH2A.**

## 6.1 Reconstitution of uH2A and Control Octamers

The purification of uH2A proved to be rather arduous and time consuming. Initial attempts to obtain sufficient quantities of uH2A from chicken erythrocytes or HeLa cell cultures and RP-HPLC proved to be too costly and time-consuming to continue. Therefore large quantities of acid extracted calf thymus histones were used and uH2A was purified with extensive liquid column chromatography and a variety of different columns. The successful purification of uH2A from each column was monitored by checking the eluted fractions using western blots with anti-ubiquitin antibodies.

Once purified, uH2A (or control H2A) was mixed with equimolar quantities of calf thymus histones H2B, H3, and H4 to form histone octamers. The octamers were then reconstituted onto nucleosomal or chromatin DNA templates (146 bp or 208-12 bp). The different constructs containing uH2A were then compared to those with control H2A using analytical ultracentrifugation and sedimentation velocity analysis in both monovalent (NaCl) and divalent ($Mg^{2+}$) ion solutions, as well as PAGE analysis and solubility assays (See Figure 62).

## 6.2 Structural Analysis of Nucleosomes Containing uH2A

Nucleosome particles containing either control H2A or uH2A were produced using two different DNA templates, the first was 146 bp, the second 208-12 bp which was digested down to 146 bp with Mnase. Nucleosome particles were analyzed using PAGE, sedimentation velocity analysis, and DNase I footprinting.

### *6.2.1 PAGE Analysis*

Figure 63 shows an SDS-PAGE of the histone proteins used for the reconstitutions. Both control (lane 2) and uH2A (lane 4) histones are shown. These were compared to the total acid extracted histones from calf thymus nuclei (lanes 1 & 3) which are identified at the side of the gel. Both the H2A and uH2A samples contain equimolar quantities of

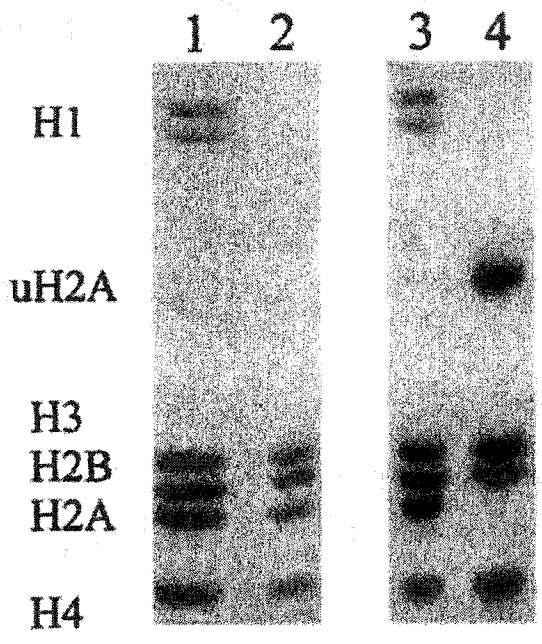


**Figure 63: SDS-PAGE of Histone Octamers Containing Either Control H2A or Purified uH2A.** Lanes 1 & 3 show a total histone marker from acid extracted calf thymus histones, the identities of the different histones are listed at the side. Control octamers are shown in Lane 2; uH2A octamers in lane 4. All samples were mixed with 2x SDS-sample buffer and boiled for 5 minutes prior to loading. The SDS-PAGE was run at 100 volts in a 0.05 M Tris, 0.38 M glycine, 0.1% SDS running buffer. Bands were visualized by Coomassie Blue staining.

histones and lane 4 clearly shows that uH2A purification was successful. The uH2A runs approximately half-way between histone H1 and H3 and western blotting with anti-ubiquitin antibodies was used to confirm its identity.

Figure 64 shows a 4% native acrylamide gel of the two different reconstituted nucleosome core particles (H2A, uH2A) compared to native nucleosomes from chicken erythrocytes (Ck) . From the gel it is apparent that the nucleosomes are stable and comparison to the marker (M) indicates that there is no free DNA (146 bp) present. All the nucleosomes appear to run normally indicating that uH2A was able to incorporate into the nucleosomes. The uH2A nucleosomes migrate more slowly in the gel which is as expected because of the added mass of the ubiquitin.

### 6.2.2 DNase I Digestion

The different reconstituted nucleosomes (H2A and uH2A) were digested with DNase I to see if the presence of the ubiquitin moiety affected DNase I digestion pattern by blocking or preventing complete access to some of the preferred cleavage sites (S1-S14). The DNase I footprint is shown in Figure 65 with the preferred cleavage sites (S2-S14) numbered at the side. The native chicken nucleosomes (Ck) and the H2A and uH2A reconstituted nucleosomes all exhibit the same digestion patterns. There are no differences apparent with the uH2A sample which indicates that the presence of ubiquitin on H2A does not impede or change the ability of DNase I to access the nucleosome during digestion. These results concur with previous studies (Kleinschmidt & Martinson 1981; Davies & Lindsey, 1994) although we were not aware of any differences in the rate of DNase I digestion between the control and uH2A samples.

### 6.2.3 Sedimentation Velocity Analysis

Nucleosomes with or without uH2A were analyzed using sedimentation velocity analysis at various salt concentrations in 10mM Tris-HCl (pH 7.5), 0.1 mM EDTA buffer. The combined results are shown in Figure 66. The sedimentation coefficients obtained are indicated by the points shown (•) for the control and (○) for uH2A nucleosomes. As the figure indicates the points for both types of nucleosomes correlate extremely well. The solid line represents the best fit line for these points while the dashed line corresponds to

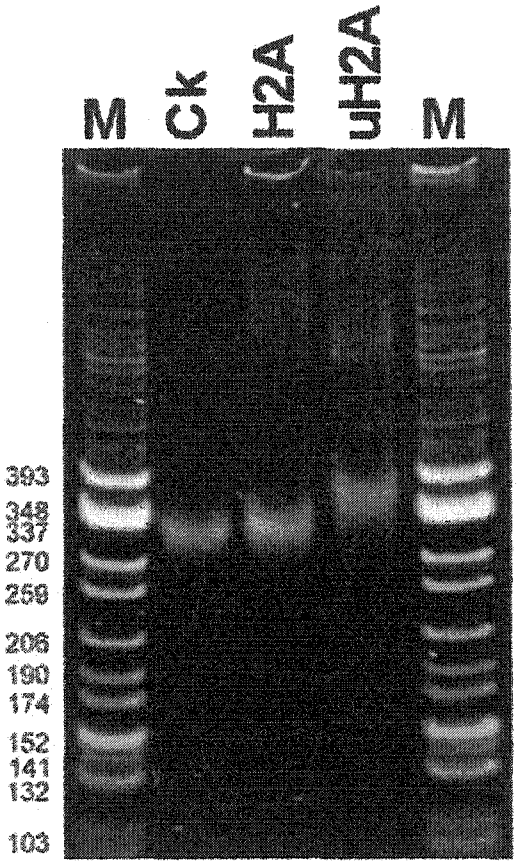


**Figure 64: 4% Native Acrylamide Gel of Nucleosomes Containing H2A or uH2A.** Reconstituted nucleosomes with H2A and uH2A were compared to native nucleosome core particles from chicken erythrocytes (Ck). M is *Cfo*I digested pBR322 DNA, the sizes of the DNA fragments produced are shown at the side. All samples were mixed with 2xNative sample buffer just prior to loading. The 4% non-denaturing acrylamide gel was run at 60 volts in a 1xE running buffer. DNA was visualized using ethidium bromide staining.

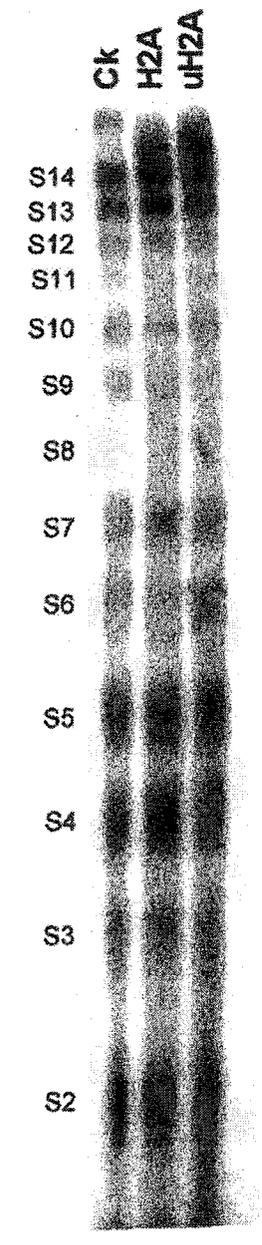


**Figure 65: DNase I Footprint of Nucleosomes Containing H2A or uH2A.** Nucleosomes containing uH2A, H2A or native nucleosomes from chicken erythrocytes (Ck) were 5' end labeled with [γ-32P]-ATP and digested with 70 units of DNase I/ml at 0°C. Samples were mixed with DNase I sample buffer and heated at 90-100°C for 10 minutes prior to loading. The 10% acrylamide (20:1 acrylamide:bisacrylamide), 7 M urea, 1xTBE denaturing gel was run at 60 watts in 1xTBE running buffer. The gel was fixed for 60 minutes, dried on filter paper and autoradiographed. S1-S14 refer to preferred DNase I cleavage sites.

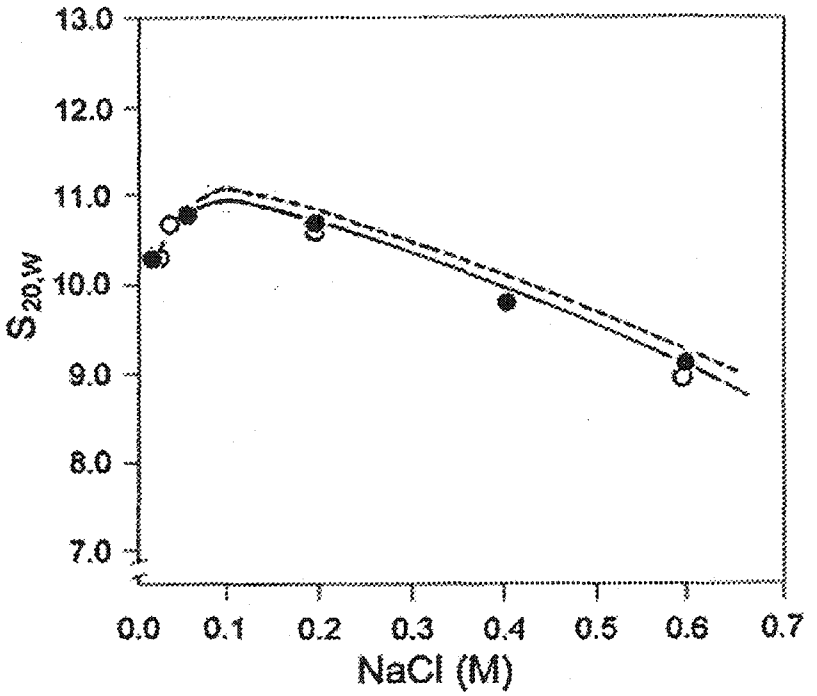


**Figure 66: Sedimentation Velocity Analysis of Nucleosomes +/- uH2A in Different NaCl Buffers.** The sedimentation coefficients ($S_{20,w}$) were determined for nucleosomes containing control H2A (●) or uH2A (○) at different salt concentrations. The solid line represents a best fit line for the nucleosome samples. The dashed line represents native nucleosomes from chicken erythrocytes. All samples were dialyzed versus buffers containing NaCl in 10 mM Tris-HCl (pH 7.5), 0.1 mM EDTA. All velocity runs were done at 20°C and 40,000 rpm in a Beckman XL-A ultracentrifuge.

native chicken erythrocyte nucleosome core particles. The results show very well that the two types of molecules were virtually the same and that the incorporation of uH2A had no significant effect on nucleosome structure.

Next we wanted to see if reconstitution with uH2A was affected by the size of the DNA fragment used in the reconstitution. Even though nucleosome assembly was not prevented with 146 bp it may be that the ubiquitin would block assembly on a longer piece of DNA or make assembly more difficult in some way. Therefore the octamers were reconstituted with the 208-12 bp DNA template and digested with Mnase to produce nucleosome core particles. Figure 67a shows the Mnase digestion of the 208-12 fibers. Fibers digested 30 minutes were then purified using a sucrose gradient and Figure 67b shows the fractions collected from that gradient. Fraction 7 was used for the sedimentation velocity analysis. As before the sedimentation coefficients were determined at different concentrations of NaCl in Tris-EDTA buffer and are shown in Figure 68. The solid triangles (▲) represent the nucleosomes produced by digestion with Mnase while the open circles (○) once again represent the uH2A nucleosomes reconstituted with 146 bp DNA as previously shown in Figure 66. Comparison shows that the nucleosome core particles produced from 208-12 were virtually identical to their 146 bp counterparts. Therefore reconstitution of uH2A into nucleosomes produces consistent results and indicate that the incorporation of uH2A was not impeded and nucleosome structure or digestion profiles were unaffected.

## 6.3 Structural Analysis of Polynucleosome Fibers Containing uH2A

While nucleosome structure does not appear to be perturbed by the presence of uH2A, given the size of the modification it still seems likely that it may have an impact on fiber folding and association. To investigate this possibility homogenous polynucleosome fibers were created by reconstituting the 208-12 chromatin DNA template with octamers containing either uH2A or H2A and comparing their folding characteristics using sedimentation velocity analysis and solubility assays.

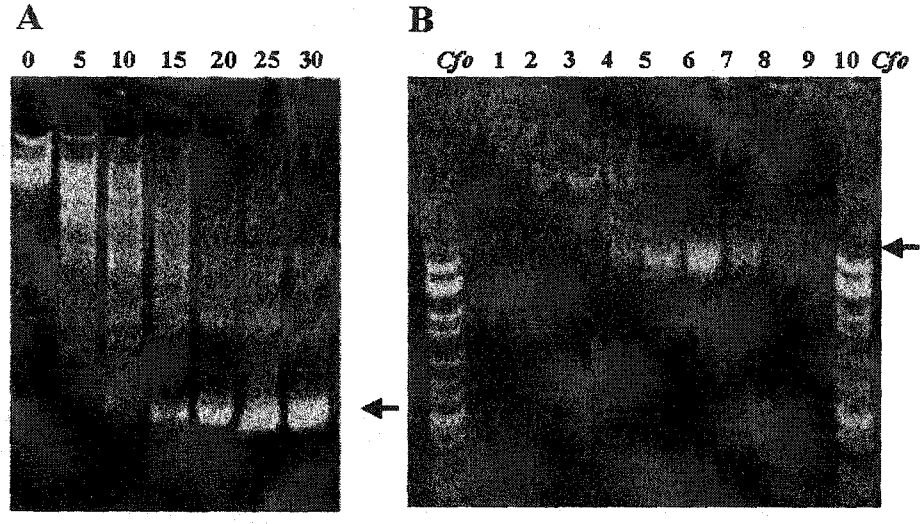


**Figure 67: Native 4% Acrylamide PAGE of Mnase Digested 208-12 Polynucleosome Fibers Reconstituted with uH2A.** **A.** 208-12 polynucleosome arrays reconstituted with uH2A and digested with 2 units/ml of Mnase. (0 to 35 refer to digestion times in minutes). **B.** Reconstituted 208-12 polynucleosome arrays digested for 30 minutes with 2 units/ml of Mnase and purified on a 5-20% sucrose gradient in 5 mM NaCl, 10 mM Tris (pH 7.5), 0.2 mM EDTA buffer and run in a SW-41 rotor at 4°C and 125,000 x g for 17 hours. One ml fractions (1-10) were collected from the bottom to the top of the gradient. *Cfo*, DNA marker created by *Cfo*I digestion of pBR322. The non-denaturing gels were run at 60 volts in 1xE running buffer and stained with ethidium bromide. On both gels the arrows point to the mononucleosome particles.

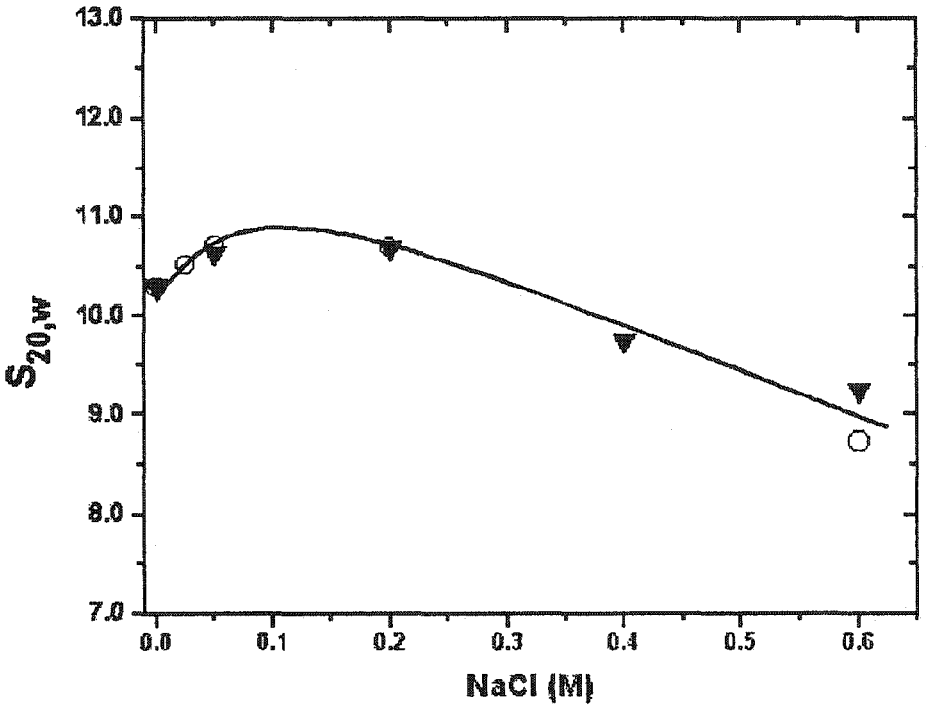


**Figure 68: Sedimentation Velocity Analysis of Nucleosomes Containing uH2A in Different NaCl Buffers.** The sedimentation coefficients ($S_{20,w}$) were determined at different salt concentrations. Both samples contain uH2A; (○) are nucleosomes reconstituted with 146 bp DNA as shown in Figure 68; (▼) are nucleosomes originally reconstituted with 208-12 bp DNA and digested with Mnase to form nucleosome core particles. All samples were dialyzed versus buffers containing NaCl in 10 mM Tris-HCl (pH 7.5), 0.1 mM EDTA. All velocity runs were done at 20°C and 40,000 rpm in a Beckman XL-A ultracentrifuge.

### 6.3.1 Solubility Assays

Increasing concentrations of divalent ions like magnesium chloride ($Mg^{2+}$) will result in the oligomerization of the polynucleosome fibers. While this reversible reaction is distinct from the *in vivo* folding process, it is still relevant because it can provide information about possible *in vivo* interactions between chromatin fibers during condensation (Schwarz *et al.*, 1996) Figure 69 shows the results of the magnesium ($Mg^{2+}$) dependent oligomerization assay with the uH2A and H2A polynucleosome fibers. Comparison of the samples show that the control fibers behave as expected and at 4 mM $MgCl_2$ about 50% of the fibers have oligomerized. However the uH2A fibers actually oligomerize at lower concentrations of $Mg^{2+}$ meaning that at 4 mM $MgCl_2$ virtually all the fibers have aggregated. This implies that the ubiquitin moiety helps the aggregation process possibly by shielding some of the DNA charge and/or the ubiquitin protein may provide additional surfaces for inter-array contacts.

### 6.3.2 Sedimentation Velocity Analysis

Reconstitution of uH2A octamers with 208-12 DNA and their subsequent digestion with Mnase had demonstrated that polynucleosome fibers with uH2A could not only be created but could also be used to form normal nucleosome particles. The structural features of these polynucleosome fibers were more closely examined using sedimentation velocity analysis in different concentrations of both NaCl and $MgCl_2$.

Figure 70 shows the combined sedimentation velocity results for uH2A (▲) and H2A (●) 208-12 fibers with varying concentrations of NaCl. From these results it appears that the uH2A fibers (▲) exhibit ionic dependent folding characteristics which are virtually identical to the control (●) fibers and are consistent with native chromatin fragments of 12 nucleosomes from chicken erythrocytes (solid line) (Garcia-Ramirez, 1992). Thus under these conditions uH2A does not appear to inhibit or change chromatin folding.

Analysis was also done with increasing concentrations of $MgCl_2$. Figure 71 shows the integral distribution of the uH2A arrays with (●) and without (○) 2 mM $MgCl_2$. Under these conditions the arrays exhibit a folding event which is typically seen with 208-12

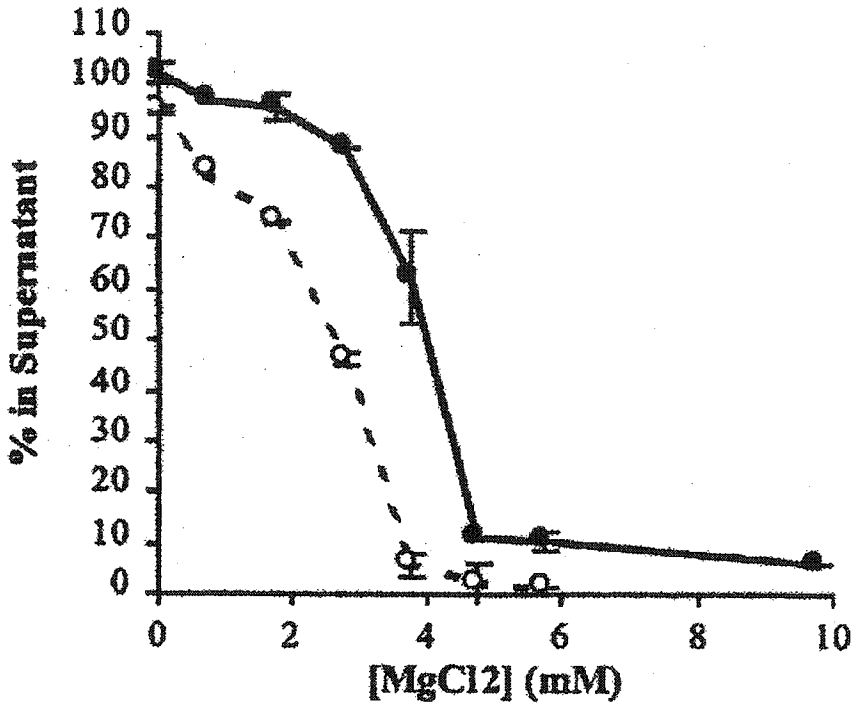


**Figure 69: Magnesium Dependent Oligomerization of Control (•) and uH2A (○) Polynucleosomal Arrays.** Arrays were incubated in increasing concentrations of $MgCl_2$ for 10 minutes at room temperature before centrifugation. Unaggregated arrays remain soluble in the supernatant as determined by $A_{260}$ measurements. Each point represents the average of two to three determinations. The % is determined via comparison to concentration at 0 mM $MgCl_2$ (100%).

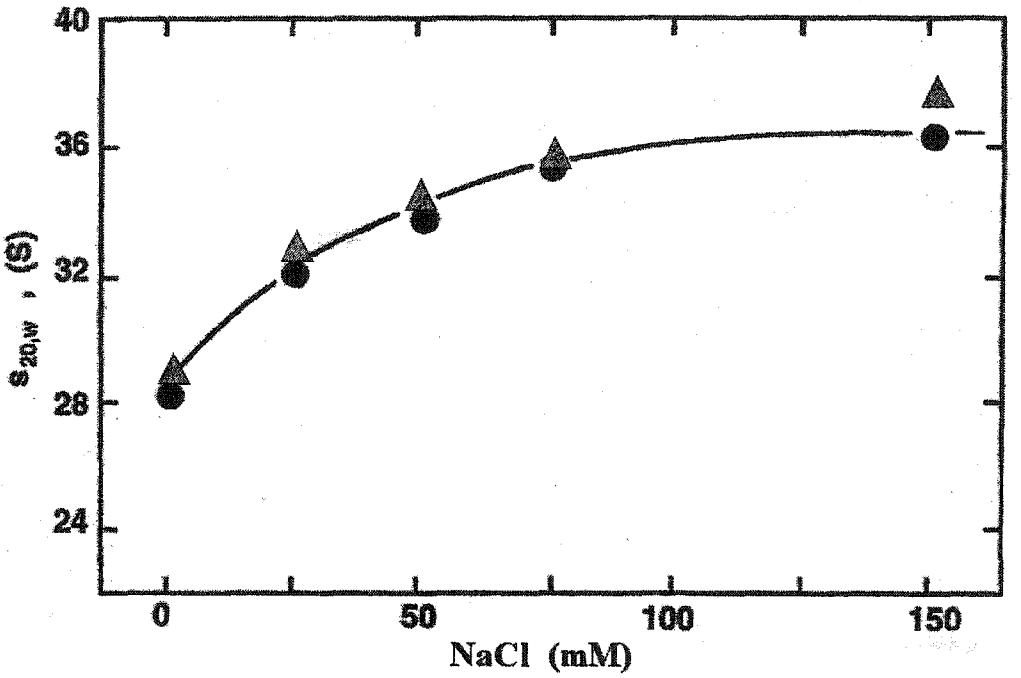


**Figure 70: Sedimentation Velocity Analysis of 208-12 Polynucleosome Arrays Reconstituted with uH2A in Different NaCl Buffers.** Sedimentation coefficients ($S_{20,w}$) of 208-12 fibers with (▲) and without (●) uH2A. The solid line represents the H1-depleted native chicken erythrocyte chromatin with and average of 12 nucleosomes (Garcia-Ramirez *et al.*, 1992). All experiments were done at 20°C and 20,000 rpm in a Beckman XL-A analytical ultracentrifuge.

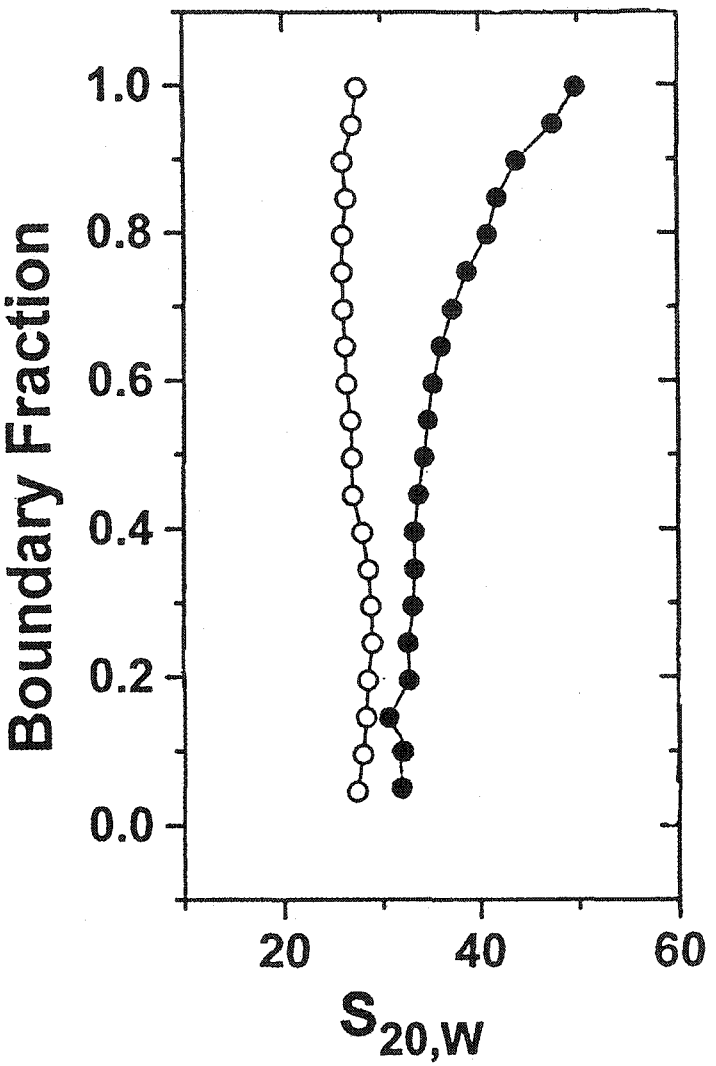


**Figure 71: Magnesium Dependence of the Sedimentation Coefficient ($s_{20,w}$) of 208-12 Polynucleosome Fibers Reconstituted with uH2A.** Integral distribution of the sedimentation coefficient of uH2A containing 208-12 nucleosomal arrays in the absence (○) or in the presence of 2 mM $MgCl_2$ (●). The integral distributions were obtained after analysis of the sedimentation boundaries using the method van Holde and Weischet (1978). All runs were done at 20°C and 20,000 rpm in a Beckman XL-A analytical ultracentrifuge.

fibers, and is referred to as the 28 S to 40 S transition. This indicates that a folding event is occurring within the uH2A fibers.

The sedimentation coefficients for both the H2A and uH2A fibers obtained at different $Mg^{2+}$ concentrations are plotted in Figure 72. This figure indicates that the sedimentation coefficients for the uH2A arrays (●,■) are on average 11% lower than the control arrays (○). It is possible that the decrease in sedimentation coefficients is due to the presence of fewer histones (we found that it was necessary to slightly undersaturate the fibers because of oligomerization problems) and/or a slight increase in the frictional parameters of uH2A arrays due to the presence of two ubiquitin molecules per nucleosome. Nevertheless, the increasing $S_{20,w}$ values for the uH2A arrays in response to the increased $MgCl_2$ concentration obviously parallel those of the control arrays. To determine the extent of folding which had occurred, the coefficients for each array were plotted relative to their respective values in 0 mM MgCl2 buffer, i.e. $S^{+MgCl}{}_2/S^{-MgCl}{}_2$. The results are shown in Figure 73 and illustrate a much closer relationship indicating that the uH2A arrays attained a degree of compaction very similar to that of the control array. Therefore there was a 35-40% increase in the sedimentation coefficient of the uH2A arrays which is consistent with the formation of an intermediately folded species such as an open helix (Hansen *et al.*, 1989; Garcia-Ramirez *et al.*, 1992; Schwarz & Hansen, 1994). Therefore even in the presence of uH2A, polynucleosome compaction is not prevented and does not appear to be severely hindered.

## 6.4 Other Possibilities?

Since uH2A did not appear to prevent nucleosome or fiber formation or folding we wanted to examine other characteristics and possibilities. Ubiquitinated histones may possibly have multiple roles or they may work in conjunction with some other modifications to elicite a stronger structural impact. The presence of uH2A has been correlated to active DNA which tends to have a more open conformation and contains acetylated histones. Therefore it is possible that the two modifications together may act to produce a more unstable nucleosome. In order to gain more insight into this possibility

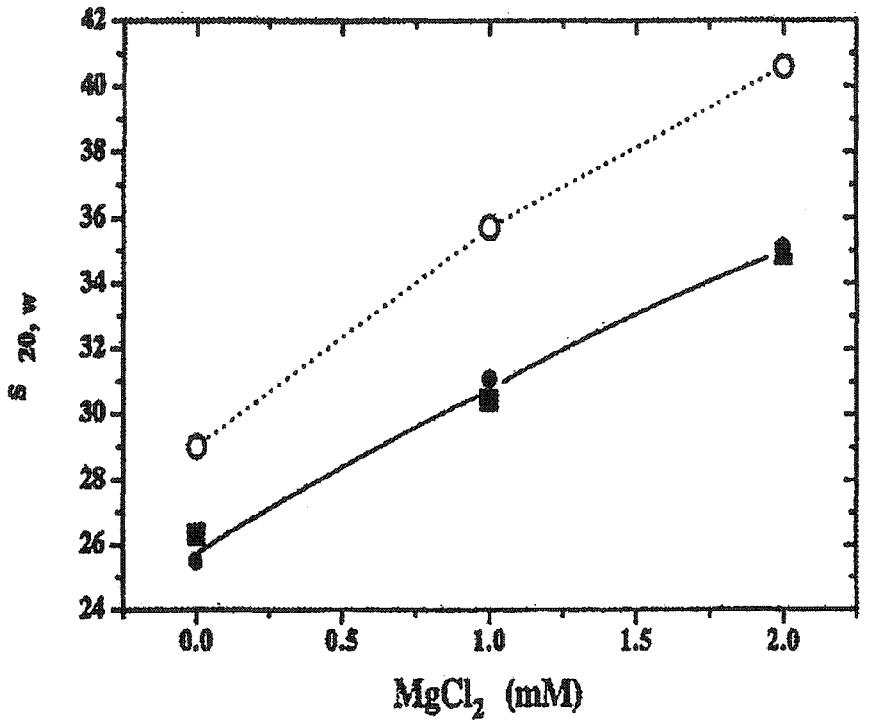


**Figure 72: Sedimentation Velocity Data for 208-12 Complexes Reconstituted with uH2A in $MgCl_2$ Buffers.** Arrays were reconstituted with native histones (○) or with octamers containing uH2A (●,■). The data shown by (●,■) were obtained from two independent reconstitution experiments. All data were recorded at 20°C and 20,000 rpm using an Beckman XL-A analytical ultracentrifuge. All samples were in $MgCl_2$ in 10 mM Tris-HCl (pH 7.5), 0.1 mM EDTA buffer.

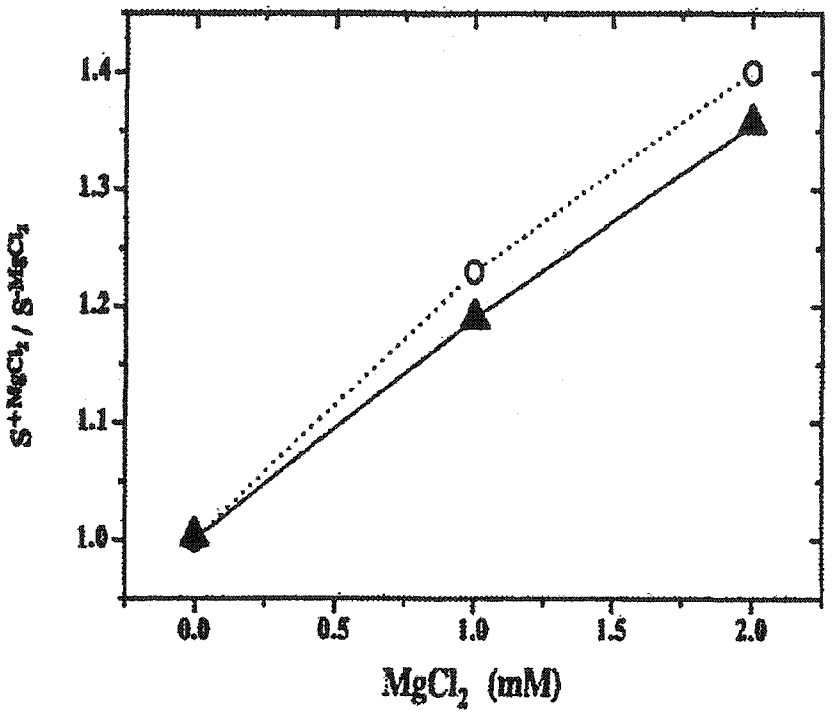


**Figure 73: Sedimentation Velocity Analysis Data for 208-12 Complexes Reconstituted with uH2A in $MgCl_2$ buffers Replotted as $S^{+MgCl_2}/S^{-MgCl_2}$.**
The results from Figure 72 were replotted so that the sedimentation coefficient of the arrays at a given magnesium concentration ($S^{+MgCl_2}$) are plotted relative to the sedimentation coefficient of the arrays in the starting buffer in the absence of magnesium ($S^{-MgCl_2}$). Nucleosomal arrays with native (○) and uH2A (▲) are shown. (▲) is the average of two sets of data (■, ●). All experiments were carried out at 20°C and 20,000 rpm in a Beckman XL-A Analytical Ultracentrifuge.

hydroxyapatite elution profiles of chromatin samples were examined. Histones H2A/H2B and H3/H4 can be eluted from a HTP column using a sodium chloride gradient. Presumably if chromatin or nucleosomes are unstable then the histones from these structures should be eluted towards the beginning of the elution peak. Conversely the histones from more stable structures will be eluted later in the peak. Since the location of ubiquitinated histones within an elution profile can be determined using western blotting it should be easy to determine if ubiquitinated histones are eluted at a specific location within the profile. In addition, if samples with different levels of acetylation are used it may be possible to see if acetylation has any effect on the elution of ubiquitinated histones. To investigate, salt extraction and the lysis of HeLa cell nuclei were used to obtain chromatin samples. Both samples were used equivalent in that they were obtained in the same way, however one sample (SII) was obtained from butyrate treated cells which will contain higher levels of acetylation, and the other (SE) was from a control sample. Each sample was loaded onto a HTP column and the histones were eluted using a 0 to 2 M salt gradient in potassium phosphate buffer (pH 6.8).

Before the elution profiles could be directly compared it was necessary to ensure that the profiles were consistent and equivalent. While every attempt was made to ensure consistency between the columns, the only way to determine if the salt gradients were accurate and equivalent was to measure and plot the salt content in the different fractions using a refractometer. By plotting these values it is possible to determine the linearity of the two gradients and to determine the fractions which are directly equivalent. Figure 74 shows the linear gradient and alignment of the two salt gradients. Figure 75 shows the plot of the two elution profiles which have been adjusted so that their fraction numbers refer to equivalent samples, and it demonstrates that the two profiles are strikingly similar.

Aliquots for selected fractions throughout the profile were run on both AU-PAGE and SDS-PAGE. The SDS-PAGE gels were western blotted to determined the location of ubiquitinated histone. Figure 76 shows the gels and western blot for the SE (■) elution profile. The SDS-PAGE (SDS) confirms the identity of the different histones, but

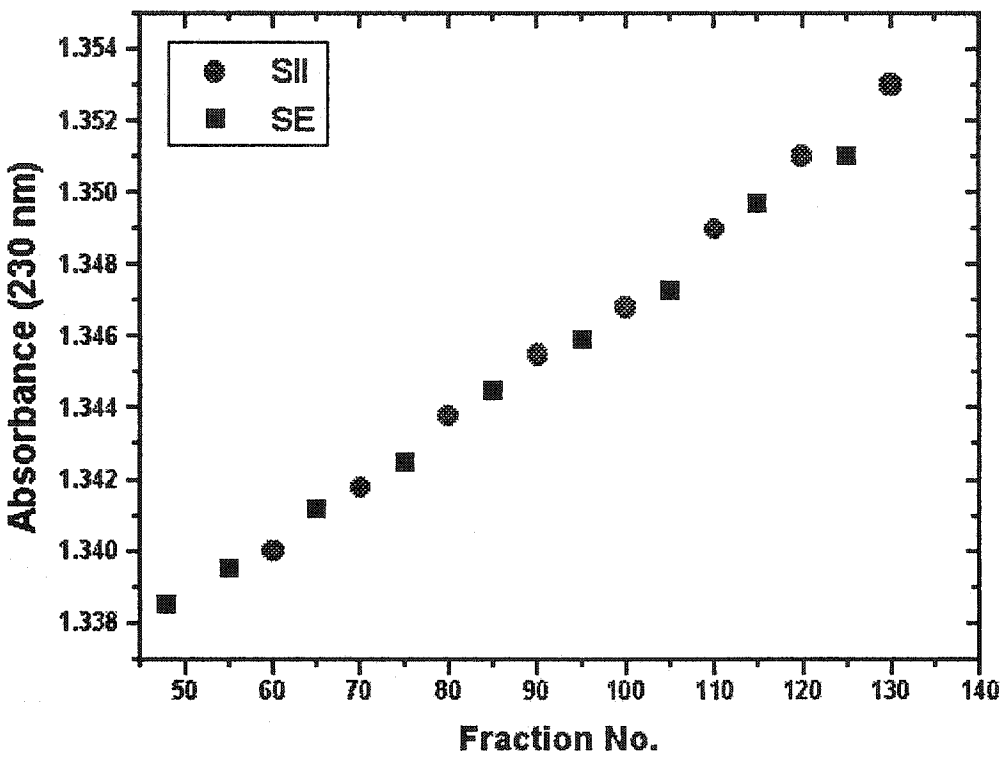


**Figure 74: Salt Gradient for HTP Elution Profiles of HeLa SII and SE Chromatin Samples.** Shows the correlation between SE and SII salt gradients and allows the correction of fraction numbers so that equivalent samples can be compared. SE and SII are equivalent samples from the salt extraction of HeLa cell nuclei; SE is from control cultures; SII from butyrate treated cultures (highly acetylated). All refractive index readings were done on a Carl Zeiss Jenna Refractometer.

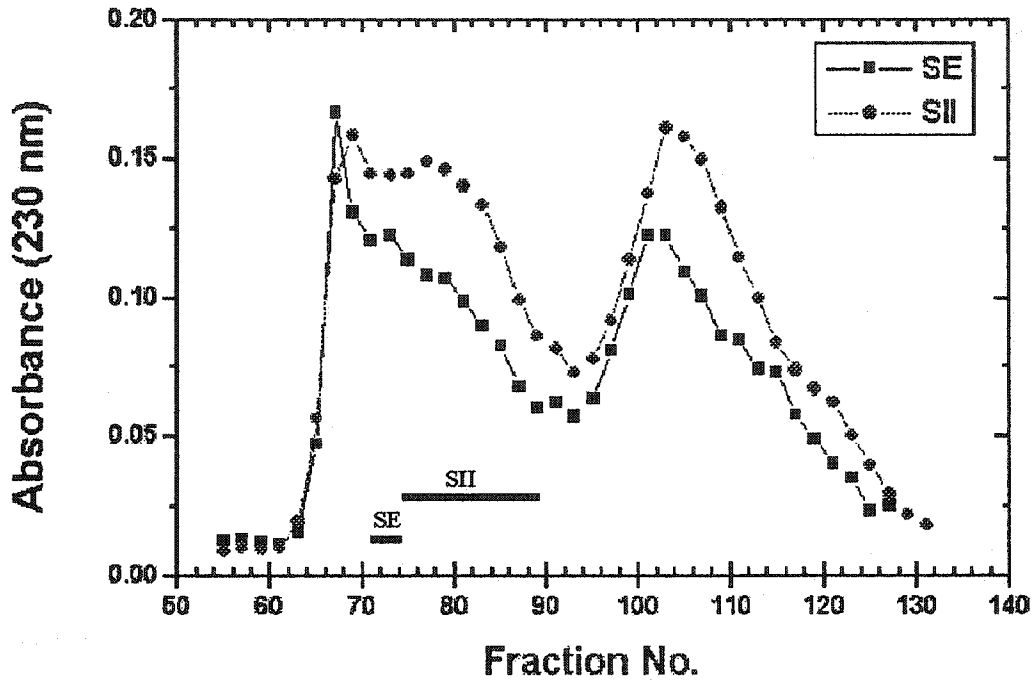


**Figure 75: HTP Elution Profiles for HeLa SE and SII Chromatin Samples.** Equivalent chromatin samples from control (SE) and butyrate treated (SII) salt extracted HeLa cell nuclei eluted from a 1.5 x 15 cm HTP column eluted with a 0 to 2 M NaCl gradient in potassium phosphate buffer (pH 6.8). Fraction numbers are equivalent for both columns and were adjusted using salt concentration refractive index readings (as per Figure 74).

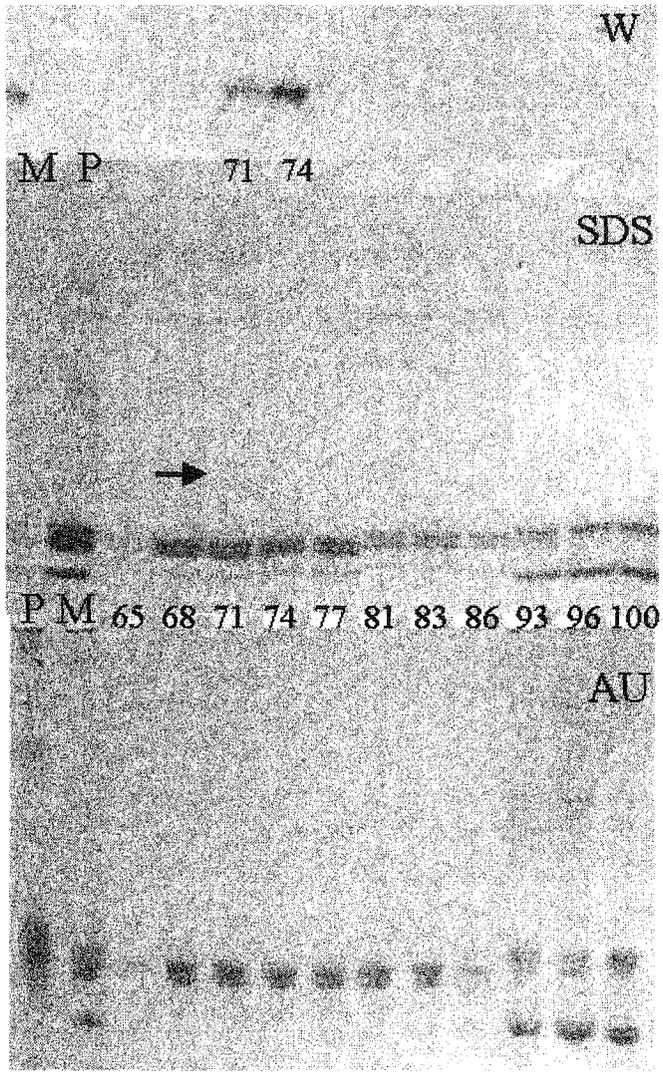


**Figure 76: PAGE and Western Blot Analysis of HTP Elution Profile of HeLa SE Chromatin Sample**. SE, control HeLa sample; AU, acetic acid urea PAGE; SDS, SDS-PAGE; W, western blot of SDS-PAGE; M, HeLa core histone marker; P, sample loaded onto HTP column. Arrow points to approximate location of ubiquitinated histones. Numbers correspond to fraction numbers in Figure 75. AU-PAGE was a 2.5 M urea, 5% acetic acid, 15% acrylamide gel run at 80 volts in 5% acetic acid running buffer and stained with Coomassie Blue. SDS-PAGE was a 6% stacking, 15% separating gel run at 100 volts in 0.05 M Tris-base, 0.38 M glycine, 0.1% SDS running buffer and stained with Coomassie Blue. Western blot of SDS-PAGE transferred onto PVDF membrane using 1/6000 rabbit anti-ubiquitin antibody and 1/3000 goat anti-rabbit HRP-conjugated secondary antibody and Rennassance® Western Blot Chemiluminescence Reagents.

ubiquitinated histones are present in such small quantities that they can not be visualized on the gel, therefore an arrow points to its approximate location as determined with western blotting and overloading of samples on SDS-PAGE. The AU-PAGE (AU) shows the same proteins but also indicates acetylation levels, which was minimal for the SE sample. The western (W) identifies two bands, one quite intense, corresponding to fractions 71 and 74. The ubiquitinated histones therefore elute within the first half of the H2A/B peak but not at the beginning of the peak which starts at fraction 65.

Figure 77 shows the equivalent fractions for the SII sample. The AU-PAGE (AU) shows that the sample is highly acetylated as expected. The SDS-PAGE (SDS) also shows the same protein distribution with an arrow pointing to the approximate location of the ubiquitinated histones. Once again, insufficient ubiquitinated histones were present to visually identify on the gel. However the western blot shows several distinct bands for ubiquitinated histones which range from fractions 74 to 89 with fractions 74 to 83 being quite intense. Figure 78 shows a direct comparison of the two western blots and their relative positions where it is obvious that in the SII fraction ubiquitinated histones are more abundant and are eluted over a much wider range and later in the elution profile than the SE sample. The elution of ubiquitinated histones towards the middle of the profile in both samples would seem to indicate that ubiquitin has more of a stabilizing effect than initially expected which appears to be enhanced in acetylated samples. However whether this is a result of a direct interaction between acetylation and ubiquitination can not be determined with these experiments.

Protamine displacement assays were also done. In these assays reconstituted nucleosomes with and without uH2A were mixed with increasing quantities of protamines to see if ubiquitination aided the process of histone replacement by protamines, an event which occurs during spermiogenesis. Initial results indicate that the presence of ubiquitin made the nucleosomes more stable as higher concentrations of protamines appeared to be required in order to displace the histones as shown in Figure 79. Therefore it appears that uH2A ubiquitination may actually produce a more stable particle which is completely contrary to initial expectations.

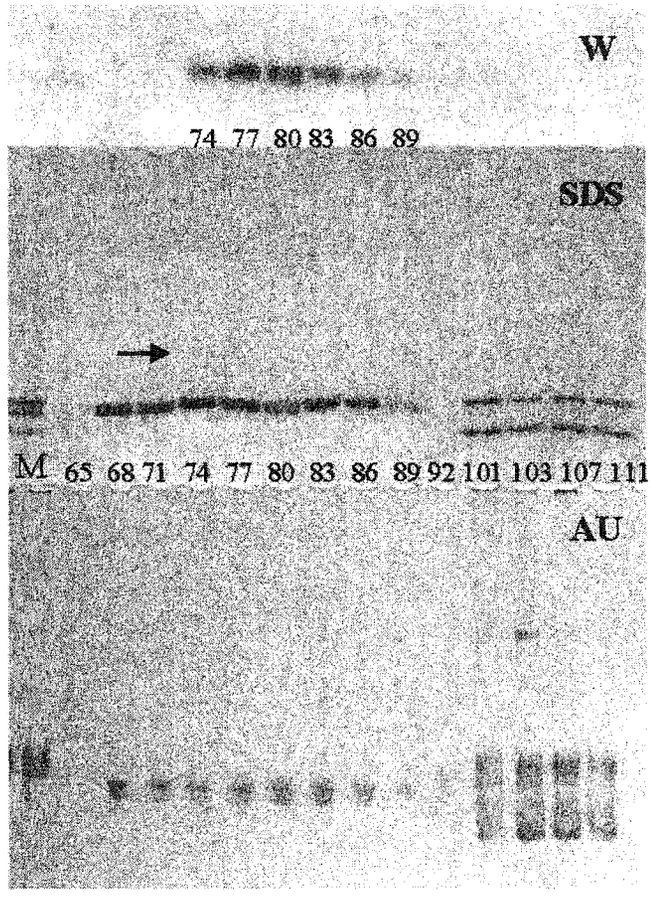


**Figure 77: PAGE and Western Blot Analysis of HTP Elution Profile of HeLa SII Chromatin Sample.** AU, acetic acid urea PAGE; SDS, SDS-PAGE; W, western of SDS-PAGE; M, HeLa core histone marker. Numbers correspond to fraction numbers in Figure 75. SII, butyrate treated HeLa sample. AU-PAGE was a 2.5 M urea, 5% acetic acid, 15% acrylamide gel run at 80 volts in 5% acetic acid running buffer and stained with Coomassie Blue. SDS-PAGE was a 6% stacking, 15% separating gel run at 100 volts in 0.05 M Tris-base, 0.38 M glycine, 0.1% SDS running buffer and stained with Coomassie Blue. Western blot was done using SDS-PAGE gel and transferring to PVDF membrane. Ubiquitinated histones were visualized using a 1/6000 dilution of a rabbit anti-ubiquitin antibody and a 1/3000 dilution of a goat anti-rabbit HRP-conjugated secondary antibody and Renaissance® Western Blot Chemiluminescence Reagents.

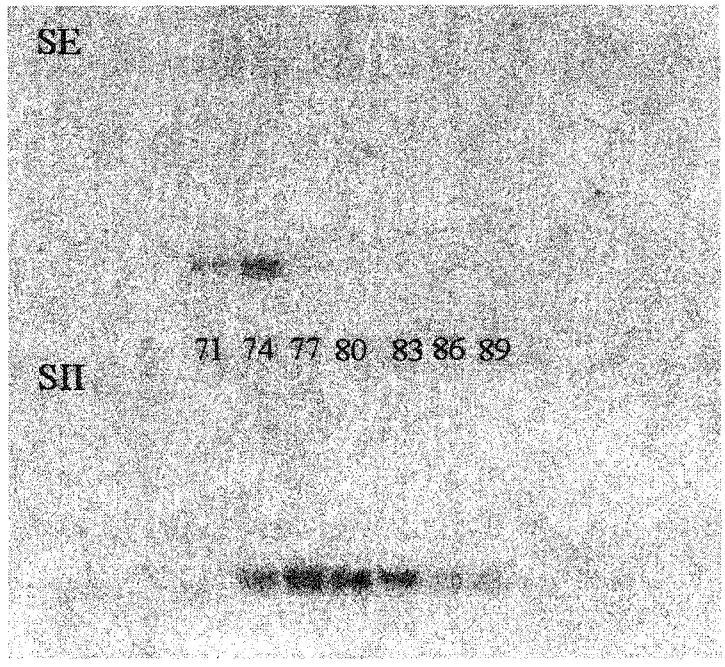


**Figure 78: Western Blots of HTP Elution Profile Fractions for SE and SII Chromatin Samples.** SE, control HeLa chromatin sample; SII, butyrate treated HeLa chromatin sample. Numbers correspond to fractions in figure 75. Ubiquitinated histones were detected using a 1/6000 dilution of a rabbit anti-ubiquitin antibody and a 1/3000 dilution of an HRP conjugated goat anti-rabbit secondary antibody and Rennaissance® Western Blot Chemiluminescence Reagents. Both westerns were of SDS-PAGE gels shown in Figures 76 and 77.

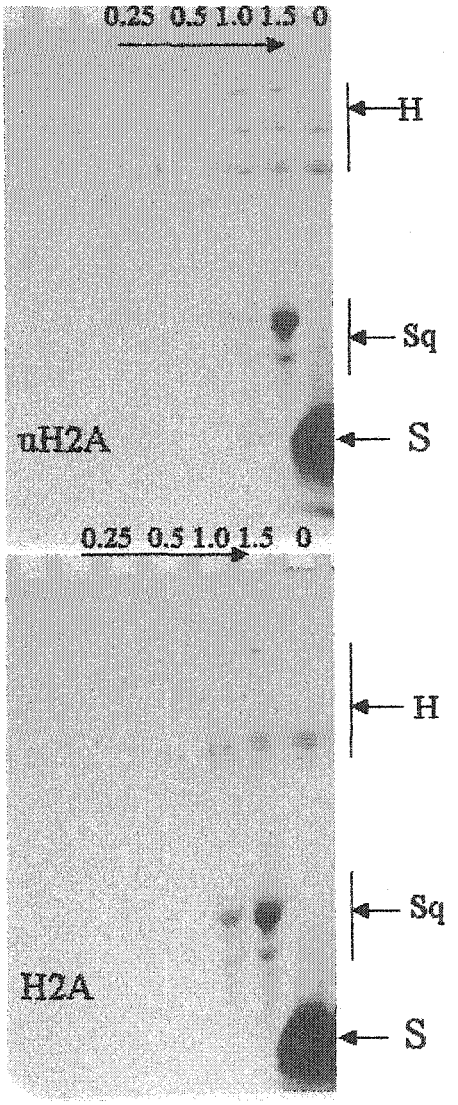


**Figure 79: AU-PAGE of Protamine Displacement Assay.** Reconstituted nucleosomes containing either uH2A or H2A with acetylated H3/H4 histones were mixed with increasing concentrations of squid protamines (Sq) to examine the ability of the protamines to displace the histones (H). All samples contained 4 μg of nucleosomes in 50 mM NaCl, 10 mM Tris-HCl (pH 7.5), 1 mM EDTA, 3 mM sodium butyrate, 2% sucrose. Numbers (0.25 to 1.5) and arrows at top of gels refer to the w/w ratio of squid protamines to nucleosomes. S, salmine (protamine from salmon). Samples were mixed with 2x AU sample buffer and loaded on to a 2.5 M urea, 5% acetic acid, 15% acrylamide gel run at 100 volts in 5% acetic acid running buffer and stained with Coomassie Blue.

## 6.5 Discussion

Ubiquitination is a bulky modification, particularly in comparison to other post-translational modifications like methylation or acetylation. While the size of this modification would indicate that it may function to prevent or hinder chromatin folding this has proven difficult to confirm *in vivo*. The *in vitro* models used here looked specifically at induced folding and oligomerization of nucleosomal arrays and the results presented indicate that contrary to expectations, uH2A did not prevent chromatin folding or association. Therefore although the histone tails are crucial for salt-induced folding of nucleosomal arrays (Garcia-Ramirez *et al.*, 1992; Moore & Ausio, 1997) the carboxyl-terminal tails of histone H2A can be ubiquitinated with little impact on the folding process. For example uH2A didn't affect the 28-40 S folding transition characteristic of histone H1-depleted chromatin in either the presence of monovalent ions (Hansen *et al.*, 1989; Garcia-Ramirez *et al.*, 1992) or in low concentrations of divalent ions (Schwarz & Hansen, 1994). Neither does it affect the maximum folding (40-55 S) transition which occurs at higher levels of histone saturation in the presence of $MgCl_2$ (Schwarz & Hansen, 1994; Tse *et al.*, 1998). Figure 80 shows a summary of the predicted and observed affects for H2A ubiquitination in both nucleosomes and chromatin. In addition, initial experiments indicate that contrary to expectations uH2A may in fact help to create a more stable nucleosome although these results are still preliminary.

An important point to remember is that the level of ubiquitination used in these assays is far greater than would be seen *in vivo*. In both the reconstituted nucleosomes and 208-12 bp polynucleosomal arrays used, there were two uH2A molecules per nucleosome whereas *in vivo* it is more common for only one H2A molecule to be ubiquitinated per nucleosome (Levinger & Varshavsky, 1980). Also little work has been done to determine the positioning and location of ubiquitinated histones *in vivo*, so it is more than likely that our *in vitro* models greatly exaggerate the amount of ubiquitination present in a similar sized native chromatin fragment.

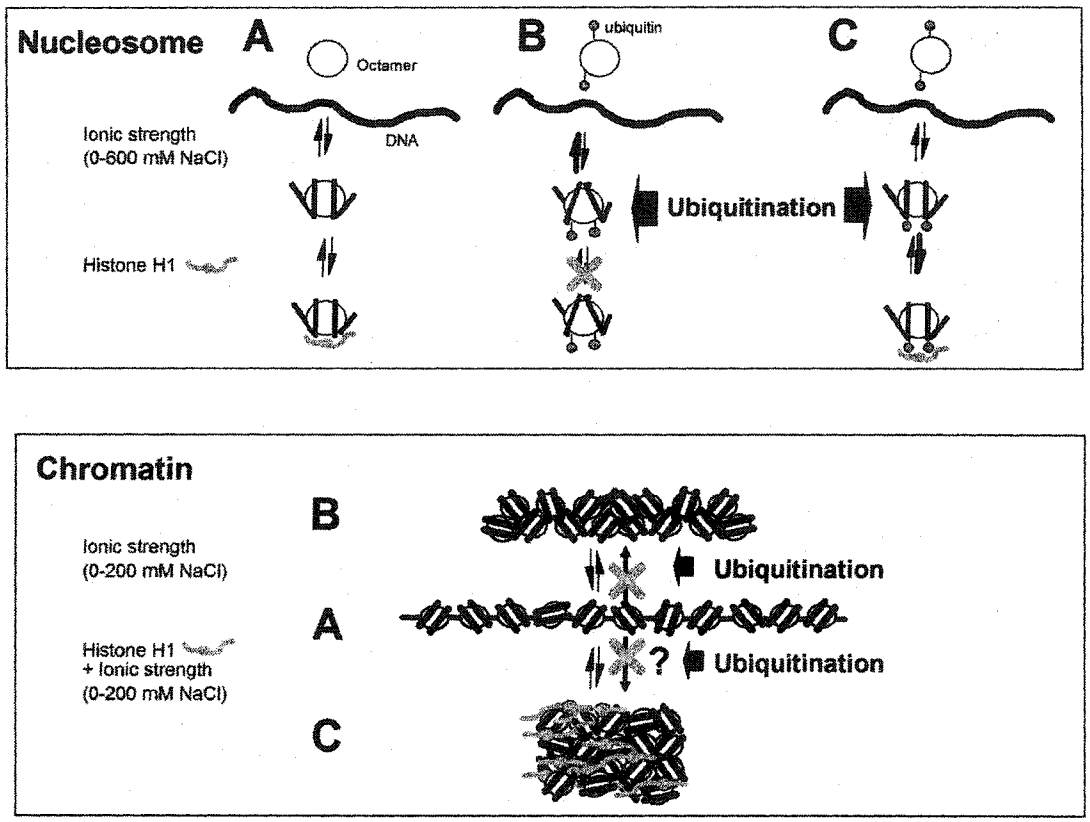


**Figure 80: Predicted and Observed Effects of H2A Ubiquitination.**
In solution nucleosomes have a reversible association equilibrium between their constitutive DNA and the histone octamer (Ausio *et al,* 1984; Ausio, 2000) which is dependent on ionic strength, concentration and temperature. Linker histones bind to nucleosomes at the DNA entry/exit point (Nucleosome A). The bulky nature of uH2A is expected to destabilize the nucleosome association-disassociation equilibrium as indicated by the thick arrow (Nucleosome B). Since H2A C-terminal tail can reach the histone H1 binding site (Usachenko *et al.,* 1994) it may interfere with H1 binding (Nucleosome B-grey cross). *In vitro* results show that uH2A does not affect stability of the nucleosome and may actually enhance the binding H1 (Nucleosome C). Chromatin fibers experience different extents of folding (Hansen & Ausio, 1992; Ausio, 2000) depending on ionic strength and H1 (Chromatin). The presence of uH2A is speculated to interfere with folding (see grey crosses). uH2A does not have any major effect on ionic strength-dependent folding of the fiber without H1 (Chromatin B). There is no information available yet for any effects when histone H1 is present (Chromatin C).

Additional investigations are required to better understand the possible structural impact of ubiquitinated histones. It will be interesting to determine if chromatin folding in the presence of histone H1 is affected by the presence of ubiquitin on histone H2A. In addition, similar experiments to those described need to be done with ubiquitinated H2B. In H2B, ubiquitin attaches to the C-terminal tail at lysine 120. However the H2B C-terminal tail is smaller than that of H2A and crystal structures indicate that it is not as accessible as the H2A protein (see Figure 10). Therefore it is entirely possible that uH2B will cause much more dramatic structural affects than its H2A counterpart and it is not inconceivable that the two histones, uH2A and uH2B, will have different structural and functional effects on chromatin dynamics.

Reconciling the physiological evidence (which associates ubiquitinated histones with such structurally opposing functions as transcription and spermiogenesis) with the *in vitro* structural results is possible. Two models have been proposed in figures 81 and 82. The first model (Figure 81) proposed that ubiquitination acts synergistically with another modification, possibly acetylation, to destabilize chromatin structure which would then allow either transcription to occur or protamine replacement of histones during spermiogenesis. Our initial experiments looking at this possibility with uH2A and acetylation do not appear to confirm this idea but it is still possible that the model is relevant with some other modification or with ubiquitinated histone H2B.

The second model (Figure 82) proposes that ubiquitination acts as a signal to recruit other proteins and possibly chromatin remodeling complexes which then disrupt nucleosome or chromatin structure allowing either transcription or chromatin compaction to occur. Recent papers by Sun & Allis (2002) and Briggs *et al.* (2002) indicate that this possibility may indeed be more probable. Their investigations have shown that ubiquitination of lysine 123 in yeast histone H2B is a prerequisite for the methylation of lysines 4 and 79 (but not lysine 36) on histone H3. Both H3 lysines 4 and 79 are required for gene silencing in yeast. Thus it appears that the H2B ubiquitination in yeast may be the first step in a pathway directly involved in gene regulation using "trans-tail" regulation, i.e. where a modification on one tail (H3 methylation) is dependent upon the modification of

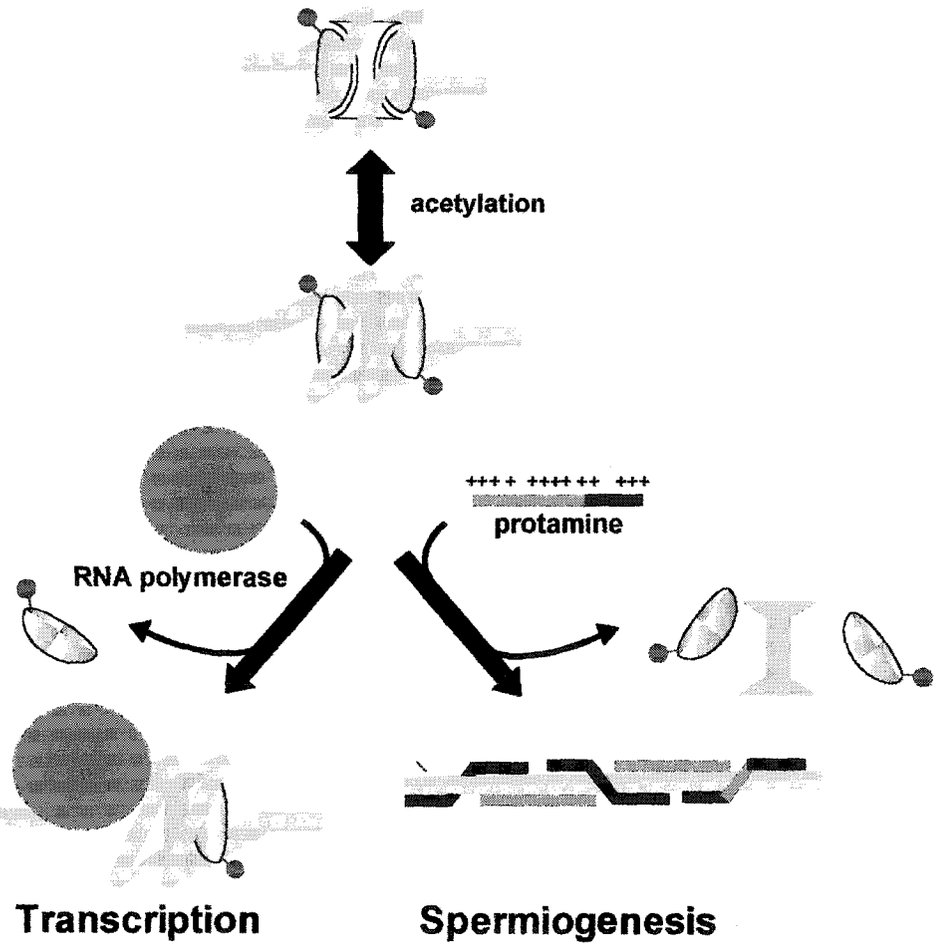


**Figure 81: Proposed Synergistic Model for Histone Ubiquitination.** Histone ubiquitination may operate synergistically with histone acetylation to destabilize the nucleosome as required by transcription and displacement of histones by protamines during spermiogenesis. The double arrow in this model indicates that acetylation could either precede or follow ubiquitination.

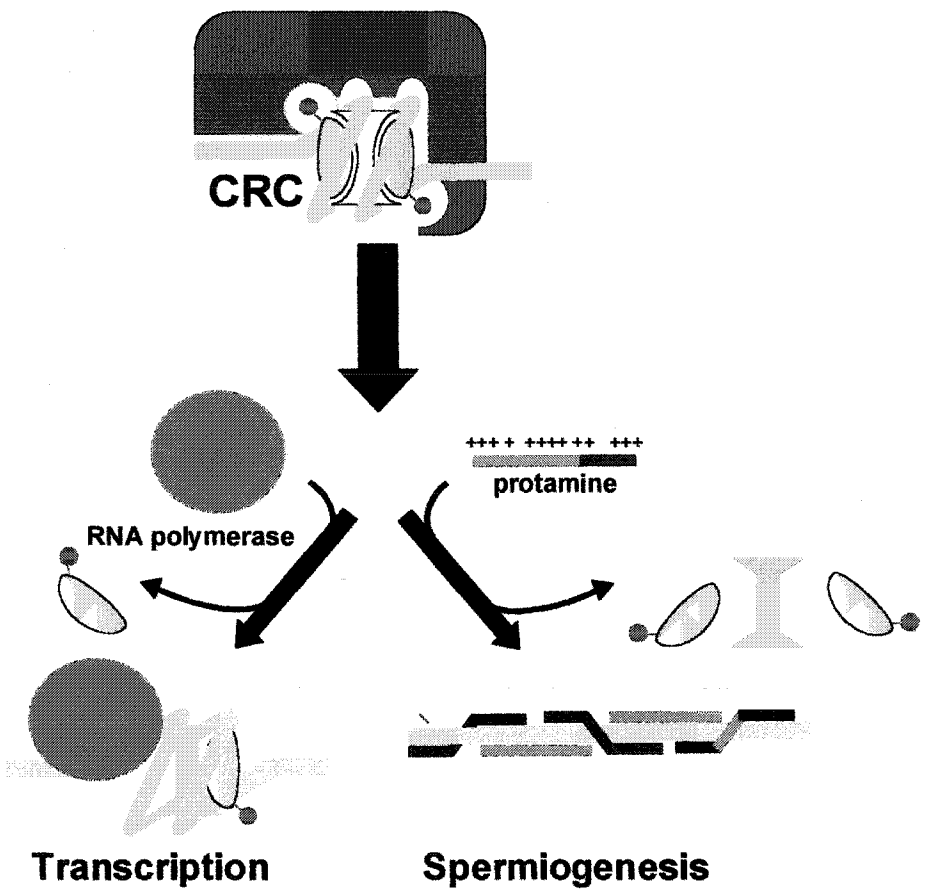


**Figure 82: Proposed Coding Model for Histone Ubiquitination.** The fact that chromatin complexes reconstituted with ubiquitinated H2A do not exhibit any major changes in conformation *in vitro* suggests that histone ubiquitination could operate as a tagging mechanism or a code for recognition by chromatin remodeling complexes such as NURF, CHRAC, or SWI/SNF that would help mediate the chromatin structural transitions during transciption or spermiogenesis.

a different histone tail (H2B ubiquitination). No doubt future investigations will help us to better understand the structural and functional importance of histone ubiquitination and its direct or indirect affects on chromatin dynamics.

# 7.0 CONCLUDING REMARKS

In eukaryotes it is chromatin rather than naked DNA which is the template for cellular processes such as transcription, replication and DNA repair. The most fundamental and basic unit of chromatin is the nucleosome and its associated histone proteins. Understanding the structure of this nucleohistone complex is fundamental to understanding the structural changes which can occur during processes such as transcription. Far from being an inert structural scaffold, chromatin is dynamic and structurally complex with different levels of compaction. An added layer to this complexity is the importance of the histone proteins. While they are considered some of the most evolutionarily conserved proteins there are still histone variants and even more numerous post-translational modifications which can occur. Since histones are such an intrinsic and essential component of chromatin, understanding the possible structural and functional impacts of their modifications may have important ramifications in understanding the structural transitions which can occur within chromatin.

This body of work has focused on the importance of the histone tails and the effect of some of their possible post-translational modifications on nucleosome and chromatin structure. It has emphasized the use of biophysical techniques such as circular dichroism and ultracentrifugation to help elucidate any structural or conformation changes. The development of a methodology to produce native-like nucleosome and polynucleosomal arrays from RP-HPLC fractionated histones (Moore *et al.*, 1997; Ausio & Moore, 1998) provides tremendous potential for investigating the importance of post-translationally modified histones (Ausio *et al.*, 2000). The data presented have shown the importance of the histone tails, particularly the H3/H4 tails, in chromatin fiber folding (Moore & Ausio, 1997) but has also demonstrated that some of the histone modifications investigated, like acetylation, have very subtle structural changes (Wang *et al.*, 2000; 2001). Indeed with ubiquitination, the huge predicted structural changes have proven to be virtually non-existent (Moore *et al.*, 2002; Jason *et al.*, 2001, 2002). The results have shown that while the histone tails have considerable importance in the inter- and intra-nucleosomal folding

events, the structural effects of some of their post-translational modifications have proven to be very subtle. Therefore it appears that the effects of histone post-translational modifications may not always be as immediately obvious as first predicted.

Careful structural investigations may sometimes preclude initial possibilities but in so doing may also lead the way to other areas of investigation and study. Indeed as one of the proposed models predicted (Figure 82), ubiquitination may act as a signal. Studies with yeast (Sun & Allis, 2002; Briggs *et al.*, 2002) have subsequently shown that ubiquitination of histone H2B is a prerequisite for methylation of specific lysines on histone H3 which in turn mediate gene silencing. Thus it appears in this case that histone ubiquitination may act as a 'master switch' in gene regulation and adds support for the idea of a 'histone code' (Strahl & Allis, 2000). No doubt the future of chromatin research will focus more intently on histone modifications and their structural effects, not just with individual modifications but more importantly with multiple or specific combinations of modifications which is far more relevant to understanding *in vivo* chromatin dynamics.

# 8.0 BIBLIOGRAPHY

Agell, N., Chiva, M., & Mexquita, C. (1983) Changes in nuclear content of protein conjugate histone H2A-ubiquitin during rooster spermatogenesis. FEBS Letters. 155 (2): 209-212.

Akhtar, A., Zink, D., & Becker, P.B. (2000) Chromodomains are protein-RNA interaction modules. Nature 407: 405-409.

Alder, A.J. & Fasman, G.D. (1974) Journal of Biological Chemistry. 249: 2911-2914.

Allfrey, V., Faulkner, R.M & Mirsky, A.E. (1964) Acetylation and methylation of histones and their possible roles in the regulation of RNA synthesis. Proceedings of the National Academy of Sciences. 51: 786-794.

Archer, S.Y. & Hodin, R.A. (1999) Histone acetylation and cancer. Current Opinions in Genetics and Development. 9: 171-174;

Arents, G., & Moudrianakis, E.N. (1995) The histone fold: a ubiquitous architectural motif utilized in DNA compaction and protein dimerization. Proceedings of the National Academy of Sciences. 92: 11170-11174.

Arents, G. Burlingame, R.W., Wang, B-C., Love, W.E., & Moudrianakis, E.N. (1991) The nucleosomal core histone octamer at 3.1Å resolution: a tripartite protein assembly and a left-handed superhelix. Proceedings of the National Academy of Sciences 88: 10148-10152.

Ausio, J. (2000) Analytical ultracentrifugation and the characterization of chromatin structure. Biophysical Chemistry. 86(2-3): 141-53.

Ausio, J. & Moore, S.C. (1998) Reconstitution of chromatin complexes from high-performance liquid chromatography-purified histones. Methods: A Companion to Methods in Enzymology. 15: 333-342.

Ausio, J., and van Holde, K.E. (1986) Histone hyperacetylation: its effects on nucleosome conformation and stability. Biochemistry. 25: 1421-1428

Ausio, J., Abbot, D.W., Wang, X. & Moore, S.C. (2001) Histone variants and histone modifications: a structural perspective. Biochemistry and Cell Biology. 79: 693-708.

Ausio, J., Dong, F., & van Holde, K.E. (1989) Use of selectively trypsinized nucleosome core particles to analyze the role of histone 'tails' in the stabilization of the nucleosome. Journal of Molecular Biology. 206: 451-463.

Ausio, J., Serger, D., Eisenberg, H. (1984) Nucleosome core particle stability and conformational change. Effect of temperature, particle and NaCl concentrations, and crosslinking of histone H3 sulfhydryl groups. Journal of Molecular Biology. 176 (1): 77-104.

Ausio, J. Borochov, N., Seger, D., Eisenberg, H. (1984) Interaction of chromatin with NaCl and MgCl2. Solubility and binding studies, transition to and characterization of the higher-order structure. Journal Molecular Biology 177: 373-398;

Avery, O.T. MacLeod, C.M. & McCarty, M. (1944) Journal of Experimental Medicine. 79: 137-158 (as communicated by van Holde, K.E. 1989. Chromatin. Springer Verlag New York Inc., New York pp. 1-15.)

Banares, J.L., Martin, A., and Parello, J. (1997) The N-tails of histones H3 and H4 adopt a highly structured conformation in the nucleosome. Journal of Molecular Biology. 273: 503-508.

Baarends, W.M., Hoogerbrugge, J.W., Roest, H.P., Ooms, M., Vreeburg, J., Hoeijmakers, J.H.J., & Grootegoed, J.A. (1999) Histone ubiquitination and chromatin remodeling in mouse spermatogenesis. Developmental Biology. 207: 322-333.

Boffa, L.C., Vidali, G., Mann, R.S., Allfrey, V.G.. (1978) Suppression of histone deacetylation in vivo and in vitro by sodium butyrate Journal of Biological Chemistry. 253(10): 3364-3366

Bohm, L., Briand, G., Sautiere, P., & Crane-Robinson, C. (1982) Proteolytic digestion studies of chromatin core-histone structure: identification of limit peptides from histone H2B European Journal of Biochemistry. 123: 299-303.

Bohm, L., Crane-Robinson, C., & Sautiere, P. (1980) Proteolytic digestion studies of chromatin core-histone structure. Identification of a limit peptide of histone H2A. European Journal of Biochemistry. 106: 525-530.

Bonner, W.M. (1988) Metabolism of ubiquitinated H2A. Current Communications in Molecular Biology The Ubiquitin System. Cold Spring Harbor Laboratory Publisher. P. 155-158.

Brehm, A., Miska, E.A., McCance, D.J., Reid, J.L., Banniser, A.J., & Kousarides, T. (1998) Retinoblastoma protein recruits histone deacetylase to repress transcription. Nature. 391: 597-600.

Briggs, S.D., Zioa, T., Sun, Z-W., Caldwell, J.A., Shabanowitz, J., Hunt, D.F., Allis, C.D., & Strahl, B.D. (2002) Trans-histone regulatory pathway in chromatin. Nature. 418: 498.

Brown, C.E., Lechner, T., Howe, L. & Workman J.L. (2000) The many HATs of transcription coactivators. Trends in Biochemical Sciences 25: 15-19.

Brownell, J.E. & Allis, C.D. (1996) Special Hats for special occasions: linking histone acetylation to chromatin assembly and gene activation. Current Opinion in Genetics and Development. 6: 176-184.

Brownell, J.E., Zhou, J., Ranalli, T., Kobayashi, R., Edmondson, D.G., Roth, S.Y., & Allis, C.D. (1996) Tetrahymena histone acetyltransferase A: a homolog to yeast Gcn5p linking histone acetylation to gene activation. Cell 84: 843-851.

Burton, D.R., Butler, M.J., Hyde, J.E., Phillips, D., Skidmore, C.J., Walker, I.O. (1978) The interaction of core histones with DNA: equilibrium binding studies. Nucleic Acids Research. 5: 3543-3663

Butler, P.J. & Thomas, J.O. (1980) Changes in chromatin folding in solution. Journal of Molecular Biology 140: 505-529

Carlson, N. & Rechsteiner, M.(1987) Microinjection of ubiquitin: intracellular distribution and metabolism in HeLa cells maintained under normal physiological conditions. Journal of Cell Biology. 104: 537-546.

Chen, H-Y., Sun, J.-M., Zhang, Y., Davie, J.R. and Meistrich, M.L. (1998) Ubiquitination of histone H3 in elongating spermatids of rat testes. Journal of Biological Chemistry. 273: 13165-13169.

Chou, P.Y. & Fasman, G.D. (1978) Prediction of the secondary structure of proteins from their amino acid sequence. Advances in Enzymology Related Areas Molecular Biology.47: 45-148.

Chung, S.Y. (1978) Characterization of the histone core complex. Proceedings of the National Academy of Sciences USA. 75: 1680-1684;

Cirillo, L.A., & Zaret, K.S. (1999) An early developmental transcription factor that is more stable on nucleosome core particles than on free DNA. Molecular Cell. 4: 961-969.

Clapier, C.R., Langst, G., Corona, D.F., Becker, P.B., and Nightingale, K.P. (2001) Critical role for the histone H4 N-terminus in nucleosome remodeling by ISWI. Molecular and Cellular Biology. 21: 875-883.

Clark, D.J., & Kumura, T. (1990) Electrostatic mechanism of chromatin folding. Journal of Molecular Biology. 211: 883-896.

Cockell, M. & Gasser, S.M. (1999) Nuclear compartments and gene regulation. Current Opinion in Genetics and Development. 9: 199-205.

Conley, B.A., Egorin, M.J., Tait, N., Rosen, D.M., Sausville, E.A., Dover, G., Fram, R.J., and Van Echo, D.A. (1998) Phase I study of the orally administered butyrate prodrug, tributyrin, in patients with solid tumors. Clinical Cancer Research. 4: 629-634.

Cook, Peter R. (2001) Principles of Nuclear Structure and Function. Wiley-Liss Inc., New York, New York.

Cotton, R.W., & Hamkalo, B.A. (1981) Nucleosome dissociation at physiological ionic strengths. Nucleic Acids Research. 9: 445-457.

Cui, Y., & Bustamante, C. (2000) Pulling a single chromatin fiber reveals the forces that maintain its higher-order structure. Proceedings of the National Academy of Sciences. 97 (1): 127-132.

Daban, J-R. (2000) Physical constraints in the condensation of eukaryotic chromosomes. Local concentration of DNA versus linear packing ratio higher order chromatin structures. Biochemistry 39 (14): 3861-3866.

Davie, J.R. (1998) Covalent modifications of histones: expression from chromatin templates. Current Opinion in Genetics and Development. 8: 173-178.

Davie, J.R. (1995) The nuclear matrix and the regulation of chromatin organization and function. International Review of Cytology. 162A: 191-249.

Davie, J.R. & Murphy, L.C. (1994) Inhibition of transcription selectively reduces the level of ubiquitinated histones H2B in chromatin. Biochemical and Biophysical Research Communications. 203: 344-350.

Davie, J.R., & Murphy, L.C. (1990) Level of ubiquitinated histone H2B in chromatin is coupled to ongoing transcription. Biochemistry. 29: 4752-4757.

Davie, J.R. & Nickel, B.E. (1987) The ubiquitinated histone species are enriched in histone H1-depleted chromatin regions. Biochimica and Biophysica Acta. 909: 183-189.

Davie, J.R. & Spencer, V.A. (2001) Signal transduction pathways and the modification of chromatin structure. Progress in Nucleic Acids Research. 65: 299-340.

Davie, J.R., Lin, R., & Allis, C.D. (1990) Timing of the appearance of ubiquitinated histones in developing new macronuclei of *Tetrahymena thermophila.* Biochemistry and Cell Biology. 69: 66-71.

Davies, N. & Lindsey, G.G. (1994) Histone H2B (and H2A) ubiquitination allows normal histone octamer and core particle reconstitution. Biochimica and Biophysica Acta. 1218: 187-193.

Deleage, G. & Roux, B. (1987) An algorithm for protein secondary structure prediction based on class prediction. Protein Engineering. 1: 289-294.

Eickbush, T.H., & Moudrianakis, E.N.& 1978 The histone core complex: an octamer assembled by two sets of protein-protein interactions. Biochemistry 17: 4955-4964.

Eisenberg, D., Weiss, R.M., & Terwilliger, T.C. (1984) The hydrophobic moment detects periodicity in protein hydrophobicity. Proceedings of the National Academy of Sciences U.S.A. 81: 140-144.

Ericsson, C., Goldknopf, I.L., & Daneholt, B. (1986) Inhibition of transcription does not affect the total amount of ubiquitinated histone 2A in chromatin. Experimental Cell Research. 167: 127-134.

Fasman, G.D., Chou, P.Y. & Alder, A.J. (1976) Prediction of the conformation of the histones. Biophysical Journal. 16: 1201-1238.

Flemming, W. (1880) Arkiv fur Microskopsch Anat. 18: 151-259. (as communicated by van Holde, K.E. 1989. Chromatin. Springer-Verlag New York Inc., New York pp.1-15.)

Gangloff, Y-G., Romier, C., Thuault, S., Werten, S., & Davidson, I. (2001) The histone fold is a key structural motif of transcription factor TFIID. Trends in Biochemical Sciences. 26 (4): 250-257.

Garcia-Ramirez, M., Rocchini, C., & Ausio, J. (1995) Modulation of chromatin folding by histone acetylation. Journal of Biological Chemistry. 270: 17923-17928.

Garcia-Ramirez, M., Dong, F., & Ausio, J. (1992) Role of the histone "tails" in the folding of oligonucleosomes depleted of histone H1. Journal of Biological Chemistry. 267 (27) 19587-19595.

Georgel, P.T., Tsukiyama, T., & Wu, C. (1997) Role of histone tails in nucleosome remodeling by *Drosophila* NURF. EMBO Journal. 16: 4717-4726.

Georgieva, E.I. & Sendra, R. (1999) Mobility of acetylated histones in sodium dodecyl sulfate-polyacrylamide gel electrophoresis. Analytical Biochemistry. 269: 399-402

Gilbrat, J.G., Garnier, J., Robson, B. (1987) Further developments of protein secondary structure prediction using information theory. New parameters and consideration of residue pairs. Journal of Molecular Biology 198: 425-443.

Goldknopf, I.L., & Busch, H. 1977. Isopeptide linkage between nonhistone and histone 2A polypeptides of chromosomal conjugate-protein A24. Proceedings of the National Academy of Sciences. 74: 864-868.

Greenfield, N. Fasman, G.D. (1969) Computed circular dichroism spectra for the evaluation of protein conformation. Biochemistry 8: 4108-4116

Grunstein, M. (1997) Histone acetylation in chromatin structure and transcription. Nature. 389: 349-352.

Gurley, L.R., Valdez, J.G., Prentice, D.A., & Spall, W.D. (1983) Histone fractionation by high-performance liquid chromatography. Analytical Biochemistry. 129: 132-144.

Haas, A.L., Bright, P.M., & Jackson, V.E. (1988) Functional diversity among putative *E2* isozymes in the mechanism of ubiquitin-histone ligation. The Journal of Biological Chemistry. 263 (26): 13268-13275.

Hallin, P., Madej, A. & Edqvist, L.E. (1985) Subunits of bovine lutropin: hormonal and immunological activity after separation with reverse phase high performance liquid chromatography. Journal of Chromatography. 294: 207-

Hamiche, Q. Sandaltzopoulos, S.R., Gdula, D.A. & Wu, C. (1999) ATP-dependent histone octamer sliding mediated by the chromatin remodeling complex NURF. Cell. 97: 833-842.

Han, M. & Grunstein, M. (1988). Nucleosome loss activate yeast downstream promoters *in vivo*. Cell. 55:1137-1145.

Hansen, J.C. & Ausio, J. (1992) Chromatin dynamics and the modulation of genetic activity. Trends in Biochemical Sciences. 17 (5): 187-191.

Hansen, J.C., Ausio, J., Stanik, V.H., & van Holde, K.E. (1989) Homogeneous reconstituted oligonucleosomes, evidence for salt-dependent folding in the absence of histone H1. Biochemistry. 28: 9129-9236.

Hansen, J.C., Tse, C., Wolffe, A.P. (1998) Structure and function of the core histone N-termini: more than meets the eye. Biochemistry. 37: 17637-17641.

Heard, E., Cler, P., & Avener, P.(1997) X-chromosome inactivation in mammals. Annual Review of Genetics. 31: 571-610.

Hebbes, T.R., Thorne, A.W. & Crane-Robinson, C. (1988) A direct link between core histone acetylation and transcriptionally active chromatin. EMBO Journal. 7(5): 1395-1402.

Hecht, A. Laroche, T., Strahl-Bolsinger, S., Gasser, S.M. & Grunstein, M. Histone H3 and H4 N-termini interact with SIR3 and SIR4 proteins: a molecular model for the formation of heterochromatin in yeast. Cell 80: 583-592.

Hennig, W. (1999) Heterochromatin. Chromosoma. 108: 1-9.

Helliger, W. Lindner, H., Hauptlorenz, S., Puschendorf, B. et al. (1988) A new h.p.l.c. isolation procedure for chicken and goose erythrocyte histones. Biochemical Journal. 255(1): 23-7.

Hershko, A. & Ciechanover, A. (1998) The ubiquitin system. Annual Review of Biochemistry. 67: 425-479.

Hilfiker,A., Hilfiker-Kleiner, D., Pannuti, A., & Lucchesi, J.C. (1997) MOF, a putative acetyl transferase gene related to the Tip60 and MOZ human genes and to the SAS genes of yeast, is required for dosage compensation in Drosophila. EMBO Journal. 16(8): 2054-60.

Howe, L.J., & Ausio, J. (1998) nucleosomal translational position, not histone acetylation, determines TFIIIA binding to nucleosomal *Xenopus laevis* 5S rRNA genes. Molecular and Cellular Biology. 18: 1156-1162.

Huang, S.Y., Barnard, M.B., Xu, M., Matsui, S., Rosse, S.M., & Garrard, W.T. (1986) The active immunoglobin kappa chain gene is packaged by non-ubiquitin-conjugated nucleosomes.

Hurley, C.K. (1977) Electrophoresis of histones: a modified Panyim and Chalkley system for slab gels. Analytical Biochemistry. 80: 624-626.

Jason, L.J.M, Moore, S.C., Lewis, J.D. & Ausio, J. (2002) Histone ubiquitination: a tagging tail unfolds. BioEssays. 24: 166-174.

Jason, L.J.M., Moore, S.C., Ausio, J. & lindsey, G. (2001) Magnesium-dependent association and folding of oligonucleosomes reconstituted with ubiquitinated H2A. Journal of Biological Chemistry. 276: 14597-14601.

Johns, E.W., (1964) Preparative methods for histone fractions from calf thymus. Biochemical Journal. 92: 55-59

Johnson, M.L., Correia, J.J., Yphantis, D.A. & Halvorson, H.R. (1998) Analysis of data from analytical ultracentrifugation by non-linear least squares techniques. Biophysics Journal. 36: 575-588

Kleinschmidt, A.M., & Martinson, H. (1981) Structure of nucleosome core particles containing uH2A (A24). Nucleic Acids Research. 9: 2423-2431.

Kornberg, R.D. (1974) Chromatin structure: a repeating unit of histones and DNA. Science 184(139): 868-871

Kornberg, R.D., & Lorch, Y. (1999) Twenty-five years of the nucleosome, fundamental particle of eukaryote chromosome. Cell. 98: 285-294.

Kossel, A. (1884) Z. Physiol Chem. 8: 511-515 (in van Holde, 1989)

Krajewski, W.A., Ausio, J. (1996) Modulation of the higher-order folding of chromatin by deletion of histone H3 and H4 terminal domains. Biochemical Journal. 316 ( Pt 2):395-400.

Krum, A., Madisen, L., Yang, Z-J., Goodman, R., Nakatani, Y., & Groudine, M. (1998) Long-distance transcriptional enhancement by the histone acetyltransferases PCAF. Proceedings of the National Academy of Sciences. 95: 13501-13506.

Kuo, M-H., Zhou, J., Jambeck, P., Churchill, M.E.A., & Allis, C.D. (1998) Histone acetyltransferase activity of yeast Gcn5p is required for the activation of target genes in vivo. Genes & Development. 12: 627-639.

Laemmli, U.K. (1970) Cleavage of structural proteins during the assembly of the head of bacteriophage T4. Nature. 227: 680-685.

Langst, G., Bonte, E.J., Corona, D., Becker, P.B. (1999) Nucleosome movement by CHRAC and ISWI without disruption or trans displacement of the histone octamer. Cell 97: 842-852.

Lee, D.Y., Hayes, J.J., Pruss, D., and Wolffe, A.P. (1993) A positive role for histone acetylation in transcription factor access to nucleosomal DNA. Cell 72: 73-84.

Lehrman, S.R., Tuls, J.L. & Lund, M. (1990) Peptide α-helicity in aqueous trifluoroethanol: correlations with predicted α-helicity and the secondary structure of the corresponding regions of bovine growth hormone. Biochemistry. 29: 5590-5596.

Levinger Varshavsky (1980) High-resolution fractionation of nucleosomes: minor particles, "whiskers," and separation of mononucleosomes containing and lacking A24 semihistone. Proceedings of the National Academy of Sciences U.S.A. 77: 3244-3248.

Lewin, B. (1997) Genes VI Oxford University Press, New York, New York. p.753-755

Lindner, H., Sarg, B., Helliger, W. (1997) Application of hydrophilic-interaction liquid chromatography to the separation of phosphorylated H1 histones. Journal of Chromatography. 782: 55-62.

Litt, M.D., Simpson, M., Recillas-Targa, F., Prioleau, M.N., Felsenfeld,G. (2001) Transitions in histone acetylation reveal boundaries of three separately regulated neighboring loci. EMBO Journal. 20 (9): 2224-2235.

Lorch, Y., Zhang, M., & Kornberg, R.D. (1999) Histone octamer transfer by a chromatin remodeling complex. Cell 96: 389-392.

Lorch, Y., LaPointe, J.W., & Kornberg, K.D. (1987) Nucleosomes inhibit the initiation of transcription but allow chain elongation with the displacement of histones. 49: 205-210.

Luger, K. Mader, A.W., Richmond, R.K., Sargent, D.F., & Richmond, T.J. (1997) Crystal structure of the nucleosome core particle at 2.8 Å resolution. Nature. 389: 251-260.

Luger, K. & Richmond, T.J. (1998a) DNA binding within the nucleosome core. Current Opinion in Structural Biology. 8: 33-40.

Luger, K. & Richmond, T.J. (1998b) The histone tails of the nucleosome. Current Opinion in Genetics and Development. 8: 140-146.

Magnaghi, J.L., Groisman, R., Naguibneva, I., Robin, P., Lorain, S., LeVillain, J.P., Troalen, F., Trouche, D., & Harel-Bellan, A. (1998) Retinoblastoma protein represses transcription by recruiting a histone deacetylase. Nature. 391: 601-604.

Martinson, H.G., True, R., Burch, J.B.E., & Kunkel, G. (1979) Semihistone protein A24 replaces H2A as an integral component of nucleosome histone core. Proceedings of the National Academy of Sciences USA. 76(3): 1030-1034.

Matsui, S-I., Seon, B.K., & Sandberg, A.A. (1979) Disappearance of a structural chromatin protein A24 in mitosis: implications for molecular basis of chromatin condensation. . Proceedings of the National Academy of Sciences USA. 76 (12): 6386-6390.

McGhee, J.D., Nickol, J.M., Felsenfeld, G., & Rau, D.C. (1983) Histone hyperacetylation has little effect on the higher order folding of chromatin. Nucleic Acids Research. 11: 4065-4075.

Megee, P.C., Morgan, B.A., Mittman, B.A. & Smith, M.M. (1990) Genetic analysis of histone H4: essential role of lysines subject to reversible acetylation. Science 247: 841-845.

Miescher, F. (1874) Ver. Naturforsch. Ges. Basel 6. 138-208. (as communicated in van Holde, K.E. 1989. Chromatin. Springer-Verlag New York Inc., New York pp.1-15.)

Miescher, F. (1871) Med-Chem Untersuch Hoppe-Selyer, pt.4 pp.441-460 (as communicated in van Holde, K.E. 1989. Chromatin. Springer-Verlag New York Inc., New York pp.1-15.)

Moazed, D., & Johnson, A.D. (1996) A deubiquitinating enzyme interactes with SIR4 and regulates silencing in *S. cerevisiae* . Cell. 86: 667-677.

Moore, S.C. & Ausio, J. (1997) Major role of the histones H3-H4 in the folding of the chromatin fiber. Biochemical Biophysical Research Communications.230(1):136-9.

Moore, S.C., Jason, L.J.M., & Ausió, J. (2002) The elusive structural impact of ubiquitinated histones. Journal of Biochemistry and Cell Biology 80 (3): 309-317.

Moore, S.C., Rice, P., Iskandar, M. & Ausio, J. (1997) Reconstitution of native-like nucleosome core particles from reversed-phase-HPLC-fractionated histones. Biochemical Journal. 328:

Mueller, R.D., Yasuda, H., Hatch, C.L., Bonner, W.M., & Bradbury, E.M. (1985) Identification of ubiquitinated histones 2A and 2B in *Physarum polycephalum.* Journal of Biological Chemistry. 260 (8): 5147-5153.

Mustkov, V., Gerber, D., Angelov, D., Ausio, J., Workman, J., and Dimitrov, S. (1998) Persistent interactions of core histone tails with nucleosomal DNA following acetylation and transcription factor binding. Molecular and Cellular Biology. 18(11): 6293-6304;

Ng, H.H. & Bird, A. (2000) Histone deacetylases: silencers for hire. Trends in Biochemical Sciences. 25: 121-126.

Nickel, B.E. & Davie, J.R. (1989) structure of polyubiquitinated histone H2A. Biochemistry. 28: 964-968.

Nickel, B.E., Allis, C.D., & Davie, J.R. (1989) Ubiquitinated histone H2B is preferentially located in transcriptionally active chromatin. Biochemistry. 28: 953-963.

Nickel, B.E., Roth, S.Y., Cook, R.G., Allis, C.D., Davie, J.R.. (1987) Changes in the histone H2A variant H2A.Z and polyubiquitinated histone species in developing trout testis. Biochemistry. 26: 4417-4421.

Noll, M. & Kornberg, R.D. (1977) Action of micrococcalnuclease on chromatin and the location of histone H1. Journal of Molecular Biology. 109:393-404

Oliva, R. & Dixon, G.H. (1991) Vertebrate protamine genes and the histone-to-protamine replacement reaction. Progress in Nucleic Acid Research Molecular Biology 40: 25-94.

Panyim, S. & Chalkley, R. (1969) High resolution acrylamide gel electrophoresis of histones. Archives of Biochemistry and Biophysics. 130: 337-346.

Paul, A-L., & Ferl, R.J. (1999) Higher-order chromatin structure: looping long molecules. Plant Molecular Biology. 41: 713-720.

Pereira, S.L., & Reeve, J.N. (1998) Histones and nucleosomes in Archaea and Eukarya: a comparative analysis. Extremophiles. 2: 141-148.

Perry, M. & Chalkley, R. (1982) Histone acetylation increases the solubility of chromatin and occurs sequentially over most of the chromatin. A novel model for the biological role of histone acetylation. Journal of Biological Chemistry. 257: 7336-7347.

Pham, A.-D., & Sauer, F. (2000) Ubiquitin-activating/conjugating activity of $TAF_{II}250$, a mediator of activation of gene expression in *Drosophila.* Science. 289: 2357-2360.

Pickart, C.M. (2001) Mechanisms underlying ubiquitination. Annual Review of Biochemistry. 70: 503-533.

Pickart, C.M. & Vella, A.T. (1988) Ubiquitin carrier protein-catalyzed ubiquitin transfer to histones. The Journal of Biological Chemistry. 263 (29): 15076-15082.

Prevelige, P.E., Jr., & Fasman, G.D. (1987) Structural studies of acetylated and control inner core histones. Biochemistry. 20: 2944-2955.

Reik, A., Gregory, P.D. & Urnov, F.D. (2002) Biotechnologies and therapeutics: chromatin as a target. Current Opinions in Genetics and Development. 12: 233-242.

Richmond, T.J., Finch, J.T., Rushton, B., Rhodes, D., Klug, A. (1984) Structure of the nucleosome core particle at 7 A resolution. Nature 311(5986): 532-537

Robzyk, K., Recht, J., & Osley, M.A. (2000) Rad6-dependent ubiquitination of histone H2B in yeast. Science. 287: 501-504.

Rubenstein, P., Sealy, L., Marshall, S., Chalkley, R. (1979) Cellular protein synthesis and inhibition of cell division are independent of butyrate-induced histone hyperacetylation. Nature 280(5724): 692-693

Schiltz, R.L., Mizzen, C.A., Vassilev, A., Cook, R.G., Allis, C.D., & Nakatani, Y. (1999) Overlapping but distinct patterns of histone acetylation by the human coactivators p300 and PCAG within nucleosomal substrates. Journal of Biological Chemistry. 274(3): 1189-1192.

Schwarz, P.M. & Hansen, J.C. (1994) Formation and stability of higher order chromatin structures. Contributions of the histone octamer. Journal of Biological Chemistry. 269: 16284-16289.

Schwarz, P.M., Felthauser, A., Fletcher, T.M., & Hansen, J.C. (1996) Reversible oligonucleosome self-association: dependence on divalent cations and core histone tail domains. Biochemistry. 35: 4009-4015.

Seale, R.L. (1981) Rapid turnover of the histone-ubiquitination conjugate protein A24. Nucleic Acids Research. 9: 3151-3158

Segawa, S-I., Fukuno, T., Fujiwara, K., & Noda, Y. (1991)Local structures in unfolded lysozyme and correlation with secondary structures in the native conformation: helix-forming or –breaking propensity of peptide segments. Biopolymers. 31: 497-509.

Sewack, G.F., Ellis, T.W., and Hansen, U. (2001) Binding of TATA binding protein to a naturally positioned nucleosome is facilitated by histone acetylation. Molecular and Cellular Biology 21: 1404-1415.

Simpson, R.T. (1991) Nucleosome Positioning: occurrence, mechanisms and functional consequences. Progress in Nucleic Acids Research. 40: 143-184.

Simpson, R.T. (1978) Structure of the chromatosome, a chromatin particle containing 160 base pairs of DNA and all the histones. Biochemistry. 17 (25): 5524-5531.

Simpson, R.T., Thoma, F., & Brubaker, J.M. (1985) Chromatin reconstituted from tandemly repeated cloned DNA fragments and core histones; a model system for study of higher order structure. Cell. 42: 799-808.

Spencer V.A. & Davie, J.R. (1999) Role of covalent modifications of histones in regulating gene expression. Gene. 240: 1-12.

Sterner, D.E. & Berger, S.L. (2000) Acetylation of histones and transcription-related factors. Microbiology and Molecular Biology Reviews. 64 (2): 435-459.

Strahl, B.D., & Allis, C.D. (2000) The language of covalent histone modifications. Nature 403: 41-45.

Sun, Z-W., & Allis, D. (2002) Ubiquitin of histone H2B regulates H3 methylation and gene silencing in yeast. Nature. 418: 104-108.

Sung, M.T. & Dixon, G.H. (1970) Proceedings of the National Academy of Sciences U.S.A. 67: 1616-1623.

Tatchell, K., & van Holde, K.E. (1977) Reconstitution of chromatin core particles. Biochemistry 16: 5295-5307.

Taunton, J., Hassig, C.A. & Schreiber, S.L. (1996) A mammalian histone deacetylase related to the yeast transcriptional regulator Rpd3p. Science. 272: 408-411.

Thoma, F. (1992) Nucleosome positioning. Biochimica and Biophysica ACTA. 1130: 1-19.

Thorne, A.W., Sautiere, P., Briand, G., & Crane-Robinson, C. The structure of ubiquitinated histone H2B. EMBO Journal. 6 (4): 1005-1010.

Tse, C., Sera, T., Wolffe, A.P., and Hansen, J.C. (1998) Disruption of higher-order folding by core histone acetylation dramatically enhances transcription of nucleosomal arrays by RNA polymerase III. Molecular & Cellular Biology 18: 4629-4638

Turner, B.M, Birley, A.J., & Lavender, J. (1992) Histone H4 isoforms acetylated at specific lysine residues define individual chromosomes and chromatin domains in Drosophila polytene nuclei. Cell. 69: 375-384.

Twyman, R.M. (1998) Advance Molecular Biology: A concise Reference. Bioscientific, New York. Chapter 3;29.

Usachenko, S.I., Bavykin, S.G., Gavin, I.M., and Bradbury, E.M. (1994) Rearrangement of the histone H2A C-terminal domain in the nucleosome. Proceedings of the National Academy of Sciences. 91: 6845-6849.

Van Holde, K. (1989) Chromatin. Springer-Verlag New York Inc., New York.

van Holde, K.E. & Weischet, W.O. (1978) Boundary Analysis of Sedimentation-velocity experiments with monodisperse and paucidisperse solutes. Biopolymers 17, 1387-1401

Verdaguer, N., Perello, M., Palau, J., & Subirana, J.A. (1993) Helical structure of basic proteins from spermatozoa. Comparison with model peptides. European Journal of Biochemistry. 214: 879-887.

Vijay-Kumar, S., Bugg, C.E., Wilkinson, K.D,., Vierstra, R.D., Hatfield, P.M., & Cook, W.J. (1987) comparison of the three-dimensional structures of human, yeast, and oat ubiquitin. Journal of Biological Chemistry. 262: 6396-6399.

Vignali, M., Hassan, A.H., Neely, K.E., & Workman, J.L. (2000) ATP-dependent chromatin-remodeling complexes. Molecular and Cellular Biology. 20 (6): 1899-1910.

Vogelaur, M., Wu, J., Suka, N., & Grunstein, M. (2000) Global histone acetylation and deacetylation in yeast. Nature. 408: 495-498

Voordow, G., Kalif, D., & Eisenberg, H. (1977) Studies of ColE1-plasmid DNA and its interactions with histones: sedimentation velocity studies of monodisperse complexes reconstituted with calf-thymus histones. Nucleic Acids Review. 4: 1207-1223.

Walia, H., Chen, H.Y., Sun, J.M., Holth, L.T., & Davie, J.R. (1998) Histone acetylation is required to maintain the unfolded nucleosome structure associated with transcribing DNA. Journal of Biological Chemistry. 273: 14516-14522.

Walker, I.O. (1984) Differential dissociation of histone tails from core chromatin. Biochemistry. 23: 5622-5628.

Wang, D., Mariggl, R., Stravopodis, D., Carpino, N., Marine J-C., Teglund, S., Feng, J., & Ihle, J.N. (2000a) EMBO Journal 19: 392-399.

Wang, X., He, C., Moore, S.C., & Ausio, J. (2001) Effects of histone acetylation on the solubility and folding of the chromatin fiber. Journal of Biological Chemistry. 276 (16): 12764-12768.

Wang, X., Moore, S.C., Laszckzak, M., & Ausio, J. (2000) Acetylation increases the α-helical content of the histone tails of the nucleosome. Journal of Biological Chemistry. 275 (45) 35013-35020.

White, C.L., Suto, R.K., & Luger, K. (2001) Structure of the yeast nucleosome core particle reveals fundamental changes in internucleosome interactions. EMBO Journal. 20 (18): 5207-5218.

Wu, R.S., Kohn, K.W., & Bonner, W.,M. (1981) Metabolism of ubiquitinated histones. Journal of Biological Chemistry. 256 (11): 5916-5920.

Xu, X., Cooper, L.G., DiMario, P.J., Nelson, J.W. (1995) Helix formation in model peptides based on nucleolin TPAKK motifs. Biopolymers. 35: 93-102.

Zlatanova, J., Leuba, S.H., & van Holde, K. (1999) Chromatin structure revisited. Critical Reviews in Eukaryotic Gene Expression. 9 (3&4): 245-255.